Enhancing Biogas Recovery from Anaerobic Co-digestion of Human Excreta and Food Waste using Response Surface Method and Biochar Additives

by

Blissbern Owusu Peprah, MSc. Environmental Engineering

A Thesis Submitted to the Deparment of Civil Engineering, Kwame Nkrumah University of Science and Technology in partial fulfillment of the requirements for the degree of

PhD. Environmental Sanitation and Waste Management

College of Engineering

Supervisor: Prof. S. Oduro-Kwarteng

Dr. Martina Francisca Baidoo

Prof. Richard Arthur

September 2023

Declaration

I hereby declare that the thesis I have undertaken is my own work and that, to the best of my knowledge and belief, it does not contain any material that has already been written or published by another person or that has been largely accepted for the award of any other degree or diploma at Kwame Nkrumah University of Science and Technology or any other educational institution, with the exception of instances where appropriate acknowledgement has been made in the text through citations or references.

....

Student Name and ID Signature Date

Certified by

....

Name of Supervisor Signature Date

Certified by

....

Name of Head of Department Signature Date

Dedication

Dedicated to God, my husband, Henry Appiagyei Osei-Owusu and my daughter Abena Appiagyei Osei-Owusu.

Abstract

Ghana shares similar challenges with other developing nations regarding waste management and access to clean energy. Fortunately, these two challenges are connected. A better waste management strategy would involve converting the organic waste fractions into biogas. Nevertheless, a thorough study of the physico-chemical characteristics of the feedstocks used in the anaerobic digestion process is essential to maximise the energy potential. Consequently, the first phase of this study examined the physico-chemical properties of some selected feedstocks, namely, human excreta (HE), food leftovers (FLO), kitchen residues (KR) and cow dung (CD) of Ghanaian origin using APHA standards and standard equipment. Results of volatile to total solid ratios (VS/TS), 0.81 ± 0.001, 0.97 ± 0.001, 0.89 ± 0.001 and 0.85 ± 0.001 for HE, FLO, KR and CD, respectively showed that all feedstocks had high biodegradable content. Although the carbon-to-nitrogen (C/N) ratios for FLO (22.14 ± 0.26), KR (23.34 ± 0.25) and CD (26.19 ± 0.47) were within the optimal range, that of HE (8.29 ± 0.09) was significantly low. With a mean alkalinity of 1219.67 ± 1.53, 630.00 ± 0.58, 590.00 ± 2.08 and 15,730.00 ± 6.00 mg $CaCO_3$ eq./L for HE, FLO, KR and CD respectively, it was observed that only CD has the optimal alkalinity value for anaerobic digestion. This brought into perspective the need for co-digestion. The second phase of the study, therefore, sought to prove the hypothesis that anaerobic co-digestion of HE, FLO and KR could generate more biogas while remaining stable if positive synergistic effects are achieved. A randomized ternary mixture design and a response surface approach were used to ascertain the relationship between substrate mixture, biogas yield, methane yield, and synergy. The findings revealed that R9(78.8 % HE:11.8 % FLO:9.4 % KR) had the highest methane yield of 764.79 mLCH_4/gVS and a synergistic index of 3.26. Additionally, the 3D response surface plots showed important and shared interactions between HE, FLO, and KR whereby the predicted responses increased with increasing HE and KR fractions and decreased with increasing FLO fractions in the substrate mixtures. In the third phase of the study, the experimental cumulative methane yield from the optimum anaerobic co-digestion ratio, R9, was fitted to five kinetic models and the cone model had the best fit recording an R^2 value of 0.9909. Finally, the effects of coconut shell (CCN) and palm kernel shell (PKN) biochar dosages (3 g, 6 g and 10 g) on the anaerobic co-digestion of HE, FLO and KR were investigated using batch mesophilic experiments. The results showed differences in the peak occurrence times and methane yields with the biochar-amended treatments peaking earlier than the control treatment. Further, methane yield (456.25 mLCH_4/gVS) increased when 3g of CCN biochar was used, depicting a 23.31 % increase compared to the control (SM=370.03 mLCH_4/gVS). However, too high CCN biochar dosages of 6 g and 10 g restricted methane production due to a potential stress on the anaerobic digestion process brought on by the accumulation of H_2 competitors of methanogens that might have cloned onto excess biochar and weakened its DIET benefit for methanogenesis. Furthermore, the methane yield was 368.69 mLCH_4/gVS, similar to that of the control (SM) when 3 g of PKN shell biochar was added to the mixture of feedstocks. Nonetheless, methane yield increased by 10.83 % when the dosage of PKN shell biochar used was increased to 6 g. Conversely, PKN10g observed a decrease in cumulative methane yield. The observed results indicate that microbial activity and kinetics could possibly be restricted by excessive dosage of biochar. This could be attributed to the possible adsorption of volatile fatty acids (VFAs) since the adsorption mechanism of biochar is not selective. Hence, higher amounts of added biochar may not necessarily correspond to higher digestion efficiency.

Contents

Declaration i

Dedication ii

Abstract iii

Table of Content iv

List of Tables xiii

List of Figures xv

1 Introduction 1

1.1 Background 1

1.2 Problem Statement 5

1.3 Research Gaps 6

1.4 Hypotheses 8

1.5 Objectives 8

1.6 Research Questions 9

1.7 Rationale and Justification of Study 9

1.8 Theoretical and Conceptual Frameworks 10

1.8.1 Theoretical Framework 10

1.8.2 Conceptual Framework 10

1.9 Organization of Thesis 13

2 Literature Review 14

2.1 Solid Waste Generation and Composition in Ghana 14

2.2 Cooking Energy Sources in Ghana 17

2.3 Biogas in Ghana 18

2.3.1 Origin of Biogas in Ghana 18

2.3.2 Household Biogas Systems 20

2.3.2.1 Types and Sizes of Biogas Digesters 20

2.3.3 Challenges with Household Biogas-Setup 21

2.3.4 Measures to Promote Household Biogas Adoption 22
2.4 Anaerobic Digestion and Biogas 23
2.4.1 Hydrolysis 23
2.4.2 Acidogenesis 25
2.4.3 Acetogenesis 26
2.4.4 Methanogenesis 26
2.5 Feedstock Types and Characteristics 27
2.5.1 Carbohydrate-Rich Substrates 28
2.5.2 Protein-Rich Substrates 28
2.5.3 Fat-Rich Substrates 29
2.6 Pretreatment 29
2.6.1 Physical Pretreatment 30
2.6.2 Thermal Pretreatment 30
2.6.3 Mechanical Pretreatment 31
2.6.4 Chemical Pretreatment 31
2.6.5 Biological Pretreatment 32
2.6.6 Microwave Pretreatment 32
2.7 Factors Affecting the AD Process 32
2.7.1 Total Solids (TS) 32
2.7.2 Volatile Solids (VS) 34
2.7.3 Chemical Oxygen Demand and Biological Oxygen Demand . 34
2.7.4 Moisture Content 35
2.7.5 Particle Size 36
2.7.6 Seeding 36
2.7.7 pH 37
2.7.8 Temperature 37
2.7.9 Mixing / Agitation 38
2.7.10 Carbon-Nitrogen Ratio (C/N) 39
2.7.11 Chemical Oxygen Demand-Nitrogen Ratio (COD/N) 39
2.7.12 Organic Loading Rate (OLR) 40
2.7.13 Hydraulic Retention Time (HRT) 40
2.7.14 Volatile Fatty Acids (VFAs) 41
2.7.15 Alkalinity 42

2.7.16 VFA/Alkalinity Ratio 43
2.7.17 Ammonia and Ammonium 43
2.8 Anaerobic Reactors 44
2.9 Biochemical Methane Potential 45
2.9.1 Compulsory Elements for the Validation of BMP Test Results 47
2.9.2 Criteria for Test Results Rejection 48
2.10 Mono and Co-digestion 48
2.10.1 Inoculum to Substrate Ratio 52
2.10.2 Human Excreta 55
2.10.3 Food Waste 55
2.11 Role of Additives in Anaerobic Co-Digestion 57
2.11.1 Biochar 58
2.11.2 Definition and Origin 58
2.11.3 Biochar Production and Characterization 59
2.11.3.1 Surface Area (SA) 61
2.11.3.2 Porosity 62
2.11.3.3 Cation Exchange Capacity (CEC) 63
2.11.3.4 Electrical Conductivity (EC) 63
2.11.3.5 Aromacity 63
2.11.4 Impact of Biochar on the Anaerobic Digestion Stages 63
2.11.4.1 Impact of Biochar on Hydrolysis 63
2.11.4.2 Impact of Biochar on Acidogenesis and Acetogenesis 64
2.11.4.3 Impact of Biochar on Methanogenesis 65
2.11.5 Biochar Adsorption Mechanism 66
2.11.5.1 Adsorption of inhibitors 67
2.11.6 Indirect and Direct Interspecies Electron Transfers (IIET and DIET) 68
2.11.7 Buffering Capacity 69
2.11.8 Immobilization of Microbial Cells 69
2.11.9 Influence of Different Types, Sizes and Quantities of Biochar on AD Process 70
2.11.10 Negative View of Biochar 73
2.12 Response Surface Methodology 73

2.12.1 Mixture Design 74
2.13 Kinetic Models 75
2.13.1 Modified Gompertz Model 75
2.13.2 Logistic Function Model 76
2.13.3 Cone Model 76
2.13.4 Fitzhugh Model 77
2.13.5 Monod Model 77

3 Materials and Methods **78**
3.1 Introduction 78
3.2 Feedstock Collection and Preparation 78
3.2.1 Human Excreta (HE) 78
3.2.2 Food Leftovers (FLO) and Kitchen Residue (KR) 79
3.3 Feedstock Sampling 82
3.4 Cow Dung (CD) Collection and Inoculum Preparation 82
3.4.1 Inoculum Preparation 83
3.5 Feedstocks and Inoculum Characterization 85
3.5.1 Proximate Analysis 85
3.5.1.1 Total Solids (TS) 85
3.5.1.2 Volatile Solids (VS) 86
3.5.1.3 Moisture Content (MC) 87
3.5.1.4 Ash Content (AC) 87
3.5.2 Ultimate Analysis 87
3.5.2.1 Determination of Total Nitrogen by Kjeldahl Digestion Method 88
3.5.2.2 Determination of Hydrogen by Titrimetric Method . 89
3.5.2.3 Determination of Total Sulphur by Spectrophotometer Method 89
3.5.2.4 Determination of Organic Carbon by Walkley – Black Wet Oxidation Method 90
3.5.2.5 C/N Ratio 90
3.5.3 Chemical Analysis 91
3.5.3.1 pH 91

3.5.3.2 Alkalinity 91
3.5.3.3 Chemical Oxygen Demand (COD) 92
3.5.3.4 Volatile Fatty Acids (VFA) 93
3.5.4 Compositional Analysis 94
3.5.4.1 Crude Fat Content 94
3.5.4.2 Crude Protein Content 95
3.5.4.3 Crude Fibre Content 95
3.5.5 Mineral Analysis 95
3.6 Additive Sampling, Preparation and Characterization 96
3.6.1 Sampling 96
3.6.2 Biochar Preparation 96
3.6.3 Biochar Characterization 97
3.6.3.1 Fourier Transform Infrared (FTIR) Analysis 97
3.6.3.2 X-Ray Diffraction (XRD) Analysis 97
3.6.3.3 X-Ray Fluorescence (XRF) Analysis 98
3.6.3.4 Brunauer-Emmett-Teller (BET) Analysis 98
3.7 Theoretical BioMethane Potential (BMP_{TH}) 98
3.7.1 Biodegradability (BD) 99
3.8 Experimental Setup 99
3.9 Biogas Collection and Measurements 101
3.9.1 Gas Composition Measurements 103
3.9.1.1 Normalizing Gas Readings 104
3.10 Synergy 105
3.11 Statistical Analysis 105
3.12 Kinetic Modeling 105
3.12.1 Modified Gompertz Model 105
3.12.2 Logistic Function Model 106
3.12.3 Cone Model 106
3.12.4 Fitzhugh Model 106
3.12.5 Monod Model 107
3.12.6 Model Evaluation 107
3.13 Response Surface Method (RSM) 108

4 Physico-Chemical Characterization of Selected Feedstocks as Co-Substrates in Household Biogas Generation in Ghana **109**

4.1 Abstract . . . 109
4.2 Introduction . . . 109
4.3 Materials and Method . . . 112
4.3.1 Biomass Collection and Preparation . . . 112
4.3.2 Proximate Analyses . . . 114
4.3.3 Ultimate Analysis . . . 114
4.3.3.1 C/N Ratio . . . 114
4.3.4 Chemical Analysis . . . 115
4.3.5 Compositional Analysis . . . 115
4.3.5.1 Crude Fat Content . . . 115
4.3.5.2 Crude Protein Content . . . 115
4.3.5.3 Crude Fibre Content . . . 115
4.3.6 Mineral Analysis . . . 116
4.3.7 Theoretical BioMethane Potential (BMP_{TH}) . . . 116
4.4 Results and Discussion . . . 117
4.4.1 Physico-Chemical Properties of Feedstocks . . . 117
4.4.1.1 Variability of Organic Matter in Feedstocks . . . 117
4.4.1.2 Variability in Chemical Composition of Feedstocks 120
4.4.1.3 Variability in Mineral Composition of Feedstocks . 123
4.4.2 Theoretical BioMethane Potential (BMP_{TH}) and Biogas Potential (BGP_{TH}) . . . 129
4.4.3 Potential, Challenges and Justification of Human Excreta as Main Substrate for Anaerobic Co-digestion in Households . . 131
4.4.4 Potential, Challenges and Justification of FLO and KR as Co-Substrate for Anaerobic Co-digestion in Households . . . 132
4.4.5 Potential, Challenges and Justification of Cow Dung as Inoculum Source for Anaerobic Co-digestion in Households . . . 132
4.5 Conclusion . . . 133

5 Anaerobic Co-Digestion of Human Excreta, Food Leftovers and Kitchen Residue: Ternary Mixture Design, Synergistic Effects and RSM Approach **135**

5.1 Abstract . . . 135
5.2 Introduction . . . 136
5.3 Materials and Method . . . 139
5.3.1 Feedstock and Inoculum Collection and Preparation . . . 139
5.3.2 Feedstock Characterization . . . 140
5.3.3 Formulation of Substrate-Mix using Mixture Design . . . 141
5.3.4 Theoretical BioMethane Potential (BMP_{TH}) . . . 143
5.3.5 Biochemical Methane Potential Test . . . 143
5.3.5.1 Biodegradability (BD) . . . 144
5.3.6 Synergy . . . 144
5.3.7 RSM Modelling . . . 144
5.3.8 Statistical Analysis . . . 145
5.4 Results and Discussion . . . 145
5.4.1 Feedstock Characteristics . . . 145
5.4.2 Daily Biogas Yields . . . 146
5.4.3 Daily and Cumulative Methane Yields . . . 148
5.4.4 Effects of VS reduction, CN Ratio, pH, Alkalinity and VFA on Biogas and Methane Yields . . . 152
5.4.5 Effect of Native Trace Elements in Substrate Mixtures on Methane Yield . . . 155
5.4.6 Synergistic Effects of Co- and Tri-digestion . . . 158
5.4.7 Modelling of Responses . . . 160
5.4.8 Response Surface Plots . . . 165
5.5 Conclusion . . . 167

6 Kinetics Study of Methane Yield from Anaerobic Co-Digestion of Human Excreta, Food Leftovers and Kitchen Residue 169

6.1 Abstract . . . 169
6.2 Introduction . . . 169
6.3 Materials and Method . . . 172
6.3.1 Feedstock and Inoculum Collection and Preparation . . . 172
6.3.2 Feedstock Characterization . . . 173
6.3.3 Biochemical Methane Potential Test . . . 173

6.3.4 Kinetics of Methane Production 174
6.3.4.1 Modified Gompertz Model 174
6.3.4.2 Logistic Function Model 174
6.3.4.3 Cone Model 175
6.3.4.4 Fitzhugh Model 175
6.3.4.5 Monod Model 175
6.3.5 Model Evaluation 175
6.4 Results and Discussion 177
6.4.1 Feedstock Characteristics 177
6.4.2 Kinetic Modeling 177
6.4.2.1 Fitzhugh Model 179
6.4.2.2 Logistic Model 180
6.4.2.3 Modified Gompertz model 181
6.4.2.4 Monod Model 183
6.4.2.5 Cone Model 183
6.5 Conclusion 185

7 Optimization of Batch Anaerobic Co-Digestion of Human Excreta, Food Leftovers and Kitchen Residue using Biochar Additives. 186

7.1 Abstract 186
7.2 Introduction 187
7.3 Materials and Methods 188
7.3.1 Origin and Properties of Feedstock and Inoculum 188
7.3.2 Feedstock and Inoculum Characterization 189
7.3.3 Biochar Preparation 190
7.3.4 Biochar Characterization 191
7.3.5 Theoretical BioMethane Potential (BMP_{TH}) 192
7.3.6 Anaerobic Digestion Set-up and Biogas Sampling 192
7.3.7 Methane-Production Determination 193
7.3.8 Biodegradability (BD) 194
7.3.9 Statistical Analysis 194
7.4 Results and Discussion 194
7.4.1 Feedstock Characteristics 194

7.4.2 Biochar Characteristics 195
7.4.2.1 X-ray fluorescence (XRF) 195
7.4.2.2 Brunauer, Emmett and Teller (BET) 198
7.4.2.3 Fourier Transform Infrared (FTIR) Analysis 199
7.4.2.4 X-ray Diffraction (XRD) 201
7.4.3 Performances of Anaerobic Co-Digestion with Biochar Samples 203
7.4.3.1 Effects of Biochar Types on Methane Yield 203
7.4.3.2 Effects of Biochar Dosage on Methane Yield 206
7.4.4 Effect of CN Ratio, pH, Alkalinity and VFAs on Methane Yield 209
7.5 Conclusion 213

8 Conclusions and Recommendations **214**
8.1 Conclusions 214
8.1.1 Overall Conclusions 220
8.2 Contribution to Knowledge 222
8.3 Implication for Further Studies 223
8.4 Recommendations 224

Bibliography **224**

List of Tables

2.1 Literature Reported TS values for Food waste, Cow dung and Human Excreta 33
2.2 Literature Reported VS values for Food waste, Cow dung and Human Excreta (*VS as % of TS) 34
2.3 Reported Moisture Content values for Food waste, Cow dung and Human excreta 36
2.4 Co-digestion Conditions and Results for Human Excreta and or Food Waste in Previous Studies (NR means Not Reported) 51
2.5 Product yield of biomass combustion on a dry basis. ((Li et al., 2020b; Masebinu et al., 2019; Luz et al., 2018)) 59

3.1 Percentage composition of FLO and KR based on wet weight 81

4.1 Percentage composition of FLO and KR based on wet weight 113
4.2 Physical, Chemical and Compositional Characteristics of HE, FLO, KR and CD (mean (standard deviation); n = 3) 118
4.3 Mineral Characteristics of HE, FLO, KR and CD (mean (standard deviation); n = 3) 126
4.4 Reported stimulatory and inhibitory concentrations of metals on anaerobic biomass (expanded from Romero-Güiza et al. (2016)) compared with values from this study 128
4.5 Theoretical Biogas and Bio-Methane Potential of HE, FLO, KR, and CD 130

5.1 Experimental Conditions for the BMP Tests. 142
5.2 Physicochemical Characteristics of Substrates [mean (standard deviation)] 145
5.3 Biogas and Methane Yields,VFA, pH, Alkalinity and VS Reduction for Different Mix Ratios of HE, FLO and KR 153
5.4 Concentration of Trace Elements in Substrate Mix 155
5.5 ANOVA Results for the RSM Models of Biogas Yield, Methane Yield and Synergy 163

5.6 RSM Performance Assessment for Biogas Yield, Methane Yield, and Synergy 164

6.1 Physicochemical Characteristics of Substrates (mean (standard deviation)) 177
6.2 Parameters for Kinetic Models 178
6.3 ANOVA Results for RSM Experiment 178

7.1 Batch experimental conditions with different biochar types. 193
7.2 Physicochemical Characteristics of Feedstocks (mean (standard deviation); n=3) 195
7.3 Percentage Chemical Composition of CCN and PKN from XRF Analyses 197
7.4 Biogas and Methane Yields,VFA, pH, Alkalinity and VS Reduction for Biochar Amended Treatments and Control(mean (standard deviation); n=3) 210

List of Figures

1.1 Theoretical Framework for Anaerobic Co-digestion of Human Excreta, Food Waste and Biochar 11
1.2 Conceptual Framework for Anaerobic Co-digestion of Human Excreta, Food Waste and Biochar 12

2.1 Solid Waste Composition in Ghana (Miezah et al.,2015) 15
2.2 Household Sources of Cooking Fuel (KITE 2008) 17
2.3 Anaerobic Digestion Stages) 24
2.4 Sources of Feedstock for Anaerobic Digestion 27

3.1 Freshly Collected and Homogenised Human Excreta 79
3.2 Sample Food Leftovers (a) Raw (b) Homogenized 80
3.3 Samples of Kitchen Residue (a) Cassava Peels, (b) Yam and Cocoyam Peels, (c) Pineapple, Avocado and Orange Peels, (d) Plantain and Banana Peels (e) Pawpaw, Watermelon and Mango Peels (d) Lettuce, Cucumber, Pepper, Tomato, Carrot, Garden Eggs and Onion Leftovers . 80
3.4 The coning and quartering method (Alakangas, 2015) 82
3.5 Freshly collected cow dung (CD) 83
3.6 Step by step procedure for inoculum preparation.(a)Freshly collected cow dung (b)Homogenised cow dung (c)Test for appropriate mix ratio (d)One part of homogenised cowdung mixed with two parts of water (e)Test for pH of slurry (f)Bottled slurry (g)Bottles placed in an incubator and connected to gas bags (h)Gas composition measurement with Biogas 5000 (i) Gas volume measurement using water displacement method. 84
3.7 (a)Electric weighing balance and (b) oven used for TS determination . 86
3.8 Furnace used for VS determination 87
3.9 pH determination using a digital pH meter 91
3.10 Potentiometric titration for alkalinity determination 92
3.11 COD determination using (a) COD HR+ vials (b) COD Heating Reactor and (c) DR 3900 Spectrometer 93

3.12 VFA determination (a)Two potentiometric titration setups for HCl and NaOH and (b) Hot plate for heating sample titrated with HCl 94
3.13 (a) Crushed coconut shells (b) Crushed oil palm kennel shells 96
3.14 (a) Coconut shell biochar (b) Oil palm kennel shell biochar 97
3.15 Schematic Batch Test Setup (A)Feedstocks used (B)Slurry from the mixture of feedstocks (C)Bottles filled with slurry and put in an incubator (D)Gas bags for the collection of gas generated 100
3.16 Bottles filled with a mix of feedstock and inoculum just before the start of the experiment 100
3.17 Bottles placed in an incubator and connected with tubes leading to the gasbags 101
3.18 Biogas collected in gas bag 102
3.19 Gas volume measurement using water displacement method 103
3.20 Gas Composition Analyser, Biogas 5000 104

4.1 (a) pH, (b) Alkalinity and (c) COD levels in HE, FLO, KR and CD . . 121
4.2 Phosphorus, potassium, calcium, magnesium and sodium contents in HE, FLO, KR and CD 124

5.1 Homogenized (a) Human Excreta (b) Inoculum (c) Food Leftovers (d) Kitchen Residue 140
5.2 Effects of different mixing ratios on daily biogas yields: (a) mono-digestion, (b) co-digestion, and (c) tri-digestion (mean±S.D; n=3) 90% of measurements have RSD of less than 10% 147
5.3 Effects of different mixing ratios on daily methane yields: (a) mono-digestion, (b) co-digestion, and (c) tri-digestion (mean±S.D; n=3) 90 % of measurements have RSD of less than 5 % 150
5.4 Effects of different mixing ratios on cumulative methane yields: (a) mono-digestion, (b) co-digestion, and (c) tri-digestion (mean±S.D; n=3) 90 % of measurements have RSD of less than 5 % 151
5.5 Effects of zinc concentrations on methane yields 156
5.6 Effects of nickel concentrations on methane yields 157

5.7 Synergy index of substrate mix at different HE/FLO/KR ratios. SI > 1 indicates synergistic effect, and SI < 1 indicates antagonistic effect (mean±S.D; n=3) 158
5.8 Effect of alkalinity on synergy index of substrate mixtures 159
5.9 Parity plots of experimental and predicted (a)biogas yield, (b) methane yield and (c) synergy as a function of the mixture components 161
5.10 (a)Three-dimensional and (b)Two-dimensional response surface plots depicting the effect of the substrate mixing ratio on biogas yield. Contour colors represent the levels of model response: blue for low and red for high responses. 165
5.11 (a)Three-dimensional and (b)Two-dimensional response surface plots depicting the effect of the substrate mixing ratio on methane yield. Contour colors represent the levels of model response: blue for low and red for high responses. 166
5.12 (a)Three-dimensional and (b)Two-dimensional response surface plots depicting the effect of the substrate mixing ratio on synergy index. Contour colors represent the levels of model response: blue for low and red for high responses. 166

6.1 Comparison of measured and projected biomethane yield (a) time trajectory for fitzhugh model (b) parity plot for the fitzhugh model 179
6.2 Comparison of measured and projected biomethane yield (a) time trajectory for the logistic model (b) parity plot for the logistic model . . 181
6.3 Comparison of measured and projected biomethane yield (a) time trajectory for modified Gompertz model (b) parity plot for the modified Gompertz model 182
6.4 Comparison of measured and projected biomethane yield (a) time trajectory for the monod model (b) parity plot for the monod model . . . 183
6.5 Comparison of measured and projected biomethane yield (a) time trajectory for the cone model (b) parity plot for the cone model 184

7.1 (a) Washed and crushed coconut shell (b) Washed and crushed oil palm kennel shell 190
7.2 (a) Coconut shell biochar (b) Oil palm kennel shell biochar 190

7.3 FTIR Spectra of CCN and PKN Biochar Samples 200
7.4 XRD Spectra of CCN and PKN Biochar Samples 201
7.5 Methane yield of CCN and PKN biochar samples at different dosages; (a) Daily methane production and (b) Cumulative methane production (values are presented as mean ± SD with n=3) 204
7.6 Methane yield of CCN samples at different dosages; (a) Daily methane production and (b) Cumulative methane production (values are presented as mean ± SD with n=3) 206
7.7 Methane yield of PKN samples at different dosages; (a) Daily methane production and (b) Cumulative methane production (values are presented as mean ± SD with n=3) 208
7.8 Initial and Final VFA Levels in Anaerobic Co-digestion Treatments . 210
7.9 Initial and Final Alkalinity Levels in Anaerobic Co-digestion Treatments 212

List of Abbreviations

HE Human Excreta

FLO Food Leftovers

KR Kitchen Residue

CD Cow Dung

AD Anaerobic Digestion

SI Synergy Index

VFA Volatile Fatty Acids

BMP Biochemical Methane Potential

SM Substrate Mixture

ISR Inoculum to Substrate Ratio

COD Chemical Oxygen Demand

TS Total Solids

VS Volatile Solids

C/N Carbon to Nitrogen Ratio

LPG Liquified Petroleum Gas

PKN Palm Kernel Nut Shell

CCN Coconut Shell

OLR Organic Loading Rate

HRT Hydraulic Retention Time

LCFA Long Chain Fatty Acids

Acknowledgment

I will first and foremost appreciate God for His loving kindness towards my life. I am also very grateful to my supervisors, Prof. S. Oduro-Kwarteng, Prof. Richard Arthur and Dr. Martina Francisca Baidoo for their immense support towards the commencement and completion of this thesis. My sincere appreciation goes to Prof. David Dotse Wemegah for his support during the entire PhD journey. I really appreciate you. To all laboratory managers and assistants especially, Ralph, thank you very much for the sleepless nights during the experimental data collection. To RWESCK-Ghana, I say a very big thank you for sponsoring my education. I wish to thank my parents for being there for me during the difficult times in this work. To my siblings George, Jeffery and Kwaku Osei-Wusu, thank you for always having my back.

CHAPTER 1

Introduction

1.1 Background

Large amounts of organic food waste and human excreta are generated daily in various Ghanaian households. The exponential rise in the production of these human-generated wastes could be attributed to increased population density, urbanization, and economic growth (Singh et al., 2021a; Kim et al., 2019b). The World Bank has reported a worldwide average daily per capita municipal solid waste generation of 0.74 kg, amounting to 2.01 billion tons of waste in 2016 (Ibikunle et al., 2019). Also, in Ghana, the waste generation rate reported by Miezah et al. (2015) is 0.47 kg/person/day, which translates into 12,710 tons of waste per day. Hence sustainable management of large quantities of waste is becoming an increasingly challenging task.

On the other hand, energy is an essential component of modern society and one of the most critical indicators of socioeconomic development. Over the years, fossil fuels have been the primary source of carbon-intensive energy supply (Kelebe et al., 2017). However, many countries are concerned about energy security because carbon-intensive energy systems rely on a finite supply of fossil fuels that are becoming more difficult and expensive to extract (Kelebe et al., 2017). Further, reliance on fossil energy sources is increasingly becoming unsustainable due to ecological and environmental challenges (Walekhwa et al., 2009).

According to Surendra et al. (2014), wood fuels, charcoal and other non-woody biomasses are also used in most households to meet energy needs for cooking. The global contribution of biomass to total energy consumption is 75–90 % (Sharma et al., 2015), with 40 % of the global population traditionally using wood biomass to meet their energy needs (O'Shaughnessy et al., 2014). In some sub-Saharan African countries, biomass utilization for cooking accounts for more than 90 % of total energy consumption (Shane et al., 2017). The increasing reliance on these woody biomasses as household energy sources has implications on the environment, human health, and food insecurity (Ghimire, 2013; Lam et al., 2011).

Mensah et al. (2016) assert that there is a high degree of inter-fuel substitution between liquified petroleum gas (LPG) and biomass-based energy types such as charcoal. This is often due to price shocks and, more importantly, erratic shortages in the supply of LPG in the Ghanaian market. In addition, Amigun et al. (2012) argue that the fuel substitution away from biomass is less likely due to low disposable incomes in urban and rural populations. As a result, there is a need to explore and exploit eco-friendly renewable energy sources and relieve households of monthly LPG purchases.

Anaerobic digestion (AD) has therefore been regarded as an appealing renewable technology for waste treatment because of its ability to convert organic matter to biogas and help alleviate energy and environmental challenges (Kim et al., 2019b). Biogas typically contains 50–70 % methane, 35–50 % carbon dioxide (Coimbra-Araújo et al., 2014; Kabir et al., 2013), and trace gases such as hydrogen sulphide depending on the type of feedstock used. For 60 % methane content, biogas has a calorific value of about 21–24 MJ/m^3 or 6 kWh/m^3 (Khan et al., 2014; Ghimire, 2013). Besides, the nitrogen, phosphorus, and potassium-rich digestate from the anaerobic digestion process could be used as fertiliser instead of the mineralised ones due to the better short-term fertilisation effect and lower pathogen content when well treated (Horváth et al., 2016; Weiland, 2010; Ward et al., 2008).

Contrary to other types of renewable energy, biogas production systems are relatively simple and can be operated on a small or large scale in urban and rural areas (Luostarinen et al., 2011). As a result, the biogas industry has been identified as being uniquely positioned to assist in the achievement of more than nine (9) of the Sustainable Development Goals (SDGs)–possibly more than any other sector (Ajieh et al., 2021). Apart from having access to clean and affordable energy, (Ezemonye et al., 2018), the issues of waste management play a unique role in facilitating the achievement of SDGs 3(good health and well-being), 6(clean water and sanitation), and 13(climate action).

Since the early 1970s, biogas distribution and use have been critical in the developing world (Shane et al., 2017). Nonetheless, biogas technology adoption in sub-

Saharan Africa (SSA) is low (Kelebe et al., 2017; Ni and Nyns, 1996). According to a study conducted in twenty-one SSA countries on the level of biogas technology adoption, the number of small and medium-sized (up to 100 m^3) biogas producing units in these countries ranged from a few in Nigeria, Uganda, and Zambia to a few more in Egypt, Ethiopia, Ghana, Cote d'Ivoire, Morocco, Rwanda, Senegal, South Africa, and Swaziland (Mshandete and Parawira, 2009). Kenya and Tanzania, however, had relatively increased numbers of over 500 and over 1000, respectively (Mshandete and Parawira, 2009). The adoption of biogas technology has been hampered by the lack of policy promoting biogas energy usage, lack of skills, rigid customs and traditions, and a lack of research and development (Ortiz et al., 2017; Chen et al., 2017; Roopnarain and Adeleke, 2017).

Furthermore, the high construction costs of some digester designs have contributed to the limited use of biogas energy in most African households (Amigun et al., 2012). According to Mohammed et al. (2017), biogas technology is characterised by high initial investment costs, typically resulting in non-monetary savings with less capital investment recovery. Also, Antwi et al. (2010) contend that renewable energy resources are generally more expensive to produce than conventional sources. Contrary to many other renewable energy technologies, almost all expenses for constructing a biogas system must be financed upfront, with meagre operational and maintenance costs.

Regardless, it is estimated that purchasing LPG over some time exceeds the cost of building and operating a biogas system over the same period, considering both monetary and environmental costs. The World Health Organization (WHO) has published guidelines for performing cost-benefit analyses on household biogas plants (Hutton et al., 2006). Meyers and Lorimor (2003) estimated an 11.4 % return on construction investment for two biogas digesters depending on the sizes and availability of local material. In contrast, Shane et al. (2017) and Mohammed et al. (2017) reported payback periods of 1.3 and 3 to 5 years (less than half the service life), respectively. The study further indicated that biogas used solely for cooking was the most viable.

Some households in Ghana, despite the initial cost, have taken the risk of investing in the biogas technology. Unfortunately, poor digester design and construction, as well as incorrect operation and lack of maintenance by users, have resulted in digesters producing little or no gas at all. According to Osei-Marfo et al. (2018), the needs of most biogas users have not been fully met, so they are only partially satisfied with the outcome of the technology. The lack of adequately trained operators and a lack of technical knowledge continue to impact the rate of biogas adoption in Africa (Parawira, 2009). According to Mengistu et al. (2016), people appear to be very concerned about whether their biogas-user neighbours, friends, and relatives have their digesters operating properly and producing enough gas before investing. This demonstrates that technical challenges limit the spread of biogas technology in Ghana.

To overcome the technical challenges that affect biogas technology, rendering it inoperable or producing less biogas, an integrated system that co-digests household waste such as human excreta (HE), food leftovers (FLO) and kitchen residue (KR) is considered in this study. The wastes chosen for this study have been selected because they are readily available in every household and may complement one another. Moreover, the feedstocks have been reported to be high in readily biodegradable organic matter and thus decomposes quickly. In addition, their high organic content and energy density make them appealing as feedstocks for biogas production (Kiran et al., 2014; Rajagopal et al., 2013). The assumption is that by combining these feedstocks, waste generated in households can be effectively managed while also producing energy for cooking purposes.

In this study, key techniques for enhanced biogas optimisation, such as co-digestion and the use of additives, are investigated. Co-digestion effects have in previous studies been evaluated from volatile solids (VS) removal rate, chemical oxygen demand (COD) removal rate, methane production and synergy index (Xie et al., 2017a). According to Shah et al. (2015), co-digestion dilutes the inhibitory effects of feedstocks, improves process stability, balances micro and macronutrients, increases organic loading with consequent higher methane yields per unit of digester volume, diversifies and synergizes the microbial communities that play a pivotal role in the methanogenesis.

1.2 Problem Statement

Household waste management and energy supply are major problems faced by most Ghanaian homes. In the case of the massive amounts of waste produced, landfilling, which has a variety of negative consequences has been the most common method of disposal. The release of greenhouse gases into the atmosphere and the seepage of leachate into soil and groundwater are two of the most prominent. Also, the country is heavily reliant on the use of fossil fuels, which are mostly in short supply. Even in their availability, fossil fuels have become more expensive, making most households unable to rely on them. The use of biogas produced from organic waste could be a solution.

Despite biogas being environmentally friendly, the digestion process of these organic materials is usually characterised by low methane yield due to some process instabilities (Tufaner and Avşar, 2016; Bo and Pin-Jing, 2014; Chen et al., 2008). Different issues, such as imbalanced C/N ratio, biodegradability, nutrient levels, and the dynamics of feedstock microorganisms, may limit process efficiency and severely inhibit methanogenesis reactions (Holliger et al., 2016). These constraints make the potential and widespread adoption of household biogas technology unappealing. Many previous studies have attempted to overcome the limitations of anaerobic mono-digestion (AD) of various feedstocks by co-digesting with other waste biomasses (Baek et al., 2020). However, anaerobic co-digestion can only produce more biogas if synergistic effects are created (Khoufi et al., 2015; Kafle et al., 2012).

Co-digestion can have antagonistic effects depending on the properties of the substrates, co-substrates and inoculum used (Xie et al., 2017b). The essential factors in this context are the type of substrate anaerobically co-digested and the selected mixing ratio (Rico et al., 2015). Nonetheless, there is considerable uncertainty regarding the evaluation of such synergistic effects (Zhou et al., 2021). Some studies have demonstrated that contradictory synergistic or antagonistic effects exist for the same raw materials and mixing ratios (Andriamanohiarisoamanana et al., 2018, 2017; Moset et al., 2017; Astals et al., 2015). Such variations have made determining whether or not a specific waste stream can produce synergistic effects when co-digested difficult and,

more importantly, determining their optimal mixing ratios (Zhou et al., 2021). As a result, a more accurate substrates and mixing ratio selection are critical for a successful co-digestion process (Kim et al., 2019a). In addition, there is the need to determine the minimal effective ratios of food waste in substrate/co-substrate mixture for the purposes of this study. This is because there is competition for food waste to be used as animal feed (Hussien et al., 2020).

1.3 Research Gaps

The increase in publications on co-digestion processes reflects its viability and suitability for improving biogas generation and environmental sustainability. However, optimising and enhancing methane generation from co-digestion systems still need more profound studies (Siddique and Wahid, 2018; Hagos et al., 2017). Feedstock characterisation remains a challenge in co-digestion systems due to the variability of feedstocks and the difference in methods and instruments utilized (Hagos et al., 2017). Furthermore, a thorough investigation of the factors influencing anaerobic co-digestion, the adjustment of operating parameters, and optimisation strategies remain elusive (Siddique and Wahid, 2018). Siddique and Wahid (2018) and Mata-Alvarez et al. (2014) assert that the environmental conditions of digesters and feedstocks used during co-digestion must be adjusted for designing universal digesters due to the imbalanced distribution of feedstocks, which impedes implementation of a scaled-up co-digestion technology (Hagos et al., 2017).

In addition, researchers from various countries have extensively studied the use of food waste for biogas production, mainly on a laboratory or pilot scale. A few studies have also been reported on the use of human excreta in anaerobic digestion systems. However, because of the variation in food waste and human excreta composition, there is a need to investigate using local food waste and human excreta (Wang, 2014). Moreover, previous researches on the co-digestion of food waste and human excreta have not provided detailed information on the effect of substrate mixing ratio and synergistic impact of co-digestion on anaerobic performance (Mata-Alvarez et al., 2014). Siddique and Wahid (2018) have reported that selecting an appropriate co-substrate

and mixing proportion is essential for the co-digestion process. This is because, improper choice of co-substrates, mixing ratios and operational states may lead to system imbalance and reduce methane generation (Siddique and Wahid, 2018).

Besides, Ma et al. (2019b) assert that different co-digested substrates and dosage ratios could significantly affect synergy during anaerobic co-digestion. As a result, Singh et al. (2021b) recommend further studies to determine the best feedstock mix ratio for optimum biogas yield. In addition, there is no reported document on the co-digestion of cooked food leftovers, kitchen residue (food preparation waste, fruit and vegetable waste) and human excreta in a mixture in the Ghanaian context. This study investigates the co-digestion of such a mixture because it includes almost all organic household waste generated.

Moreover, most studies have concluded that future research should focus on low-cost biogas enhancement for small and medium-sized households (Luo et al., 2020; Pellegrini et al., 2018; Heubeck et al., 2007). The use of additives is one such low-cost methods. However, an additive such as biochar is a complex material with variable properties that are dependent on different production parameters. The adsorbing efficiency of biochar is impacted by contact time, operating temperature, adsorbent and adsorbate dosages, particle size and pore distribution, surface chemistry, and pH (Hadi et al., 2015; Yargicoglu et al., 2015; Li et al., 2014). Nonetheless, Pan et al. (2019) recommend that studies aimed at improving AD performance efficiency focus on interactions between biochar properties and dosages.

Further, the use of additives in AD is not fully understood in practice. Due to significant differences in digestion substrates and AD operational procedures, many challenges are associated with using additives in AD systems. To address the various shortcomings, efforts must be made to improve the overall efficiency of the anaerobic digestion process in biogas plants to make this technology popular in various households (Sreekrishnan et al., 2004). Finally, coverage of the use of biochar additives in the co-digestion of human excreta and food waste has not been documented.

1.4 Hypotheses

This thesis proposes the use of human excreta and food waste as potential main substrate and co-substrate, respectively, in combination with biochar additives as a way to improve the anaerobic co-digestion process of household organic waste. The following hypotheses are proposed:

(i) Physico-chemical properties of the individual feedstocks may likely enable a more robust and stable co-digestion process.

(ii) Different co-digestion mixing ratios of substrate and co-substrate significantly impact the synergy and biogas production of the anaerobic digestion process. Finding the optimal mix ratio of human excreta and food waste will thus increase biogas production.

(iii) Different kinetic models may provide a different fit to experimental data.

(iv) Incorporating a carbon-based additive, such as biochar may aid in microbial immobilization and increase the buffer capacity of the co-digestion mixtures.

(v) The biogas and methane yields may vary depending on the type and dose of additive used. Finding the best mix of additive types and doses in the co-digestion mixture will boost biogas production.

1.5 Objectives

The main objective of the study is to enhance biogas recovery from the anaerobic co-digestion treatment of human excreta and food waste for household cooking purposes in Ghana. The specific objectives are :

(i) To identify and characterize potential feedstocks and inoculum for household biogas production in Ghana.

(ii) To investigate the optimal mixing ratios of human excreta, food leftovers and kitchen residues using RSM and BMP.

(iii) To determine the fitness of batch experimental data to kinetic models.

(iv) To determine the effect of different biochar types and doses on biogas yield.

1.6 Research Questions

(i) Does the physico-chemical properties of feedstocks lead to enhanced biogas and methane yields?

(ii) What optimum mixing ratios of human excreta, food leftovers and kitchen residue will give a positive synergy and high biogas and methane yields?

(iii) Which kinetic model will best fit the experimental data?

(iv) What biochar type, and dose can increase biogas and methane yields?

1.7 Rationale and Justification of Study

The low adoption of the biogas technology in Ghana seems not to portray the urgent need of the country to manage the enormous amounts of biodegradable waste generated and the energy crises, considering the favourable temperatures that could support the fermentation process (Mwirigi et al., 2014). This research is therefore engineered to build on the available knowledge and add value to the community and industry in the areas listed below:

Improvement of waste management: Using the anaerobic digestion system, waste is managed and treated well to produce biogas and other beneficial products. Also, Masebinu et al. (2019) have reported a 20 % volume reduction waste due to the diversion of the organic fractions of municipal solid waste from landfills compared to direct landfilling.

Environmental safety and climate change: This treatment reduces greenhouse gas (GHG) emissions by replacing fossil fuels and capturing methane from organic waste. Also, the odour and other unesthetic challenges from waste is reduced.

Energy: Availability of green energy and low consumption of fossil fuels.

Agricultural benefits: Use of digestate as bio-fertiliser.

Financial benefits: The provision of a sustainable system will be able to save households of the money used in purchasing LPG and the country the enormous amounts of money used in managing waste. Also, the in situ anaerobic digestion of household waste will lead to the reduction of operational cost for collection and transport of waste.

1.8 Theoretical and Conceptual Frameworks

1.8.1 Theoretical Framework

The fundamental theoretical approach to this study stems from a scientific and technological process of biochemically degrading organic waste via anaerobic digestion, as shown in Figure 1.1. Household waste (food waste and human excreta) and a carbon-based additive are used as feedstock. Physical and mechanical pretreatments are applied to the feedstock. The pretreated feedstock is then digested anaerobically to produce biogas.

1.8.2 Conceptual Framework

The conceptual approach to achieving the outlined objectives of this study is presented in Figure 1.2. The process begins with the preparation and characterisation of feedstock, inoculum and additives. The optimum mixing ratio is then determined for the substrate (human excreta) and co-substrate (food waste types). Furthermore, the interaction between the feedstocks is studied using a response surface model. Also, the experimental data are fitted to different kinetic models to determine the best fit. Finally, the optimum additive type, size and dose are determined in the quest to enhance biogas generation.

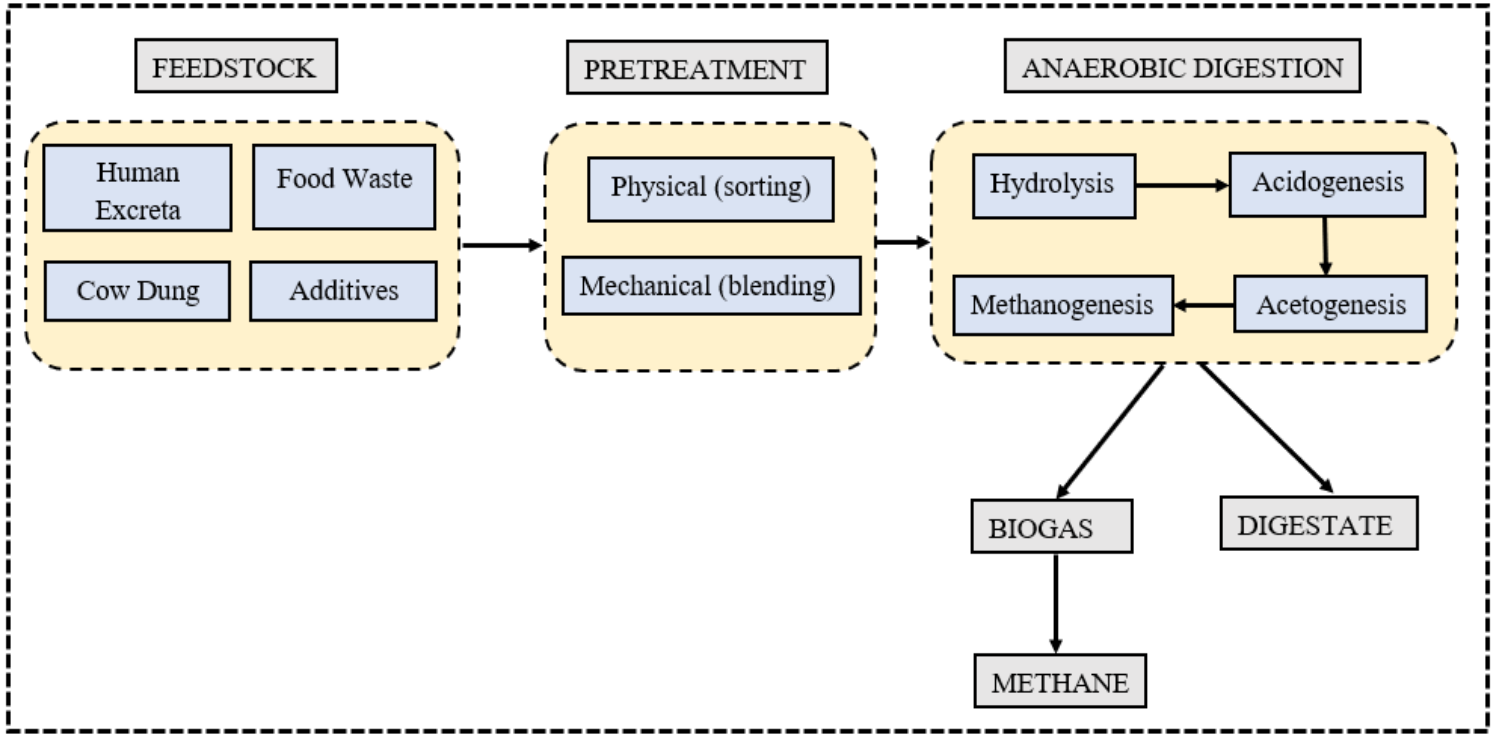

Figure 1.1: Theoretical Framework for Anaerobic Co-digestion of Human Excreta, Food Waste and Biochar

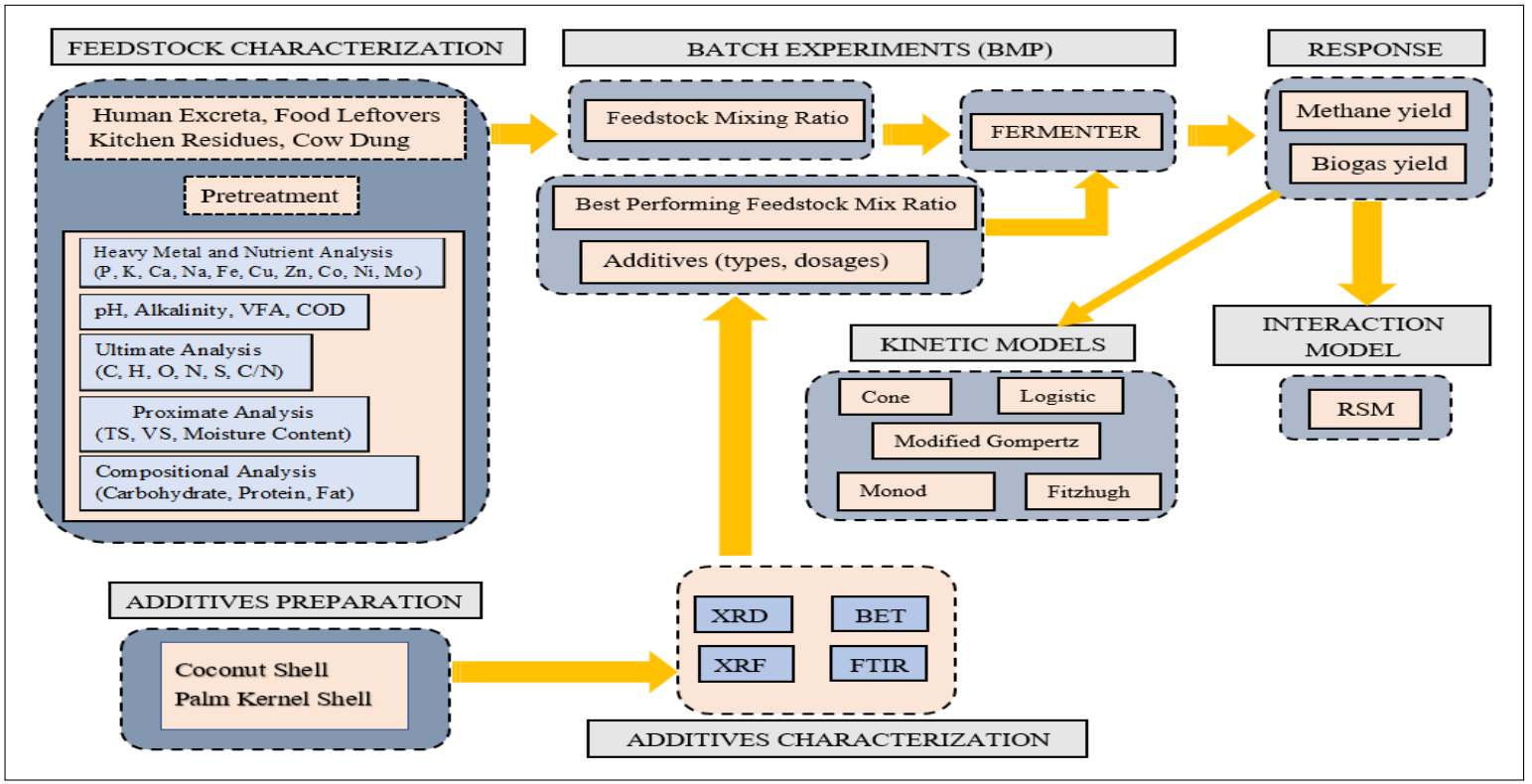

Figure 1.2: Conceptual Framework for Anaerobic Co-digestion of Human Excreta, Food Waste and Biochar

1.9 Organization of Thesis

This thesis is composed of eight chapters that adhere to the manuscript-based format. In the first chapter, an overview of the research background, gaps, and problem statement are provided. Reasons to conduct research on the selected topic are also provided. Finally, the objectives of the thesis, conceptual and theoretical frameworks are stated. This is continued with an extensive literature review in the second chapter. In chapter three, the materials and instruments used as well as the methods adhered to in this study are documented. Chapters four to seven contain a brief introduction, approach and methods, results and discussions for each of the specific objectives stated.

In chapter four, a detailed characterization of the feedstocks chosen for this study is presented. Given the aim of favouring synergy and optimising methane production, the interaction studies (using the response surface model and mixture design) between human excreta, food leftovers and kitchen residue are documented in chapter five. As kinetic models have become very essential, especially in aiding design, the experimental data are fitted to different kinetic models in chapter six. In chapter seven, the effects of different additives and doses are studied to identify the best performing. Finally, chapter eight presents general conclusions for the study and outlines some recommendations.

CHAPTER 2

Literature Review

2.1 Solid Waste Generation and Composition in Ghana

Effective waste management has proven to be a major challenge in Ghana, due to the lack of necessary waste management facilities and in some cases, technological know-how (Fei-Baffoe et al., 2014). According to Miezah et al. (2015), the waste generation rate in Ghana is 12,710 tons per day for a population of 27,043,093. This value is expected to have increased with the increase in population. Furthermore, Kemausuor et al. (2018) and Sakah et al. (2017) claim that cities with 600-800 tons of waste per day have a significant biogas generation potential. Also, specific waste generation rates in Ghana are 0.318 kg/person/day for biodegradable waste (organics and papers), 0.096 kg/person/day for non-biodegradable waste (metals, glass, textiles, leather, and rubbers), and 0.055 kg/person/day for miscellaneous (inert) waste (Miezah et al., 2015).

The recorded waste generation rates differ by geographical location, with the forest and coastal zones producing more waste than the savannah and northern zones. Also, the average waste generation rates by metropolises, municipalities, and districts are 0.63 kg/person/day, 0.40 kg/person/day, and 0.28 kg/person/day, respectively (Miezah et al., 2015). Additionally, Miezah et al. (2017) have reported 70 % to 80 % municipal solid waste generation per day by households with 50 % to 70 % biodegradable fraction. Although Ghana has several sanitation laws, their implementation and enforcement have not been realized (Ofori-Boateng et al., 2013). As a result, only about 44 % of the wastes generated in the various metropolises are collected, leaving a massive 56 % backlog (Abalo et al., 2018). Backlogs of waste are typically burned, buried, or disposed of in other inappropriate ways. From the 2010 housing and population census, 37.7 % of households were reported to be in the practice of disposing of waste in open places such as public dumps (GSS, 2010).

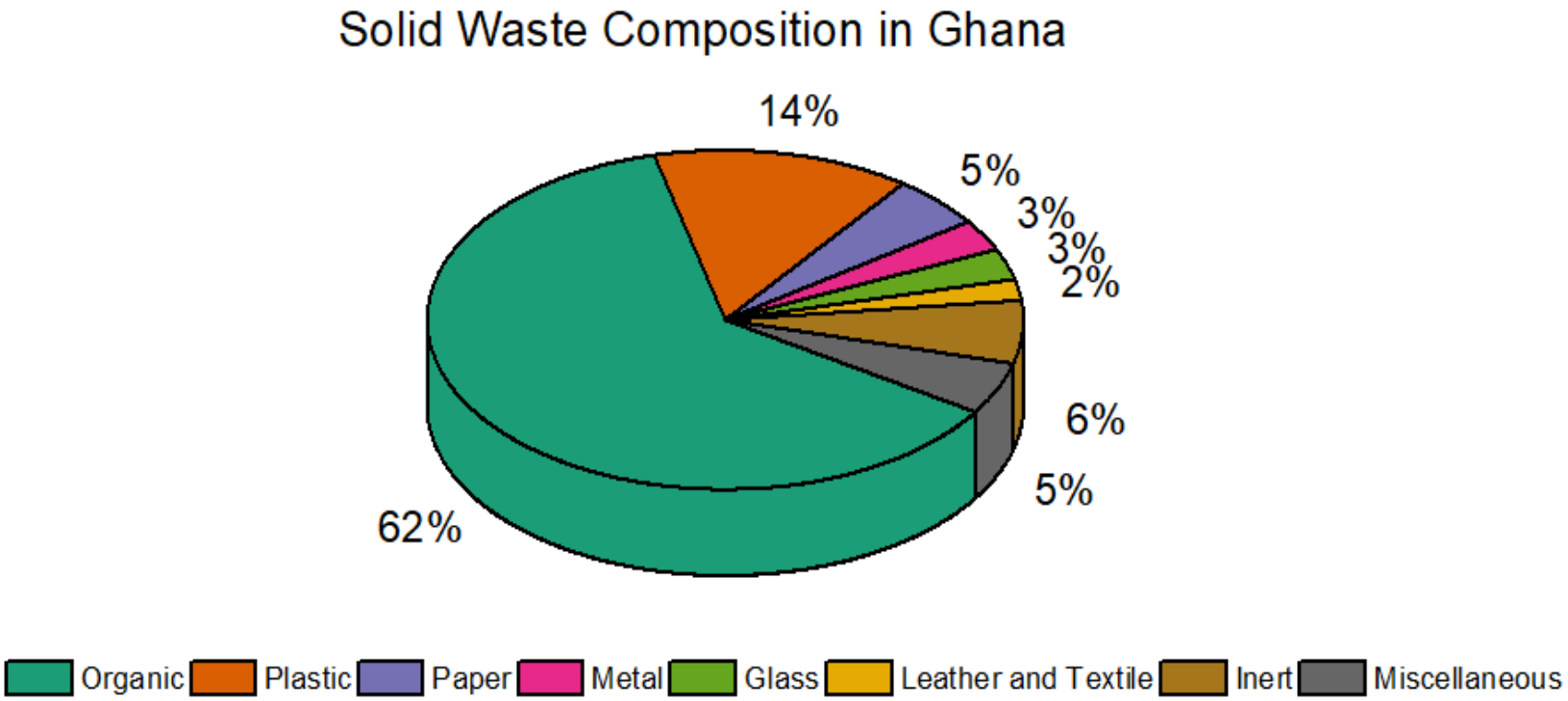

Figure 2.1: Solid Waste Composition in Ghana (Miezah et al.,2015)

Further, 23.8 % of households were documented to be using public waste containers, 10.7 %, burning their waste and 14.4 % having their waste collected (GSS, 2010). Until the Lavender Hill treatment center was built, human excreta was often mechanically or manually collected and discharged untreated on open ground, in drainage systems, water bodies, or even into the sea (Shih et al., 2017; Agyei et al., 2011; Kuffour et al., 2009). The data on waste composition clearly shows that organic fractions are the most abundant in Ghana (Figure 2.1). This high biogenic content demonstrates how well the waste portion is suited for bioconversion processes (Zhang et al., 2014). However, Ghana's large amount of waste does not correspond to the available waste management infrastructure, human resources, or logistics for effective and efficient management (Fei-Baffoe et al., 2016). Ghana has over 35 institutionalized treatment plants, but only a few are operational for waste treatment (Abalo et al., 2018).

Furthermore, landfilling is the primary method of waste management in Ghana. This practice is of great concern because the landfills are mostly open dumps with no leachate or gas collection systems, posing serious health risks (Mensah and Larbi, 2005). Waste management has therefore become a major bottleneck for Ghana's economy and environmental organizations (Abiti et al., 2017). It should be emphasized that waste management extends far beyond collection and disposal to include the generation of income and other resources, the creation of jobs, cost savings, and environmental protection. Most likely, the amount of waste produced in Ghana has the potential to generate revenue for the government through recycling, cost savings, and taxes.

However, Ghana spends vast sums of money on solid waste management whereas other countries generate income, raw materials, and energy from waste (Monney et al., 2013; Bernardo et al., 2007). According to Abalo et al. (2018), the Accra Metropolitan Assembly spends approximately GHC 6.7 million per year on waste collection and transportation and GHC 550,000.00 per month on landfill maintenance and waste contractor payment. As a result, it is critical for Ghana to investigate sustainable waste management and environmental protection methods. Landfilling should be the last resort for waste management in Ghana, not the first.

2.2 Cooking Energy Sources in Ghana

The availability of an efficient and dependable energy source in Ghana cannot be overstated in an era when the country is still struggling with energy scarcity. Although Ghana passed the "Renewable Energy Act," Act 832, in 2011 to address the development, management and utilization of renewable energy, little progress has been made in the renewable energy sector (Ahiataku-Togobo, 2016). Most households still rely on wood biomass, charcoal, or liquefied petroleum gas (LPG) for cooking purposes.

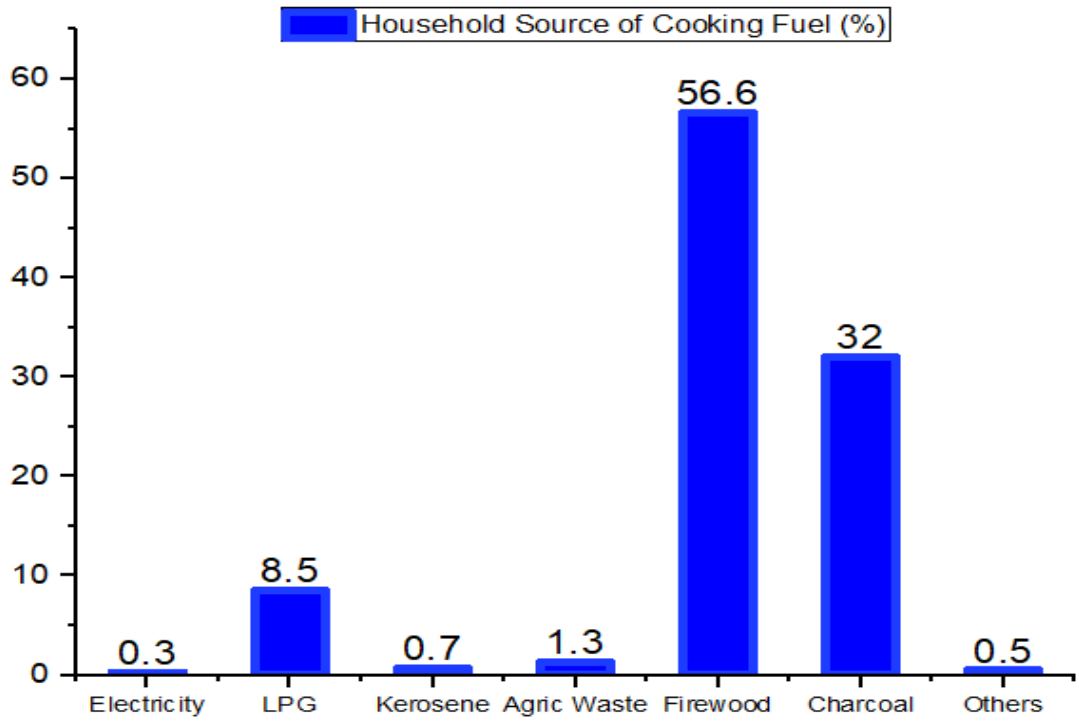

Figure 2.2: Household Sources of Cooking Fuel (KITE 2008)

According to Mensah et al. (2016), there is a high inter-fuel substitution between LPG and other biomass-based energy types like charcoal, fuelwood and kerosene. This is often due to price shocks and most importantly, erratic shortages in the supply of LPG in the Ghanaian market. A study from KITE (2008) depicts the different sources of cooking fuel in Ghana (Figure 2.2).

According to the same study, the percentages of LPG, electricity, kerosene, agricultural residue, firewood, charcoal, and other alternatives as household sources of cooking fuel in the Ashanti region of Ghana are 0.6, 7.5, 0.7, 0.1, 50.6, 39.9, and 0.5 % respectively (KITE, 2008). The distribution demonstrates a higher use of firewood and charcoal. This is comparable to the reported 80 % use of wood fuel in sub-Saharan Africa reported by (Okello et al., 2013). However, firewood and charcoal place an undue strain on forest reserves, resulting in deforestation. A sustainable and clean energy source for cooking is therefore required. As a solution, more appropriate energy sources have been proposed, the most prominent of which is energy from waste (Gyamfi et al., 2015).

According to Abalo et al. (2018), using waste to generate sustainable and environmentally friendly fuels such as biogas is not a novel idea however, the concept has not received the necessary attention in Ghana. That notwithstanding, Lwiza et al. (2017) reports that households can significantly benefit from the biogas technology because it reduces the need for alternative cooking fuels. Some studies have found that biogas is associated with less fuel wood use; 30–60 % in China, depending on the province (Gosens et al., 2013) , 50–60 % in Peru (Garfí et al., 2012) and 60 % in Nepal (Singh and Maharjan, 2003).

2.3 Biogas in Ghana

2.3.1 Origin of Biogas in Ghana

The origin of biogas technology in Ghana can be traced back to the late 1960s; however, it did not receive the attention it required until the mid-1980s (Bensah and Brew-Hammond, 2010). Prior to the 1980s, the primary goal was to provide energy for domestic cooking, but most biogas plants failed soon after the project began, due to a lack of technical know-how (Ahiataku-Togobo, 2008). The Ministry of Energy sought assistance from China to train some staff and other state institutions at the Biogas Research and Training Centre (BRTC) in Chengdu, China, to encourage technology transfer to Ghana (Lybæk et al., 2017). The technology was disseminated in cattle-raising communities as demonstration programs between the 1980s and the early 1990s. Dung

and night soil were used as feedstock materials (Lybæk et al., 2017; Arthur et al., 2011). German Appropriate Technology Exchange (GATE) of GIZ (formerly GTZ), Bremen Overseas Research and Development Association (BORDA), and the Catholic Secretariat in Ghana also provided support for demonstration and training programs (Arthur et al., 2011).

It should be mentioned that the Ministry of Energy built the first biogas demonstration plant, a 10 m^3 Chinese fixed dome digester, in 1986 at the Shai Hills with support from the Chinese government (Ahiataku-Togobo, 2008). The "Integrated Rural Energy and Environmental Project" at Apollonia also saw the building of nineteen fixed-dome digesters. In 1987, two household demonstration plants were also built at Jisonayilli and Kurugu in the Northern Region, with financial assistance from the United Nations Children Fund. Following that, the Apollonia biogas plant was built, which produced electricity for domestic use and bio-slurry for agricultural use (Edjekumhene et al., 2001). Ghana's Ministry of Energy launched the Appolonia biogas project in 1992 (Arthur et al., 2011). For several years, the project performed satisfactorily. Ownership issues, lack of feedstock materials, plant operation and maintenance issues, socio-cultural attitudes against the use of faecal-based slurry, and inadequate involvement of women in decision-making limited its potential (Bensah and Brew-Hammond, 2010; Boakye, 2008).

The Ministry of Energy's interest in biogas dissemination waned in 1993 and subsequent years, owing primarily to a lack of donor support and unmet expectations of the Appolonia projects. In 1996, the ministry attempted to rekindle government interest by funding a study to assess biogas resources in Greater Accra, Volta, and the Northern Regions. This research was intended to be the first step in the planning and development of a National Biogas Program (Ampofo, 1996). Little has been done to advance the biogas program since the study was completed and the report was handed to the ministry. Despite the lack of a clear biogas policy or framework, many biogas service providers are involved in constructing biogas plants in Ghana (Arthur et al., 2011). Small biogas digesters are currently installed in both domestic and institutional settings to receive and hygienically treat black water from flush toilets (Lybæk et al.,

2017).

2.3.2 Household Biogas Systems

Acquisition of household biogas digesters is a sustainable way of assisting low-income families in meeting their basic energy needs and improving their living standards (Ferrer-Martí et al., 2018). According to Bedi et al. (2017) and Rajendran et al. (2012), household digesters reduce the amount of organic household waste while significantly reducing energy-related expenditures and the use of firewood. This is because when operating at full capacity, a biogas plant has the potential to replace up to 2208 kg and 3319 kg of firewood per year for a 4 m^3 and 6 m^3 plant, respectively (Gwavuya et al., 2012). Gosens et al. (2013) reported a nearly ceased LPG usage by household biogas users in their dataset, including poor and relatively well-off households. The study's findings are attributed to the possibility of biogas and LPG being nearly perfect substitutes because they are both dedicated cooking fuels. However, because LPG is expensive, households have a strong incentive to reduce its use (Gosens et al., 2013).

2.3.2.1 Types and Sizes of Biogas Digesters

The fixed-dome, floating drum, and puxin digeste are the three main types of biogas digesters that have been designed, tested, and disseminated in Ghana. The fixed dome model developed by China and the floating drum model developed by India have continued to perform to this day (Datong, 1989). The design of the digester varies according to geographical location, substrate availability, and climatic conditions (Rajendran et al., 2012). A digester used in mountainous areas, for example, is designed to have less gas volume to avoid gas loss. According to Bensah and Brew-Hammond (2010), the dome design is used in 80 % of biogas plants distributed in Ghana, making them the most popular. This is because they are less expensive than floating drum digesters.

As of 2011, over 240 digesters with capacities ranging from 6 to 10 m^3 had been installed in Ghana (Duku et al., 2011b). Bensah et al. (2015) reported an increase in excrement-based biogas plants due to the high demand of digesters that treat faecal sludge from flushed toilets. According to Bensah and Brew-Hammond (2010), most

household and institutional biogas plants have volumes of 10 m^3 and 50 m^3, respectively, where the retention time is the criterion in sizing the digesters. Also, Abbas et al. (2017) asserts that the most feasible size for a household system is 10 m^3 because it meets the cooking needs of a typical family.

Chen et al. (2013) found that ground temperature is the most critical factor influencing the amount and rate of biogas production. Because of geothermal energy, it is preferable to have digesters underground in tropical countries (Bin, 1989) . Most biogas plants in rural China are built 2 m underground (Chen et al., 2013). Likewise, most of the biogas plants in Ghana are placed underground. The temperature in a 2 m deep biogas plant is roughly equivalent to the average ground temperature at 1.6 m depth (Gl et al., 1993). According to Chen et al. (2013), the temperature at a depth of 2 m ranges from $8\,^{\circ}$C to $25\,^{\circ}$C. Even though the minimum temperature for biogas production is $10\,^{\circ}$C , biogas production is most rapid when temperatures exceed $20\,^{\circ}$C (Ma, 2003). The measured temperature for an underground biogas plant in Ghana was approximately $22\,^{\circ}$C - $25\,^{\circ}$C.

Moreover, the building materials (brick, cement, plastic, reinforced fibre, and metal materials) used in constructing biogas digesters directly impact the temperature (Obileke et al., 2021). Hence a bricks or cement biogas digester is recommended for households because of its ability to maintain a higher slurry temperature without the use of additional heating (Obileke et al., 2021). Also, findings from Obileke et al. (2021) show that most household biogas digesters are built with bricks and cement because of their rigidity, robustness, and longevity. That notwithstanding, soft bags or plastic digesters are likely substitutes in areas where logistics and transportation may be difficult due to their lightweight and low cost (Obileke et al., 2021; Abbas et al., 2020). Furthermore, fixed biogas plants (brick, concrete) are 1.27 times more expensive than portable biogas plants (plastics) (Abbas et al., 2020).

2.3.3 Challenges with Household Biogas-Setup

Household biogas digester programs are frequently promoted without any systematic planning (Ferrer-Martí et al., 2018). As a result, most plants fail shortly after the

project's completion. Poor digester design and construction, lack of feedstocks, balloon gasholders breakdown and gas leakages, maintenance services and operational knowledge have been reported as some of the reasons rendering the household biogas technology unapealing (Bensah and Brew-Hammond, 2010). Some studies have revealed that households that abandoned biogas technology did so within four years of its installation, even though its lifespan is estimated to be twenty-five years (Lwiza et al., 2017). According to Osei-Marfo et al. (2018), the needs of most biogas users have not been fully met, and people are only partially satisfied with the technology's outcome. Mengistu et al. (2016) assert that people appear to be very concerned about whether their biogas user neighbours, friends, and relatives benefit well before investing.

Furthermore, there is a lack of data on the financial viability of biogas plants (Mohammed et al., 2017). Because of the high cost of constructing a digester, most households have been slow to embrace the biogas technology (Antwi et al., 2010). According to Mohammed et al. (2017), anaerobic digestion technology is characterized by high initial investment costs, typically resulting in non-monetary savings with less capital investment recovery. Without subsidies, the payback period of 11 to 14 years, based solely on energy cost savings from investing in a digester, may be too long to justify the investment (Bedi et al., 2017). Gwavuya et al. (2012) discovered rates of return above 10 %, whereas Adeoti et al. (2000) reports rates of return of around 18 % for a 6 m^3 plant of similar design in Nigeria.

2.3.4 Measures to Promote Household Biogas Adoption

To realize the untapped potential of the biogas technology, both governmental and non governmental sectors must work together to facilitate its dissemination (Surendra et al., 2014). Some recommendations to overcome the challenges associated with household biogas dissemination and adoption include implementing policy and providing financial incentives and technical (construction, operation, and maintenance) training. Since existing policies for household biogas projects focus primarily on construction assistance while ignoring management and maintenance, alternative policies must be investigated to balance the construction and operation (Wang et al., 2016; Feng et al.,

2012).

In addition to policy development, steps should be taken to improve follow-up services and biogas plant management (Chen et al., 2010b). To overcome the financial component of biogas technology dissemination, financial incentives such as soft loans and subsidies should be introduced (Osei-Marfo et al., 2018; Arthur et al., 2011). Furthermore, stakeholders and the government must establish a regulatory body to oversee the activities of biogas service providers in Ghana (Osei-Marfo et al., 2018) . Finally, biogas service stations are required to provide follow-up services (Chen et al., 2017).

2.4 Anaerobic Digestion and Biogas

Anaerobic digestion (AD) is a collection of biochemical processes that occur without oxygen and involve a consortium of microorganisms breaking down complex biodegradable organic matter to produce biogas and digestate (Grando et al., 2017; Kadam and Panwar, 2017). The primary components of biogas are methane (CH_4) and carbon dioxide (CO_2), which are typically in the proportions of 50-80 % methane and 30-50 % carbon dioxide. Water vapour, hydrogen sulfide, ammonia, carbon monoxide, nitrogen and hydrogen are also produced during the AD process (Matheri et al., 2017). However, trace gases must be removed from the gas before usage (Kadam and Panwar, 2017). This is because water vapour, when combined with H_2S on metal surfaces, has corrosive properties and reduces the heating value. Likewise, hydrogen gas is corrosive. As illustrated in Figure 2.3, the AD process involves biochemical steps namely hydrolysis, acidogenesis, acetogenesis, and methanogenesis (Siddique et al., 2015a,b; Deublein and Steinhauser, 2011).

2.4.1 Hydrolysis

Hydrolysis, the first step in the AD process, involves microorganisms breaking down complex organic polymer chains (primarily carbohydrates, proteins, and lipids) that cannot be transported across cell membranes into smaller molecules such as monomers and oligomers (Matheri et al., 2017). This breakdown is caused by enzymes secreted by facultative/obligate anaerobic hydrolytic bacteria (Paritosh et al., 2017). Proteolytic

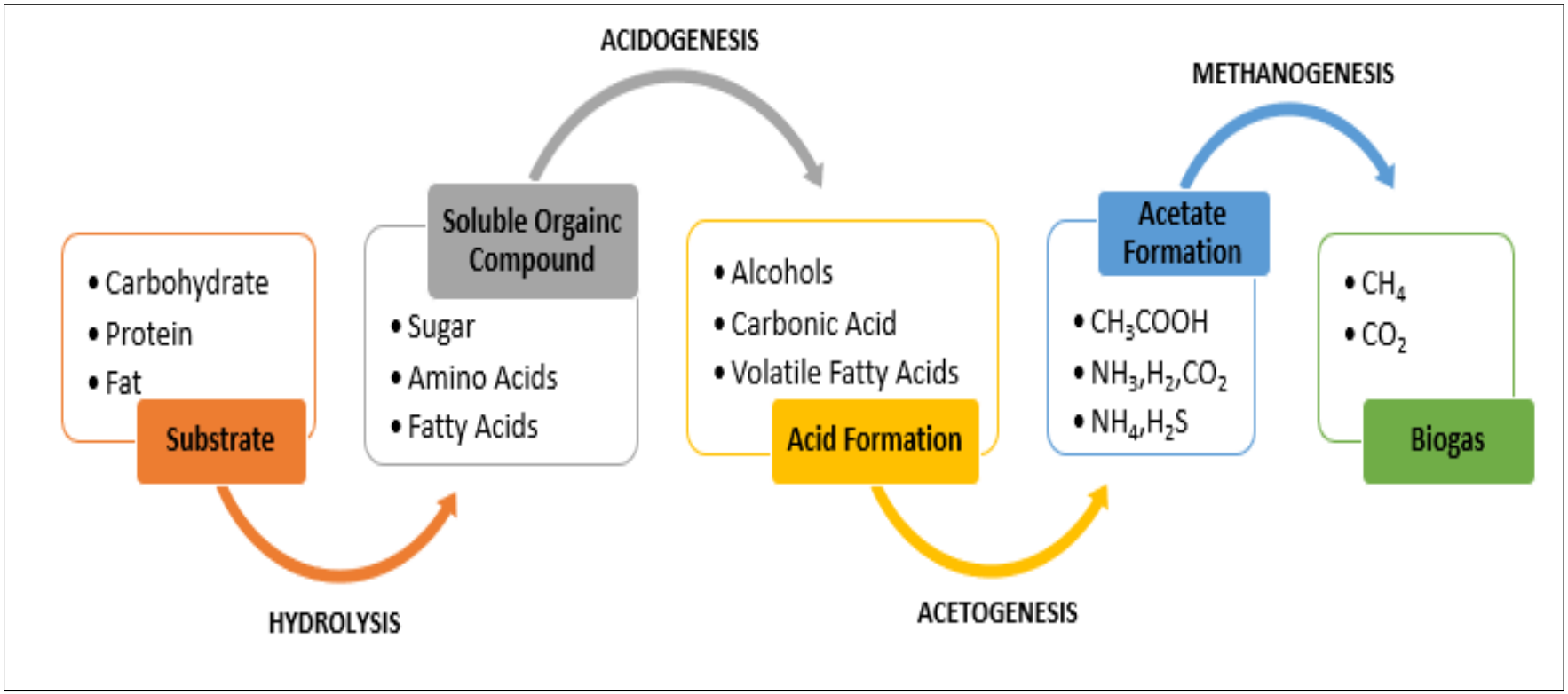

Figure 2.3: Anaerobic Digestion Stages

bacteria produces proteases, which catalyze protein hydrolysis into amino acids. Cellulolytic and xylanolytic bacteria also produce cellulases and xylanases to degrade carbohydrates in the form of cellulose and xylan to glucose and xylose, respectively. In Equation 2.1, glucose molecules are produced by starch hydrolysis.

$$nC_6H_{10}O_5 + nH_2O \rightarrow nC_6H_{12}O_6 \tag{2.1}$$

Similarly, lipolytic bacteria produces lipases that degrade lipids into long-chain fatty acids and glycerol. Hydrolysis can occur at varying rates depending on the substrate and is frequently referred to as a rate-limiting step in the AD process (Paritosh et al., 2017). According to Mital (1997), the hydrolysis rate is relatively slow. It is affected by the substrate's nature and size, bacterial concentration, pH, enzyme production, bioreactor temperature, and enzyme adsorption onto substrate particles. Streptococcus and Enterobacter are the genera of anaerobes responsible for hydrolysis (Bryant, 1979).

2.4.2 Acidogenesis

In the next step of the AD process, known as acidogenesis, the hydrolysis products are converted into carbon dioxide, hydrogen, ammonia, and volatile fatty acids (acetate, propionate, butyrate, valerate, and isobutyrate). During acidification, facultative anaerobic bacteria use oxygen and carbon, resulting in an anaerobic condition. When the AD process is working properly, the majority of the organic material (about 70 %) is directly transformed into methanogenic substrates (acetate, carbon dioxide, and hydrogen), while a significant portion (approximately 30 %) is transformed into lower fatty acids and alcohols (Paritosh et al.,2017). Methane can be produced directly from acetate, carbon dioxide, and hydrogen. However, if the hydrogen produced is not consumed quickly enough, the formation of volatile fatty acids and alcohols increases, throwing the AD process out of balance (Schink,1997). Syntrophic acetogenic bacteria can further degrade other VFAs (propionate, butyrate, valerate, and isobutyrate) to form acetate and hydrogen.

2.4.3 Acetogenesis

The VFAs and alcohol produced during the fermentation step are oxidized to acetate (Equation 2.2), while protons are reduced to hydrogen during the acetogenesis step. This process is aided by acetogenic bacteria from the genera *Syntrophomonas* and *Syntrophobacter*. Acetogenesis is a critical step in the AD that necessitates close collaboration between the organisms that perform oxidation and the methane-producing microorganisms active in the next stage of actual methane formation (Schink, 1997). During acetogenesis, hydrogen is constantly consumed, keeping the concentration of hydrogen at a manageable level. Thus, acetogenic bacteria coexist with hydrogenotrophic methanogens, which remove excess hydrogen and use it to produce methane. The acetogenesis stage essentially demonstrates how efficient the biogas production process is because acetate reduces to produce 70 % methane (Paritosh et al., 2017).

$$nC_6H_{12}O_6 \rightarrow 3nCH_3COOH \tag{2.2}$$

2.4.4 Methanogenesis

The last stage of the AD process is where archaea methanogens produce methane from carbon dioxide, hydrogen, and acetate. Methanogenesis is the driving force behind the anaerobic degradation process because it produces energy under standard conditions. Methane is produced through carbon dioxide reduction or acetic acid fermentation. The acetate degrading route, consisting of the slowest growing and most sensitive organisms, generates 70 % of the methane produced (Bułkowska et al., 2015). As a result, acetate is an essential methane precursor (Equation 2.3). On the other hand, the hydrogen path is the H_2 utilizing route with a high growth rate and less sensitive organism (Bułkowska et al., 2015). The remaining 30 % of methane is produced through the reaction of hydrogen and carbon dioxide (Equation 2.4). Because of the existence of the acetate and hydrogen pathways, the methanogenic bacteria that produce methane are classified as acetoclastic methanogens and hydrogenotrophic methanogens (Matheri et al., 2017). Moreover, methanogenesis is rate-limiting due to the vulnerability of the diverse microbes.

$$CH_3COOH \rightarrow CH_4 + CO_2 \tag{2.3}$$

$$CO_2 + 4H_2 \rightarrow CH_4 + 3H_2O \tag{2.4}$$

2.5 Feedstock Types and Characteristics

In the context of anaerobic digestion, feedstock refers to any substrate that anaerobic bacteria and archaea can convert to biogas. According to Paritosh et al. (2017), feedstocks type, quality, and quantity directly impact biogas yield and quality. Figure 2.4 depicts biomass types used as feedstock for biogas production (Möller and Müller, 2012; Labatut and Scott, 2008).

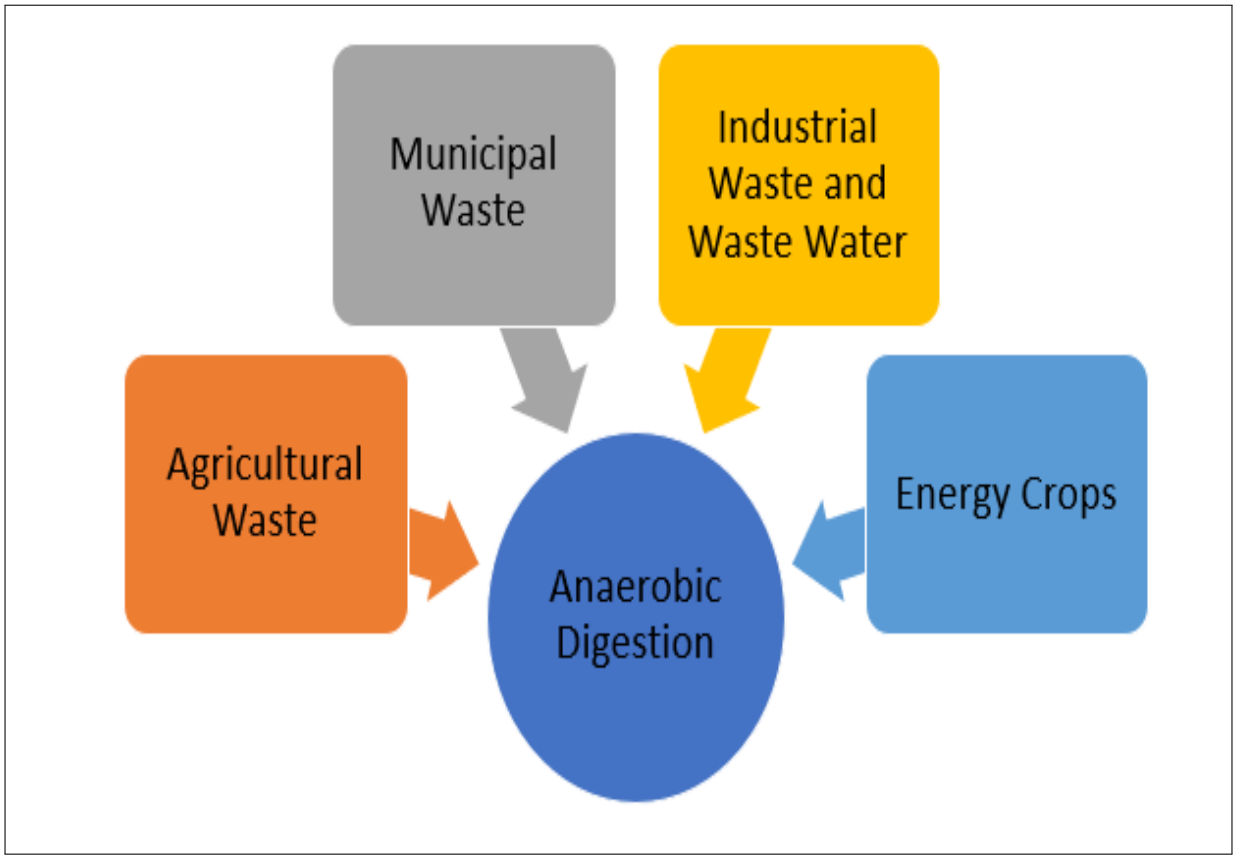

Figure 2.4: Sources of Feedstock for Anaerobic Digestion

It ranges from simple wastewater to complex high-solid waste. The nutrient content

of these feedstocks varies, as does their ability to generate biogas. Also, the composition of substrates has a substantial impact on the efficiency of biogas production (Steffen et al., 1998). Carbohydrates, proteins, and lipids are the most common chemical components of organic feedstock (Siddique and Wahid, 2018; Hagos et al., 2017). To enrich microorganisms, create nutritional balance, and reduce inhibitors, feedstock used in anaerobic digestion should contain optimum amounts of carbohydrates, lipids, and fats that are easily accessible. Carbohydrates and proteins have faster conversion rates but produce less biogas (Chiu and Lo, 2016). Conversely, lipids have the greatest biogas yield but need to be retained for a longer period of time since they degrade slowly (Esposito et al., 2012).

2.5.1 Carbohydrate-Rich Substrates

Carbohydrates, also known as sugars, are found in varying amounts in almost all substrates. Rice, pasta, cassava, yam, and potatoes are rich in simple sugars, disaccharides, and polysaccharides. Starch is the most common polysaccharide, consisting of straight or branched glucose chains. Plant-derived substrates are also carbohydrate-rich despite their difficulty in degrading (Hagos et al., 2017). A high sugar concentration may cause a rapid accumulation of VFA in the biogas digester and a decrease in pH (Paritosh et al., 2017). Feedstocks with high concentrations of sugars are therefore mixed with feedstocks with lower content of easily degradable organic components to create a balanced environment for the AD process.

2.5.2 Protein-Rich Substrates

Proteins are also vital constituents of organic substrates. Abattoir waste, farmhouse waste (pig and chicken manure) and stillage from ethanol industries have high protein proportions, while domestic wastewater and food waste have less protein (Hagos et al., 2017). Proteins have different forms of amino acids. Of all the various forms of amino acids in proteins, one thing stands typical: they have the amine group (-NH_2) (Kallistova et al., 2014; Wagner et al., 2013). Protein-rich substrates tend to generate substantially high amounts of methane (Murovec et al., 2015).

2.5.3 Fat-Rich Substrates

Organic materials with high-fat content are produced by slaughterhouses, edible oil industries, dairy product industries, and food manufacturing industries. Triglycerides, a type of fat, degrade into glycerol and long-chain fatty acids (LCFAs), the most common of which are palmitic, stearic, and oleic acids (Dasa et al., 2016). Glycerol converts quickly to biogas and has a high biogas yield due to its easily degradable nature (Achinas et al., 2017; Braun, 2007, 1982). Lipids have a higher theoretical methane potential than carbohydrates and proteins, ranging between 850 and 1050 L/kg VS (Rasit et al., 2015). However, the decomposition of LCFAs is a complex process. Hence, lipids are usually unsuitable for mono-digestion, owing to LCFAs inhibition (Rasit et al., 2015).

High concentrations of LCFAs may lead to blockages and anaerobic microbial inhibitions in anaerobic digesters (Cavaleiro et al., 2008). At elevated temperatures, they can cause foaming due to their detergent properties (Nguyen et al., 2017; Kallistova et al., 2014). Therefore, excessive production of LCFAs may lead to system malfunctioning (Chow et al., 2015). Stearic and oleic acids have a detrimental effect on the methanogenesis stage at concentrations of 0.2–0.5 g/L (Chen et al., 2008; Angelidaki and Ahring, 1992). Also, LCFAs inhibition of 5 g/L can be expected when digesting food waste since it is usually rich in lipids (Mirmohamadsadeghi et al., 2019). Conversely, volatile fatty acids (VFAs) are formed in the acidogenesis stage if LCFAs are not inhibited.

2.6 Pretreatment

Biodegradation of some biomasses may be difficult due to their intrinsic properties and the inability of microorganisms to break them down easily. The biodegradability of biomass may be hampered by fibre strength, lignin content, crystalline structure, cellulosic polymers, pretreatment time, humidity, and substrate surface properties. Pretreatment is one of the techniques for improved biogas optimization. Various pretreatment methods such as physical, mechanical (ultrasound, high pressure, and lysis), thermal, chemical (ozonation, alkali), and biological can be used to reduce the recalcitrance of biomass (Kondusamy and Kalamdhad, 2014; Wang and Zhao, 2009; Cozzolino et al.,

1992). Combinations of pretreatment types can also be used to improve anaerobic digestion efficiency. On the contrary, some combinations of pretreatment may decrease degradability due to intermediate inhibitory formation in some cases (Salminen et al., 2003).

Pretreatment increases the surface area and accessibility of the substrates to microorganisms, facilitating the conversion of polymers to monomers. Furthermore, pretreatment of biomass before AD reduces retention time and the final amount of sludge (Shah et al., 2015; Li et al., 2010). Moreover, pretreatment increases chemical oxygen demand and releases the substrates' intracellular nutrients (Neshat et al., 2017). Because the AD stages directly affect mass transfer and food availability, pretreatment aids the rate-limiting stages (Gomec et al., 2002). Although pretreatment may improve substrate degradation and process efficiency, it does not always yield higher biogas (Achinas et al., 2017). Pretreatments are primarily applied to one of the co-substrates, obviously the one with the poorer biodegradability, rather than the entire mixture to reduce costs in anaerobic co-digestion (Mata-Alvarez et al., 2014). The various types of pretreatment methods are listed below.

2.6.1 Physical Pretreatment

Waste sorting is required to biologically treat some types of waste, such as municipal solid waste. Source-separation or hand sorting techniques can be used.

2.6.2 Thermal Pretreatment

Liquid hot water is another name for thermal pre-treatment. It entails heating feedstock to approximately $220\,^{\circ}$C at a given pressure (Wang et al., 2012). However, the feedstock is cooled to a lower temperature before feeding. Thermal pretreatment removes pathogens, improves dewatering performance, and reduces digestate viscosity. It may, however, result in the loss of volatile organics. The impact of thermal pretreatment is determined by the biodegradable material and mesophilic and thermophilic conditions (Wang et al., 2012). For sewage sludge, an optimum temperature of $160\,^{\circ}$C-$180\,^{\circ}$C and a treatment time of 30-60 minutes have been reported (Gavala et al., 2003; Van Haandel and Lettinga, 1994). Pretreatment at a moderate temperature of $70\,^{\circ}$C has also been

documented, but it requires more time (Ferrer et al., 2008). The increase in biogas production caused by thermal pretreatment is associated with COD solubilization.

2.6.3 Mechanical Pretreatment

Mechanical disintegration of substrates reduces the particle size and increases the medium's specific surface area, facilitating the hydrolytic step (Zhang et al., 2014; Luste et al., 2009). This is significant because COD degradation is slowed when the specific surface area is not exposed (Matheri et al., 2017). Therefore, mechanical grinding is required for food waste since it accelerates substrate solubilization (hydrolysis and acidogenesis), thereby improving anaerobic digestion (Nah et al., 2000). According to Wang et al. (2012), the relationship between particle size and biogas production rate is inversely proportional. Sharma et al. (1988) discovered that substrates with particle sizes of 0.088 mm and 0.40 mm are ideal for optimized biogas production compared to 1.0, 6.0, and 30.0 mm particle sizes. According to Agyeman and Tao (2014), reducing particle size to 2.5–8 mm could improve methane production.

2.6.4 Chemical Pretreatment

Chemical pre-treatment is the process of removing biodegradable material through the use of alkalis and strong acids in the digestion process (Matheri et al., 2017). The bonds of feedstock materials are frequently broken down via a chemical pretreatment procedure (Siddique and Wahid, 2012). Hence, one of the most efficient methods for complex matter solubilization is alkali treatment. NaOH, KOH and some other substances are added to fermenters when the pH needs to be adjusted by increasing the alkalinity. Kim et al. (2003) report an efficiency ranking of NaOH > KOH > $Mg(OH)_2$ > $Ca(OH)_2$ when making a choice of chemical to use. Corn husks were steeped in a NaOH solution for five days before being co-digested with cow dung and methane yield was observed to have increased from 60 % to 80 % (Mel et al., 2015). However, excessive Na^+ or K^+ concentrations may result in AD inhibition (Neves et al., 2006). Additionally, acid pre-treatments or oxidative methods improve feedstock digestibility and hydrolysis rate, particularly lignin (Matheri et al., 2017).

2.6.5 Biological Pretreatment

Biological pretreatment does not necessitate the use of any toxic chemicals. However, it is susceptible to environmental factors. Slow hydrolytic enzymes and fungi are commonly used to improve feedstock degradation (Tisma et al., 2017). According to Patinvoh et al. (2016), pretreating with *Bacillus sp.* generates roughly twice as much methane as untreated feedstock. Ziemiński and Kowalska-Wentel (2015) also found that hydrolytic-enzymes pretreated sugar beet pulp silage and vinasse produced 28 % more biogas than untreated material with the same mixing ratio.

2.6.6 Microwave Pretreatment

Microwave (MW) irradiation improves substrate degradability and increases biogas production (Wang and Li, 2016). Siddique et al. (2017) found that microwave pretreatment of waste-activated sludge increased biogas production by 53 %. In addition, Microwave pretreatment before sludge digestion boosted biogas generation by 45-79 % according to Zhen et al. (2017).

2.7 Factors Affecting the AD Process

The performance of biogas plants can be improved by studying and monitoring changes in parameters such as pH, temperature, loading rate, agitation, C/N ratio, VFA and others. Any significant change in these parameters can affect biogas production (Gashaw, 2014; Dioha et al., 2013). Nonetheless, optimizing process factors affecting biogas production is complex, with several interactive controlling parameters. Some of the factors that influence the AD process are discussed below.

2.7.1 Total Solids (TS)

TS is a term used to describe the dry matter content of a substrate. Mechanical components of AD plants, such as pumps and stirrers, are influenced by TS concentrations because they can effectively process substrates within a specific range of TS concentrations. Wet AD systems are typically fed substrates with a TS content of less than 10 %, implying that a large amount of water is required in digesters when dealing with high solid organic wastes. According to Kigozi et al. (2013), the optimum TS range for wet

AD of food waste is between 6 % and 9 %. Similarly, Arifan et al. (2021) and Wang et al. (2020) recorded an optimum solid content of 7-10 % and 5–15 % respectively for biogas production. Arifan et al. (2021) further reports that the AD process for total solids under 7% was unstable, while total solids above 10 % occasionally resulted in fermenter overload. Table 2.1 shows some TS values of feedstocks from literature.

Table 2.1: Literature Reported TS values for Food waste, Cow dung and Human Excreta

Feedstock Type	Total Solids (%)	Reference
Food waste	21.6	Paritosh et al. (2017)
Food waste	24.6	Dhamodharan et al. (2015)
Food waste	22.0	Pax et al. (2020)
Human Excreta	18.0	Singh et al. (2021b)
Cow Dung	22.7	Arifan et al. (2021)
Cow Dung	20.2	Dhamodharan et al. (2015)
Cow Dung	32.8	Pax et al. (2020)
Cow Dung	20	Singh et al. (2021b)

Human excreta has TS values ranging from 14 to 37 % (Miller et al., 2015; Rose et al., 2015; Wignarajah et al., 2006). Uncu and Cekmecelioglu (2011) and Ohkouchi and Inoue (2006) have also reported TS values of 38.7 % and 24.1 % respectively for food waste. It is important to note that traditional food structure and composition variations affect the solid content (Bodík and Miroslavakubaská, 2014). Besides, Yavini et al. (2014) claim that an increase in TS values decreases water volume and reduces microbial activity and biogas yield. Due to reduced methanogen mobility, a higher solids concentration would imply a longer retention time for the degradation and digestion process (Kossmann and Pönitz, 1999). Yi et al. (2014) confirmed that the relative abundance of the genus *Methanoculleus* decreased with increasing TS contents, indicating that *Methanoculleus* contributed less to methane production in high-solids AD than in low-solids AD.

2.7.2 Volatile Solids (VS)

VS concentration is the organic fraction of TS and is expressed as a percentage of TS in grams per kilogram. Even though VS represents the total concentration of dry organic matter, it is important to note that not all of this may be available for anaerobic digestion. VS can be used to assess the degree of degradation in an AD process in that simultaneous measurements of VS concentration in the feed and the digested end-product can be used to evaluate process efficiency. Significantly higher VS reductions may be obtained for simpler substrates. However, a decrease in VS removal rate can indicate a process imbalance, which might not be apparent until the process is severely harmed. The determination of VS is analytically simple. Yet, it is subject to errors due to non-representative samples and analytical inaccuracy. Because some volatile materials evaporate during the TS determination, the VS determination is likely to underestimate the organic material contained in the sample. Table 2.2 displays some VS values from literature.

Table 2.2: Literature Reported VS values for Food waste, Cow dung and Human Excreta (*VS as % of TS)

Feedstock Type	Volatile Solids (%)	Reference
Food waste	91.9*	Paritosh et al. (2017)
Food waste	20.3	Dhamodharan et al. (2015)
Food waste	90.7*	Pax et al. (2020)
Human Excreta	81.0*	Singh et al. (2021b)
Cow Dung	18.1	Arifan et al. (2021)
Cow Dung	15.3	Dhamodharan et al. (2015)
Cow Dung	96.0*	Pax et al. (2020)
Cow Dung	88.0*	Singh et al. (2021b)

2.7.3 Chemical Oxygen Demand and Biological Oxygen Demand

The Chemical Oxygen Demand (COD) measures the oxygen equivalent of the organic matter content of a sample that is susceptible to oxidation. COD is commonly used as a control tool in anaerobic systems, determining the organic (degradable) material

content of feedstocks (Matheri et al., 2017; Curry and Pillay, 2012). Most likely, the strength of the COD of a feedstock has a significant impact on the final amount of biogas yield and the methane content (Ghani and Idris, 2009). According to Ahmed et al. (2019), COD levels in human excreta range from 800 to 24000 mg/l. Koné and Strauss (2004) also reported a COD range of 1200-7800 mg/l for Human excreta. Metcalf and Eddy (2003) also discovered a COD range of 5000-80000 mg/l for faecal sludge. On the other hand, Bodík and Miroslavakubaská (2014) reported a COD range of 150000-510000 mg/l for food waste. Dhamodharan et al. (2015) found COD concentrations in cow dung and food waste to be 21.6 and 78.4 g/l, respectively. Also, COD concentrations in human excreta and cow dung were 92.8 and 280.0 g/l, respectively (Singh et al., 2021b). Because COD is a defined test, the degree of sample oxidation can be influenced by digestion time, reagent strength, dilution factor, and sample COD concentration.

Biological Oxygen Demand (BOD) is also the amount of oxygen consumed by organic and inorganic compounds oxidized by the biological-oxidation effect under specific conditions (Pujar et al., 2030). Because BOD is primarily a biochemical parameter, it generally reflects the biodegradability of organic matter in the substrate (Kjeldsen et al., 2002; Kjeldsen and Christophersen, 2001). It is expected that BOD and COD values decrease over time during anaerobic digestion due to reducing organic pollutants (Gashaw, 2016). As a result, the BOD: COD ratio is a good indicator of the degrees of biological and chemical decomposition and can be used to predict the degradation of organic matter (Gashaw, 2016).

2.7.4 Moisture Content

Microbial community in the AD process rely on water to survive, making moisture content a critical parameter. However, maintaining the same water availability throughout the digestion cycle is challenging. As anaerobic digestion progresses, water added at a high rate is gradually reduced to a lower level (Gashaw, 2016). High moisture content is likely to affect process performance by dissolving readily degradable organic matter, whereas low moisture content can kill some microorganisms, resulting in process failure (Igoni et al., 2008). As a result, operating within an optimal moisture

content range is required. It has been reported that the highest methane production rates occur at humidity levels ranging from 60 to 80 % (Gashaw, 2016). Table 2.3 displays some moisture content values from literature.

Table 2.3: Reported Moisture Content values for Food waste, Cow dung and Human excreta

Feedstock Type	Moisture Content (%)	Reference
Food waste	78.0	Pax et al. (2020)
Cow dung	67.2	Pax et al. (2020)
Cow dung	66.0	Singh et al. (2021b)
Human Excreta	84.0	Singh et al. (2021b)

2.7.5 Particle Size

Particle size affects AD process kinetics due to the availability of specific surface area for microorganism use (Lesteur et al., 2010). The available substrate surface area for microbes may be reduced by larger particles, which can also clog systems. On the other hand, microorganisms have access to more specific surface area when particles are smaller, resulting in increased feed availability for bacteria (Vigueras-Carmona et al., 2016; Mshandete et al., 2006). However, the formation of soluble organic compounds like volatile fatty acids is accelerated by excessive substrate particle size reduction, which also speeds up the steps of hydrolysis and acidogenesis. (Izumi et al., 2010).

By reducing food waste particle size from 8 to 2.5 mm, Agyeman and Tao (2014) boosted the methane output by 10-29 %. According to Izumi et al. (2010), reducing the average particle size of food waste from 2.14 to 1.02 mm doubled the maximum substrate utilization rate coefficient. In addition, Li et al. (2021) used maceration to reduce the particle size of cow dung by physically chopping, grinding, and blending. The study recorded higher methane production using these mechanisms compared to non-treated cow dung.

2.7.6 Seeding

The microorganism type and population required for acid fermentation and methane formation are present to some extent in most substrates, but their numbers may be in-

sufficient. As a result, inoculum must be introduced into the AD process. Usually, the inoculum is degassed by pre-incubating for 2 to 5 days to deplete the biodegradable material and reduce methane production (Filer et al., 2019; Angelidaki et al., 2009). Angelidaki et al. (2009) recommend that the pre-incubation be performed at the same temperature as the process temperature from which the inoculum was originally obtained.

2.7.7 pH

pH is one of the essential parameters for AD due to the sensitivity of microorganisms to pH variations and its effect on the solubilization of organic matters (Feng et al., 2015). However, different microbes require different optimal pH values at each stage of the AD process, although most of them prefer neutral pH conditions. Inability to keep the pH within a safe range could lead to reactor failure (Chen et al., 2008). Hydrolyzing and acidogenic microorganisms prefer pH values between 5.5 and 6.5 (Kallistova et al., 2014). Nonetheless, Hagos et al. (2017) extend the range for acidogenesis microorganisms (fermentative bacteria) to 4.0–8.5 because they are less sensitive to pH and can tolerate changes.

Also, many researchers have discovered that maintaining a pH between 6.8 and 7.2 is preferable for maximum methane yield (Lemmer et al., 2017; Gashaw, 2014). Conversely, pH levels between 6.0 and 6.5 inhibit the activity of methane bacteria (Gashaw, 2014). Also, when the pH level exceeds 8.5, it creates an unfavourable environment for methanogenic bacteria (Matheri et al., 2017). Walker (2009) recommend a pH between 7.0 and 8.0 for protein degradation, while carbohydrate degradation requires a pH between 6.0 and 9.0. The concentrations of total ammonia nitrogen (TAN) and volatile fatty acid (VFA) are highly related to pH, making them the primary parameters of pH balance management (Fisgativa et al., 2016).

2.7.8 Temperature

Temperature selection and control are critical in AD because they drive the functions of microorganisms. According to Divya et al. (2015), temperature variations can affect microbial growth and significantly reduce biogas production. It is necessary to

consider the microorganisms present and the conditions under which they can survive in order to operate at the optimal temperature (Matheri et al., 2017). AD temperature ranges are divided into three categories: psychrophilic, mesophilic, and thermophilic. Psychrophilic is a temperature range of less than $10\,°C$, whereas mesophilic operates in a temperature range of $20-45\,°C$, with an optimum temperature of $35\,°C$. Furthermore, thermophilic is above $50\,°C$, with $55\,°C$ being the most commonly used operating temperature (Matheri et al., 2017).

Mesophilic and thermophilic environments are frequently used in AD. However, considering that a wider variety of microorganisms are supported by the mesophilic process than the thermophilic process, the former is more stable (Yang et al., 2018). While thermophilic bacteria can develop slowly in mesophilic temperatures, mesophilic bacteria cannot thrive in thermophilic temperature ranges. On the contrary, thermophilic temperatures positively affect the metabolic rate of microorganisms, resulting in a faster digestion process (Sreekrishnan et al., 2004). However, they are difficult to control and may require additional energy to maintain the reactor's constant temperature (Hagos et al., 2017). Also, as the temperature rises, the solubility of CO_2 decreases (Siddique and Wahid, 2018). With lower temperatures in mesophilic digesters, CO_2 dissolves faster and produces carbonic acid when it reacts with water, increasing the system's acidity (Siddique and Wahid, 2018).

The methanogenic bacteria that aid in the production of biogas are susceptible to temperature changes, and the ideal temperature is from $33\,°C$ to $38\,°C$. Low temperatures impede the formation of biogas, whereas high temperatures kill the bacteria that produce it (Gashaw, 2014). In order to maintain a constant temperature, the structure for producing biogas is typically built underground. (Sibisi and Green, 2005). Although the rate of gas production increases with temperature, the content of methane decreases (Dai et al., 2017).

2.7.9 Mixing / Agitation

The substrate concentration, temperature, nutrients, and other operating conditions are uniform when mixing is done. The stirring of the digester influences the distribution of

microorganisms by ensuring intimate contact between microorganisms and substrate, resulting in a better digestion process (Wang et al., 2017a). Most importantly, mixing releases trapped gas bubbles in digester content and reduces solids buildup or sedimentation (Kigozi et al., 2013). Stirring can be accomplished by installing specific mixing devices in the reactor, such as a scraper or a piston. In addition, other methods, such as daily slurry feeding rather than periodic feeding, provide the desired mixing effect (Gashaw et al., 2014). Furthermore, gas recirculation has been shown to improve mixing (Sreekrishnan et al., 2004).

2.7.10 Carbon-Nitrogen Ratio (C/N)

The carbon to nitrogen (C/N) ratio of an organic material impacts the AD process. While carbon provides energy for microorganisms, nitrogen is used by bacteria that produce methane to meet their protein requirements (Matheri et al., 2017). When C/N is high, nitrogen (N) is rapidly depleted, VFAs accumulate and biogas production is reduced (Siddique and Wahid, 2018). Lower C/N values result in higher ammonia concentrations, which stifle microbial growth (Siddique and Wahid, 2018). Because AD consumes carbon faster, a high percentage is required to operate at maximum efficiency (Matheri et al., 2017). As a result, the AD process is more stable when the C/N ratio is between 20 and 30, with the majority of the carbon being readily degradable (Haider et al., 2015). Co-substrates are added in anaerobic co-digestion processes to maintain an optimal C/N in digesters (Moset et al., 2017).

2.7.11 Chemical Oxygen Demand-Nitrogen Ratio (COD/N)

The COD/N ratio of the substrate is an important parameter to consider when producing biogas. The optimal COD/N range for anaerobic digestion is 350/7 – 1000/7 (Gashaw, 2014). Microbial growth in the digester is hampered if the ratio is greater or lesser than the optimal range. According to Gashaw (2014), biogas produced at COD/N ratios of 500/7 and 600/7 was nearly equal in quantity, whereas biogas produced at 400/7 was less than that produced at 500/7, 600/7, and 700/7.

2.7.12 Organic Loading Rate (OLR)

The organic loading rate is defined as the amount of organic solids loaded per unit time and volume of a digestion process. OLR is essential in optimizing microorganism activity since different microbial groups are unlikely to grow at the same rate due to substrate concentration (Neshat et al., 2017). Also, because organic loading rate is inversely proportional to methane production, when the organic loading rate exceeds the capacity of the microbial inoculum, volatile fatty acids (VFAs) accumulate in the medium, causing a drop in pH and reducing methanogenic activity (Dixon et al., 2007). During overloading, gas production initially increases before abruptly decreasing. This is because process imbalance takes time to manifest. During extreme overloading, methane concentration decreases as CO_2 concentration rise, owing to the inability of H_2-using methanogens to consume CO_2.

Paudel et al. (2017) showed that OLR of 1.24 gVS/L/d was optimal for methane production and organic removal in a two-stage continuously stirred tank reactor operating at 37 °C. Also, a study conducted in Pennsylvania on a 100 m^3 biogas plant operating on manure found that increasing the OLR from 346 kgVS/d to 1030 kgVS/d increased gas yield from 67 to 202 m^3/d (Gashaw, 2014). On the other hand, El-Mashad et al. (2008) discovered that the digester treating food waste was not stable at the OLR of 4.0 gVS/L/d or the reduced OLR of 2.0 gVS/L/d because it contained high concentrations of volatile fatty acid and produced low biogas. According to Ahring et al. (1995), acetate accumulated faster than any other VFA after organic overloading. Therefore, there is an optimum feed rate for a specific size of plant that will produce the most gas and beyond which further increases in substrate quantity will not produce more gas proportionately (Gashaw, 2014).

2.7.13 Hydraulic Retention Time (HRT)

The hydraulic retention time (HRT) is the time that microorganisms spend consuming and synthesizing substrates in a digester (Siddique and Wahid, 2018). The required retention time for the completion of the AD reactions varies depending on the technology, process temperature, microbe nature, and waste composition (Matheri et al.,

2017). Although a short retention time is desired to reduce digester volume and investment cost, a trade-off must be struck to achieve the desired operational conditions, which maximize either methane production or organic matter removal (Li et al., 2015a). If the HRT is shorter than the microbe generation times, the microbes are washed out, failing the AD system (Dareioti and Kornaros, 2015). Hence, the longer a substrate is exposed to the reaction conditions, the more complete its degradation becomes (Gashaw, 2014).

Moreover, Xie et al. (2017a) report that increasing HRT increases the concentration of VFAs. Furthermore, Gashaw (2014) claims that the reaction rate decreases as the residence time increases. An excessively long HRT may result in nutrient deficiency and the eventual death of microorganisms (Siddique and Wahid, 2018). It is reported that HRT in tropical countries ranges from 30 to 50 days, while in colder climates, it can reach 100 days (Gashaw, 2014). Paudel et al. (2017) also reported an optimal HRT of 8 hours and 20 days in the acidogenic and methanogenic stages for maximum hydrogen and methane production.

2.7.14 Volatile Fatty Acids (VFAs)

VFAs are acidogenesis intermediates formed from monomers such as monosaccharides, amino acids, and long-chain fatty acids (Fisgativa et al., 2016). It contains acetic, propionic, butyric, and in some cases, valeric and caproic acid. The levels of acetic acid to propionic acid, in particular, make a strong statement about the stability and efficiency of the AD process (Scherer, 2007). The production of VFAs in the early stages of digestion may lower the pH in the digester and inhibits microorganism methanogenic activity (Anggarini et al., 2015). If acetogens do not develop sufficiently to consume the available VFA due to TAN inhibition, VFA may accumulate in the digester (Fisgativa et al., 2016).

Additionally, the washout of microbes caused by high OLR may result in system acidification, given that acidifying microorganisms grow faster than methanogens (Drosg et al., 2013). The accumulation of VFAs indicates that the inhibition of the

methanogenesis process has begun (Xie et al., 2017a). Nonetheless, in anaerobic co-digestion systems with a high buffering capacity, microbial communities, particularly the indigenous community of methanogenic archaea, can withstand high VFA concentrations (Franke-Whittle et al., 2014).

According to Bedoić et al. (2020), the inhibition threshold for VFAs in food waste is 16.5–18.0 gCH_3COOH/L. A proper balance of carbohydrates and proteins and proper pH control are required to avoid inhibition from VFA concentrations (Capson-Tojo et al., 2017, 2016). Nasrin et al. (2021) found that initial VFA concentrations ranged between 0.16 and 0.21 g/L for all test groups in their study of kitchen waste (KW) with varying TS content. After fermentation, the final VFA values of KW at various TS contents ranged between 0.27 and 0.90 g/L. To allow anaerobic fermentation to proceed normally, the concentration of volatile fatty acids, mainly acetic acid, should be less than 2000 mg/l (Yadvika et al., 2004). Similarly, Nandi et al. (2020) assert that VFA concentrations greater than 3 g/L may cause process failure.

2.7.15 Alkalinity

Alkalinity can be described as the ability of a system to buffer against acidification. It measures the liquid capacity of the reactor to neutralize acids by absorbing hydrogen ions without causing a significant pH change. A solution's buffer capacity is linked to the presence of acid-alkaline pairs. It is thus significantly impacted by carbonate and bicarbonate presence, VFAs, phosphate, and ammonia. Alkalinity is lost by the production and accumulation of VFAs (Fagbohungbe et al., 2017). Because of the positive Gibbs free energy, which is considered the rate-limiting step of anaerobic digestion, the degradation rate of VFAs such as propionate and butyrate is generally slow (Zhang et al., 2018b). As a result, alkaline chemicals such as sodium bicarbonate, sodium hydroxide, sodium carbonate, and sodium sulphide are commonly used to control severe acidification and maintain a suitable pH (6.8–7.2) for CH_4 production (Zhang et al., 2018b; Esposito et al., 2012).

Some feeds have a relatively high buffer capacity to compensate for minor pH changes. Hence, it may be impossible to detect initial acid accumulation in some

substrates, such as manure, by measuring pH. According to Scherer (2007), liquid manure has a buffer capacity of up to 21000 mg$CaCO_3/L$, which helps to stabilize the anaerobic digestion process. If the raw material's alkalinity is relatively constant, an increasing acid accumulation in the anaerobic digestion process can only be detected if the alkalinity is measured. VFA consumes alkalinity before a drop in pH can be directly detected. However, the pH value should not be used as a process stability indicator in a well-buffered system since changes in pH caused by VFA accumulation are constantly controlled (Björnsson et al., 2000). Filer et al. (2019) recommend that alkalinity be kept at around 3000 mg$CaCO_3/L$ to maximize methane yield.

2.7.16 VFA/Alkalinity Ratio

According to Feng et al. (2013), the VFA/Alkalinity ratio has three critical levels used in assessing the stability of anaerobic digestion: (1) 0.4 is stable; (2) 0.4–0.8 may exhibit some instability; and (3) >0.8 indicates significant instability. As a result, the inoculum and substrate volumes used to prepare the slurry have to be adjusted during the planning stage to be less than the first critical level, which is 0.4.

2.7.17 Ammonia and Ammonium

Ammonia is produced as a byproduct of the biological breakdown of nitrogenous matter (Yenigün and Demirel, 2013). It is essential to distinguish between two types of inorganic ammonia nitrogen that are commonly found during fermentation. The first is total ammonia nitrogen (TAN), which refers to both ammonia $(NH_3 - N)$ and ammonium $(NH_4 - N)$ nitrogen that is present in the liquid phase during the process (Bedoić et al., 2020; Yenigün and Demirel, 2013). The second type is free ammonia which is the concentration of unionized ammonia (NH_3) in the same liquid phase (Bedoić et al., 2020). Free ammonia is undissociated and toxic (Mata-Alvarez, 2002). According to Miron et al. (2000), ammonia inhibition is caused by free ammonia, which easily permeates cell membrane.

The toxicity limits for free ammonia described in literature varies greatly, with concentrations ranging from 50 to 1,500 $mgNH_3 - N/L$ (Krakat et al., 2017). On the contrary, Pind et al. (2003) report a wide range of ammonia inhibition between 2500

– 11000 $mgNH_3 - N/L$. Also, Yirong et al. (2017) have shown ammonia inhibition threshold concentrations ranging from 2000 to 6000 $mgNH_3 - N/L$. Furthermore, when the total nitrogen concentration exceeds 5,000 $mgNH_3 - N/L$, the hydrolysis and acidogenesis conversion ratio decrease (Krakat et al., 2017). However, ammonia concentrations less than 200 $mgNH_3 - N/L$ are said to be beneficial to the AD process (Gashaw, 2016). Hence microorganisms cannot thrive in substrate containing ammonia concentrations greater than 200 $mgNH_3 - N/L$, and methanogens are the least tolerant and easily killed by ammonia inhibition (Gashaw, 2016). Euryarchaeota (methanogens) are the anaerobic degrading microorganisms most affected by elevated ammonia levels (>1,800 $mgNH_3 - N/L$) and the first to be inhibited (Krakat et al., 2017).

When bacteria degrade proteins, ammonium ions are released. Although ammonium serves as a nitrogen source for microbial growth, it may also inhibit methanogenic metabolism (Procházka et al., 2012). According to Gashaw et al. (2014), ammonium is less toxic than ammonia and only disrupts bacterial activity at extremely high concentrations. Bacterial growth is inhibited at ammonium concentrations ranging from 1,500 to 10,000 $mgNH_4 - N/L$, while 30,000 $mgNH_4 - N/L$ is toxic (Sumardiono et al., 2013). Inhibition levels of 1700-14000 $mgNH_4 - N/L$ have been reported by Krakat et al. (2017) and Chen et al. (2008).

2.8 Anaerobic Reactors

An anaerobic reactor is a closed tank where various biochemical processes, such as fermentation, occur under controlled conditions. Because the system is closed, optimal conditions and process regulation and control are possible. Multiple reactors have emerged over time, emphasising the kind of waste to be anaerobically treated. Anaerobic digesters are classified based on several factors, including whether the biomass is attached to a surface (attached growth) or can freely mix with the reactor liquid (suspended growth). The number of stages and total solids concentration in the reactor can also classify the reactor. Anaerobic reactors can be batch or continuous, wet, semi-dry, dry, single, double, or multi-phase. The wet anaerobic digestion system contains 15-30 % TS, while the dry system contains 30-60 % TS (Muhammad Nasir et al., 2012).

According to Muhammad Nasir et al. (2012), the wet anaerobic system can use waste directly as received. In contrast, the dry anaerobic system requires waste water content to be reduced to about 12 % of total solids. Dry anaerobic digestion produces less methane and has a lower VS reduction than wet anaerobic digestion due to VFA transport limitations (Nagao et al., 2012). Anaerobic reactors include; (a) Conventional Reactors such as the Anaerobic Sequencing Batch Reactor, Continuous Stirred Tank Reactor and Anaerobic Plug-Flow Reactor (b) Sludge retention reactors such as Anaerobic Contact Reactor, Up-Flow Anaerobic Sludge Bed Reactor, Up-Flow Anaerobic Solid-State Reactor, Anaerobic Baffled Reactor and Internal Circulation (c) Anaerobic Membrane Reactors such as Anaerobic Filter Reactor, Anaerobic Fluidized Bed Reactor and Expanded Granular Sludge Blanket (Saitawee et al., 2014).

2.9 Biochemical Methane Potential

The biochemical methane potential test has been widely accepted by academic researchers and technical practitioners for determining the maximum methane production of various substrates (Filer et al., 2019; Hafner et al., 2018; Ariunbaatar et al., 2016). The methane produced in the batch assay by the mixture of substrates and active anaerobic inoculum is recorded until the methane production reduces to small volumes and eventually stops (Holliger et al., 2016; Angelidaki et al., 2009). The test is inexpensive and easy to repeat. Biodigestibility, biodegradability, bioavailability, reaction-rate kinetics, anaerobic activities, and inoculum influence can be assessed using BMP tests (Wang et al., 2017a).

The first protocol for BMP tests was proposed in 1979 (Owen et al., 1979). Since then, several additional guidelines have been proposed (VDI, 2006; Holliger et al., 2016; Angelidaki et al., 2009). In contrast to chemical (e.g., pH and COD) and biochemical (e.g., BOD) parameter testing, no standardized procedure or information is available for BMP tests (Rice et al., 2012). There have been numerous suggested international and national protocols, each requiring its own set of serum bottles, test inoculum, food-to-microorganism ratios, nutrients, and methane measurement tools (Filer et al., 2019). Furthermore, most methodologies lack transparency in experimental design. For instance, test setup data, such as slurry volumes used (mainly not shown

in some papers), COD mass balance, or the number of bottles used, would be helpful for new labs as a comparison model (Filer et al., 2019).

Results from BMP tests can be used to characterize and evaluate the optimal design and performance of the anaerobic co-digestion process (Da Silva et al., 2018). BMP testing has therefore become an important study in assessing the feasibility of implementing and optimizing (e.g. Co-digestion) a full-scale plant (Lippert et al., 2018; Koch et al., 2016). Holliger et al. (2016) compared the volume of methane predicted by BMP data to the volume of methane measured onsite from a full-scale installation over a 7- to 9-month period. The authors discovered that the BMP weekly methane production rates were comparable and followed a similar pattern. Furthermore, Li et al. (2017) found that BMP degradation rate information could be used as a practical tool for evaluating process performance in full-scale biogas processes. Nonetheless, BMP tests can take a long time, ranging from 20 days to more than 100 days for different substrates (Raposo et al., 2012).

Even though many guidelines for BMP testing have been proposed, results published in peer-reviewed journals show that critical experimental design or execution flaws are still common (Koch et al., 2019). Koch et al. (2019) proposed a powerful but simple method for evaluating the quality of BMP measurements. While predicting the methane potential of an unknown substrate is difficult, Koch et al. (2019) hypothesized that the specific methane production (SMP) curve for most substrates should have a similar shape. Significant deviation from this typical response indicates issues that must be addressed to obtain reliable results. So far, the German VDI 4630 is the only BMP guideline that discusses, albeit briefly, the typical shape of SMP curves.

Furthermore, the guideline only provides hypothetical idealized curves rather than actual measurements, and it is unclear what might cause each response. To demonstrate this concept and establish relationships between flaws in experiments, SMP curves, and BMP values, Koch et al. (2019) reproduced some common experimental mistakes. The flaws investigated were inoculum storage (2 weeks at various temperatures), inoculum dilution with water (no dilution to 1:2 dilution), and inoculum-to-substrate ratio (from

2.00 to 0.05). SMP curves were evaluated using common kinetic models. All flaws affected the SMP curves, but excessive dilution and meagre inoculum-to-substrate ratio had the most outstanding effects on the SMP curves and the BMP curves (Koch et al., 2019). There was a clear lag phase of more than ten days in the most extreme case (ISR of 0.05), and the resulting BMP was 15 % lower than in the reference case.

2.9.1 Compulsory Elements for the Validation of BMP Test Results

Validation criteria for obtained results have been documented by Holliger et al. (2016). The validation criteria either define a positive control's methane yield range or focus on the relative standard deviations among replicates to guarantee high test reproducibility (Koch et al., 2019). The conditions below must be met for BMP test results to be validated (Holliger et al., 2016);

(i) All tests must be performed in at least three duplicates.

(ii) In addition, blank assays (background methane production from the inoculum) and (or) positive controls (e.g., microcrystalline cellulose, tributyrin) must be performed.

(iii) The duration of the BMP tests should not be predetermined, and trials should only be terminated when daily methane production during three consecutive days is <1 % of the accumulated volume of methane (i.e., BMP 1 %);

(iv) The BMP is expressed as the volume of dry methane gas under standard conditions (273.15 K and 101.33 kPa) per mass of volatile solids (VS) added, with the unit $NLCH_4$ kg/VS;

(v) The BMP of the substrate and the positive control is determined by subtracting the methane production of the blanks from the gross methane production of the substrate/positive control assays;

(vi) For the calculation of the BMP of the substrate and the positive control, the standard deviation of the blanks must be taken into account

2.9.2 Criteria for Test Results Rejection

Test results must be rejected if at least one of the following criteria is met (Holliger et al., 2016);

(i) If the relative standard deviation (RSD) of the blank or the positive control is greater than 5 %, even after applying a statistical test to eliminate a single outlier

(ii) If the RSD of a homogenous substrate is greater than 5 %, even after applying a statistical test to eliminate a single outlier

(iii) If the RSD of a heterogeneous substrate is greater than 10 %, even after using a statistical test to remove a single outlier

(iv) If the BMP of the positive control is less than 85 % and greater than 100 % of the theoretical

Several inoculum-substrate ratios (ISRs) should be tested in parallel if substrate inhibition is suspected. Indicative values for operational parameters of the digester that are most likely to provide a high-quality inoculum are:

(i) pH: between 7.0 and 8.5

(ii) VFA: less than 1.0 gCH_3COOH/L

(iii) NH_4^+: less than 2.5 $gN - NH_4/L$

(iv) Alkalinity: greater than 3 $gCaCO_3/L$

2.10 Mono and Co-digestion

In the AD process, one or more substrates can be used to produce biogas. Mono-digestion uses a single feedstock or substrate, whereas co-digestion refers to the simultaneous use of two or more substrates or feedstocks. Based on their VS contents, the feedstock with the greater mixture content in a co-digestion process is considered the main substrate, while the one with the lower content is regarded as the co-substrate (Chiu and Lo, 2016). Several studies on anaerobic mono-digestion with different biomasses have been conducted; however, direct utilization of a single substrate

is difficult due to nutritional imbalance, a lack of diverse microorganisms, and the effect of operational factors (Hagos et al., 2017). As a result, the anaerobic co-digestion technique is recommended.

Co-digestion, also known as "co-fermentation," is a promising option for overcoming the drawbacks of mono-digestion and improving the economic viability of AD plants due to increased methane production (Gashaw, 2014; Mata-Alvarez et al., 2014). Some key characteristics, such as co-substrate composition and induced inhibitors, may impact the anaerobic co-digestion system (Xie et al., 2016). The primary benefit of co-digestion is the increased yield of biogas. Biogas production can be increased by up to 400% depending on the substrate type, concentration, and flow rate (Cavinato et al., 2010; Alatriste-Mondragón et al., 2006).

Co-digestion improves the synergistic effects of fermentative bacteria while also accelerating the hydrolysis rate (Xu et al., 2018; Ebner et al., 2016). Additionally, co-digestion digesters can operate at organic loading rates (OLR) and volatile fatty acid (VFA) concentrations as high as 10 $kgVS/m^3/d$ and 8 g/L, respectively (Shah et al., 2015). Furthermore, other authors have demonstrated that co-digestion reduces hydraulic retention time, HRT (Matheri et al., 2017). In addition, the process is advantageous as shown below (Shah et al., 2015; Astals et al., 2014; Mata-Alvarez et al., 2014);

(i) Enhances process stability and nutrient balance

(ii) Inhibitory/toxic substances are diluted and buffer capacity boosted

(iii) Improves synergistic effects of microorganisms

(iv) Increases biodegradable organic matter load

(v) Encourages economic benefits from sharing apparatus and costs

Co-digestion studies of sewage sludge and food waste have been shown to be effective due to the balancing of the high nitrogen content with the carbon content of food waste (Chua et al., 2013). Soyingbe et al. (2019) concluded that co-digesting faecal

sludge with various types of organic feedstock materials effectively produced biogas and nutrient-rich bio-slurries as organic fertilizer. According to Yusuf et al. (2011), co-digesting substrates stabilize the feed, thereby improving the C/N ratio and decreasing nitrogen concentration. Using a co-substrate with low nitrogen and lipid content is likely to reduce the problems associated with the accumulation of intermediate volatile compounds and high ammonia concentrations (Khalid et al., 2011).

Lavagnolo et al. (2017) investigated the co-digestion of brown water and kitchen waste. The study discovered that the mixtures performed significantly better than the individual substrates, with a maximum methane yield of 520 $mlCH_4/gVS$. Similarly, a batch co-digestion of sanitary wastewater and kitchen waste with different mix ratios of 100:0, 75:25, 50:50, 25:75, and 0:100 by volume at room temperature for 30 days revealed that the highest biogas yield was obtained from a mix ratio of 25:75, and the lowest from a mix ratio of 0:100 (Minale and Worku, 2014). Furthermore, Rajagopal et al. (2013) discovered that batch anaerobic co-digestion of brown water and food waste generated more methane (0.54–0.59 LCH_4/gVS_{added}) than individual substrates. Adding a co-substrate (e.g., brown water) to food waste could improve the stability of the anaerobic digestion process by providing additional nutrients and maintaining buffer capacity, according to Lim et al. (2013). Table 2.4 shows co-digestion conditions and results for human excreta and or food waste in previous studies.

Despite its benefits, anaerobic co-digestion is a complex organic waste treatment process, and permanent solutions for its stability and optimization are yet to be discovered (Hagos et al., 2017). Because of its high biodegradability, organic loading

Table 2.4: Co-digestion Conditions and Results for Human Excreta and or Food Waste in Previous Studies (NR means Not Reported)

Feedstock	Vial Volume (ml)	Inoculum	Temperature (°C)	pH	Mixing (rpm)	Duration (days)	Biogas yield (ml/g VS)	Methane yield ($mLCH_4$/g VS)	Reference
Untreated Food Waste	400	Municipal andbIndustrial Biowastes	37	8	84	35	NR	501	Tampio et al. (2014)
Autoclaved Food Waste	400	Municipal andbIndustrial Biowastes	37	8	84	35	NR	445	Tampio et al. (2014)
Food Waste	250	NR	35	NR	150	70	NR	247	Kim et al. (2014)
Feaces	250	NR	35	NR	150	70	NR	220	Kim et al. (2014)
Feaces and Food Waste	250	NR	35	NR	150	70	NR	254	Kim et al. (2014)
Feacal Sludge	500	Anaerobic Digester Effluent	35	7.74	NR	33	NR	242	An et al. (2017)
Human Excreta	500	Digested Sewage Sludge	35	7.36	20	25	NR	254	Fagbohungbe et al. (2015)
Food Waste	500	NR	38	7.18	100	28	940	496	Bodík and Miroslavakubaská (2014)
Food Waste	125	Anaerobic Digester Effluent	32	7.5	NR	40	897	NR	Prabhu et al. (2015)
Septage	125	Anaerobic Digester Effluent	32	7.5	NR	40	96	NR	Prabhu et al. (2015)
Food Waste and Septage (1:1)	125	Anaerobic Digester Effluent	32	7.5	NR	40	693	440	Prabhu et al. (2015)
Food Waste and Septage (2:1)	125	Anaerobic Digester Effluent	32	7.5	NR	40	818	444	Prabhu et al. (2015)
Food Waste	610	Cow manure	37	NR	90	45	370	229	Paritosh et al. (2017)
Food Waste	500	Sewage Treatment Sludge	35	NR	80	30	NR	400-420	Rajagopal et al. (2013)
Brown Water	500	Sewage Treatment Sludge	35	NR	80	30	NR	260-300	Rajagopal et al. (2013)
Food Waste and Brown Water	500	Sewage Treatment Sludge	35	NR	80	30	NR	300	Rajagopal et al. (2013)
Food Waste, Cow Dung and Food Oils	1000	NR	35	NR	NR	35	2914	NR	Hussien et al. (2020)
Food Waste	300	Wastewater Treatment Effluent	35	4.6	NR	63	943	NR	Muratçobanoğlu et al. (2020)
Cow Dung	300	Wastewater Treatment Effluent	35	7.2	NR	63	699	NR	Muratçobanoğlu et al. (2020)
Domestic Sewage Sludge and Food Waste	500	Palm Oil Mill Effluent	37	NR	100	12	NR	620	Sulaiman and Seswoya (2019)
Cow Dung	500	Cow Dung	35	NR	NR	45	193	NR	Venkateshkumar et al. (2020)
Food Waste and Brown Water	30000	Anaerobic Treatment Sludge	37	7-7.5	NR	20	NR	700	Paudel et al. (2017)
Food Waste and Sludge	500	Anaerobic Treatment Sludge	30	NR	NR	30	660	NR	Latha et al. (2019)
Kitchen Waste and Brown Water	120	Anaerobic Treatment Sludge	35	7	NR	28	NR	520	Lavagnolo et al. (2017)
Food Waste and Brown Water	5000	Anaerobic Treatment Sludge	35	NR	80	150	1540	924	Lim et al. (2013)
Kitchen Waste and Sanitary Waste Water	5000	Cow Manure	25	7.2	NR	30	65600	NR	Minale and Worku (2014)
Human Excreta,Food Waste and Toilet Paper	120	Digested Sewage Sludge and Food Waste	35	NR	Manual Shaking	40	NR	350	Kim et al. (2019b)
Kitchen Waste, Food, Fruit,Vegetable Waste	500	Digested Sludge	37	8	NR	28	614	354	Li et al. (2020a)

rates in co-digestion must be carefully monitored, especially when co-digesting food waste with manure or leachate, which can lead to process saturation and failure (Chen et al., 2010a). Rajagopal et al. (2013) described the disadvantages of co-digesting brown water and food waste, with the authors observing higher biogas production and biodegradation efficiencies for the mono-digestion. The biogas yields obtained for brown water, food waste, and their mixture were 876, 421, and 300 L/kgVS added, respectively. The results showed that brown water produced the highest amount of biogas, methane and VS reduction. The lower biogas yield of the mixture shows that the addition of food waste inhibited the process (Lim, 2011).

Furthermore, due to differences in metabolic properties, nutritional requirements, growth rates, and optimal operational factors, co-digestion in a one-stage digester is difficult (Hubenov et al., 2015). To overcome the challenges and complexities of the anaerobic co-digestion process, it is critical to design appropriate reactors, develop characterization methods, and categorize organic materials based on their biodegradability, accessibility, and availability (Hagos et al., 2017).

2.10.1 Inoculum to Substrate Ratio

The inoculum to substrate ratio (IRS) is an important parameter for assessing the anaerobic biodegradability of solid wastes, specifically the degradation of VS of organic material (Ahou et al., 2021). Because of the different compositions of the microbial consortia within inoculum, the source of inoculum is considered to have a significant role in substrate degradation efficiency, particularly for the complex mix of substrates (Dechrugsa et al., 2013). Some experimental data have shown that the ultimate methane yields and rates of methane production are dependent on the inoculum used, specific substrates and optimum proportions used (Yoon et al., 2014; Eskicioglu and Ghorbani, 2011). Beyond a certain threshold, the use of more inoculum in the anaerobic digestion process has no significant effect on biogas generation (Rakić et al., 2022). Furthermore, excessive inoculum use increases digester volume unnecessarily (Sri Bala Kameswari et al., 2012).

Owen et al. (1979) proposed an ISR of 1 as a baseline for the organic fraction of solid waste. Also, Rakić et al. (2022) discovered that an ISR ratio of 1.0 was optimal. However, some authors state that for some substrates, increasing the ISR to 2 may be required (Raposo et al., 2011; Chynoweth et al., 1993). VDI (2006) recommends determining methanogenic power using an ISR ratio greater or equal to 2 (% volatile matter basis). Fagbohungbe et al. (2015) also found that the ISR of 2 produced the most methane of 254 $mlCH4/gVS$ and the most pathogen removal with values of 2.7×10^4 and $2.5 \times 10^3 CFU/ml$, respectively, for E.coli and faecal coliform bacteria. Except for the ISR of 2, all other ISR conditions saw significant reductions in methane production after 24 hours. The increase in methane production rates was sustained in the ISR of 2 for 96 hours before plateauing (Fagbohungbe et al., 2015).

Given that an ISR greater than or equal to 2 has never been reported as inhibitory, Raposo et al. (2011) propose making this ratio mandatory for standardized tests. The German standard VD1 4630 recommends substrate concentrations of around 10 g VS/L with inoculum concentrations of 1.5 to 2 % to achieve an inoculum to substrate ratio of 2 (Raposo et al., 2012). According to Rodriguez-Chiang and Dahl (2015), the lower the ISR, the longer the period over which methane is produced. Alternatively, the higher the ISR, the earlier the maximum production rate peaks are observed. This could be due to the higher microbial activity present when a more significant amount of inoculum is used at higher ratios. Hence, increasing the ISR increases the number of active methanogens in the inoculum, reducing the time for a sufficient methanogenic population to grow to initiate methanogenic activity.

Furthermore, the tested substrate determines the optimal ISR (Rakić et al., 2022). According to Holliger et al. (2016), VS-based ISRs should be between two and four for most applications. To limit acidification reactions in highly degradable substrates with diverse microbial dynamics, such as food waste, a high Inoculum-to-Substrate Ratio (ISR) (greater than or equal to four) is usually required (Lü et al., 2012). More substrate dilution, equivalent to increasing ISR, may help improve practical methane yield (Dechrugsa et al., 2013).

Although this is a good starting point for ISR selection, different substrates and inoculum may react differently (Elbeshbishy et al., 2012). Large inoculation volumes have been found to ensure high microbial activity, low risk of overloading, and low inhibition risk (Angelidaki and Sanders, 2004). These findings are consistent with those of Raposo et al. (2008), who reported that a significant change in inoculum to substrate ratio could result in differences in biogas production. There are two general rules to follow when narrowing down the ISR options. One suggestion is that for readily biodegradable substrates, the inoculum volume should be greater than the substrate or an ISR greater than or equal to 2 be used to reduce acidification or inhibition problems (Liu, 1996).

The second rule is that an ISR less than 2 should be used for substrates with a high content of non-biodegradable organics. However, regardless of these guidelines, a series of ISRs for a new substrate should be tested to obtain consistent BMP values (Yoon et al., 2014). Hashimoto (1989) discovered a significant reduction in biogas yield for batch fermentation of wheat straw using ISR less than 0.25. Similarly, an ISR of 0.25 resulted in the lowest methane yield (110 $mlCH_4/gVS$) and pathogen removal values (Sri Bala Kameswari et al., 2012). This demonstrates that when ISR decreases, methanogenic activity slows, resulting in a decrease in biogas generation. According to Sri Bala Kameswari et al. (2012), increasing ISR from 0.25 to 2.30 resulted in 145–391 ml of biogas generation per gram of VS added. In addition, increasing the ISR from 0.50 to 1.00 resulted in a significant increase in biogas generation. Furthermore, when ISR was increased from 1.00 to 2.30, biogas generation increased by 1.5–2.12 % (Sri Bala Kameswari et al., 2012).

Zhou et al. (2011) added to the consensus by reporting that ISRs between 1 and 3 were the most effective for AD operation and methanogenesis. Furthermore, ISRs 2 and 1 appeared to have the shortest residence times, whereas ISRs 0.5, 0.3, and 0.25 had increased residence times of 2, 6, and 15 days, respectively. Cabbai et al. (2013) confirm ISR 3 as a good ratio for equilibrated anaerobic process conduction. Regardless, Moset et al. (2015) demonstrated that the impact of the ISR in the range of 0.25-2.5 gVS is substrate type dependent.

2.10.2 Human Excreta

Human excreta (HE) is the general term for the raw (or partially digested) slurry or solid that a person passes. It comprises of varying concentrations of settled solids and other non-faecal matter (Jeuland et al., 2004), and its management is a significant problem in most sub–Sahara African countries, including Ghana. However, HE may hold the key to energy security and employment creation as it contains resources that can be mined for valuable purposes (Fanyin-Martin et al., 2017). Each day, humans excrete in the order of 30 g of carbon (90 g of organic matter), 10×10^{12} g of nitrogen, 2 g of phosphorus and 3 g of potassium (Strauss et al., 2003). The source, physical composition, storage, oxygen availability during storage, temperature and moisture content influence the quality of HE.

2.10.3 Food Waste

Food waste (FW) is the discarded foodstuff, mainly consisting of unsold food, food preparation leftovers and uneaten food from households, restaurants and large producers such as collective caterers and supermarkets (Mao et al., 2015). Both developed and developing nations have between 15 and 63 % of their municipal waste streams being FW (Zhang et al., 2014). FW is typically a heterogeneous substrate, comprising proteins, lipids, carbohydrates, organic acids, traces of inorganic compound and fibers that contain both readily fermentable and refractory complex organics (Luo and Angelidaki, 2012). It has high moisture content (MC), high content of volatile organic solids, and it is a readily biodegradable organic substrate (Paritosh et al., 2017).

The mono-digestion of FW is easy to acidify, inhibiting methanogens and producing less methane (Lin et al., 2011). According to Chua et al. (2013), the microbial population in a co-substrate like sludge is able to digest food waste and cause a quick enhancement in waste degeneration. In addition, it increases the nutrient level and adds moisture to the rather solid household food waste content (Spierling, 2011). Ikpe et al. (2019) studied the biogas yield of different food substrates such as beans, rice, yam, fufu, ripe plantain, gari, corn, unripe plantain, sweet potatoes, banana, pineapple and water melon. Gari yielded the highest raw biogas of 140 g and highest purified biogas

of 110 g. This was followed by fufu and yam which yielded raw biogas of 120 g and purified biogas of 90 g. Among the aforementioned substrates digested, sweet potatoes had the lowest raw biogas yield of 70 g with the lowest purified biogas yield of 50 g.

Nasrin et al. (2021) assessed the methane potential of kitchen waste at different total solids (TS) content. Kitchen wastes such as spoiled rice, brinjal, potato, papaya, tomato, fish and poultry parts, which are easily decomposed, were selected for this study. Batch experiments were set up under ambient temperature. Kitchen waste was added to the batch digester at different TS content (5, 7, 10, 12 and 15 %) and sealed for 146 days until the gas production stopped. Substrate characteristics were analyzed before and after the anaerobic digestion. The highest methane yield was 78.12 L/kg VS at 15 % TS content followed by 12, 10, 7 and 5 % (Nasrin et al., 2021).

Kitchen residue (KR) and fruit and vegetable waste (FVW) are a major part of food waste from households. KR comprises bits of food peels and residues left before cooking in kitchens (Li et al., 2020a). KR can be utilized to produce biogas due to its high biodegradability, calorific value and nutritive value to microbes (Iqbal et al., 2014). That notwithstanding, KR has a low buffering capacity. Therefore, at a lower ISR poor methane production performance was found (Li et al., 2013). FVW, on the other hand, are the waste generated from fruits and vegetables mainly in the markets and households. FVW is characterized by high-volatile solids and biodegradability (Ward et al., 2008).

FVW contain 8–18 % total solids (TS), with a total volatile solids (VS) content of 86–92 % (Bouallagui et al., 2005). The organic fraction includes about 75 % easy biodegradable matter (sugars and hemicellulose), 9 % cellulose and 5 % lignin. The COD/N ratio of FVW is balanced, being around 100/4 (Bouallagui et al., 2005). Moreover, FVW is a kind of high C/N biowaste, and KR has a low C/N which can lead to poor stability of digesters (Vats et al., 2019; Wang et al., 2014c). Li et al. (2020a) showed that co-digestion with FVW and KW could improve methane production.Co-digestion of FVW and KR or food leftovers (FLO) has been proposed (Wang et al., 2014c; Lin et al., 2011). However, the feasibility of tri-digestion with these three

wastes and comparison of microbial community change in anaerobic mono, co and tri-digestion are unclear.

Longjan and Dehouche (2020) studied the anaerobic digestion of food wastes such as yam peel, cassava peel, cocoyam peel and plantain peel. Of all the samples tested, yam peel was shown to have the highest biogas potential. In contrast, cassava peel has the lowest bioenergy potential due to its cyanide content, which is toxic to anaerobic digestion microbes. Also, preliminary study on biogas production of cassava peels showed their low biogas potential probably as a result of its toxic cyanogenic glycosides content (Cruz et al., 2021; Aisien et al., 2020). Also the drop in pH at the beginning of the AD process of cassava causes the death of microbial methanogens due to rapid acid formation (Kohmuean et al., 2020).

2.11 Role of Additives in Anaerobic Co-Digestion

AD treatment of biowastes is mainly faced with intermediate inhibition, system instability, and low methane yield (Shen et al., 2020). Many attempts have been made to increase gas production during the biogas AD process, and one of such is the introduction of accelerants or additives (Mao et al., 2015). The adsorption of a substrate on the surface of such additives results in localized substrate concentration, favorable conditions for microbe growth, and rapid gas production. Additives come in several types, namely;

(i) Greenery biomass (e.g., algae).

(ii) Biological additives (fungi, enzymes, microbial consortium): In contrast to fungal activity, a microbial consortium basically causes an incremental availability of cellulose and hemicellulose as well as digestibility.

(iii) Inorganic additives: Chemical reagents such as alkali, acid and oxidative reagents as well as inorganic salts, zeolite, macro nutrients and trace elements.

(iv) Carbon-based accelerants: Ggraphene, carbon nanotube, biochar, activated carbon, carbon cloth and carbon felt.

For the purposes of this study, biochar is further reviewed.

2.11.1 Biochar

Recent research has shown that biochar, a by-product of biomass pyrolysis, is a viable substitute for the industrial-grade carbon-based adsorbent employed in AD (Shen et al., 2020; Masebinu et al., 2019). Biochar is extensively explored as a functional carrier in AD processes because it has a specific surface area and lots of pores in comparison to conventional carriers as zeolite, clay, ceramic, and plastic materials (Ye et al., 2018). Results of previous studies and recent reviews indicate that the use of biochar effectively shortens the lag phase of the AD process, improves methane production and alleviates inhibiting stress by acting as sorbent for hydrophobic inhibitors (Shen et al., 2020; Luo et al., 2015). It also focuses on essential mechanisms such as microbial immobilization, interspecies electron transfer, buffer potential and nutrient retention (Zhang et al., 2018b).

In addition to substrate type and inoculum characteristics, biochar dosage, properties, and particle size greatly influence AD performance (Pan et al., 2019). However, Shao et al. (2019) asserts that the ability of biochar to facilitate anaerobic digestion is restricted to stressed surroundings. This section summarizes the influence of biochar in enhancing and equilibrating the hydrolysis, acidogenesis, acetogenesis, and methanogenesis stages of AD. Also, its ability to serve as a conduit for bioelectrical connections, support microbial colonization and reinforce buffer capacity is discussed (Pan et al., 2019).

2.11.2 Definition and Origin

Biochar is a solid carbonaceous material obtained from the thermochemical conversion of biomass in an oxygen-depleted environment (Tan et al., 2017). Biochar consists of fixed carbon, labile carbon and other volatile compounds, in addition to moisture and ash components (Quan et al., 2016). Biochar application started with it being used for soil amendment. For some time now, biochar has been utilized in anaerobic digestion as an additive. The significant mechanisms of biochar studied for its effective functions are associated with its favourable physico-chemical properties, such as high CEC, large porosity, and surface area (SA) (Sanchez-Monedero et al., 2018).

2.11.3 Biochar Production and Characterization

The production of biochar is influenced by various process parameters such as temperature, residence time, heating rate, and pressure, which impact its yield, properties (amorphous or porous, shape, size), and quality (chemical composition) (Tripathi et al., 2016). Furthermore, the composition, structure, and inherent binding of the original biomass also play a role in determining the physicochemical properties of biochar (Ruan et al., 2019). Biomass used in biochar production primarily consists of cellulose, hemicellulose, lignin, along with smaller amounts of pectin, protein, extractives, and ash (Fabbri and Torri, 2016). Typically, cellulose, hemicellulose, and lignin account for 40-60 %, 20-40 %, and 10-25 % of the biomass material on a dry basis, respectively (Quan et al., 2016).

During thermal decomposition, the structural components of biomass (cellulose, hemicellulose, and lignin) undergo a series of reactions, including dehydration, cross-linking, depolymerization, fragmentation, rearrangement, repolymerization, condensation, and carbonization at different temperatures (Qambrani et al., 2017). Thermochemical conversion techniques like hydrothermal carbonization (HTC), torrefaction, pyrolysis (Py), and gasification (Gs) are commonly employed for biomass treatment, each requiring specific temperature ranges as shown in Table 2.5 (Luz et al., 2018).

Table 2.5: Product yield of biomass combustion on a dry basis.((Li et al., 2020b; Masebinu et al., 2019; Luz et al., 2018))

Feedstock Process	Temperature (°C)	Residence Time	Biochar
Fast Pyrolysis	300-1000	Short (< 2 s)	12 %
Slow Pyrolysis	300-650	Long (5 mins-2 h)	30 %-60 %
Gasification	>800	Moderate (10-20 s)	10 %
Hydrothermal Carbonisation	180-300	1-16 h	50-80 %
Torrefaction	-290	10-60 min	80 %

The three conversion processes - pyrolysis, gasification, and hydrothermal carbonization (HTC) - can transform biomass into biochar, condensable liquid (bio-oil), and non-condensable gases (syngas). The specific product and its application depend on

the type of biomass used and the thermal conditions utilized during devolatilization (Masebinu et al., 2019; Tripathi et al., 2016).

Biochar is typically used to refer to the solid product of pyrolysis, whereas hydrochar and char are terms used to describe the solid materials generated during HTC and gasification processes, respectively (Pecchi and Baratieri, 2019). For the purpose of this study, the focus will be on biochar produced through slow pyrolysis. Slow pyrolysis occurs within a temperature range of 400-600 °C, with a long residence time (several hours) and a low heating rate. Slow pyrolysis is preferred for biochar production due to its favorable characteristics, including surface area, pore structure, and cation exchange capacity (CEC) (Luz et al., 2018). It is widely acknowledged as the most effective pyrolysis method, with biochar yields ranging from 30 % to 60 % and a specific surface area below 400 m^2/g (Li et al., 2020b).

Biochar produced at lower temperatures exhibits higher acidity, polarity, lower aromatic content, and hydrophobicity. As the process temperature increases, the presence of acid functional groups (-OH and -COOH) and biochar yield decrease, while alkaline functional groups, pH, and ash content in biochar increase (Li et al., 2020b). The rise in pH value of biochar with increasing pyrolysis temperature can be attributed to the enrichment of non-pyrolyzed inorganic elements and the presence of salts, such as carbonates and chlorides of potassium and calcium (Gaskin et al., 2007). According to Weber and Quicker (2018), most types of biochar exhibit alkaline properties, with pH values ranging from 8.2 to 12.4. For pyrolysis temperatures above 500 °C, the pH value of biochar derived from different biomass materials typically falls within the range of 10-12.

Under severe pyrolysis conditions, the presence of carboxyl and acidic groups in biochar decreases, resulting in an increase in alkalinity and pH when the biochar is suspended (Ronsse et al., 2013). This increase in pH can also be attributed to the reduction of acid functional groups and the polymerization/condensation reactions of aliphatic compounds on the biochar (Manyà, 2012). As mentioned previously, temperature is a key parameter that influences the quality of biochar. The physicochemical

characteristics of biochar, including specific surface area (SA) and cation exchange capacity (CEC), vary depending on the pyrolysis temperature and feedstock source (Ahmad et al., 2014). Optimal biochar production, considering both economic feasibility and feedstock nature, is typically achieved at temperatures ranging from 450 to 600 °C (Tripathi et al., 2016). With increasing pyrolytic temperature, more volatiles are released, resulting in cracks and pores within the microstructure of the remaining solid(Masebinu et al., 2019). However, if the temperature rise is uncontrolled and volatilization exceeds the optimal level, the pores may become wider and the Brunauer-Emmett-Teller (BET) surface area of the biochar may decrease (Masebinu et al., 2019).

2.11.3.1 Surface Area (SA)

The characteristics of biochar (ash content, porous structure and surface area) influence its efficacy. The surface area increases with the release of volatiles from the biomass (Li et al., 2020b). Regardless of the type of raw material used, the development of a biochar microstructure and the increased surface area have been widely observed with an increased pyrolysis temperature (Liu et al., 2020). As reported by Zhao et al. (2017), increase in pyrolysis temperatures above 400 °C leads to a gradual increase in the biochar specific surface area (SSA) and at 600 °C the highest SSA was achieved for all the feedstock tested.

Increase in SSA of biochar produced from woody and herbaceous biomass are more pronounced at a prodution temperature higher than 450 °C as a result of severe degradation and decomposition of them at elevated temperatures (Zhao et al., 2017). As the temperature rises further (> 900 °C), the number of pores may be reduced by the ordering of the structure, pore expansion, and/or the merger of adjacent pores, while some pores may be blocked by the softening and melting of ash (Li et al., 2020b). According to Cantrell et al. (2012), the biochar yield remains consistent when the temperature exceeds 400 °C. However, when the temperature falls below 400 °C, there is a decrease in the biochar yield due to the loss of volatile matter and non-condensable gases such as methane and carbon dioxide.

In addition to the temperature, the residence time of a slow pyrolysis process can also affect the surface areas of biochar. A rise in residence time results in a further increase of surface area at certain temperatures (Xie et al., 2022). A high SA of the biochar assures more effectiveness for the interaction with the surrounding microorganisms (González et al., 2009). The SA of biochar varies significantly depending on the feedstock used for its production. For instance, woody biochar derived at 650 °C exhibited an average SA of 255 m^2/g (Mukherjee et al., 2011). In contrast, poultry litter and swine solids biochar had much lower SA of 51 and 4 m^2/g, respectively (Cantrell et al., 2012). The lower SA observed in manure-based biochar can be attributed to the higher degradability of the organic matter present in manure. Pan et al. (2019) discovered that the lower lignin and cellulose content in manure leads to an undesirable biochar structure with slower development of the aromatic structure.

2.11.3.2 Porosity

The availability of a habitat for microorganisms is closely connected to the porous structure and specific surface area (SA) of biochar (Sanchez-Monedero et al., 2018). Depending on the size, pores can offer micro-habitats both for oxic and anoxic conditions (Ladygina and Rineau, 2013). Different support materials possessing porous and non-porous configurations have often been investigated to improve bio-methanation (Arif et al., 2018). The support materials have a significant impact on the start-up and efficiency of the AD process because the primary film formation of biomass is fundamental for further biofilm growth and stability (Arif et al., 2018).

Porosity is characterized in terms of the average diameter. Micropores present a diameter lower than 2 nm, thus affecting the SSA and absorption characteristics. Meso and Macro porosity are characterized by pore diameters of 2–50 nm and greater than 50 nm [59], respectively (Luz et al., 2018). Therefore, the biochar pore size distribution is an important factor that needs to be keenly studied to understand the possible interactions with organisms. Microorganisms can find an appropriate habitat to proliferate depending on the pore size distribution. Typical sizes of such microorganisms are bacteria (between 0.3 and 13 μm), fungus (between 2 and 80 μm) and protozoa (between 7 and 30 μm) (Luz et al., 2018; Lee et al., 2013). A porous material en-

hances biofilm development significantly compared to more smooth media (Patel and Madamwar, 2000). It acts as a shield for the selective microorganisms involved in the AD process under acid stress conditions (Luo et al., 2015).

2.11.3.3 Cation Exchange Capacity (CEC)

CEC represents the biochar capability of exchanging cations with organic or inorganic matter. A high CEC value reflects a high superficial negative charge, and consequently, a high number of cations can be accepted (Mengel, 1993).

2.11.3.4 Electrical Conductivity (EC)

EC is used to evaluate the biochar conductivity capabilities, vital for the syntrophic activities of microbes (Zhang et al., 2018b). It is proportional to the ionic content of the bio-reactor, and its determination can be used to evaluate VFA, cation concentrations, and total alkalinity (Aceves-Lara et al., 2012).

2.11.3.5 Aromacity

The Aromaticity quantifies how carbon is bound in polycyclic aromatic ring structures (Manyà et al., 2014). Fixed carbon content is strongly correlated to biochar aromaticity (Hood-Nowotny, 2016).

2.11.4 Impact of Biochar on the Anaerobic Digestion Stages

2.11.4.1 Impact of Biochar on Hydrolysis

The addition of biochar improves the efficiency of the hydrolysis stage in breaking down proteins, polysaccharides, and lipids (Pan et al., 2019). As a result, biochar addition can be viewed as a mechanical pretreatment for promoting hydrolysis by damaging the cell membrane of insoluble matter, thereby increasing the availability of macromolecular organics (Duan et al., 2019; Hassanein et al., 2019). Not only do biochar supplements disrupt insoluble matter cell walls, but they also activate the protease, amylase, cellulase, dextranase, and lipase enzymes (Pan et al., 2019; Yang and Wang, 2019).

According to Pan et al. (2019), when the functional genes associated with hydrolases were investigated further, more protease and dextranase genes were discovered in the presence of biochar. Also, Giwa et al. (2019) discovered that *Sedimentibacter Tissierella* and *Syntro-phomondaceae*, which are essential for hydrolysis and carbohydrate fermentations, were enriched in a biochar-added reactor. Further, biochar can be used to promote electron transfer, which is beneficial to the hydrolysis reaction (Velimirovic et al., 2016). Ma et al. (2019b) found an increment in hydrolysis of particulate organics at the early periods of the anaerobic digestion process when biochar was added, reflecting in the higher contents of total carbon, dissolved organic and inorganic carbon of digestate.

2.11.4.2 Impact of Biochar on Acidogenesis and Acetogenesis

Biochar has demonstrated high efficacy in anaerobic digestion by the promotion of the acid formation processes(Liu et al., 2021; Puyol et al., 2018). During acidogenesis and acetogenesis, biochar supplementation can stimulate the timely production and degradation of VFAs. This is because the biochar intensely activates anaerobic functional microorganisms that produce acetic acid (Pan et al., 2019). Martínez et al. (2018) found that adding biochar to the co-digestion of sewage sludge and citrus peel at 37 °C increased the concentrations of acetic, propionic and butyric acids.

Similarly, Giwa et al. (2019) discovered an increase in acetic acid when 0.25 g/d of biochar was added to the anaerobic digestion of vegetable, meat, fish, and bone waste at temperatures of 35 and 37 °C. Biochar, on the other hand, had little effect on propionic and I-butyric acid in their study. Wang et al. (2018a) performed fermentative co-digestion of foodwaste and dewatered sewage sludge at 35 °C using biochar produced from sawdust, wheat bran, peanut shell, and sewage sludge at three pyrolysis temperatures of 300, 500, and 700 °C. According to the findings, biochar supplementation stimulated the timely production of VFAs dominated by acetate in significant amounts.

In terms of the influence of pyrolysis temperatures, the study found that biochar pyrolyzed at higher temperatures of 500 and 700 °C had a significant influence on VFA

production. Sunyoto et al. (2016) investigated the effect of biochar on VFA generation and reduction in a two-phase batch anaerobic digestion experiment. The lag phase of the biochar-amended digesters was 5.5-5.9 days, compared to a control of 10 days. They came to the conclusion that biochar promotes VFA accumulation during hydrolysis and reduction during methanogenesis, resulting in a 41.6 % increase in specific biomethane.

Furthermore, Cai et al. (2016) showed that adding biochar reduced the lag phase by 10.9-20.0 %, 43.3-54.4 %, and 36.3-54.0 %, respectively, at ISRs of 2, 1, and 0.8. Luo et al. (2015) observed biochar inducing a 38 % reduction in lag phase. Finally, Sunyoto et al. (2016) studied the addition of biochar to a two-phase AD system for foodwaste and discovered that the lag time for H_2 and CH_4 production decreased by 21.4-35.7 % and 41-45 %, respectively, as both VFAs degradation and methane production potential were increased.

2.11.4.3 Impact of Biochar on Methanogenesis

Methanosaeta, *Methanobacterium*, *Methanolinea* and *Methanosarcina* are the dominant methanogens in biochar-augmented anaerobic digester (Kumar et al., 2021; Li et al., 2019a; Ma et al., 2019a). Similarly, Shen et al. (2017) discovered a biochar-induced selective colonization of *Methanosarcina*. According to Lü et al. (2016), biochar improves methanogenesis by assisting *Methanosaeta* in becoming resistant to higher VFA levels and enriching the *Methanosarcina*. Li et al. (2018c) discovered that biochar addition facilitated thermophilic co-digestion of foodwaste and waste activated sludge, with the relative abundance of *Syntrophothermus*, *Methanosaeta*, and *Methanosarcina* increasing from 3.6- 4.7 %, 30.0-43.9 %, and 11.1- 15.8 %, respectively.

According to Luo et al. (2015), when digesting glucose, the addition of biochar promoted an increase in archaea, which facilitated an increase in CH_4 production and a reduction in acidification. Also, Luo et al. (2015) observed a 70.6 % increase in methanogenesis rate. According to Lü et al. (2019), biochar increased methane production by 32.5-13.3 % for mesophilic and thermophilic oil digestion, respectively.

2.11.5 Biochar Adsorption Mechanism

The surface of biochar consists of both carbonized and non-carbonized fractions, creating a heterogeneous surface with different sorption mechanisms. Sorption occurs when the interfacial layer of a solid sorbent increases in density during the exchange of molecules with a fluid called the sorbate. Pignatello (2011) categorize sorption into three routes: chemisorption, physisorption, and ion-exchange. Chemisorption, which involves strong covalent bonds and orbital mixing, is less common in environmental systems. Physisorption, on the other hand, can be further divided into adsorption and absorption. Adsorption occurs when molecules settle on the surface or form layers on the adsorbent, while absorption refers to the condensation of molecules into the pores of the adsorbent.

The adsorption process on biochar is facilitated by hydrogen bonding, electrostatic attraction, ion exchange, or the hydrophobic effect. The rate of adsorption of organic pollutants on biochar is influenced by their solubility, as interactions occur primarily at hydrophobic sites. Thus, if a soluble pollutant possesses a hydrophobic functional group, it can be attached to hydrophobic biochar (Masebinu et al., 2019). The sorption of organic pollutants onto biochar through pore-filling depends on the total volume of micropores and mesopores (Rosales et al., 2017). Alkaline biochar surfaces can precipitate water-soluble contaminants. For organic molecules, hydrophobic interactions and hydrogen bonding are important mechanisms, while Van der Waals forces of attraction induced by the biochar's surface chemistry are common for organic compounds (Fagbohungbe et al., 2017). Generally, the adsorption capacity of biochar increases as the ionic radius of the pollutant decreases, facilitating better penetration onto the biochar surface (Ahmad et al., 2014).

Biochar surfaces typically carry a negative charge as a result of the dissociation of oxygen-containing functional groups. This negative charge facilitates the electrostatic attraction of positively charged organic compounds (Qambrani et al., 2017; Ahmad et al., 2014). However, when the pyrolytic temperature exceeds 450 °C, the biochar

becomes less polar and more aromatic due to the loss of oxygen and hydrogen functional groups (Ahmad et al., 2014). This change affects the biochar's adsorption capacity for polar organic contaminants in aqueous solutions. Ahmad et al. (2014) observed that the electrostatic repulsion between negatively charged organic compounds on biochar can promote hydrogen bonding, leading to adsorption. As the hydrogen bonding between water and oxygen functional groups diminishes, hydrophobic sites become more attractive to non-polar contaminants. The adsorption process occurs in three stages: the transfer zone (continuous adsorption), the clean zone (no adsorption), and the exhausted zone (equilibrium) (Kizito et al., 2017, 2015).

2.11.5.1 Adsorption of inhibitors

Inhibitors, including long chain fatty acids (LCFAs), ammonia, limonene, heavy metals, and phenols, can undergo degradation or transformation into other metabolites, which can be just as inhibitory as the original compounds (Duetz et al., 2003). The addition of biochar to anaerobic digestion systems has been shown to adsorb inhibitors due to its porous structure and large surface area (Li et al., 2019a). The adsorption process involves various mechanisms such as physical adsorption, surface precipitation, complexation, pore filling, hydrogen bonding, electrostatic attraction, and ion exchange (Li et al., 2019a).

Adsorbed ammonia can react with functional groups on the biochar surface, forming amines and amides, thereby reducing the accumulation and mobility of ammonia as a direct inhibitor without affecting the anaerobic digestion process (Xie et al., 2022). Apart from direct inhibitors, indirect inhibitors such as volatile fatty acids (VFAs) can be formed during the anaerobic digestion process. The addition of alkaline biochar can help regulate the pH value in the anaerobic digestion system and increase methane yield (Li et al., 2019a). Fagbohungbe et al. (2016) reported that the use of biochar with a pH of 6.9 can enhance biogas production.

The sorption capacity of biochar with different organic and inorganic materials has been extensively reported in the literature but with regard to most inhibitory compounds during AD it has not been well documented (Mohan et al., 2014). This may be

attributed to the uncertainty surrounding the addition of biochar to AD systems. Adsorbents like biochar are not selective during sorption; hence, there is the possibility that some of the essential nutrients or useful metabolites will be adsorbed during the AD process (Fagbohungbe et al., 2017).

2.11.6 Indirect and Direct Interspecies Electron Transfers (IIET and DIET)

Interspecies electron transfers can be achieved using insoluble materials like humic compounds or conductive substances and has been found to play important roles in improving the performance of anaerobic digestion (Lovley, 2017). Both indirect interspecies electron transfer (IIET) and direct interspecies electron transfer (DIET) play roles in microbial interactions (Zhang et al., 2018b). In comparison to IIET, the DIET pathway exhibits more stable and rapid consumption of substrates and intermediates, with an electron transfer speed 106 times faster than IIET (Yang et al., 2017; Cruz Viggi et al., 2014).

Through DIET, electrons can be transferred via conductive cell-to-cell connections, enabling co-metabolism of target substrates, as described by Wegener et al. (2015). The enhancement of electron transfer can lead to improved acetate-methanogenesis, as indicated by (Pan et al., 2019). Furthermore, DIET does not rely on complex enzymatic steps for the generation, consumption, and diffusion of redox mediators (Baek et al., 2018). DIET has been found to be possible through diffusive soluble electron carriers such as hydrogen or formate (Shao et al., 2019; Ye et al., 2018; Lovley, 2017). Strategies for DIET have been reported to consist of three possible types through conductive pili with cytochromes attached, outer membrane proteins and electrically conductive materials (Kouzuma et al., 2015).

Addition of conductive materials such as carbons into bio-CH_4 digesters has been found to stimulate DIET process within a wide range of microbes that cannot generate conductive nanowires like geobacter species (Liu et al., 2012). This is because carbon-based materials have favourable physico-chemical properties (including fine

pore structure, good electrical conductivity, large porosity, and surface area) contributing to the DIET (Liu et al., 2021). Syntrophic partners can be enriched on the surface of conductive carbons and they can take advantage of them as electrical conduits for electron exchange. This pathway can be metabolically favorable as these materials may mitigate the energy investment by microbes for the synthesis of conductive pili (Zhao et al., 2015).

2.11.7 Buffering Capacity

During anaerobic digestion (AD), the accumulation of acid is a common occurrence that reduces the system's buffer capacity (Chen et al., 2008; Ward et al., 2008). Fluctuations in pH within AD processes are typically caused by factors such as feedstock composition, high organic loading rates (OLR), and microbial inhibition, as highlighted in the review by Masebinu et al. (2019). However, the buffer capacity of AD can be increased or maintained by adding alkali compounds or controlling the OLR, as suggested by Ward et al. (2008). Biochar, due to its acid-buffering properties, has significant potential for enhancing anaerobic digestion processes (Wang et al., 2017b).

Additionally, Zhang et al. (2018b) demonstrated that the alkalinity of biochar increases with higher pyrolysis operating temperatures. This finding is supported by Komnitsas et al. (2015), who reported an increase in the pH of biochar with rising pyrolytic temperatures, resulting from the liberation of oxygenated carbon and deprotonation of the biochar surface. Depending on the ash composition within the biochar, its introduction to an anaerobic digestion system can increase alkali content, leading to beneficial effects on process performance (Romero-Güiza et al., 2016).

2.11.8 Immobilization of Microbial Cells

Microbial immobilization refers to the process of microbial cells colonizing the surface of a stable solid material, as explained by Fagbohungbe et al. (2017). Physical immobilization of microbes has been shown to increase biomass retention time by keeping the biomass inside porous structures, reducing the distance between syntrophic bacteria and methanogens (Kumar et al., 2021; Zhang et al., 2018b). Biochar has emerged as an effective medium for providing attachment sites for key microbes and enhancing

their contact with the fermentation substrate (Wang et al., 2017b). The large surface area of biochar facilitates biofilm formation and efficient colonization of microorganisms (Zhang et al., 2018b; Sharma et al., 2015).

The macropores within biochar support the attachment of bacterial cells (Fagbohungbe et al., 2017), while the abundant pores provide a habitat for immobilized microbes, leading to an improved digestion process (Xu et al., 2018). The binding or colonization of microbial communities in anaerobic digestion enables interspecies electron transfer and reduces the washout rate of active microbes (Lü et al., 2019). Numerous studies have demonstrated that the addition of biochar enhances microbial metabolism and growth by providing a favorable support system (Cai et al., 2016; Sunyoto et al., 2016).

In their study, Cooney et al. (2016) investigated the impact of biochar on improving the retention of microbial species that facilitate the rapid degradation of greasy wastewater in a packed bed anaerobic digestion process. They found that biochar promoted the formation of microbial biofilms, which supported the colonization of acidogens, acetogens, and methanogens, resulting in a 69 % reduction in chemical oxygen demand (COD). The presence of biochar in the biofilm led to an average methane (CH_4) concentration of 60 % and approached the theoretical CH_4 production rate, indicating high efficiency.

Similarly, Sawayama et al. (2004) compared dispersed and immobilized cells and observed that the biomass and methane production rate of the immobilized cells were higher. Additionally, Luo et al. (2015) noted the colonization of *Methanosarcina* on biochar material during anaerobic digestion of a glucose solution. In comparison to the study without biochar, methane production was significantly increased by 86.6 %.

2.11.9 Influence of Different Types, Sizes and Quantities of Biochar on AD Process

In a study conducted by Fagbohungbe et al. (2016), the researchers examined how different types of biochar and their ratios influenced the anaerobic digestion of citrus

peel waste in a batch process at a temperature of 35 °C. They combined wood biochar (WB), coconut shell biochar (CSB), and rice husk biochar (RHB) with citrus peel at a 1:1 mixing ratio based on the dry weight of the total solid. The results indicated that CSB resulted in the highest methane production, while WB led to the shortest lag phase before methane production began. The researchers also tested different ratios of WB to citrus peel (1:3, 1:2, 1:1, and 2:1) under the same experimental conditions, finding that a decrease in the proportion of biochar increased the microbial lag phase.

Another study by Linville et al. (2017) found that increasing the dosage of biochar and using smaller particle sizes enhanced the adsorption of NH_3 during a batch anaerobic digestion process. Additionally, Lü et al. (2016) investigated the effect of biochar particle size on NH_4^+ adsorption efficiency in a batch anaerobic digestion using glucose as the substrate. They discovered that biochar particles with sizes ranging from 2.5 to 5 mm, 0.5 to 1 mm, and 75 to 150 μm reduced the lag phase by 23.9%, 23.8%, and 5.9%, respectively, under highly stressed anaerobic digestion conditions. Furthermore, the CH_4 production rate increased by 47.1 %, 23.5 %, and 44.1 %, respectively, corresponding to the order of the different particle sizes. This increase was attributed to the enhanced colonization of *Methanosarcina*. The researchers concluded that selecting biochar particles of appropriate sizes is crucial for facilitating the colonization of microbial cells.

Several studies have examined the influence of biochar particle size on its performance in various processes. Smaller particle sizes have been found to reduce mass transfer limitations and increase the forces that facilitate the penetration of the adsorbate into the adsorbent (Daifullah and Girgis, 1998). This enhanced penetration is attributed to the larger surface area available in smaller-sized biochar, resulting in improved adsorption outcomes. However, the response time for methane production may be slower with smaller-sized biochar. Conversely, larger-sized biochar has been shown to alleviate the effects of pH more quickly, leading to greater production in a shorter period (Luz et al., 2018). Additionally, larger adsorbate sizes can obstruct smaller sorption sites, affecting overall performance (Duku et al., 2011a).

Studies have reported different findings regarding biochar particle size. For instance, as the particle size of biochar increases, the adsorption of NH_4^+-N from digestate decreases (Kizito et al., 2015). Conversely, reduced particle size results in improved biochar performance due to increased surface area (Masebinu et al., 2019). Notably, biochar with a particle size of 75 μm exhibited superior results compared to 2-5 mm and 0.5-1 mm treatments, including shorter lag phases and increased methane production (Pan et al., 2019). Furthermore, investigations on various biochar types, such as rice husk biochar, shrub biochar, peanut shell biochar, straw biochar, sawdust biochar, and coconut shell biochar, revealed that the cumulative methane yield was higher when coconut shell biochar was present compared to control groups without biochar (Shen et al., 2020).

Interestingly, anaerobic digestion tests with biochars showed a secondary methane yield peak, while control groups did not exhibit this phenomenon. Moreover, an optimal dosage of straw biochar (e.g., 2 %) improved cumulative methane yield, but excessive addition (4 %) inhibited anaerobic digestion (Shen et al., 2020). In a study conducted by Meyer-Kohlstock et al. (2016), the impact of biochar addition on biogas and methane yields was investigated. The researchers found that adding 5 % biochar increased both yields by approximately 5 %, while an addition of 10 % resulted in a 3 % increase. However, the authors noted that although higher biochar dosages led to increased methane content in biogas and substrate degradation rates, inhibition of the process occurred at higher dosages due to elevated concentrations of alkali metals beyond acceptable limits.

Similarly, Sunyoto et al. (2016) examined the effect of pine sawdust biochar, obtained at 650 °C, on methane production in two-phase anaerobic digestion of aqueous carbohydrates. Different biochar addition ratios were tested in comparison to a control reactor without biochar, all incubated at 35 °C. The cultures with 8.3 and 16.6 g/L biochar additions exhibited improved cumulative methane production, while those with 25.1 and 33.3 g/L biochar additions showed a reduction compared to the control. The highest methane production increase of 6 % was observed with an 8.3 g/L biochar

addition, while the lowest decrease of 13 % resulted from a 33.3 g/L biochar addition. However, at all concentrations, the addition of biochar shortened the lag phase of methane production by 41-45 %.

2.11.10 Negative View of Biochar

Biochar has been shown to only help strained situations brought on by external voltage or microbial inactivity, and it had little to no effect on situations that were functioning normally, which could be attributed to the finding that biochar enriched DIET-capable *Methanosarcina* and *Methanosaeta* which are sensitive to stress (Shao et al., 2019). Also, potential H_2 competitors (e.g. Hydrogenophaga) of methanogens could also clone onto biochar that weakened its DIET benefit for methanogenesis. This was observed throughout sequencing when suspended microbes which cannot conduct DIET with biochar, were far more extensive than those attached to additives. Finally, according to Liu et al. (2021), it is necessary to discuss the dosages, outcomes, and applications of each additive. Summarizing the impact of various additives on the efficiency of anaerobic digesters has thus become a crucial area of study in recent years.

2.12 Response Surface Methodology

Biogas production could be significantly enhanced via optimization of parameters which affect biogas plants (Yılmaz and Şahan, 2020). However, traditional methods are inappropriate for optimization studies due to the need for numerous tests that consume a great amount of time and materials (Safari et al., 2018). Statistical programs are widely used as optimization approaches in the literature to overcome these limitations. A mathematical technique called response surface methodology (RSM) is used to approximate the response of the dependent variable within the limits of the experimental design and to describe the combined effects of several independent variables on it (Gunes et al., 2021; Baek et al., 2020). The RSM investigates an appropriate approximation relationship between input and output variables and identify the optimal operating conditions for a system under study or a region of the factor field that satisfies the operating requirements (Farooq et al., 2013; H Pishgar-Komleh et al., 2012).

2.12.1 Mixture Design

Experiments adhering to mixture designs are a unique case of response surface experiments where the response depends on the proportions of the various mixture components. Mixture experiments occur when studying the composition of materials and the effects of the material compositions on one or more responses of interest. The most commonly used mixture design is the optimal design. The goal is to find the blend of the different mixtures that gives the maximum yield of response. When working with mixtures, the response is a function of the proportions. In order to keep track of the proportions, there must be a constraint that keeps a constant total in every run of the design. This makes mixture DOEs (Design of Experiments) unique from other types of designs.

Using the mixture design and RSM, Baek et al. (2020) examined the impacts of various substrate compositions on methane yield and synergy index. According to the authors, regardless of the substrate mixing ratio, cow manure, food waste, and pig manure could all be digested together without significantly losing any of their methane potential (i.e., little antagonistic effect). However, the co-digestion circumstances where the food waste fraction was larger than approximately 50 % were expected to have an antagonistic effect by the response surface model. To prevent the potential antagonistic effect, which is minor, and to maximize the benefit from the co-synergistic digestion's effect, authors advised limiting the food waste portion in the substrate combination below 50 %.

The design of experiments (DoE) is the most important aspect of RSM. The DoE is focused on the selection of the most suitable points where the response should be well examined. The mathematical model of the process is mostly related to design of experiments. Thus, the selection of experiment design has a great effect in determining the correctness of the response surface construction. The advantages offered by the RSM can be summarized as determining the interaction between the independent variables, modeling the system mathematically, and saving time and cost by reducing the number of trials (Boyacı, 2005). However, the most important disadvantage of the response surface method is that the experimental data are fitted to a polynomial

model at the second level. It is not correct to say that all systems with curvature are compatible with a second-order polynomial model.

2.13 Kinetic Models

2.13.1 Modified Gompertz Model

A Gompertz curve or model, named after Benjamin Gompertz, is a sigmoid function. It is a type of mathematical model for a time series, where growth is slowest at the start and end of a time period. The modified Gompertz model has been proven as an excellent empirical non-linear regression model (Pramanik et al., 2019). Modified Gompertz model equation is a modified form of the Gompertz equation which is commonly used to simulate the cumulative biogas production (Lim et al., 2022). This model assumes that cumulative biogas production is a function of hydraulic retention time (Krishania et al., 2013). It has also been widely used to simulate the performance of methane production and the lag period in an anaerobic co-digestion process.

Yusuf et al. (2011) used the modified Gompertz model to fit the cumulative daily biogas production of digesters co-digesting cow dung and horse dung. The modified Gompertz equation was observed to adequately describe biogas production with a good fit of (R^2) 0.996, 0.998 and 0.997 for digesters A (100 % horse dung), B (75 % horse dung and 25 % cow dung) and C (50 % horse dung and 50 % cow dung), respectively. Kafle and Kim (2012) compared the modified Gompertz and first-order kinetics models and showed that, better fitting result was found for the modified Gompertz model. Budiyono and Sumardiono (2014) have also applied the modified Gompertz equation in their work and found the model to give a good fit.

Simulation results of accumulated biogas production for sheep paunch manure showed that modified Gompertz equation had higher R^2 values that ranged from 0.9965 to 0.999 compared to R^2 values of first order kinetic equation that ranged from 0.9769 to 0.9827 (Lawal et al., 2016). Latinwo and Agarry (2015b) studied th codigestion of sewage sludge and municipal waste and reported that Modified Gompertz plot had higher correlation (R^2 values of 0.9947) than exponential rise to maximum plot for

simulating cumulative biogas production. Furthermore, a study by Casallas-Ojeda et al. (2020) on the simultaneous incidence of two significant variables in the anaerobic digestion of foodwaste were evaluated. The study showed that the Gompertz kinetic model fit the process dynamics better and with a lower error than the first-order model.

2.13.2 Logistic Function Model

A time-dependent process is described by a logistic kinetic model, in which the growth is exponential at first and then slows down and reaches a plateau in the end after reaching saturation (Burnham, 2017). Hence, the logistic function model is suitable for an initial exponential increase and a final stabilization at the highest production level, which assumes that the rate of biogas production is proportional to the quantity of biogas already produced (Donoso-Bravo et al., 2010). Latinwo and Agarry (2015b) reported that logistic function model showed better correlation of cumulative biogas production. For cumulative biogas production simulation of sewage sludge and municipal waste, logistic growth plot had higher correlation than exponential rise to maximum plot with R^2 values of 0.9141 for exponential rise to maximum plot and 0.9886 for logistics model (Latinwo and Agarry, 2015b).

Moreover, Sedighi et al. (2022) investigated the potential for biogas production from the anaerobic co-digestion of the organic fraction of municipal solid waste and sewage sludge after physical and chemical pretreatments at three inoculum-to-substrate (IS) ratios (ISR: 2, 4 and 6) and three levels of total solids (TS: 3, 5 and 7 %). A series of experiments were further carried out in laboratory-scale (1-L) single-stage digesters in batch mode at the temperature of 35 °C for 50 days. The kinetic study of the mesophilic anaerobic co-digestion additionally showed that logistic function (LF) provided a reasonably accurate description of biogas production (Sedighi et al., 2022).

2.13.3 Cone Model

Researchers, such as Zahan et al. (2018), Li et al. (2015b) and Pitt et al. (1999) have analyzed the cone model to better model the cumulative biogas production. Bedoić et al. (2020) reported that kinetic analysis using the cone model showed that foodwaste has a shape factor, n = 1.6, and a reaction rate constant between 0.145 and 0.200

d^{-1}. Zhen et al. (2016) reported that cone model in anaerobic digestion of food waste gave a similar shape factor (1.3) and rate constant (0.126 d^{-1}). Also, Venkateshkumar et al. (2020) observed R^2 and root mean square error (RMSE) values to be between 0.9622–0.9960 and 0.9418–3.8794, respectively.

Further, a study by Prajapati et al. (2018) reported R^2 values between 0.9592 and 0.9929, and RMSE values lesser than 12.1. Li et al. (2015b) compared three kinetics models, including first-order kinetics, the transfer function model and the cone model for different livestock manures as feedstocks and with different substrate concentrations. The results showed that the cone model had better performance than the first-order and the transfer function models. El-Mashad (2013) observed that the Cone model best described the cumulative biogas production data, whereas the exponential model was the worst predictor of the experimental data.

2.13.4 Fitzhugh Model

The Fitzhugh model is an extension of the first order model with the introduction of the constant n (Ihoeghian et al., 2022). Hydrolytic constant,k, which is fitted by Fitzhugh model, can be applied to represent the hydrolytic rate of digestive system (Li et al., 2018d). In general, a higher k value indicates a higher hydrolytic rate of digester system (Yang et al., 2022). k and n values were validated in El-Mashad (2013) for k less than 0.30 and n less than 4.81. R^2 and root mean square error (RMSE) values were observed to lie in the ranges from 0.9022 to 0.9837 and 0.9995 to 12.9987, respectively for anaerobic co-digestion of cow dung and cotton seed hull (Venkateshkumar et al., 2020).

2.13.5 Monod Model

Lawrence and McCarty (1969) applied the monod model to anaerobic digestion processes. Since then, it has been widely used, especially with soluble substrates. Due to the high error values for the anaerobic co-digestion of food waste and meat and bone meal, Bedoić et al. (2020) discovered that monod kinetics proved to be the least suitable of the models examined.

CHAPTER 3

Materials and Methods

3.1 Introduction

The sampling methods, locations, materials, and instruments used in this research are all covered in this chapter. Further included are the inoculum and additive preparation processes. Also, the approaches utilized to examine the physical and chemical makeup of the feedstocks and additives used in this study are discussed. Additionally, the different feedstock ratios used and the experimental matrix are reported. Furthermore, the procedures for determining the theoretical biomethane potential of cow dung, food leftovers, kitchen residues and human excrement are presented. There is also a description of the procedure for determining biodegradability, synergistic effects, and gas measurement. Finally kinetic models, the response surface method, and other statistical analyses are provided.

3.2 Feedstock Collection and Preparation

3.2.1 Human Excreta (HE)

Human excreta (H.E.) was the primary feedstock for this investigation, and it was freshly obtained from a KVIP in Ayeduase, a suburb of Kumasi. Samples were sorted to remove any inorganic substance and homogenised (Figure 3.1).

Figure 3.1: Freshly Collected and Homogenised Human Excreta

3.2.2 Food Leftovers (FLO) and Kitchen Residue (KR)

Food leftovers (FLO), (Figure 3.2) in this study are cooked foods that go uneaten and kitchen residues (KR) (Figure 3.3) consist of waste from food preparation as well as leftover fruits and vegetables. Over the course of four weeks, FLO and KR were collected from households of staff and the canteen at a Senior High School in Kumasi. Components and compositions of FLO and KR are specified in Table 3.1. FLO and KR were manually sorted to remove non-biodegradable fractions after which the organic fractions were shredded into smaller pieces, blended and homogenized into a slurry to maintain a particle size below 3mm using a household food grinder and a 3mm sieve. Samples were frozen at a temperature of $-20\,^{\circ}$C before use. The frozen samples were allowed to thaw at a temperature of $4\,^{\circ}$C and used within a day to prevent biological decomposition.

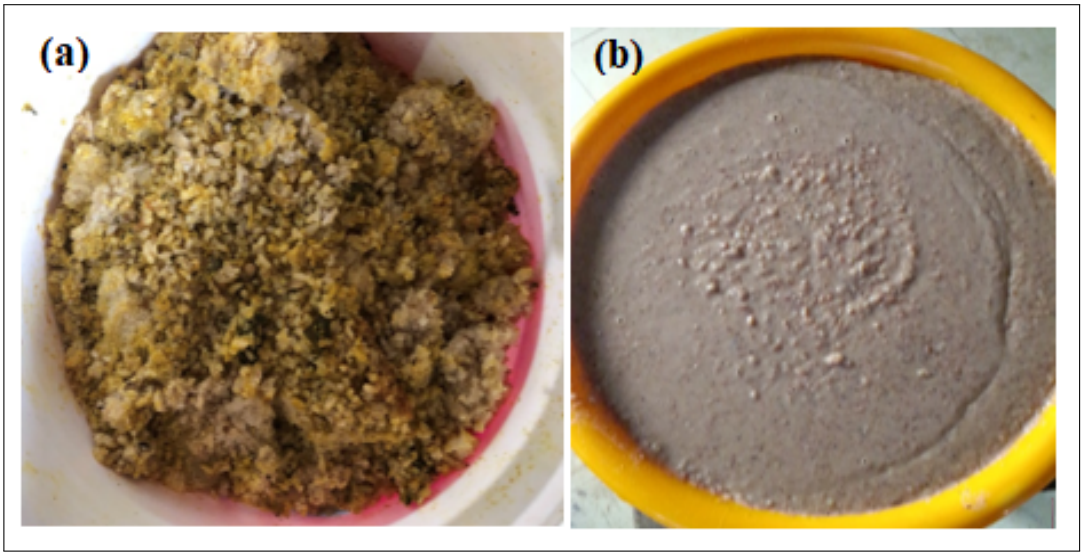

Figure 3.2: Sample Food Leftovers (a) Raw (b) Homogenized

Figure 3.3: Samples of Kitchen Residue (a) Cassava Peels, (b) Yam and Cocoyam Peels, (c) Pineapple, Avocado and Orange Peels, (d) Plantain and Banana Peels (e) Pawpaw, Watermelon and Mango Peels (d) Lettuce, Cucumber, Pepper, Tomato, Carrot, Garden Eggs and Onion Leftovers

Table 3.1: Percentage composition of FLO and KR based on wet weight

KR Components	% Composition (% wet weight)	FLO Components	% Composition (% wet weight)
Pawpaw peels	3.04	Rice	27.58
Watermelon peels	4.53	Cassava / Fufu	17.52
Avocado peels	3.12	Kenkey (cooked fermented corn dough)	14.66
Banana peels	2.59	Banku (cooked fermented cassava and corn dough)	12.80
Mango peels	4.00	Bread and Vegetables Sauce	4.19
Orange peels	5.87	Plantain	6.58
Pineapple peels	3.28	Kontomire (Boiled Cocoyam Leaves)	2.06
Onion peels	4.98	Gari and Beans	3.09
Lettuce, Cucumber, Pepper, Tomato, Carrot, Garden Eggs	8.48	Fish	0.12
Cocoyam peels	3.19	Egg	0.05
Plantain peels	12.47	Yam	11.35
Yam peels	20.91	-	-
Cassava peels	23.54	-	-

3.3 Feedstock Sampling

FLO and KR were sampled using the coning and quartering method shown in Figure 3.4 in an effort to obtain a more homogeneous representation (Alakangas, 2015). The samples were fully combined, piled into cone shapes, then separated into two and four portions, respectively, by flattening each pile. The diagonally opposed quarters were taken, either for laboratory analysis or, if a smaller quantity was needed, the procedure was repeated.

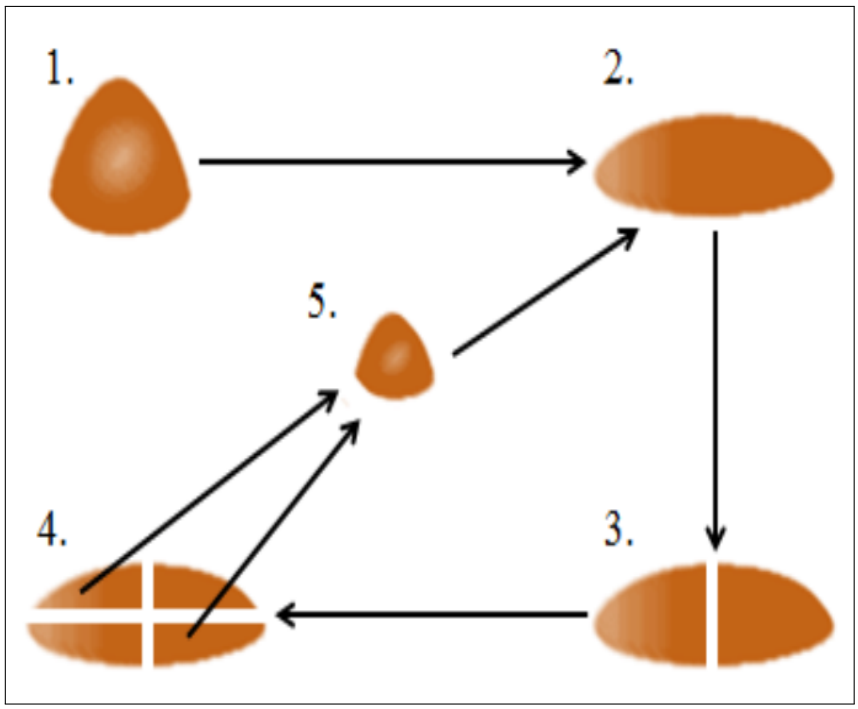

Figure 3.4: The coning and quartering method (Alakangas, 2015)

3.4 Cow Dung (CD) Collection and Inoculum Preparation

In this work, CD was employed as an inoculum. Fresh cow dung was collected (Figure 3.5) from the Department of Agriculture's farm at KNUST.

Figure 3.5: Freshly collected cow dung (CD)

3.4.1 Inoculum Preparation

The cow dung which was used as inoculum source was pounded and hand-mixed to homogenise. The homogenised CD was gently mixed with water to test for various TS values, and a final mixing ratio of 1:2 (one part of the CD to two parts of water) was chosen. Per the mixing ratio, a slurry was made, and a pH of 7.8 was measured. The CD slurry was placed in 1000 mL bottles. An anaerobic environment was established in the bottles. Using a 60 % active volume and a 40 % headspace each bottle was filled with 575 g of CD slurry at 5.2 % TS. For 60 days, the bottles were kept in an incubator at a temperature of $30\,^{\circ}$C. Biogas volumes were monitored using the water displacement method, and a biogas 5000 was used to analyse the gas composition. The procedure has been shown in the steps in Figure 3.6(a-i)

Figure 3.6: Step by step procedure for inoculum preparation.(a)Freshly collected cow dung (b)Homogenised cow dung (c)Test for appropriate mix ratio (d)One part of homogenised cowdung mixed with two parts of water (e)Test for pH of slurry (f)Bottled slurry (g)Bottles placed in an incubator and connected to gas bags (h)Gas composition measurement with Biogas 5000 (i) Gas volume measurement using water displacement method.

3.5 Feedstocks and Inoculum Characterization

Characterization of the feedstocks (HE, FLO, and KR) and inoculum were carried out to understand the physico-chemical features of the feedstocks being used, and also to determine the suitability of each feedstock for biogas production. Standard methods were employed for the proximate, ultimate, chemical and mineral analysis (APHA, 1998).

3.5.1 Proximate Analysis

The total solids (TS), volatile solids (VS), moisture content (MC), and ash content (AC) of HE, FLO, KR, and CD were measured using proximate analysis in accordance with APHA (American Public Health Association) Standards. The analysis were carried out at the Environmental Quality Engineering Laboratory, KNUST, Ghana. All analysis were carried out in triplicates with the average values and standard deviations reported.

3.5.1.1 Total Solids (TS)

The APHA method 2540 B was used to determine the TS of the feedstocks (APHA, 1998). 5g of each sample was measured with an Ohaus Explorer Ex 324 electronic balance (Figure 3.7a) and dried at $105\,^{\circ}$C in an electric vacuum Lanphan DZF-6090 oven (Figure 3.7b) for 24 hours, followed by cooling in a desiccator and weighing. Equation 3.1 was used in determining the TS.

$$\%TS = \frac{W_{total} - W_{dish}}{W_{sample} - W_{dish}} \times 100 \tag{3.1}$$

where W_{total} is the mass of the dried sample and dish (g), W_{dish} is the mass of dish (g), and W_{sample} is the mass of the fresh sample and dish (g).

Figure 3.7: (a)Electric weighing balance and (b) oven used for TS determination

3.5.1.2 Volatile Solids (VS)

The APHA method 2540 E (APHA, 1998) was employed for VS determination. Samples from the total solids test were taken for further heating in a Lanphan Atmosphere Furnace-SA2-4-17TP (Figure 3.8) at a temperature of $550\,^{\circ}$C for 4 hours to burn all the organic matter. Equation 3.2 was used to determine the VS.

$$\%VS = \frac{W_{total} - W_{volatile}}{W_{total} - W_{dish}} \times 100 \tag{3.2}$$

where W_{total} is the mass of the dried sample and dish (g), W_{dish} is the mass of dish (g), and $W_{volatile}$ is the mass of the burnt sample and dish (g).

Figure 3.8: Furnace used for VS determination

3.5.1.3 Moisture Content (MC)

The substrate MC was expressed by the weight difference between the initial weight of the sample and the TS. MC was determined according to Equation 3.3 (Singh et al., 2021a).

$$\%Moisture = 100 - TS\% \tag{3.3}$$

3.5.1.4 Ash Content (AC)

The AC in percentage was calculated as per Equation 3.4 (Singh et al., 2021a).

$$\%Ash = 100 - (Moisture\% + VS\%) \tag{3.4}$$

3.5.2 Ultimate Analysis

Ultimate analysis was conducted at the laboratories of Department of Agriculture and Department of Natural Resources, KNUST. The amount of carbon (C), hydrogen (H),

nitrogen (N), oxygen (O), and sulphur (S) in the feedstocks were determined using standard procedures (APHA, 1998). The total amount of sulphur was quantified using the spectrophotometer method (Singh et al., 1999), and the percentage of total nitrogen was computed using the Kjeldahl method (Bremner, 1965). Titrimetry (McLean, 1965) was used to determine the amount of hydrogen, and the Walkley-Black Wet Oxidation method was used to obtain the amount of organic carbon (Heanes, 1984; Nelson, 1982). The oxygen content was calculated using Equation 3.5 (Fajobi et al., 2022).

$$\%O = 100 - (C + H + N + S + AC)\% \tag{3.5}$$

3.5.2.1 Determination of Total Nitrogen by Kjeldahl Digestion Method

Kjeldahl digestion method was used in the determination of total nitrogen as reported by Bremner (1965). A 500 ml long-necked Kjeldahl flask was filled with 1 g of sample that was oven dried and pulverized to pass through a 0.5 mm sieve. Prior to weighing, sample was evenly mixed. The mixture was moistened by adding 10 ml of distilled water and allowed to sit for 10 minutes. An amount of 10 ml of concentrated H_2SO_4 and one spatula full of Kjeldahl catalyst (a combination of one part selenium, ten parts copper sulphur, and one hundred parts sodium sulphur) was added. After being digested for 1.5 hours, the product became colorless or light greenish.

After the flask had cooled down, it was decanted into a 50 ml volumetric flask. To make up the difference, the digest was added to a 50 ml volumetric flask after the digestion flask has been cleaned with distilled water. A pipette was used to transfer an aliquot of 10 ml of the digest into the Kjeldahl distillation device, and 90 ml of distilled water was then added. An amount of 20 ml of 40 % NaOH was also added. In a 250 ml conical flask, 100 ml of distillate was collected over 10 ml of 4 % boric acid and three (3) drops of mixed indicator. The collected distillate (100 ml) was titrated with 0.l N HCl until the blue color turned grey and then abruptly flashed to pink. Equation 3.6 was then applied to obtain the % nitrogen.

$$\%N = \frac{(a - b) \times 1.4 \times N \times V}{S \times t} \tag{3.6}$$

where *a* is ml HCl used in the sample titration, *b* is ml HCl used in the blank titration, *N* is Normality of standard HCl, *V* is total volume of digest, *S* is mass of oven dried sample taken for digestion and *t* is volume of aliquot taken for distillation (10ml)

3.5.2.2 Determination of Hydrogen by Titrimetric Method

Titrimetric method was used to determine the percentage of hydrogen, as reported by McLean (1965). In a 2L volumetric flask, about 1.2 L distilled water was added. An amount of 400 ml 80 % Hydrochloric acid and 133 ml of 70 % Nitric acid were also added. The mixture was then diluted to 2L to form an Acqua-regia. A 2 mm sieve was used to filter 3g of dry sample before being weighed into a digestion flask. Acqua-regia was added and digested for 10 minutes. The content of the digested mixture was filtered into a 100 ml volumetric flask and adjusted with distilled water. 10 ml of the digest was measured into the Erlenmeyer flask. About 5 drops of phenolphthalein indicator was added to the digested mixture. With 0.05 N NaOH, the digest was titrated to a pink end point. The volume of NaOH used (V) to reach the end point of titration was recorded. Applying Equation 3.7 yielded the % hydrogen content.

$$\%H = \frac{V \times 0.05 \times 100}{W} = V \times 1.67 \tag{3.7}$$

where *V* is volume of NaOH used (ml), 0.05 N is Normality of NaOH and *W* is weight of sample used

3.5.2.3 Determination of Total Sulphur by Spectrophotometer Method

The spectrophotometer method described by Singh et al. (1999) was turbidimetrically used to determine total sulphur content. Di-acid (HNO_3-HClO_4) digestion was used. Six serial standards of 5, 10, 20, 30, 40 and 50 mg/L were prepared from a pure sodium sulphate compound. 5 % of Barium chloride (BaCl) was also prepared from a pure compound and 0.5 % of gum acacia-acetic acid (GAAA) was prepared. 2 ml of each serial standard and 2 ml of unknown extracts were pipetted into labelled test tubes, respectively. 0.5 ml of GAAA and 1.0 ml of BaCl were added to each tube, respectively. All tubes were incubated for 30 minutes at room temperature. The spectrophotometer read the turbidity intensity at 420 nM. From the serial standards and their corresponding optical densities, a calibration curve was constructed. The concentration of sulfur

in the unknown extracts was determined using the graph.

3.5.2.4 Determination of Organic Carbon by Walkley – Black Wet Oxidation Method

The methods described by Heanes (1984) and Nelson (1982) were adapted to determine the organic and total carbon contents of feedstocks. An amount of 0.5 g of the sample was weighed into a 500 ml Erlenmeyer flask. It is recommended that samples be ground to pass through a 0.5 mm sieve and mixed thoroughly before weighing. From a burette, exactly 10 ml of 1.0 N $K_2Cr_2O_7$ solution was added and followed by 20 ml of 97 % H_2SO_4. The mixture was swirled to ensure that the solution was in contact with all the particles of the sample. The flask and content were allowed to cool on an asbestos sheet for 30 minutes. An amount of 200 ml distilled water and 10 ml of orthophosphoric acid were added. Also 2.0 ml of diphenylamine indicator was added. The content of the flask was titrated with 0.5 N ferrous sulphate solution until the colour changed to dark blue and then to a green end– point. The titre value was recorded and corrected for the blank solution. Equation 3.8 was used to estimate % carbon.

$$\%C = \frac{M \times (V_{blank} - V_{sample}) \times 0.003 \times 1.33 \times 100}{g} \tag{3.8}$$

where *M* is Molarity of $FeSO_4$, V_{blank} is ml $FeSO_4$ of blank titration, V_{sample} is ml $FeSO_4$ of sample titration, *g* is mass of sample taken in gram, *0.003* is milli-equivalent weight of C in grams (12/4000), *1.33* is correction factor used to convert the wet combustion C value to the true C value since the wet combustion method is about 75 % efficient in estimating C value, (i.e. 100/75 = 1.33). NB: Organic matter content is determined using the formula: % Organic C × 1.724 (1.724 is the Van Bemellean factor).

3.5.2.5 C/N Ratio

The C/N ratio of the samples was calculated using Equation 3.9. (Dahunsi et al., 2019; Anderson and Ingram, 1993).

$$C/N = \frac{\%Carbon}{\%Nitrogen} \tag{3.9}$$

3.5.3 Chemical Analysis

3.5.3.1 pH

A digital Hanner H1 98136 pH meter (Figure 3.9) was used to measure pH.

Figure 3.9: pH determination using a digital pH meter

3.5.3.2 Alkalinity

The alkalinity of each feedstock was determined according to the APHA method 2320B using potentiometric titration in Figure 3.10 (APHA, 1998). A 100 ml sample was put in a conical flask with a magnetic stirrer while a burette was filled with 0.025N sulphuric acid solution (H_2SO_4). The initial pH of the sample was measured. The standard acid was titrated against the sample until a pH between 4.5 was reached. After each titration, the volume of the titrant and pH were recorded. Alkalinity was then determined using Equation 3.10.

$$Alkalinity(mg/L) = \frac{A \times N \times 50000}{B} \tag{3.10}$$

where A is the volume of standard acid used (ml), B is the volume of sample used (ml) and N is the normality of standard acid.

Figure 3.10: Potentiometric titration for alkalinity determination

3.5.3.3 Chemical Oxygen Demand (COD)

The COD of each feedstocks was determined by adapting to the HACH COD method using the HACH COD HR+ (200-15000 mg/L) test vials (Figure. 3.11a) and HACH DR 3900 spectrophotometer. The method involved simple digestion for 2 hrs at 150 °C using the HACH COD Heating Reactor (Figure. 3.11b) before examining the absorbance equivalent concentration. The vial was cleaned ahead of reading. The COD HR program from the DR 3900 Spectrophotometer (Figure. 3.11c) was chosen. After reading the blank vial, the sample vial was put into the cell holder and read. Results were displayed in mg/L COD.

Figure 3.11: COD determination using (a) COD HR+ vials (b) COD Heating Reactor and (c) DR 3900 Spectrometer

3.5.3.4 Volatile Fatty Acids (VFA)

The VFA was determined titrimetrically after diluting 1 g of the samples to 100 mL and titrating with 0.1 N hydrochloric acid (HCl) until the pH was 3.0. (Figure 3.12a). The samples were then heated (Figure. 3.12b) for 3 to 5 minutes to remove CO_2. After cooling, the samples were again titrated with 0.1 N sodium hydroxide (NaOH) until the pH reached 6.5 (Figure 3.12a). Equation 3.11 was used to determine the VFA (Singh et al., 2019a,b, 2021a).

$$VFA(mg/L) = \frac{(B \times 100) - (A + 100)}{99.23} \times dilution factor \times 60 \qquad (3.11)$$

where *A* is the volume of HCl consumed and *B* is the volume of NaOH consumed during the titration.

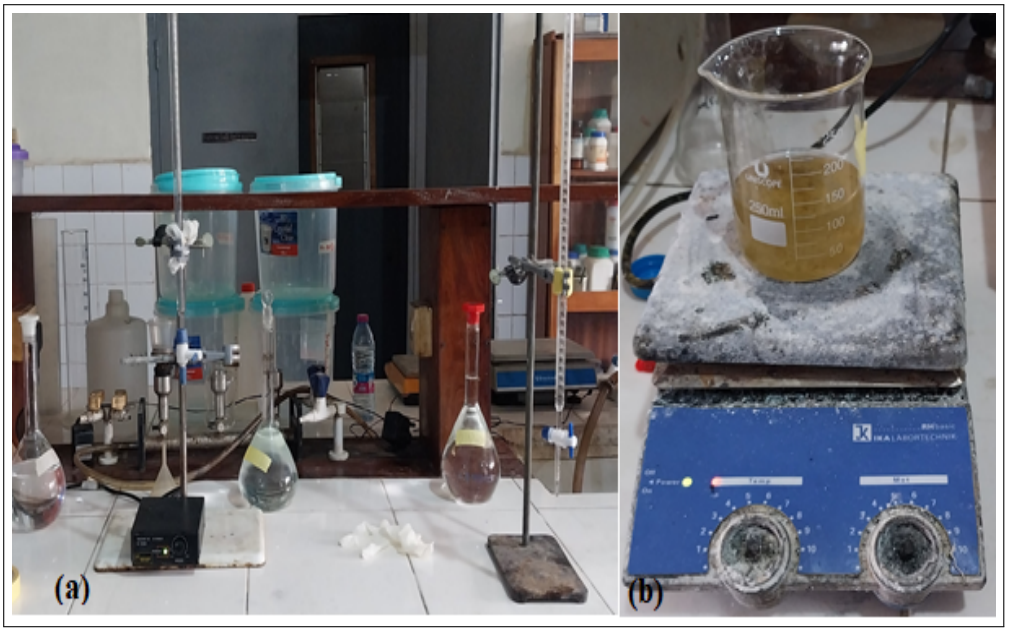

Figure 3.12: VFA determination (a)Two potentiometric titration setups for HCl and NaOH and (b) Hot plate for heating sample titrated with HCl

3.5.4 Compositional Analysis

3.5.4.1 Crude Fat Content

Samples of each feedstock was extracted with ether to get the ether extract (fat) using method AOAC 2003.05 (AOAC, 1990, 2006). The method quantified the amount of crude fat in dry samples using the randall modification of standard soxhlet extraction. After the ether had been distilled, the residue was weighed to ascertain the weight of the extract. A Soxhlet was used to carry out the ether extraction. The extraction flask was heated to 110 °C for approximately 5 minutes, cooled, and then weighed to determine the ether extract. The Soxhlet extraction device's bottom tubes received the sample packet. The material was extracted with petroleum ether for three hours without interruption using mild heating. The extraction flask was disconnected, and it was allowed to cool. The ether was evaporated on a water bath until there was no longer any ether odour. It was cooled down even further to room temperature. The extract and extraction flask were then reweighed, and the results were reported. Equation 3.12 is used to calculate the percentage of ether extract.

$$\%Ether\ Extract = (\frac{B}{C}) \times 100 \tag{3.12}$$

where B = ether extract weight, C = sample weight

3.5.4.2 Crude Protein Content

Crude protein was calculated from nitrogen (N) determination using AOAC Method 984.13 (AOAC, 1995). A 6.25 conversion coefficient was used to calculate protein concentration from measured total Kjeldahl nitrogen (TKN), as shown in Equation 3.13.

$$\%Crude\ Protein = Total\ Nitrogen(N_T) \times 6.25(Protein\ Factor) \tag{3.13}$$

3.5.4.3 Crude Fibre Content

Carbohydrates were calculated as the mass-balance difference of the crude fat, protein, moisture and ash determinations (AOAC, 1990). Equations 3.14 and 3.15 provide the general formulas.

$$\%Carbohydrate = \%TS - (\%AC + \%Fat + \%Protein) \tag{3.14}$$

$$\%Carbohydrate = 100\% - (\%AC + \%MC + \%Fat + \%Protein) \tag{3.15}$$

3.5.5 Mineral Analysis

Potassium (K) and sodium (Na) contents were analysed using flame photometry (Barnes et al., 1945). Also calorimetric determination of phosphorus (P) was done using vanadium phosphomolybdate method specified by APHA (1992). Calcium (Ca) and magnessium (Mg) contents were determined using atomic absorption spectroscopy (AAS) with model VGP 210 from Buck Scientific (Katz and Jenniss, 1983). PerkinElmer's NexION 2000 ICP-MS was used to detect the amount of nickel (Ni), molybdenum (Mo), chromium (Cr), cobalt (Co), cadmium (Cd), zinc (Zn), copper (Cu), selenium (Se), manganese (Mn) and iron (Fe) in the feedstocks after acid digestion.

3.6 Additive Sampling, Preparation and Characterization

3.6.1 Sampling

The coconut shells (Figure 3.13a) and oil palm kennels shells (Figure 3.13b) were

Figure 3.13: (a) Crushed coconut shell (b) Crushed oil palm kennel shells

collected from the markets within the Kumasi Central Business District. The biomasses were thoroughly washed with distilled water severally to ensure the removal of impurities.

3.6.2 Biochar Preparation

The crushed and washed samples were incubated at 105° C for 24 h to dry. The samples were put in crucibles, covered and put in the furnace and slowly pyrolysed to $600\,^{\circ}$C for two hours at a heating rate of $5\,^{\circ}$C/min. Subsequently, the biochar was washed with distilled water (Figure 3.14). Biochar was then ground in a household blender for 1 min at the 'Low' setting. The biochar samples was then sieved to separate out sizes of less than 600 μg diameter. The biochar samples of size less than 600 μg at dosing amounts of 3, 6 and 10 g were utilized for the experiment.

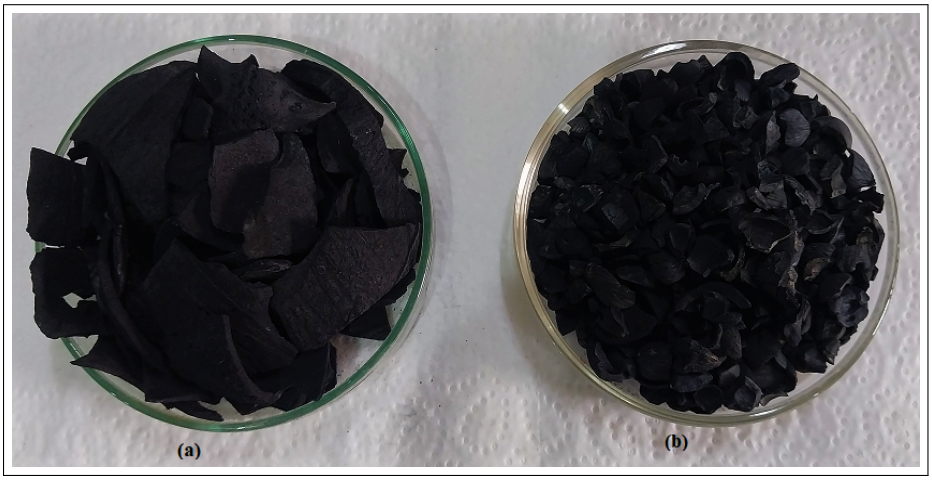

Figure 3.14: (a) Coconut shell biochar (b) Oil palm kennel shell biochar

3.6.3 Biochar Characterization

3.6.3.1 Fourier Transform Infrared (FTIR) Analysis

FTIR spectroscopy reported by Liu et al. (2015), was employed to investigate the structural features and molecular composition of biochar samples. This was performed at the KNUST Central Laboratory. All infrared spectra were collected with an FTIR Bruker Alpha FTIR spectrometer equipped with platinum attenuated total reflectance (ATR-FTIR, Bruker, Karlsruhe, Germany). The ATR-FTIR diamond crystal and all accessories were thoroughly cleaned with isopropanol between samples and background scans. The spectra were measured from 4000 cm^{-1} to 400 cm^{-1} with a scanning time of 32 s at a spectral resolution of 4 cm^{-1}. The spectra were obtained with the OPUS software (Bruker, Karlsruhe, Germany).

3.6.3.2 X-Ray Diffraction (XRD) Analysis

X-ray Diffraction (XRD) technique as described by Khan et al. (2020) and Chauhan and Chauhan (2014), was used to elucidate the crystalline nature of the biochar samples. This was performed at the Department of Physics, University of Ghana. The scattering of X-rays from atoms produced a diffraction pattern that contained information about the atomic arrangement in crystal. XRD patterns of biochar were obtained

on a powder X-ray diffractometer Model Philips with $CuK\alpha$ radiation having a scanning speed of $0.04\,°$/s.

3.6.3.3 X-Ray Fluorescence (XRF) Analysis

X-ray fluorescence (XRF) spectroscopy documented by Abdel-Fattah et al. (2015) was used to determine the elemental and oxide compositions of the samples using a Rigaku NEX CG XRF. This was performed at the Department of Earth Science, University of Ghana.

3.6.3.4 Brunauer-Emmett-Teller (BET) Analysis

BET surface analysis described by Abdel-Fattah et al. (2015), was carried out at the Centre for Genetic Engineering and Bioinformatics Technology, Federal University of Technology, Minna (Niger State), Nigeria using a Nova 4200e surface area and pore analyzer (Quantachrome Instruments, USA). The pore volume and pore diameter were determined using the method of Barrett–Joyner–Halenda (BJH). The samples were degassed at $250\,°$C for 3h prior to analysis. Nitrogen was used as the adsorptive gas at 77 K.

3.7 Theoretical BioMethane Potential (BMP_{TH})

The empirical relationship between the feedstock components were determined using Equation 3.16 by Buswell and Mueller (1952) and Buswell and Boruff (1932).

$$C_aH_bO_c + (a - \frac{b}{4} - \frac{c}{2}) \times H_2O \rightarrow (\frac{a}{2} + \frac{b}{8} - \frac{c}{4}) \times CH_4 + (\frac{a}{2} - \frac{b}{8} + \frac{c}{4}) \times CO_2 \tag{3.16}$$

When ammonia and hydrogen sulphide were released from protein-containing substrates, a modified Buswell equation by Boyle (1976) was used, as shown in Equation 3.17.

$$C_aH_bO_cN_dS_e + (a - \frac{b}{4} - \frac{c}{2} + \frac{3d}{4} + \frac{e}{2}) \times H_2O \rightarrow (\frac{a}{2} - \frac{b}{8} + \frac{c}{4} + \frac{3d}{8} + \frac{e}{4}) \times CO_2 + (\frac{a}{2} + \frac{b}{8} - \frac{c}{4} - \frac{3d}{8} - \frac{e}{4}) \times CH_4 + d \times NH_3 + e \times H_2S \quad (3.17)$$

The theoretical methane yield was derived from the empirical formulae $C_aH_bO_cN_dS_e$ and estimated using Equation 3.18, based on the atomic composition of the substrate (Steffen et al., 2016; Fagbohungbe et al., 2015; Raposo et al., 2013).

$$BMP_{TH} = (\frac{(\frac{a}{2} + \frac{b}{8} - \frac{c}{4} - \frac{3d}{8} - \frac{e}{4}) \times 22400}{12a + b + 16c + 14d + 32e}) \quad (3.18)$$

3.7.1 Biodegradability (BD)

The extent of anaerobic biodegradability, BD, was calculated by dividing experimental methane yield (BMP_{exp}) by the theoretical methane potential (BMP_o) according to the Equation 3.19 (Wang et al., 2014a).

$$BD(\%) = (\frac{BMP_{exp}}{BMP_o}) \times 100 \quad (3.19)$$

3.8 Experimental Setup

The batch experiment was set up as shown schematically in Figure 3.15. For the determination of the BMP of HE, FLO, KR and cellulose, the experiments were performed in triplicates using 500 ml bottles with a total working volume of 325ml (60 %) as shown in Figure 3.16. The inoculum and substrates were added at a ratio of 1 based on VS (Holliger et al., 2016). Bottles containing cellulose were used as positive controls whereas the bottles with only inoculum were used as blanks. The bottles were kept in a temperature-controlled incubator at 30 ± 1°C (Figure 3.17).

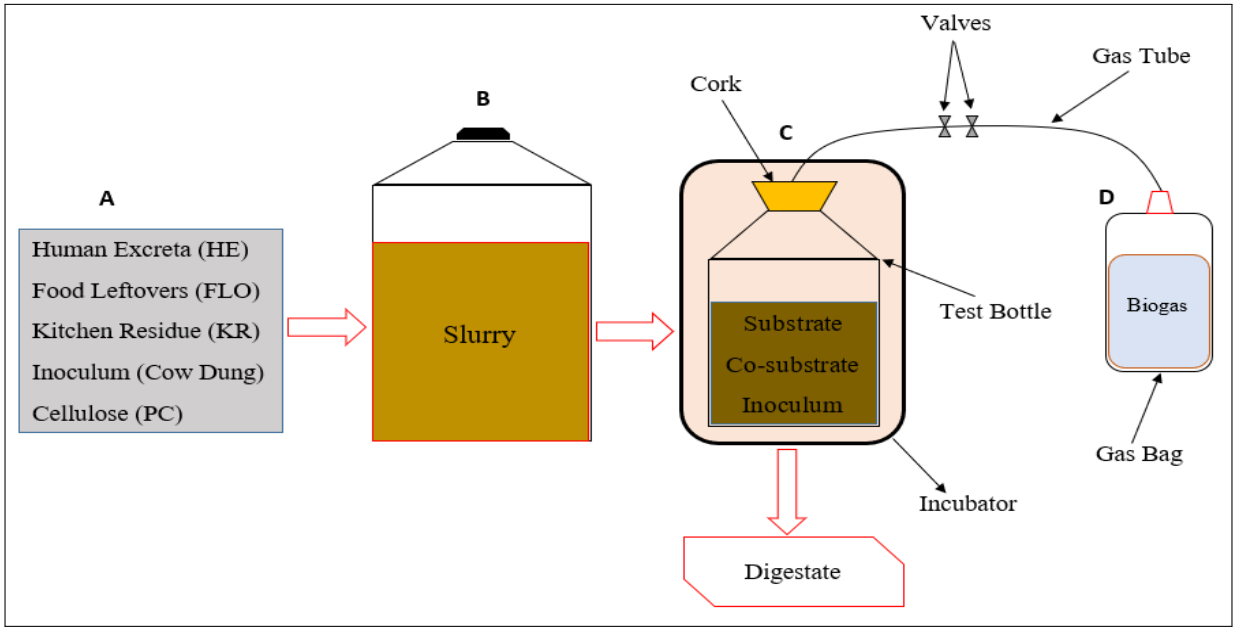

Figure 3.15: Schematic Batch Test Setup (A)Feedstocks used (B)Slurry from the mixture of feedstocks (C)Bottles filled with slurry and put in an incubator (D)Gas bags for the collection of gas generated

Figure 3.16: Bottles filled with a mix of feedstock and inoculum just before the start of the experiment

Figure 3.17: Bottles in an incubator and connected with tubes leading to the gasbags

3.9 Biogas Collection and Measurements

The entire bottle and gas collection setup were built to create an anaerobic condition using epoxy and silicone sealants. The bottles were connected to gas bags through polypropylene tubing (Figure 3.18).

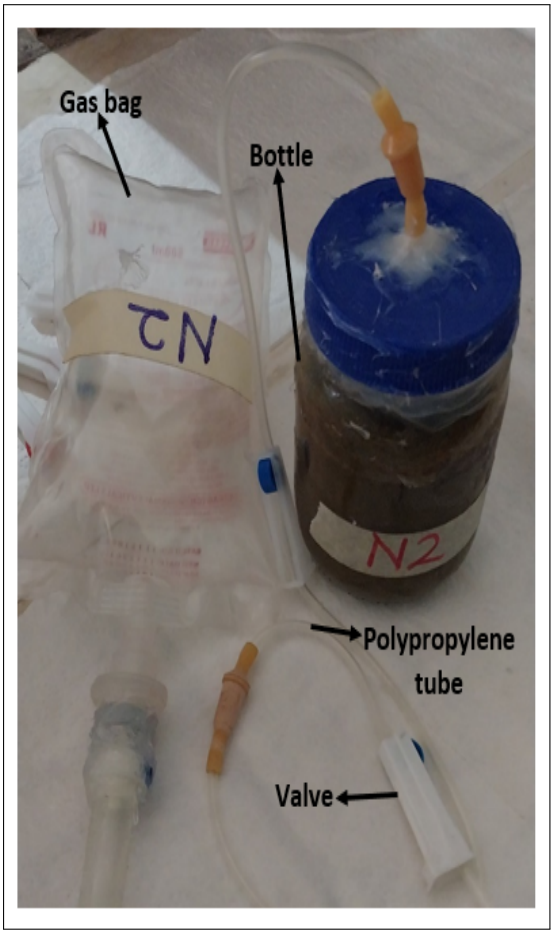

Figure 3.18: Biogas collected in gas bag

The volume of generated biogas in the gas bags was determined adhering to the downward water displacement technique (Filer et al., 2019) using an inverted glass chamber of 1000 mL capacity as shown in Figure 3.19.

Figure 3.19: Gas volume measurement using water displacement method

3.9.1 Gas Composition Measurements

Composition of biogas (methane, carbon dioxide, hydrogen sulfide and ammonia) was measured with a portable Biogas 5000, Geotech UK) analyzer (Figure 3.20). The individual volumes of the various component gases were then estimated Equation 3.20 (Singh et al., 2021a).

$$Component\ Gas(ml) = Biogas \times (\frac{Component\ Gas(\%)}{100}) \tag{3.20}$$

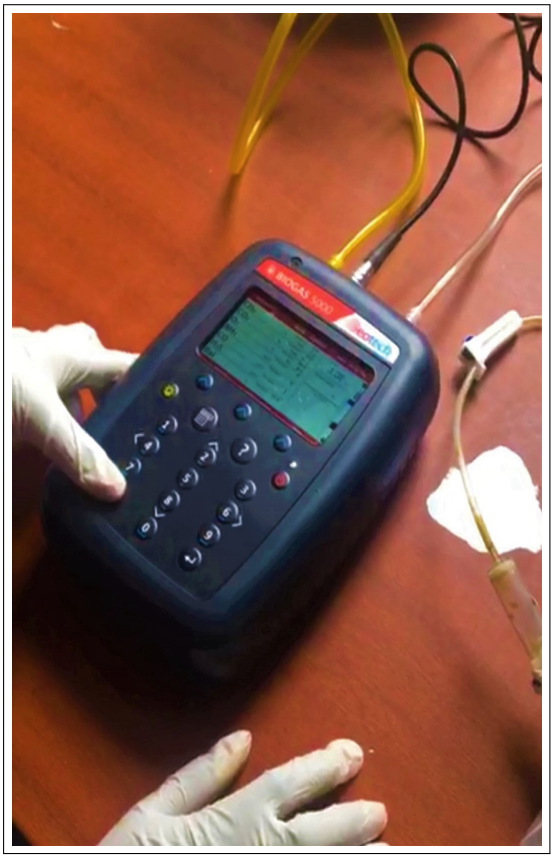

Figure 3.20: Gas Composition Analyser,Biogas 5000

3.9.1.1 Normalizing Gas Readings

The gas volume normalization was based on the ideal gas law, PV = nRT. *P* is the pressure of the gas, *V* is the volume of the gas, *n* is the number of moles of gas, *T* is the temperature of the gas and *R* is the ideal gas constant. For the experimental setup with the gas bag and water column, the actual room temperature *(Tr)* and atmospheric pressure *(Pr)* were recorded at the same time as the gas volume *(V)* was measured. These values were used for gas volume normalization under standard temperature *(To)* and pressure *(Po)* according to Equation 3.21 (Wang et al., 2014a).

$$V_{STP} = (\frac{V \times T_o \times P_r}{T_r \times P_o}) \tag{3.21}$$

3.10 Synergy

Synergy index (SI) was determined as the ratio of methane yield of the co-digestion substrates $(M_{i,n})$ to the weighted average $(M_{oi,n})$ based upon VS content (% VS) of the methane yield of individual substrate. This was calculated using Equation 3.22 (Hou et al., 2020; Ebner et al., 2016).

$$SI = (\frac{M_{i,n}}{M_{oi,n}}) = (\frac{M_{i,n}}{\sum_i^n \%VS_i M_{o,i}}) \tag{3.22}$$

where subscripts 'i' through 'n' denote the co-digested substrates and $\sum_i^n \%VS_i$=1. An SI greater than one (>1) implies a synergistic impact, while an SI less than one (<1) indicates an antagonistic effect.

3.11 Statistical Analysis

Samples were analysed in triplicates and reported as the mean value ± standard deviation (SD) in results and discussion. One-way analysis of variance (ANOVA) was then used to test the Statistical significance of different digesters. Also, Tukey's honestly significant difference (HSD) test was used for the pairwise comparison of the mean biomethane composition obtained during co-digestion using Minitab v.19 software. *($p < 0.05$)* was used as threshold for statistical significance.

3.12 Kinetic Modeling

Five kinetic models namely, modified gompertz , logistic function, cone, fitzhugh and monod models were selected to fit the data for biogas generated from the experiment. The models were fitted to the experimental data to determine the kinetic constants. The equations for the various kinetic models used in this study are presented in the subsections below.

3.12.1 Modified Gompertz Model

The modified Gompertz equation is presented as shown in Equation 3.23 (Budiyono and Sumardiono, 2014; Yusuf et al., 2011).

$$Y = Aexp(-exp[\frac{R_m e}{A}(\lambda - t) + 1]) \tag{3.23}$$

where *Y* is the cumulative methane yield at any time, *t* ($mlCH_4/gVS$), *A* is the simulated maximum methane yield ($mlCH_4/gVS$), R_m is the maximum methane production rate ($mlCH_4/gVS/day$), *e* is Euler's function with a value of 2.718282, λ is the lag phase for methane production (day) and t is the time in (day).

3.12.2 Logistic Function Model

The logistic kinetic model equation was used as shown in Equation 3.24.

$$Y = (\frac{A}{1 + exp[4R_m\frac{\lambda - t}{A} + 2]}) \tag{3.24}$$

where *Y* is the cumulative methane yield at any time, *t* ($mlCH_4/gVS$), *A* is the simulated maximum methane yield ($mlCH_4/gVS$), R_m is the maximum methane production rate ($mlCH_4/gVS/day$) and λ is the lag phase for methane production (day).

3.12.3 Cone Model

The cone model described by Bedoić et al. (2020); Ma et al. (2019b) was used as shown in Equation 3.25.

$$Y = (\frac{A}{1 + (k \times t)^{-n}}) \tag{3.25}$$

where *Y* is the cumulative methane yield at any time, *t* ($mlCH_4/gVS$), *A* is the simulated maximum methane yield ($mlCH_4/gVS$), *k* is the rate constant and *n* is the dimensionless shape factor.

3.12.4 Fitzhugh Model

The Fitzhugh kinetic model described by Pitt et al. (1999) was applied as shown in Equation 3.26.

$$Y = A(1 - exp(-kt)^n) \tag{3.26}$$

where *Y* is the cumulative methane yield at any time, *t* ($mlCH_4/gVS$), *A* is the simulated maximum methane yield ($mlCH_4/gVS$), *k* is the rate constant and *n* is the dimensionless shape factor.

3.12.5 Monod Model

The monod model described by Lawrence and McCarty (1969) was applied as shown in Equation 3.27.

$$Y = A \times (\frac{k \times t}{1 + (k \times t)}) \tag{3.27}$$

where *Y* is the cumulative methane yield at any time, *t* ($mlCH_4/gVS$), *A* is the simulated maximum methane yield ($mlCH_4/gVS$) and *k* is the rate constant.

3.12.6 Model Evaluation

Experimental validation was done for each kinetic model to make sure the expected biogas yields matched the results of the experiments. Equations 3.28–3.34 provided statistical measures of the goodness of fit for the models, using coefficient of determination (R^2), adjusted (R^2), Akaike's information criterion *(AIC)* and error terms such as the mean square error *(MSE)*, root mean square error *(RMSE)*, standard error of prediction *(SEP)* and mean absolute error *(MAE)* (Venkateshkumar et al., 2020; El-Mashad, 2013)

$$R^2 = 1 - (\frac{\sum_{i=1}^{n}(P_i - (P_i)^{est})^2}{\sum_{i=1}^{n}(P_i)^{est} - P_{avg})^2}) \tag{3.28}$$

$$AdjustedR^2 = 1 - [(1 - R^2) \times (\frac{n-1}{n-N-1})] \tag{3.29}$$

$$AIC = nln(\frac{RSS}{n}) + 2(N+1) + \frac{2(N+1)(N+2)}{(n-N-2)} \tag{3.30}$$

$$MSE = 1/n \sum_{i=1}^{n} (P_i)^{est} - (P_i)^2 \tag{3.31}$$

$$RMSE = \sqrt{1/n \sum_{i=1}^{n} ((P_i)^{est} - (P_i))^2} \tag{3.32}$$

$$SEP = (\frac{RMSE}{P_{avg}}) \times 100 \tag{3.33}$$

$$MAE = 1/n \sum_{i=1}^{n} |(P_i)^{est} - (P_i)| \tag{3.34}$$

where *n* is the number of data points, Pi^{est} is the estimated value, *Pi* is the experimental value, P_{avg} is the average experimental value, *N* is the number of model parameters and *RSS* is the residual sum of squares.

3.13 Response Surface Method (RSM)

The percentages of HE, FLO, and KR in the substrate combinations (ranging from 0 to 100 %) were utilized as independent variables to calculate the yields of biogas, methane, and synergy (Baek et al., 2020). A sequential process of experimental data collection, polynomial equation construction, and model suitability assessment was used for RSM. In order to predict the responses of biogas and methane yields as well as synergy, progressively more complicated polynomials were fitted to the experimental data. Using backward stepwise regression, the best response surface model was chosen. The experimental matrix was produced and the RSM calculations for model selection were carried out using the Design Expert 13 program from Stat-Ease, Minneapolis, Minnesota, USA.

CHAPTER 4

Physico-Chemical Characterization of Selected Feedstocks as Co-Substrates in Household Biogas Generation in Ghana

4.1 Abstract

Biogas substitution for Liquefied Petroleum Gas (LPG) in households would be the long-awaited solution to the problems of increasing cost of energy and large amounts of household human-generated waste. Nevertheless, a thorough study of the physico-chemical characteristics is essential to maximise the energy potential of such waste biomass. Consequently, this study examined the physico-chemical properties of chosen feedstocks, namely, Human Excreta (HE), Food Leftovers (FLO), Kitchen Residue (KR) and Cow Dung (CD) of Ghanaian origin using APHA standards and standard equipment. Results for volatile to total solid ratios (VS/TS) were 0.81±0.001, 0.97±0.0 01,0.89±0.001 and 0.85±0.001 for HE, FLO, KR and FLO respectively. The results showed that all feedstocks had higher biodegradable content making them desirable for biogas production. The C/N ratios determined from the elemental compositions were 8.29±0.09, 22.14±0.26, 23.34±0.25 and 26.19±0.47 for HE, FLO, KR and CD, respectively. Although C/N ratio for FLO, KR and CD were within the optimal range, that of HE was significantly low. With a mean alkalinity of 1219.67±1.53, 630.00±0.58, 590.00±2.08 and 15730.00±6.00 mg/L for HE, FLO, KR and CD respectively, it was observed that only CD has the optimal alkalinity value for anaerobic digestion. This brings into perspective the need for co-digestion.

4.2 Introduction

Ghana shares similar challenges with other developing nations regarding waste management and access to clean energy. Fortunately, these two challenges are connected. A better waste management strategy would involve turning the organic waste fractions produced in these nations into biofuels. In many Ghanaian households, substantial

amounts of organic food waste and human excrement are produced daily (Arthur et al., 2020) . Increased population density, urbanisation, and economic expansion are known to contribute to the exponential rise in the quantity of human-generated waste (Singh et al., 2021b; Kim et al., 2019b). The world bank has reported a worldwide average daily per capita municipal solid waste generation of 0.74 kg, which amounted to 2.01 billion tonnes of waste in 2016 (Ibikunle et al., 2019).

Additionally, Miezah et al., 2015 reported that Ghana generates 12,710 tonnes of waste per day, which translates into a waste generation rate of 0.47 kg/person/day. However, only about 44 % of solid wastes generated in Ghanaian metropolis are properly collected and disposed of (Abalo et al., 2018), with rural residents receiving worse service (Ketibuah et al., 2004; Boadi and Kuitunen, 2003). Also, less than 30 % of urban residents have acceptable household toilet facilities (Boateng, 2015; Mensah and Larbi, 2005). However, Arthur et al. (2020) reported an increased value of 38.6 % for rural users of flush and non-flush toilet facilities.

That not withstanding, waste management practices in Ghana mostly focus on fostering service access and disposal. Bukari et al. (2019) argues that certain solid waste disposal activities such as landfilling are unnecessary and that reuse of waste contributes to the improvement of livelihoods of urban households. With the rising pattern of urban garbage output, finding sustainable strategies to achieve waste management goals and the sustainable development goals (SDGs) 3(good health and well-being), 6(clean water and sanitation), and 13(climate action) has become difficult for governments and city authorities. Nevertheless, better alternatives are provided by examining the waste management hierarchy. The preferred fundamental waste management techniques in the waste management hierarchy are avoidance, reduction, reuse, recycling, energy recovery, and trash disposal (Zeng et al., 2010). According to Bukari et al. (2019), families could explore energy recovery and other alternative ways of using their solid waste.

Reliance on fossil fuels is becoming increasingly unsustainable due to ecological and environmental issues (Walekhwa et al., 2009). Also, people in rural regions are

mostly known for their usage of woody biomass, typically in the form of charcoal or firewood for cooking purposes. Sharma et al. (2015) has reported that the global contribution of biomass to total energy consumption is between 75 % and 90 %, with 40 % of people using agricultural biomass such as wood fuel, charcoal, and other non-woody biomasses traditionally to meet household energy needs (O'Shaughnessy et al., 2014; Surendra et al., 2014; Karekezi, 2002). In some Sub-Saharan African nations, wood biomass for cooking makes up more than 90 % of all energy use (Shane et al., 2017). However, there are consequences for the environment, human health, and food insecurity due to the rising use of these woody biomasses as home energy sources (Ghimire, 2013; Lam et al., 2011).

Also, Mensah et al. (2016) found that LPG and biomass-based energy sources like charcoal have continually been substituted for one another significantly. This is frequently brought on by price shocks and, more significantly, by sporadic shortages of LPG in the Ghanaian market. Additionally, Amigun et al. (2012) contend that low disposable incomes in urban and rural populations make the fuel transition from wood biomass less likely. It is therefore necessary to investigate and utilize eco-friendly renewable energy sources, in order to relieve households of their need to purchase LPG regularly. Environmentally friendly and sustainable renewable energy alternatives, such as biogas from anaerobic digestion process is being recommended to address the issue.

Having stated that, it is imperative to gather as much data about the physical, biological, and chemical compositions of selected feedstocks. This is because, the characteristics of individual feedstocks and have immediate impact on biogas output, anaerobic degradation stability, and startup procedure (Gaballah et al., 2020; Lohani and Havukainen, 2018). Further, data on feedstocks can be used to determine the theoretical methane potential (VDI, 2006; Browne and Murphy, 2013; Drosg et al., 2013; Angelidaki et al., 2009). Although the effectiveness and suitability of various anaerobic digestion feedstocks for biogas recovery have been well documented, indigenous feedstock characterisation is of utmost importance. The potency of any selected feedstock for energy recovery is influenced by the peculiarities or uniqueness of locations,

atmospheric conditions, and nutrition (Fajobi et al., 2022). This highlights the need for appropriate characterisation of locally sourced feedstock to determine their eligibility as substrates for the anaerobic digestion process (Fajobi et al., 2022).

Human Excreta (HE), Food Leftovers (FLO), Kitchen Residue (KR) and Cow Dung (CD) are the feedstocks characterised in this study. It is crucial to determine their physico-chemical properties through standard procedures because of the variability in their availability, energy production methods, and limited information on their suitability as anaerobic co-digestion feedstocks. This study examines the emphasized feedstocks by considering proximate, ultimate, compositional, and mineral analyses. This finding will serve as a reference for biogas producers and stakeholders who desire to extract energy from the examined feedstocks.

4.3 Materials and Method

4.3.1 Biomass Collection and Preparation

Fresh HE was collected from a KVIP at Ayeduase in Kumasi, Ghana. FLO and KR were also collected from households of staff and the canteen at a Senior High School in Kumasi following the coning and quartering method detailed in chapter 3. Fresh CD was collected from the animal farm of the Department of Agriculture, KNUST. Components and compositions of FLO and KR are specified in Table 4.1. FLO, KR and CD were manually sorted to remove non-biodegradable fractions before organic fractions were shredded into smaller pieces, blended and homogenized into a slurry to maintain a particle size below 3 mm using a household food grinder and 3 mm sieve. Samples were frozen at a temperature of $-20\,^{\circ}$C before use. The frozen samples were allowed to thaw at a temperature of $4\,^{\circ}$C and used within a day to prevent biological decomposition.

Table 4.1: Percentage composition of FLO and KR based on wet weight

KR Components	% Composition (% wet weight)	FLO Components	% Composition (% wet weight)
Pawpaw peels	3.04	Rice	27.58
Watermelon peels	4.53	Cassava / Fufu	17.52
Avocado peels	3.12	Kenkey (cooked fermented corn dough)	14.66
Banana peels	2.59	Banku (cooked fermented cassava and corn dough)	12.80
Mango peels	4.00	Bread and Vegetables Sauce	4.19
Orange peels	5.87	Plantain	6.58
Pineapple peels	3.28	Kontomire (Boiled Cocoyam Leaves)	2.06
Onion peels	4.98	Gari and Beans	3.09
Lettuce, Cucumber, Pepper, Tomato, Carrot, Garden Eggs	8.48	Fish	0.12
Cocoyam peels	3.19	Egg	0.05
Plantain peels	12.47	Yam	11.35
Yam peels	20.91	-	-
Cassava peels	23.54	-	-

4.3.2 Proximate Analyses

The APHA method 2540 B was used to determine the total solids (TS) content of the feedstocks using a Lanphan DZF-6090 drying oven (APHA, 1998). Also, APHA method 2540 E (APHA, 1998), was employed for volatile solids (VS) determination using a Lanphan Atmosphere Furnace-SA2-4-17TP. The moisture content (MC) and Ash content (AC) of the feedstocks were estimated according to Equations 4.1 and 4.2 (Singh et al., 2021a).

$$\%MC = 100 - TS\% \tag{4.1}$$

$$\%AC = 100 - (MC\% + VS\%) \tag{4.2}$$

4.3.3 Ultimate Analysis

Ultimate analysis was conducted at the Department of Agriculture and Department of Natural Resources, KNUST. The levels of carbon (C), hydrogen (H), nitrogen (N), oxygen (O), and sulphur (S) in the feedstocks were determined using standard procedures (APHA, 1998). The total amount of sulphur was quantified using the spectrophotometer method (Singh et al., 1999), and the percentage of total nitrogen was computed using the Kjeldahl method (Bremner, 1965). Titrimetry (McLean, 1965) was employed to determine the amount of hydrogen, and the Walkley-Black Wet Oxidation method was used to obtain the amount of organic carbon (Heanes, 1984; Nelson, 1982). Using Equation 4.3 (Fajobi et al., 2022), the oxygen content was calculated.

$$\%O = 100 - (C + H + N + S + AC)\% \tag{4.3}$$

4.3.3.1 C/N Ratio

The C/N ratio of the feedstocks was calculated using Equation 4.4. (Dahunsi et al., 2019; Anderson and Ingram, 1993).

$$C : N = \frac{\%Carbon}{\%Nitrogen} \tag{4.4}$$

4.3.4 Chemical Analysis

The alkalinity of each feedstock was determined according to the APHA method 2320B using Potentiometric titration (APHA, 1998). A digital Hanner H1 98136 pH meter was used to measure pH. The COD of each feedstock was also determined by adapting to the HACH COD method using the HACH COD HR+ (200-15000 mg/L) test vials and DR 3900 spectrophotometer.

4.3.5 Compositional Analysis

4.3.5.1 Crude Fat Content

Samples of each feedstock was extracted with ether using method AOAC 2003.05 (AOAC, 1990, 2006). Equation 4.5 is used to calculate the percentage of ether extract.

$$\%EtherExtract = (\frac{B}{C}) \times 100 \tag{4.5}$$

where *B* = ether extract weight, *C* = sample weight

4.3.5.2 Crude Protein Content

Crude protein was calculated from nitrogen (N) determination using AOAC Method 984.13 (AOAC, 1995). A conversion coefficient of 6.25 was used to calculate protein concentration as shown in Equation 4.6.

$$\%Crude\ Protein = Total\ Nitrogen(N_T) \times 6.25(Protein\ Factor) \tag{4.6}$$

4.3.5.3 Crude Fibre Content

Carbohydrates were calculated as the mass-balance difference of the crude fat, protein, moisture and ash determinations (AOAC, 1990). Equations 4.7 and 4.8 provide the general formula.

$$\%Carbohydrate = \%TS - (\%AC + \%Fat + \%Protein) \tag{4.7}$$

$$\%Carbohydrate = 100\% - (\%AC + \%MC + \%Fat + \%Protein) \tag{4.8}$$

4.3.6 Mineral Analysis

Potassium (K) and sodium (Na) contents were analysed using flame photometry (Barnes et al., 1945). The calorimetric determination of phosphorus (P) was done using vanadium phosphomolybdate method specified by APHA (1992). Calcium (Ca) and magnessium (Mg) contents were determined using atomic absorption spectroscopy (AAS) with model VGP 210 from Buck Scientific (Katz and Jenniss, 1983). PerkinElmer's NexION 2000 ICP-MS was used to detect the amounts of nickel (Ni), molybdenum (Mo), chromium (Cr), cobalt (Co), cadmium (Cd), zinc (Zn), copper (Cu), selenium (Se), manganese (Mn) and iron (Fe) in the feedstocks.

4.3.7 Theoretical BioMethane Potential (BMP_{TH})

The empirical relationship between the components of the feedstocks were determined using a modified Buswell equation by Boyle (1976), as shown in Equation 4.9.

$$\begin{aligned} C_aH_bO_cN_dS_e + (a - \frac{b}{4} - \frac{c}{2} + \frac{3d}{4} + \frac{e}{2}) \times H_2O \rightarrow (\frac{a}{2} - \frac{b}{8} + \frac{c}{4} + \frac{3d}{8} + \frac{e}{4}) \times CO_2 + \\ (\frac{a}{2} + \frac{b}{8} - \frac{c}{4} - \frac{3d}{8} - \frac{e}{4}) \times CH_4 + d \times NH_3 + e \times H_2S \end{aligned} \tag{4.9}$$

The theoretical methane yield was estimated using Equation 4.10 (Scherer et al., 2021; Steffen et al., 2016; Fagbohungbe et al., 2015; Raposo et al., 2013).

$$BMP_{TH} = (\frac{(\frac{a}{2} + \frac{b}{8} - \frac{c}{4} - \frac{3d}{8} - \frac{e}{4}) \times 22400}{12a + b + 16c + 14d + 32e}) \tag{4.10}$$

4.4 Results and Discussion

4.4.1 Physico-Chemical Properties of Feedstocks

The physical and chemical characteristics of the selected feedstocks are summarized in Table 4.2.

4.4.1.1 Variability of Organic Matter in Feedstocks

The TS content of FLO (25.65±0.02 %) and CD (24.71±0.18 %) were higher than that of HE (11.32±0.03 %) and KR (9.42±0.01 %) as shown in Table 4.2. Nonetheless, higher TS values in FLO and CD may limit the mobility of methanogens, leading to longer retention times (Kossmann and Pönitz, 1999). FLO has been reported to have a TS range of 18.1–37.8 % (Dhamodharan et al., 2015; Zhang et al., 2014; Uncu and Cekmecelioglu, 2011; Wang and Zhao, 2009; Ohkouchi and Inoue, 2006), with a typical TS content of 20 % for cooked food (Pax et al., 2020; Paritosh et al., 2017). Bodík and Miroslavakubaská (2014), emphasized that traditional food structure and composition variations affect the solid content of food waste from different locations.

The TS content of KR in this study (9.42 %) was as low as the value of 12.23 % reported by Li et al. (2020a) due to the high moisture content of kitchen residues like fruit and vegetable waste. Literature reports TS values of HE ranging from 14 % to 37 %, which is higher than the value obtained in this study (Singh et al., 2021b; Miller et al., 2015; Rose et al., 2015; Wignarajah et al., 2006). Also, the reported TS content range of CD is 20.0 % to 32.8 % (Singh et al., 2021b; Arifan et al., 2021; Pax et al., 2020; Dhamodharan et al., 2015), and the TS value of CD from this study (24.71 %) falls within this range. In addition, Table 4.2 shows the moisture content of HE, FLO, KR, and CD in this study. It was observed that HE and KR had higher moisture content than FLO and CD. This is beneficial for co-digestion, as it helps to maintain desirable moisture levels (Karki et al., 2021). The moisture content values reported in this study are similar to those reported by Singh et al. (2021b) for HE (84.0 %) and CD (66.0 %), Parra-Orobio et al. (2018) for FLO (76.0 %) and CD (67.2 %) and Oladejo et al. (2020) for CD (85.6 %) and FLO (81.1 %) respectively.

Table 4.2: Physical, Chemical and Compositional Characteristics of HE, FLO, KR and CD (mean (standard deviation); n = 3)

	Analysis	HE	FLO	KR	CD
Proximate Analysis	TS(% wet weight)	11.32 (0.03)	25.65 (0.02)	9.42 (0.01)	24.71 (0.18)
	VS (% of TS)	81.02 (0.05)	96.89 (0.06)	88.59 (0.09)	85.29 (0.03)
	VS (%)	9.17 (0.02)	24.85 (0.01)	8.35 (0.02)	21.08 (0.16)
	VS/TS	0.81 (0.001)	0.97 (0.001)	0.89 (0.001)	0.85 (0.001)
	MC (% wet weight)	88.68 (0.03)	74.35 (0.02)	90.58 (0.01)	75.29 (0.18)
	AC (% wet weight)	2.15 (0.01)	0.80 (0.02)	1.08 (0.01)	3.63 (0.02)
Compositional Analysis	Carbohydrate(% dry weight)	NA	56.88 (0.04)	63.67 (0.01)	64.40 (0.02)
	Crude protein (%)	NA	19.58 (0.03)	11.82 (0.01)	12.56 (0.01)
	Crude fat (% dry weight)	NA	3.22 (0.02)	0.36 (0.01)	0.61(0.01)
Ultimate Analysis	Carbon (%)	44.92 (0.02)	46.93 (0.03)	44.03 (0.03)	52.71 (0.03)
	Hydrogen (%)	7.71 (0.02)	8.24 (0.02)	10.96 (0.04)	6.29 (0.02)
	Nitrogen (%)	5.36 (0.07)	2.12 (0.03)	1.89 (0.02)	2.01 (0.03)
	Sulphur (%)	0.32 (0.03)	0.18 (0.03)	0.33 (0.02)	0.59 (0.02)
	Oxygen (%)	39.55 (0.09)	41.73 (0.04)	41.47 (0.04)	34.76 (0.05)
	C/N	8.39 (0.09)	22.14 (0.26)	23.34 (0.25)	26.19 (0.47)

NA means Not Analysed

Zhang et al. (2012) reported a range of 69-93 % for moisture content of FLO and KR. Studies have shown that the moisture content of biomass affects its calorific value (Ahmed et al., 2019). It is therefore crucial to operate within an optimal moisture content range as extremely high or low moisture content can negatively impact process performance. Igoni et al. (2008) reported that extremely high moisture content is likely to affect process performance by dissolving readily degradable organic matter, whereas extremely low moisture content can kill some microorganisms, resulting in process failure. According to Gashaw (2016), methane production is at its greatest at humidity levels between 60.0 % and 80.0 %. The VS values of HE, FLO, KR, and CD are also shown in Table 4.2. VS is an essential parameter in determining the organic content and energy potential of feedstocks.

High VS values recorded for all feedstocks indicate the presence of readily biodegradable organic matter (Capson-Tojo et al., 2017). Literature reported values for HE (81.0 %) (Singh et al., 2021b), FLO (90.7-91.9 %) (Pax et al., 2020; Paritosh et al., 2017; El-Mashad and Zhang, 2010), and CD (88.0-96.0 %) (Singh et al., 2021b; Pax et al., 2020) are consistent with values reported in this study. In addition, the VS/TS ratio is an important indicator of biodegradable content (Li et al., 2013), and FLO had the highest VS/TS ratio of 0.97. Zhang et al. (2012) reported a VS/TS of 0.85-0.96 for FLO. The higher VS of FLO explains its lower ash content in comparison to HE, KR, and CD. VS of TS and actual VS reported by Li et al. (2020a) for KR were 85.94 % and 10.51 %, respectively. These values are quite close to that obtained in this work for KR (88.59 % and 8.35 %). However, the actual availability of organic matter for biogas production is limited by microbial uptake for growth.

The carbohydrate, protein, and fat contents of HE, FLO, KR, and CD are presented in Table 4.2. Carbohydrates ranged from 56.88 % to 64.40 %, while protein content ranged from 11.82 % to 19.58 % of dry weight, and fat content ranged from 0.36 % to 3.22 % for FLO, KR, and CD respectively. Fisgativa et al. (2016) documented the carbohydrate and protein contents of food waste to be 36.4 %VS and 21.0 %VS, respectively. Carbohydrates, also known as sugars, vary in amounts in almost all substrates. Rice, pasta, cassava, yam, and potatoes are rich in simple sugars, disaccharides,

and polysaccharides. Starch is the most common polysaccharide, consisting of straight or branched glucose chains.

Plant-derived substrates are also carbohydrate-rich despite their difficulty in degrading due to lignin presence (Hagos et al., 2017). High sugar concentrations can cause the rapid accumulation of volatile fatty acids (VFAs) and decreased pH in the biogas digester (Paritosh et al., 2017). High protein substrates however, generate substantial amounts of methane (Hagos et al., 2017). Also, fats have a high biogas yield although long chain fatty acid decomposition is complex (Rasit et al., 2015).

4.4.1.2 Variability in Chemical Composition of Feedstocks

The C, H, N, S, and O contents were in the range of 44.92±0.02 % – 52.71±0.03 %, 6.29±0.02 % - 10.96±0.04 %, 1.89±0.02 % - 5.36±0.07 %, 0.18±0.03 % - 0.59±0.02 % and 34.76±0.05 % - 41.73±0.04 % respectively for HE, FLO, KR and CD (Table 4.2). C and O had the highest contents for all feedstock types, while N and S recorded the lowest values. N and S contents are expected to be low during anaerobic digestion in order to reduce the quantity of trace gases (hydrogen sulphide, ammonia) produced. Correspondingly, the C/N ratios are reported on Table 4.2. Singh et al. (2021b) documented C/N ratios of 12.0 and 24.0 for HE and CD, whilst Paritosh et al. (2017) and Arifan et al. (2021) reported C/N ratios of 20.4 and 28.7 for food waste and CD respectively. Dhamodharan et al. (2015) and Zhang et al. (2007) have also reported a C/N of 14.7–36.4 for FLO.

Generally, a C/N ratio of 20-30 gives a more stable AD process (Dar et al., 2021; Rahman et al., 2017; Chiu and Lo, 2016; Haider et al., 2015). Dadaser-Celik et al. (2016), achieved the highest gas production with a C/N ratio of 28. Contrarily, Guarino et al. (2016) reported an optimum C/N ratio range of 9 to 50 and the value for HE (8.39) was close to the lower threshold of the range. Although the C/N ratio for HE was low, that for FLO, KR and CD were within the recommended C/N range of 20 to 30, for anaerobic digestion (Table 4.2). While carbon provides energy for microorganisms, nitrogen is used by bacteria that produce methane to meet their protein requirements (Matheri et al., 2017). When C/N is high, nitrogen (N) is rapidly depleted, microbial

activity is limited, VFAs accumulate, and biogas production is reduced (Siddique and Wahid, 2018).

Lower C/N values result in higher ammonia concentrations, which stifle microbial growth (Siddique and Wahid, 2018). Research has proven that co-digestion of feedstock such as HE, FLO, KR and CD can help balance and maintain optimum C/N levels (Karki et al., 2021; Hagos et al., 2017). It is therefore recommended that substrates with low C/N ratios be mixed with those with high C/N ratios for better AD performance (Rouf et al., 2010).

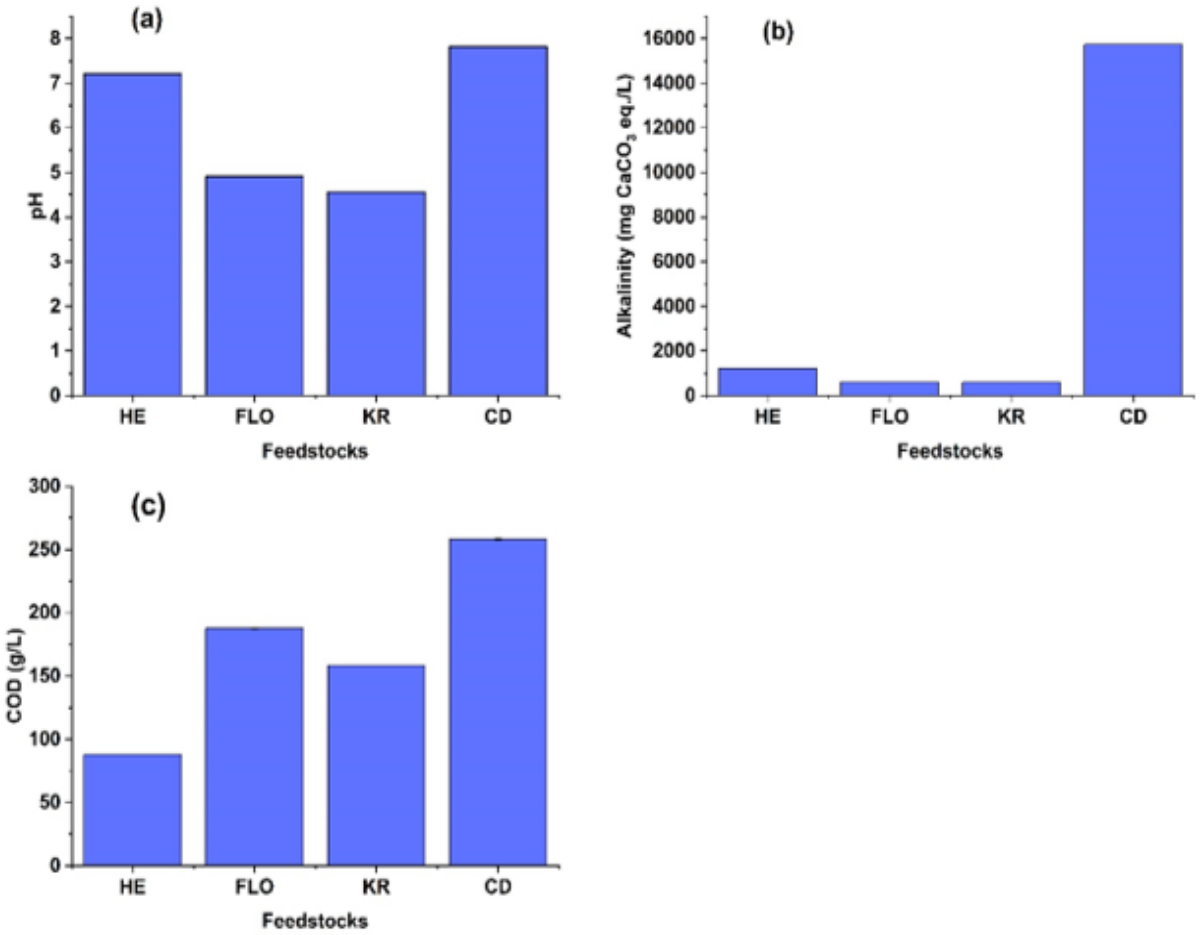

Figure 4.1: (a) pH, (b) Alkalinity and (c) COD levels in HE, FLO, KR and CD

Mean pH values of 4.91±0.01 and 4.56±0.01 in the acidic range were obtained for FLO and KR respectively, while HE and CD, with respective pHs of 7.21 ± 0.01 and

7.82 ± 0.02, were within the suitable range for AD (Figure 4.1a). The pH of HE was slightly above neutral (Figure 4.1a). Fanyin-Martin et al. (2017) reported a pH of 7.48 ± 0.33, 7.41 ± 0.36 and 7.87 ± 0.37 for HE from public septage, private septage and pit latrine, respectively. Also, Fisgativa et al. (2016), documented an average pH of 5.1±0.7, for food waste from 65 different studies. Similarly, Zhang et al. (2018c) and Shamurad et al. (2020) reported low pH values of 3.5 and 4.3, respectively, for FLO and KR. The low pH recorded for food waste could be attributed to the possible presence of carbohydrate-containing food materials, which can be converted to volatile fatty acids (Pramanik et al., 2019).

The low pH range is favourable for fermentative bacteria that could easily develop during the first few hours of the AD process. However, a higher pH is necessary for the digester to favour the development of methanogen microorganisms. In addition, pH values of 8.7 (Bah et al., 2014), 7.3 (Zhai et al., 2015) and 7.67 (Egwu et al., 2021) have been reported in literature for CD. These values are in the optimum range, just like what is reported in this study. Gashaw (2016) reported that reducing the pH of CD from 7.5 to 7.0 increased methane production by four times.

Nonetheless, the AD process can tolerate a pH range of 6.6 to 8.0 (Gashaw, 2014). When the pH level exceeds 8.5, it creates an unfavourable environment for methanogenic bacteria (Gashaw, 2014). The pH of a media during anaerobic digestion is one of the essential parameters due to the sensitivity of microorganisms to pH variations and its effect on the solubilisation of organic matter (Feng et al., 2015). The inability to keep the pH within a safe range could lead to reactor failure (Chen et al., 2008).

Alkalinity values for HE, FLO, KR and CD for this study are shown in Figure 4.1b. The alkalinity represents the buffering capacity in the biogas production system to maintain pH (Sawasdee et al., 2021). A major part of the alkalinity of a feedstock is required to buffer the CO_2, leaving only a small amount of "reserve alkalinity" to neutralize the VFAs. A high alkalinity value allows the system to absorb the VFAs produced, without leading to sharp decrease in pH (Gómez-Quiroga et al., 2020). Alkalinity values of 1200 mg $CaCO_3 L^{-1}$ for KR (Li et al., 2013), 825 mg $CaCO_3$ L^{-1} for

FLO (Chen et al., 2015), 980 mg $CaCO_3$ L^{-1} for sludge (Chen et al., 2015), 19550 mg $CaCO_3$ L^{-1} for CD (Egwu et al., 2021), and 38050 mg $CaCO_3$ L^{-1} for CD (Gómez-Quiroga et al., 2020) have been documented.

It is clear from this study and that of other researchers that CD has high alkalinity and could serve as a good buffer source when used as co-substrate or inoculum source during the anaerobic process. However, the alkalinity values for FLO (630 mg $CaCO_3$ L^{-1}) and KR (589 mg $CaCO_3$ L^{-1}) in this study do not fall within the optimal range; hence, the need for co-digestion with high alkalinity feedstocks. Mshandete et al. (2004) and Filer et al. (2019) recommend that alkalinity be kept at 3000 mg $CaCO_3$ L^{-1} to maximize methane yield. Alternatively, Georgacakis et al. (1982) propose alkalinity of at least 6000 mg $CaCO_3$ L^{-1} for anaerobic digestion. However, Scherer et al. (2021) recently found that alkalinity of 10,000 mg $CaCO_3$ L^{-1} yielded almost 100% biodegradation of organics.

Most likely, the COD strength of a feedstock has a significant impact on the final amount of biogas and methane yields (Ghani and Idris, 2009). As shown in Figure 4.1c, the high COD values obtained for HE, FLO, KR and CD show that the feedstocks have great potential during biogas generation. COD value was highest in CD (258115 mg/L), followed by FLO (187730 mg/L), KR (158327 mg/L) and HE (87682 mg/L) in this study. COD levels reported in literature for HE ranged from 800 to 92600 mg/L (Ahmed et al., 2019; Kim et al., 2019b; Fanyin-Martin et al., 2017; Koné and Strauss, 2004; Metcalf and Eddy, 2003).Moreover, some authors documented a COD range of 143000 - 510000 mg/L for FLO (Kim et al., 2019b; Bodík and Miroslavakubaská, 2014; Fisgativa et al., 2016). Furthermore, Singh et al. (2021b) reported a COD concentration of 280000 mg/L for CD.

4.4.1.3 Variability in Mineral Composition of Feedstocks

Trace elements are essential for microbial growth and have been reported to improve AD operation even in reactors with high organic loadings and contribute to reduction in the VFAs (Banks et al., 2012). Sodium (Na), calcium (Ca), potassium (K), phosphorus (P), and Magnesium (Mg) are essential constituents of biomass that maintain

the metabolic activities of microorganisms in anaerobic digestion (Zhang et al., 2018a, 2011). For the purposes of green energy generation, effluent and solid sludge reuse, it is essential to analyse the presence of indigenous micro and macro nutrients in feedstocks prior to the commencement and during the anaerobic digestion process (Arthur and Scherer, 2020). The macronutrient content (P, K, Ca, Mg and Na) for HE, FLO, KR and CD in this study ranged between 17.63 mg/L and 4184.83 mg/L (Figure 4.2).

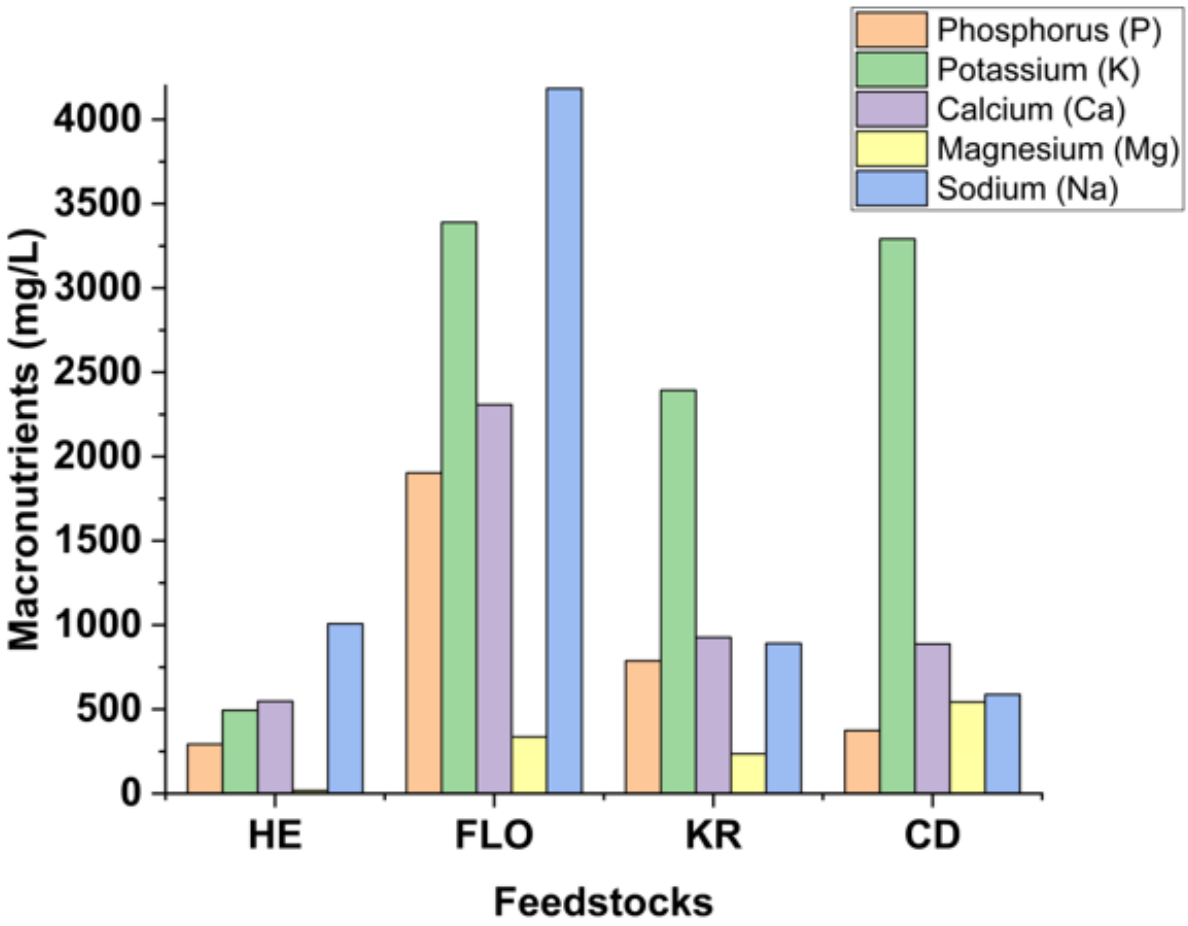

Figure 4.2: Phosphorus, potassium, calcium, magnesium and sodium contents in HE, FLO, KR and CD

In this study, FLO had the highest Na (4184.83 mg/L), P (1902.67 mg/L), Ca (2308.33 mg/L) and K (3390.00 mg/L) levels, while CD had the highest Mg (543.33 mg/L) level (Figure 4.2). Na, K and Ca are more prevalent in FLO and may contribute to salt inhibition (Mirmohamadsadeghi et al., 2019). For K, Mg, Na, P and Ca content in FLO, Fisgativa et al. (2016) reported mean values of 12000.00, 2000.00, 22000.00, 5000

and 16000 mg/L respectively. Comparatively, the K, Mg, Na, P and Ca levels of FLO in this study (Figure 4.2) were lower. Further, Ahmed et al. (2019) reported Ca, Mg, Na and K values of 90.00, 10.00, 530.00 and 710.00 mg/L respectively while Fagbohungbe et al. (2015) documented 20700.00, 2.00, 900.00 and 890.00 mg/L respectively for HE. These values are higher than what were obtained in this study (Figure 4.2).

For pit, public and private septage, Fanyin-Martin et al. (2017) obtained 520.00, 230.00 and 140.00 mg/L respectively, for phosphorus. The phosphorus level for this study (292.33 mg/L) lies within the range reported by Fanyin-Martin et al. (2017). Further, Shen et al. (2015a) obtained 6000.00, 9400.00, 2300, 16000 and 8600 for P, K, Na, Ca and Mg in CD. However, the K, Mg, Na, P and Ca levels of CD in this study (Table 4.3) were lower than what is reported in literature.

According to Chen et al. (2008), the presence of Na, K, Mg, and Ca can be inhibitory and toxic at certain concentrations. Na, for example, inhibits at a threshold concentration between 8000 mg/L and 12000 mg Na/L (Li et al., 2019b; Anwar et al., 2016). However, after microorganism adaptation, concentrations up to 15000 mg/L are tolerated (Speece, 1983). Conversely, at concentrations of 350–400 mg/L, Na creates an ideal environment for methanogens (Chen et al., 2008). On the other hand, the presence of Ca has a threshold value of about 7000 mg Ca/L (Lo et al., 2012), with the optimum calcium concentration being between 150 and 300 mg Ca/L (Paritosh et al., 2017; Jackson-Moss et al., 1989; Huang and Pinder, 1995). Nonetheless, Kugelman and McCarty (1965) reported a toxicity threshold as low as 200 mg/L. Also, the potassium (K) inhibition threshold is around 7500 mg K/L (Chen and Cheng, 2007).

At relatively low concentrations, micronutrients (trace metals) are critical cofactors in numerous enzymatic reactions involved in the biochemistry of methane formation (Arthur et al., 2022). Enzymes such as hydrogenase (containing Fe and or Ni) and formate dehydrogenase (containing Fe, Se, and Mo) release electrons from H_2 and HCOOH during interspecies hydrogen/formate transfer (Banks et al., 2012). The Fe, Ni, Zn, Cr, Co, Cu, Cd, Mo, Mn and Se levels of HE, FLO, KR and CD in this study are summarized in Table 4.3. For all trace elements, a suitable concentration range

Table 4.3: Mineral Characteristics of HE, FLO, KR and CD (mean (standard deviation); n = 3)

Analysis	HE	FLO	KR	CD
Iron, Fe (mg/L)	2.64 (0.001)	11.86 (0.004)	5.64 (0.003)	14.18 (0.001)
Nickel, Ni (mg/L)	0.34 (0.001)	0.09 (0.001)	0.06 (0.001)	1.43 (0.01)
Zinc, Zn (mg/L)	1.36 (0.001)	7.40 (0.001)	9.76 (0.005)	1.29 (0.001)
Chromium, Cr(mg/L)	0.36 (0.001)	0.06 (0.002)	0.02 (0.001)	4.32 (0.001)
Cobalt, Co (mg/L)	0.013 (0.0002)	0.005 (0)	0.003 (0)	0.203 (0.001)
Copper, Cu (mg/L)	0.95 (0.001)	0.23 (0.001)	0.36 (0.001)	1.25 (0.001)
Cadmium, Cd (mg/L)	0.003 (0)	0.002 (0)	0.004 (0)	0.01 (0.001)
Molybdenum, Mo (mg/L)	0.58 (0.001)	0.03 (0.001)	0.01 (0)	3.04 (0.01)
Manganese, Mn (mg/L)	0.23 (0.001)	0.59 (0.001)	0.38 (0.002)	1.84 (0.001)
Selenium, Se (mg/L)	0.004 (0)	0.002 (0)	0.003 (0)	0.014 (0.0001)

between the maximum nutrient requirements and inhibition is established (Brulé et al., 2013).

In this study, Fe, Zn and Mn for all feedstocks lie outside the stimulatory concentration range, while Ni, Cr, Co, Cu, Cd and Se lie within (Table 4.4). Mo lies within the stimulatory concentration range for FLO and KR, but lies outside the range for CD and HE. The micronutrients in HE are in the order Fe>Zn>Mn>Cu>Mo>Cr>Ni>Co>Se>Cd, whereas those in FLO are in the order Fe>Zn>Mn>Cu>Ni>Cr>Mo>Co>Cd=Se. KR on the other hand, have micronutrients in the order Zn>Fe>Mn>Cu>Ni>Cr>Mo>Cd>Co =Se and CD, in the order Mn>Fe>Zn>Cr>Mo>Ni>Cu>Co>Cd=Se. Lin (1992) opined that the relative toxicity of heavy metals to acetic acid degradation in mesophilic anaerobic digestion of sewage sludge was Cd>Cu>Cr=Zn>Pb>Ni. Evaluating heavy metal toxicity during anaerobic digestion of sewage sludge, Ahring and Westermann (1985) revealed severe inhibition at various concentrations for certain heavy metals, such as 70 to 400 mg/L for Cu, 200 to 600 mg/L for Zn, and 10 to 2000 mg/L for Ni.

Ni, Co, and Fe, have received the most attention in recent studies because they are essential cofactors of carbon monoxide dehydrogenase and other enzymes involved in acetoclastic methanogenesis (Choong et al., 2016; Romero-Güiza et al., 2016; Kida et al., 2001). Fe is used in the transport system of methanogenic bacteria to convert CO_2 to CH_4, and it serves as both an electron acceptor and donor (Vintiloiu et al., 2013). Fe also acts as a binding component in sulfide precipitation, controlling the level of hydrogen sulfide in the biogas (Gustavsson et al., 2013). Additionally, optimum Fe content in AD is likely to increase the rate of methane formation by activities of microorganisms such as *Methanosarcina barkeri* (Lin et al., 1990).

Cobalt (Co), a metal-ligand for vitamin B12, influences *methyl transferase* activity, a methyl transport component (Schattauer et al., 2011). This Co property allows microbes to degrade methanol (Romero-Güiza et al., 2016). Furthermore, Ni serves as a core element for *coenzyme F430*, which is involved in autotrophic methanogenesis (Romero-Güiza et al., 2016). Zn acts as a structural ion in the transesterification factor and is involved in the function of enzymes involved in methanogenesis, such as

Table 4.4: Reported stimulatory and inhibitory concentrations of metals on anaerobic biomass (expanded from Romero-Güiza et al. (2016)) compared with values from this study

Trace Element	Values from this Study (mg/L)	Stimulatory Concentration (mg/L)	Inhibitory Concentration (mg/L)	References
Ca	547.50-2308.33	100<Ca<1035	300<Ca<8000	Lo et al. (2012) Yuan et al. (2010) Chen et al. (2008) Tan et al. (2009)
Mg	17.63-543.33	<720	NR	Lo et al. (2012)
Na	588.33-4184.83	100<Ca<350	3500<Na<8000	Lo et al. (2012)
K	494.50-3393.00	<400	400<K<28934	Lo et al. (2012) Tan et al. (2009)
Fe	2.64-14.18	<0.3	NR	Worm et al. (2009)
Ni	0.06-1.43	0.03<Ni<27	35<Ni<1600	Altaş (2009) Fermoso et al. (2009) Ma et al. (2009) Gikas (2007) Li and Fang (2007) Kida et al. (2001)
Zn	1.29-9.76	0.03<Zn<2	7.5<Zn<1500	Altaş (2009) Fermoso et al. (2009) Ma et al. (2009) Worm et al. (2009) Li and Fang (2007)
Cr	0.02-4.32	0.01<Cr<15	27<Cr<2500	Altaş (2009) Lin and Shei (2008) Li and Fang (2007)
Co	0.003-0.203	0.03<Co<19	35<Co<950	Fermoso et al. (2009) Ma et al. (2009) Worm et al. (2009) Lin and Shei (2008) Gikas (2007) Kida et al. (2001)
Cu	0.23-1.25	0.03<Cu<2.4	12.5<Cu<350	Altaş (2009) Ma et al. (2009) Lin and Shei (2008) Li and Fang (2007)
Cd	0.002-0.01	<1.6	36<Cd<3400	Altaş (2009) Li and Fang (2007) Yue et al. (2007)
Mo	0.01-3.04	<0.05	NR	Worm et al. (2009)
Mn	0.23-1.84	<0.027	NR	Worm et al. (2009)
Se	0.002-0.014	<0.04	NR	Worm et al. (2009)

NR means Not Reported

coenzyme *M methyltransferase* (Romero-Güiza et al., 2016). On the other hand, Cu is required for coenzyme Q and biological electron transport (Fermoso et al., 2008; Sauer and Thauer, 2000; Metcalf and Eddy, 2003).

Mn is an electron acceptor in anaerobic respiration processes and Mo, is found in enzymes like formate dehydrogenase (FDH), which catalyzes formate production by propionate oxidizers (Banks et al., 2012; Fermoso et al., 2009; Langenhoff et al., 1997). Schmidt et al. (2014) reports a rapid accumulation of VFAs when Fe and Ni are depleted, whereas Co and W have long-term effects. Fermoso et al. (2009) illustrated the fundamental role of these micro nutrients by demonstrating their interactions with microbe cells. Overall, the elements in methanogens cells were in the following order Fe>Zn>Ni>Cu=Co=Mo>Mn. Also, Schönheit et al. (1979) discovered that *Methanobacterium thermoautotrophicum* grew in response to trace elements of Fe>Ni>Co=Mo.

Zhang et al. (2015a) documented the effects of Fe (5.0 mg/L), Co (1.0 mg/L), Ni (1.0 mg/L), and Se (0.2 mg/L) on the AD of FLO. The authors reported that without trace elements, a VFA concentration of 30,000 mg/L inhibited methane production. In contrast, the digesters with added trace elements had a stable performance with a high methane yield of 465.4 mL CH_4/gVS. For further justification, Zhang et al. (2015b) demonstrated that trace elements (Fe, Co, Mo, Ni) supplementation recovered unstable mono-digestion of food waste from process imbalance, as evidenced by increased CH_4 yields from 384.1 to 456.5 mL CH_4/gVS added, decreased the concentration of propionate from 899.0 to 10.0 mg/L, and increased pH from 6.9 to 7.4.

4.4.2 Theoretical BioMethane Potential (BMP_{TH}) and Biogas Potential (BGP_{TH})

The molecular formulas and product equations for HE, FLO, KR and CD summarized in Table 4.5 were determined using the results from the ultimate analysis. The BGP_{TH}

Table 4.5: Theoretical Biogas and Bio-Methane Potential of HE, FLO, KR, and CD

Biomass	Molecular Formula	Product Equation	BGP_{TH} (mL/gVS)	BMP_{TH} (mL CH_4/gVS)	$\%\, CH_4$
HE	$C_{3.74}\ H_{7.65}\ O_{2.47}\ N_{0.38}\ S_{0.01}$	2.06CH_4 + 1.67CO_2 + 0.38NH_3 + 0.01H_2S	946.93	472.50	49.90
FLO	$C_{3.91}\ H_{8.17}\ O_{2.61}\ N_{0.15}\ S_{0.01}$	2.27CH_4 + 1.64CO_2 + 0.15NH_3 + 0.01H_2S	918.72	512.05	55.74
KR	$C_{3.67}\ H_{10.87}\ O_{2.61}\ N_{0.13}\ S_{0.01}$	2.49CH_4 + 1.18CO_2 + 0.13NH_3 + 0.01H_2S	864.09	563.91	65.26
CD	$C_{4.39}\ H_{6.24}\ O_{2.17}\ N_{0.14}\ S_{0.02}$	2.37CH_4 + 2.02CO_2 + 0.14NH_3 + 0.02H_2S	1058.94	552.27	52.15

and BMP_{TH} of HE, FLO, KR and CD were subsequently calculated (Table 4.5). The percentage methane composition lay within 49.9-65.3 %. The BGP_{TH} and BMP_{TH} usually assumes that 100 % of the substrate is biodegradable, but in reality, only 40-90 % of the material is converted into biogas (Curry and Pillay, 2012). Fagbohungbe et al. (2015) reported biomethane yields of 290 mL/gVS and 566 mL/gVS for substrate to inoculum ratios of 0.5 and 1 respectively during anaerobic digestion of HE. The methane yield of HE in this study therefore lies within the range reported by Fagbohungbe et al. (2015).

Also, Zhang et al. (2007) documented methane outputs of 348 and 435 mLCH_4/gVS for FLO after 10 and 28 days of digestion respectively. Similar methane production from FLO was measured by other authors in the range of 401-529 mLCH_4/gVS (Browne and Murphy, 2013; El-Mashad and Zhang, 2010). Additionally, Ebner et al. (2016) reported bio-methane potentials for FLO and KR ranging from 165 to 496 mLCH_4/gVS. The highest methane production was in materials rich in lipids or rapidly degradable carbohydrates. The biomethane potential for FLO in this study lies within the range reported in literature, while KR in this study is higher than the range reported. This is however expected because of the variability of food waste. Furthermore, Sandhu and Kaushal (2022b) after digesting breeding manure, reported optimum values of 1104.77 ml and 1465.22 ml for methane and biogas respectively.

4.4.3 Potential, Challenges and Justification of Human Excreta as Main Substrate for Anaerobic Co-digestion in Households

HE was chosen as substrate in this study because of its availability in every household and its ability to be easily digested anaerobically. From the results of this study and other studies, HE possesses very important nutrients that can support its valorization. Also, the pH and alkalinity lie within the optimum range for a successful AD process. The methane content reported in this study for HE is 53.2 %. Relatively, a low methane yield of 48 % was observed when Gao et al. (2019) treated black water with lower free ammonia concentrations of 26 and 60 mg/L. Also, the C/N ratio of 8.39 obtained for HE in this study is very low. This is similar to the low C/N ratio of 7.9 reported

by Afifah and Priadi (2017). That notwithstanding, HE can be co-digested with co-substrates (FLO, KR or CD) higher in C/N ratio. Finally, it is recommended to connect HE directly to the biogas system without any direct human contact due to the high bacteria load.

4.4.4 Potential, Challenges and Justification of FLO and KR as Co-Substrate for Anaerobic Co-digestion in Households

The composition of FLO and KR strongly depend on different eating and cooking habits (Zhang et al., 2014). Hence, it could be said that their characteristics vary from place to place. From this work, the C/N ratios of FLO (22.1) and KR (23.3) were found to be within the optimum range for anaerobic digestion. However, the pH (4.9 and 4.6) and alkalinity (630 and 590 mg/L) values for FLO and KR respectively were significantly low. As these values cannot support a stable AD process, FLO and KR are recommended to be used as potential co-substrates for household biogas generation. With this, a substrate like HE with optimum alkalinity and pH level could be added during the digestion of FLO and KR.

Optimal methane and biogas values of the co-digestion of FLO and substrates like algae, chicken, fish mixed and cow manure have been reported to be 1345.97 ml, and 2244.58 ml, respectively (Kaushal et al., 2022). Also, optimum values of cumulative biogas and methane were found to be 3401.8 ml and 2266.3 ml respectively when KR such as apples, vegetables, fruit pulp wastes as well as algae, pond sludge and CD were co-digested (Sandhu and Kaushal, 2022a). FLO and KR are better of co-substrates because, even though they are readily available in large amounts in households, it is possible that there is competition for the use of FLO and KR as feed for household animals.

4.4.5 Potential, Challenges and Justification of Cow Dung as Inoculum Source for Anaerobic Co-digestion in Households

There are two major advantages of using CD for co-fermentation or as inoculum. First, it provides nutrients like trace metals, vitamins, and other substances needed for mi-

crobial growth (Ya'aba and Ramalan, 2021). This is confirmed by the mineral analysis of CD in this work. Secondly, it helps to balance pH and increase buffering ability (Gashaw et al., 2014). The pH (7.8) and alkanity (15730 mg/L) of CD in this study are within the optimum range and can support a successful AD process. The high buffering capacity of CD makes the process more resistant to VFA accumulation and thus mitigates inhibition processes (Gashaw et al., 2014). Further, Font-Palma (2019), reported that the C/N ratio of CD fell in the optimal range (20–30) for AD. Similarly, the C/N ratio obtained for CD (26.2) in this study is within the optimal range.

Further, CD harbours a rich microbial diversity, containing different species of bacteria (Randhawa and Kullar, 2011; Nene, 1999). Many distinct bacterial genera, including *Citrobacter koseri*, *Enterobacter aerogenes* , *Escherichia coli*, *Klebsiella oxytoca*, *Klebsiella pneumoniae*, *Kluyvera spp.*, *Morgarella morganii*, *Pasteurella spp.* , *Providencia alcaligenes*, *Providencia stuartii*, and *Pseudomonas spp.*, have been isolated from cow dung by Sawant et al. (2007). Ya'aba and Ramalan (2021) confirmed the above by isolating *Escherichia coli*, *Bacillus sp.* , *Pseudomonas sp.*, *Staphylococcus sp.*, and *Proteus sp.* from a CD digester before, during and after the anaerobic digestion period. Complex organic matter, such as lignocelluloses, chitin, cellulose, xylose, and xylem, is degraded by these bacteria (Martens et al., 2009). Because of the above characteristics, the use of CD as inoculum or co-substrate during the AD process is justified.

4.5 Conclusion

The suitability of HE, FLO, KR and CD for household biogas production has been established since all feedstocks contain readily available biodegradable components that can easily be converted to biogas. However, HE, proposed as the main substrate for household biogas generation, has a very low C/N ratio, which could lead to low AD performance. Hence, using small portions of FLO and KR as co-substrates will balance the C/N ratio during co-digestion. Also, CD as inoculum will be a good source of microbial community and buffer. This information was established through the results obtained for the various characterizations done in this study, which mostly met the requirements for suitable anaerobic digestion feedstock(s) available in literature.

Therefore, HE, FLO, KR and CD are recommended to be very well developed as feed-stock sources for household biogas generation.

CHAPTER 5

Anaerobic Co-Digestion of Human Excreta, Food Leftovers and Kitchen Residue: Ternary Mixture Design, Synergistic Effects and RSM Approach

5.1 Abstract

Anaerobic digestion of multiple substrate can generate more biogas while remaining stable if positive synergistic effects are achieved. The type of substrates that are anaerobically co-digested and the mixing ratio used are the most important variables as each substrate has unique set of characteristics. Optimizing the volatile solids (VS), C/N and volume ratios by testing various substrate mixing ratios is a popular method for determining the best-performing ratio of substrate mixture. Although the conventional one-factor-at-a-time approach to multivariate process optimization is frequently discussed in literature, it is ineffective. It also necessitates numerous experimental runs in addition to the possibility of inaccuracy. In contrast, the ternary mixture design and the response surface approach has reportedly been found to quicken the process of testing different mixing ratios with high accuracy without running several experiments. Therefore, a randomized ternary mixture design without blocking and a response surface approach are used in this work to ascertain the relationship between substrate mix and biogas yield, methane yield, and synergy. The findings of the experiment revealed that R9(78.8:11.8:9.4) had the highest methane production of 764.79 mLCH_4/g VS and a synergistic index of 3.26. Additionally, the 3D response surface plots from the response surface model showed important and shared interactions between Human Excreta, (HE), Food Leftovers (FLO), and Kitchen Residue (KR). HE and KR had a similar positive synergistic effect on biogas yield, methane yield, and synergy, which was not the case for FLO. Also, the response surface plots showed that the predicted responses increased with increasing HE and KR fractions and decreased with increasing FLO fractions in the substrate mixtures.

5.2 Introduction

Human excreta and food waste are considered to be readily available human-generated waste that could be used for the production of biogas in households (Appiagyei Osei-Owusu et al., 2023). It is estimated that one-third of the world's population, approximately 2.4 billion urban dwellers, rely on onsite sanitation system installations such as public latrines and septic tanks (Appiah-Effah et al., 2014). In Ghana, about 58 % of the entire population rely on cesspit and Kumasi Ventilated Improved Pit (KVIP) latrines (Appiah-Effah et al., 2014). Furthermore, Arthur et al. (2020) has reported that 38.6 % of rural dwellers in Ghana use flush and non-flush toilet facilities. Unfortunately, the liquid waste is disposed of untreated and indiscriminately into drainage ditches and open urban spaces (Ahmed et al., 2018b; Ofori-Amanfo et al., 2018).

Very few human excrement treatment facilities are available to treat the volumes of liquid waste generated, thus making the treatment abysmal (Ahmed et al., 2018a). Also, several studies indicate that 55–80 % of municipal solid waste from developing countries are generated from households (Okot-Okumu, 2012; Nagabooshnam, 2011; Nabegu, 2010). In Ghana, 8389 tonnes (constituting about 66 % of total household waste) of household organic wastes are reported to be generated per day in a study conducted by (Miezah et al., 2015).

Waste management, therefore, has become a major bottleneck for Ghana's economy considering the large volumes of solid and liquid waste generated (Abiti et al., 2017). The amount of waste produced in Ghana can most likely generate revenue for the government through recycling and energy generation (Monney et al., 2013). However, the country spends vast sums of money on solid waste management (Abalo et al., 2018). Therefore, it is imperative that Ghana look into environmentally and financially viable sustainable solutions. Anaerobic digestion (AD), due to its capacity to transform organic material into biogas, mostly CH_4 and CO_2 has been regarded as an appealing method for treating high-strength organic wastes (Kim et al., 2019b).

Further, decentralized AD treatment is now widely recognized as a viable waste management strategy (Kyere et al., 2019). The idea of decentralized treatments was first focused on the separation of grey (from the sink, shower, and laundry) and black (containing feces and urine) water, which were subsequently treated and recycled on-site (Elmitwalli et al., 2006). Currently, source-separable waste streams like food waste are included in decentralized treatments. According to Kyere et al. (2019), a decentralized treatment system that incorporates AD may offer a cheap supply of energy for on-site use.

Different feedstocks influenced by the uniqueness of locations can be used to generate biogas (Fajobi et al., 2022). However, many of these feedstocks cannot solely produce the desired biogas yield due to their characteristics (Appiagyei Osei-Owusu et al., 2023). As a result, multiple feedstocks are co-digested to produce biogas with the characteristics of the feedstock used highly influencing the biogas yield (Pöschl et al., 2010). Khoufi et al. (2015) and Kafle et al. (2012) state that anaerobic co-digestion can maintain process stability with a higher rate of biogas production if substrates synergise. The most important factors in this situation are the kinds of anaerobically co-digested feedstocks (Rico et al., 2015).

As different substrates have different properties, the percentage of co-digested substrates that are mixed together affects the synergic activity of anaerobic co-digestion (Ma et al., 2019b; Chiu and Lo, 2016). Selecting co-substrates that are suitable and have the right mixing ratio is thus critical for improved biogas production due to the presence of native trace elements or sufficient buffer capacity (Mata-Alvarez et al., 2014). The C/N ratio can be optimized as a common method of determining the substrate mixing ratio. Besides, controlling the VS is another typical approach to manage the mixing ratio of substrates (Chiu and Lo, 2016).

Furthermore, previous studies have evaluated synergic co-digestion effects from indicators, such as volatile solid (VS) removal rate, COD removal rate, methane production and synergy index (Xie et al., 2017a). However, depending on the properties of the co-substrates, co-digestion might occasionally have an antagonistic effect (Xie

et al., 2017b). Therefore, carefully selecting co-substrates and their mixing ratio is critical for a successful co-digestion process and improved biogas yield (Kim et al., 2019a). The mixture of different substrates is a strategy to increase the performance of a digester in order to ensure an optimal feedstock composition and enhance biogas production (Mata-Alvarez et al., 2000). That notwithstanding, Oladejo et al. (2020) and Lindmark et al. (2014) recommend that the mixing hydrodynamics in anaerobic co-digestion methods be done in the correct proportion to provide adequate contact surfaces between the digesting substrate and bacteria.

According to Andriamanohiarisoamanana et al. (2018) and Andriamanohiarisoamanana et al. (2017) investigations using the same feedstock and the same mixing ratio have reported conflicting results regarding synergic or antagonistic effects. Due to these variances, it has been challenging to assess whether or not a particular waste stream can have synergistic benefits when digested together and, more significantly, to establish the best mixing ratios (Moset et al., 2017; Astals et al., 2015). This makes the setting or location where feedstocks are taken and the experiments done very important. Consequently, Hagos et al. (2017) suggested investigating local or indigenous feedstocks, such as food waste and human excreta, due to the variation in composition across different settings.

The goal of the current study is to examine the possibilities for using AD in onsite treatment of human excreta (HE), food leftovers (FLO), and kitchen residues (KR), the major human-generated organic wastes. A reference biochemical methane potential test (BMP), which could ultimately reveal methane yields of these wastes has been demonstrated in this study (Filer et al., 2019; Koch et al., 2019; Holliger et al., 2016; Raposo et al., 2011; Angelidaki et al., 2009). In addition, the mixtures of these wastes are established at various mixing ratios to investigate the impact of various substrate properties and compositions on methanogenic performance without the addition of any external additives such as buffer or trace elements. Also, the minimal effective ratios of FLO and KR are determined in substrate mixture because there is competition for food waste to be used as animal feed (Hussien et al., 2020). The effect of mixing ratios on biogas yield, methane yield and synergy index is modelled and described using

Response Surface Methodology (RSM).

The use of food waste for biogas production has been extensively studied however information on the use of human excreta or a combination of foodwaste and human excreta are scarce (Paritosh et al., 2017). Therefore, this is a unique study in that no data has been reported on the optimum mixing ratios for the co-digestion of HE, FLO and KR in the Ghanaian context. The results of this study will serve as a guide for the setup and operation of co-digestion systems for the on-site treatment of household generated waste

5.3 Materials and Method

5.3.1 Feedstock and Inoculum Collection and Preparation

Fresh HE (Figure 5.1 a) was collected from a KVIP at Ayeduase in Kumasi, Ghana. Fresh cow dung was collected from the animal farm of the Department of Agriculture, KNUST. Anaerobically mono-digested cow dung (Figure 5.1 b) with a pH of 7.8 and alkalinity of 8150mg/L was used as inoculum. The inoculum was degassed for two weeks under mesophilic condition $(30\,^{\circ}\text{C})$ until no gas production prior to use. The total solids (TS) and volatile solids (VS) of the inoculum were 3.80 ±0.14 % and 78.29 ±0.12 %, respectively. FLO and KR were also collected from households of staff and the canteen at a Senior High School in Kumasi, Ghana. FLO (Figure 5.1 c) was mainly composed of milled rice, cassava, fufu, kenkey, yam, egg, fish, gari, beans, bread, banku, kontomire (cocoyam leaves) and some vegetable sauce. These are very common foods eaten in most houses in Ghana.

KR (Figure 5.1 d), on the other hand, comprised of milled cassava peels, yam peels, cocoyam peels, plantain peels, lettuce residue, cucumber residue, tomato residue, carrot residue, garden eggs residue, avocado peels, banana peels, mango peels, orange peels, pineapple peels, onion peels, pawpaw peels and watermelon peels. FLO and KR were manually sorted to remove non-biodegradable fractions such as polyethene bags before organic fractions were shredded into smaller pieces, blended and homogenized into a slurry to maintain a particle size below 3mm using a household food grinder and

3mm sieve (Figure 5). Samples were frozen at a temperature of $-20\,^{\circ}$C before use. The frozen samples were allowed to thaw at a temperature of $4\,^{\circ}$C and used within a day to prevent biological decomposition.

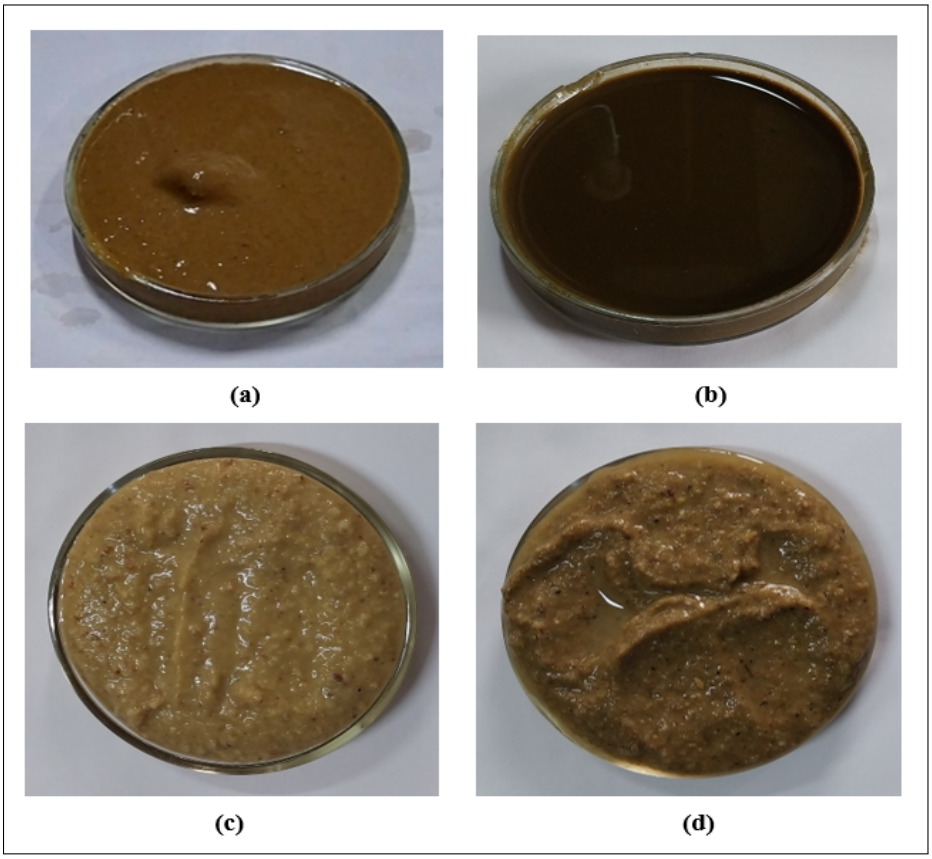

Figure 5.1: Homogenized (a) Human Excreta (b) Inoculum (c) Food Leftovers (d) Kitchen Residue

5.3.2 Feedstock Characterization

The physical and chemical compositions of the feedstocks (HE, FLO, and KR) were evaluated before and after digestion using standard procedure (APHA, 1998). The feedstock were analyzed for pH, total solid (TS), volatile solid (VS), organic carbon content, total nitrogen content, hydrogen content, oxygen content, sulphur content, C/N ratio, alkalinity and volatile fatty acids (VFA). The pH was analyzed using a digital hanner H1 98136 pH meter. The TS and VS were analyzed using APHA methods 2540 B and APHA method 2540 E, respectively (APHA, 1998). Total nitrogen was calculated following the Kjeldahl method (Bremner, 1965), and the total amount of

sulfur was determined using the spectrophotometer method (Singh et al., 1999). Hydrogen was determined using titrimetric method (McLean, 1965) and organic carbon by Walkley – Black Wet Oxidation Method (Heanes, 1984; Nelson, 1982).

The oxygen content was calculated as the positive difference between 100 and the sum of C, H, N, S, and ash content (AC) (Fajobi et al., 2022). The C/N ratios of the samples was calculated by dividing the measured value of C and N (Dahunsi et al., 2019; Anderson and Ingram, 1993). Also, the alkalinity was determined according to the APHA method 2320B using Potentiometric titration (APHA, 1998). VFA was determined titrimetrically (Singh et al., 2021a, 2019a,b). PerkinElmer's NexION 2000 ICP-MS was used to detect the amounts of nickel (Ni), molybdenum (Mo), zinc (Zn) and iron (Fe) in the feedstocks. All results are reported as the mean ± standard deviation.

5.3.3 Formulation of Substrate-Mix using Mixture Design

A no-block, randomised ternary mixture experimental design with three variables serving as mixture components was adopted in this study to formulate the substrate mix from HE, FLO and KR. Sixteen substrate mixtures with different mixing ratios (VS basis) of HE, FLO and KR were generated in total. The Design Expert software version 13 (Stat-Ease, Minneapolis, MN, USA) was used to generate the experimental matrix. The different mix ratios of HE, FLO and KR in the substrate mixtures (from 0 to 100 %) (Table 5.1) were used as independent variables (input factors) to estimate the responses of biogas yield, methane yield and synergy. Equations 5.1 and 5.2 show the relationship between the components of the mixture which also represent factors of the design.

$$0 \leq HE, FLO, KR \leq 100 \tag{5.1}$$

$$HE + FLO + KR = 100 \tag{5.2}$$

For each of the runs *(Ri)*, there were three bottles (triplicates) that were used. Ri_a, Ri_b and Ri_c, where *i* starts from 1 to 16 (Table 5.1).

Table 5.1: Experimental Conditions for the BMP Tests.

Ratio $(HE:FLO:KR)^a$	$HE(g)^b$	$FLO(g)^b$	$KR(g)^b$	$Inoculum(g)^b$	$Cellulose(g)^c$	C:N Ratio
R1(100:0:0)	75.00	0.00	0.00	233.00	0.00	11.79
R2(0:100:0)	0.00	32.00	0.00	233.00	0.00	28.84
R3(0:0:100)	0.00	0.00	84.00	233.00	0.00	20.36
R4(0:50:50)	0.00	16.00	42.00	233.00	0.00	27.85
R5(50:50:0)	37.00	16.00	0.00	233.00	0.00	15.45
R6(50:0:50)	37.00	0.00	42.00	233.00	0.00	12.92
R7(66.7:33.3:0)	50.00	11.00	0.00	233.00	0.00	11.89
R8(66.7:0:33.3)	50.00	0.00	28.00	233.00	0.00	12.44
R9(78.8:11.8:9.4)	59.00	4.00	8.00	233.00	0.00	23.98
R10(54.7:21.8:23.5)	41.00	7.10	20.00	233.00	0.00	22.53
R11(32.1:25.2:42.7)	24.00	8.00	36.00	233.00	0.00	17.10
R12(0:33.1:66.9)	0.00	11.00	56.00	233.00	0.00	13.51
R13(33.3:66.7:0)	25.00	22.00	0.00	233.00	0.00	23.27
R14(16.7:16.6:66.7)	12.00	5.00	56.00	233.00	0.00	26.27
R15(33.4:33.3:33.3)	25.00	11.00	28.00	233.00	0.00	15.21
R16(16.7:66.7:16.6)	12.00	22.00	14.00	233.00	0.00	23.63
Blank^d	0.00	0.00	0.00	233.00	0.00	22.88
Positive Control(PC)^e	0.00	0.00	0.00	233.00	7.00	21.89

$a: VS\ basis, b: Wet-weight\ basis, c: Dry-weight\ basis, d: Only\ inoculum, e: Composed\ of\ pure\ cellulose\ and\ inoculum.$

5.3.4 Theoretical BioMethane Potential (BMP_{TH})

The empirical relationship between the components of the feedstocks were determined using a modified Buswell equation by Boyle (1976), as shown in Equation 5.3.

$$C_aH_bO_cN_dS_e + (a - \frac{b}{4} - \frac{c}{2} + \frac{3d}{4} + \frac{e}{2}) \times H_2O \rightarrow (\frac{a}{2} - \frac{b}{8} + \frac{c}{4} + \frac{3d}{8} + \frac{e}{4}) \times CO_2 + (\frac{a}{2} + \frac{b}{8} - \frac{c}{4} - \frac{3d}{8} - \frac{e}{4}) \times CH_4 + d \times NH_3 + e \times H_2S \tag{5.3}$$

The theoretical methane yield was estimated using Equation 5.4 (Scherer et al., 2021; Steffen et al., 2016; Fagbohungbe et al., 2015; Raposo et al., 2013).

$$BMP_{TH} = (\frac{(\frac{a}{2} + \frac{b}{8} - \frac{c}{4} - \frac{3d}{8} - \frac{e}{4}) \times 22400}{12a + b + 16c + 14d + 32e}) \tag{5.4}$$

5.3.5 Biochemical Methane Potential Test

In 500 mL bottles with a working capacity of 300 mL, BMP tests of the different mixtures were carried out. 233 g of the inoculum and 7 g VS of a substrate combination were put into each bottle. A 1:1 inoculum to substrate ratio (ISR) (VS basis) was adhered to. In total, 18 BMP runs (16 runs with the substrate mixtures (Table 5.1), one with the inoculum-only control and one run with a positive control of pure cellulose) were carried out in triplicates making 54 trials. The BMP bottles were tightly sealed, incubated at $30\,^{\circ}$C and manually shaken daily for 60 days, and biogas production and composition were monitored daily.

The generated biogas was collected in gas bags and measured through downward water displacement technique using an inverted glass chamber of 1000 mL capacity (Filer et al., 2019). The measured biogas was corrected to standard conditions of ($0\,^{\circ}$C) and 1 atm. Biogas composition was also determined with a portable Biogas 5000, Geotech UK) analyzer. VDI.4630 (2016) assume a substrate usage of 5 % during

the fermentative stage and 3 % during the methanogenic stage, for a total microbial biomass utilization of 8 % over the entire process. In this study, 8 % was used for specific methane correction.

5.3.5.1 Biodegradability (BD)

The extent of anaerobic biodegradability, BD, was calculated by dividing experimental methane yield (BMP_{exp}) by the theoretical methane potential (BMP_o) according to the Equation 5.5 (Wang et al., 2014a).

$$BD(\%) = (\frac{BMP_{exp}}{BMP_o}) \times 100 \tag{5.5}$$

5.3.6 Synergy

Synergy index (SI) was determined as the ratio of methane yield of the co-digestion substrates $(M_{i,n})$ to the weighted average based upon VS content (% VS) of the methane yield of individual substrate $(M_{oi,n})$. This was calculated according to Equation 5.6 (Hou et al., 2020; Ebner et al., 2016).

$$SI = (\frac{M_{i,n}}{M_{oi,n}}) = (\frac{M_{i,n}}{\sum_i^n \%VS_i M_{o,i}}) \tag{5.6}$$

where subscripts *i* through *n* denote the co-digested substrates and $\sum_i^n \%VS_i$=1. An SI greater than one (>1) implies a synergistic impact, while an SI less than one (<1) indicates an antagonistic effect.

5.3.7 RSM Modelling

A sequential process of experimental data collection, polynomial equation construction, and model suitability assessment was used for RSM. This was done through multiple regression analysis in order to assess the relationship between mixture components and the responses of biogas yield, methane yield and synergy. Increasingly polynomials were fitted to the experimental data to model the response surfaces (Baek et al., 2020). Anova and performance assessment results for the modeling, parity as well as 3D response surface plots were generated to show the effect of the interaction

between input variables and the responses.

5.3.8 Statistical Analysis

Samples were analysed in triplicates and reported as the mean value ± standard deviation (SD) in results and discussion. One-way analysis of variance (ANOVA) was then used to test the statistical significance of different digesters. Also, Tukey's honestly significant difference (HSD) test was used for the pairwise comparison of the mean biomethane composition obtained during co-digestion using Minitab v.19 software. *($p < 0.05$)* was used as threshold for statistical significance.

5.4 Results and Discussion

5.4.1 Feedstock Characteristics

Table 5.2 provides information on the properties of the feedstocks (HE, FLO, and KR) employed in this study. The TS concentrations for HE, FLO, and KR were 11.34 ± 0.14, 25.80 ± 0.32 and 9.44 ± 0.00 %, respectively, while the VS contents were 82.81 ± 0.84, 83.99 ± 0.61 and 88.10 ± 0.37 %. These values are similar to what is reported by Appiagyei Osei-Owusu et al. (2023). According to Capson-Tojo et al. (2017) and Li et al. (2013), feedstocks with high VS and VS/TS values (Table 5.2) may contain organic materials that are highly biodegradable.

Table 5.2: Physicochemical Characteristics of Substrates [mean (standard deviation)]

Parameter	HE	FLO	KR
TS (%)	11.34 (0.14)	25.80 (0.32)	9.44 (0.00)
VS (% TS)	82.81 (0.84)	83.99 (0.61)	88.10 (0.37)
VS/TS	0.83 (0.001)	0.84 (0.001)	0.88 (0.001)
pH	7.1 (0.1)	5.0 (0.1)	5.3(0.1)
C (%)	61.22 (0.02)	41.16 (0.01)	38.10 (0.01)
N (%)	7.32 (0.02)	1.26 (0.01)	1.30 (0.02)
H (%)	9.02 (0.02)	9.52 (0.01)	8.52 (0.01)
O (%)	12.25 (0.01)	45.66 (0.01)	43.72 (0.01)
S (%)	0.200 (0.00)	0.135 (0.00)	0.031 (0.00)
C/N	8.36 (0.01)	32.59 (0.13)	29.34 (0.44)

KR, such as leftover fruits and vegetables, has a high moisture content, contributing to the low TS of KR. Neves et al. (2009) and Carucci et al. (2005) have reported that majority of fruit and vegetable wastes contain high levels of volatile solids and easily biodegradable organic matter, but they lack total solids. In most cases, they hydrolyze quickly, producing acids that decrease the pH and limit the growth of methanogens (Ward et al., 2008). While the pH values of FLO (5.0 ± 0.1) and KR (5.3 ± 0.1) were in the acidic range, that of HE (7.1 ± 0.1) was almost neutral. The presence of food components containing carbohydrates, which can be converted to monosaccharides and then volatile fatty acids during the AD process, may result in the low pH and buffer capacity of FLO and KR that was observed (Pramanik et al., 2019).

The C/N ratios for HE, FLO and KR, respectively, were 8.36±0.01, 32.59±0.13 and 29.34 ±0.44 based on the elemental compositions. The AD process is often more stable at a C/N ratio of 20 to 30, with most of the carbon content being easily degradable (Dar et al., 2021; Rahman et al., 2017; Chiu and Lo, 2016; Haider et al., 2015). HE in this study had a low C/N ratio consistent with the 12.0 reported by Singh et al. (2021b). However, the C/N ratios of FLO and KR are within the 20 to 30 range that Scherer et al. (2021) proposed for anaerobic digestion. In order to improve AD performance, feedstocks with low C/N ratios should be combined with feedstocks with high C/N ratios for better anaerobic digestion performance (Rouf et al., 2010).

5.4.2 Daily Biogas Yields

Figure 5.2 displays the daily biogas production from the studies of the mono, co-, and tri-digestion. On the first day, the daily biogas production ranged from 11.40 to 128.33 mL/gVS, demonstrating a rapid startup of the process. HE, FLO, and KR contained substantial amounts of components such as carbohydrates that were simple to digest and their conversion could happen extremely quickly. Figure 5.2a demonstrates that on day 3, following the first peak, the biogas yield in the mono-digestion of FLO and KR significantly dropped. This was most likely caused by a drop in system pH brought on by converting organic matter in the FLO and KR to VFA, whose buildup might have prevented biogas synthesis (Lin et al., 2011).

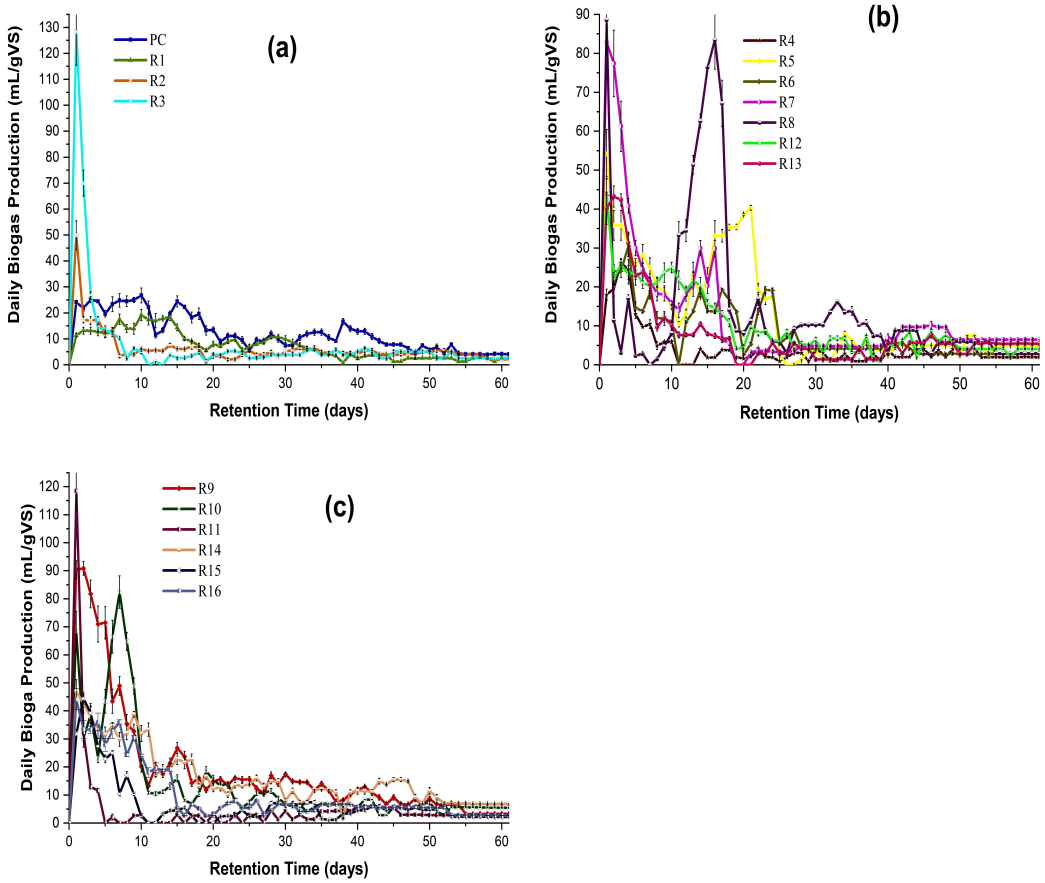

Figure 5.2: Effects of different mixing ratios on daily biogas yields: (a) mono-digestion, (b) co-digestion, and (c) tri-digestion (mean±S.D; n=3) 90% of measurements have RSD of less than 5%

As illustrated in Figure 5.2b, the co-digestion of HE and FLO (R5, R7, R13) and HE and KR (R6, R8) similarly showed possible minor acidification with a decrease in biogas on days 3 and 4. However, the acidification was relatively mitigated compared with the mono-digestion of individual feedstock because of the alkalinity levels (3437.50-5975.00 mg/L) of all treatments and the buffer from HE. In contrast, negligible acidification was observed in the tri-digestion (Figure 5.2c), which yielded higher biogas production (322.75-1167.62 mL/gVS) by day 61. The highest cumulative biogas production was 1167.62 mL/gVS, corresponding to the tri-digestion R9 of HE/FLO/KR (78.8:11.8:9.4).

In comparison with the mono-digestion AD tests, the results demonstrated that multiple substrate digestion (R9,R10,R14 and R15) had a superior capacity for buffering

(alkalinity range of 3537.50-6587.50 mg/L) and was relatively stable for the production of biogas. Singh et al. (2021b) reported increased daily biogas output for the co-digestion of human excreta, cow dung, and poultry litter as opposed to mono-digestion, further demonstrating the more reliable performance of the mixed feedstock digestion system.

5.4.3 Daily and Cumulative Methane Yields

Methane production profiles varied between the 16-substrate mixing ratio runs. These variations were more pronounced throughout the study, especially during the first two weeks of incubation (Figure. 5.3). This was unsurprising as there were different combinations of feedstocks in the bottles. The daily methane production increased to a peak and then drastically decreased in the first ten to fifteen days in all the mono digestion tests (Figure. 5.3a). The co-digestion and tri-digestion experiments also revealed a consistent pattern in the daily methane output, which peaked at high levels before gradually declining to essentially no methane production (Figures. 5.3b and c).

The daily methane productions from the HE-added reactors R5, R7, R8, R9, and R10 were higher than those from reactors without HE over the first seven days (Figures 5.3b and c). Independent of the mixing ratios, the peak values of R5, R7, R8, R9, and R10 were observed earlier than those linked to HE mono-digestion. This held true, in particular, for feedstocks containing 50 % or more HE (R5, R7, R8, R9 and R10, Figures 5.3b and c). This observation might be due to the quick hydrolysis and fermentation of biodegradable organics in HE, FLO, and KR (Hou et al., 2020).

Although R5,R7, R8, R9, and R10, as all other mixtures, hydrolyzed quickly, the process was remarkably steady compared to the other mix ratios with less or no HE. This was evident by comparing the initial and final alkalinity (4537.00-6587.50 mg/L and 1362.50-2987.50 mg/L respectively), initial and final pH (7.1-7.9 and 6.1-6.6 respectively) and initial and final VFA concentrations (2309.79-3555.38 and 1082.33-1680.94 respectively) as shown in Table 5.3. Additionally, the use of readily biodegradable materials such as carbohydrates from FLO and KR may explain why the peak

values of daily methane production from the HE-added reactors were observed to experience a gradual reduction, while reactors with no HE sharply declined after the first few days.

As can be seen, R9 recorded the highest daily methane production of all the reactors, peaking at 59.51 mLCH_4/gVS whereas R5,R7, R8 and R10 peaked at 36.78, 52.33, 57.25 and 55.71 mLCH_4/gVS respectively. Further, the reactors with high HE ratios produced more methane daily. This finding suggests that increasing the amount of HE added to FLO and KR is advantageous for increasing methane generation, probably because of the alkalinity and pH of HE. Additionally, this could be associated with native nutrients or trace elements in HE (Hou et al., 2019).

The cumulative methane yields from the mono-digestion of HE (R1), FLO(R2), KR (R3), and cellulose (positive control, PC) are 253.89, 135.27, 198.86, and 435.36 mLCH_4/gVS, respectively, as shown in Figure 5.4a. Also, the cumulative methane yields from the co-digestion and tri-digestion tests are shown (Figures 5.4b and c, Table 5.3). It was discovered that the mono-digestion tests for FLO and KR produced less methane than the mixed groups. This might be explained by the high levels of VFA buildup (Capson-Tojo et al., 2016) in FLO and KR (R2:4141.89 mg/L and R3: 3543.28 mg/L, respectively) as well as the lower levels of alkalinity in FLO (R2:1775.0 mg/L) and KR (R3:1900.0 mg/L).

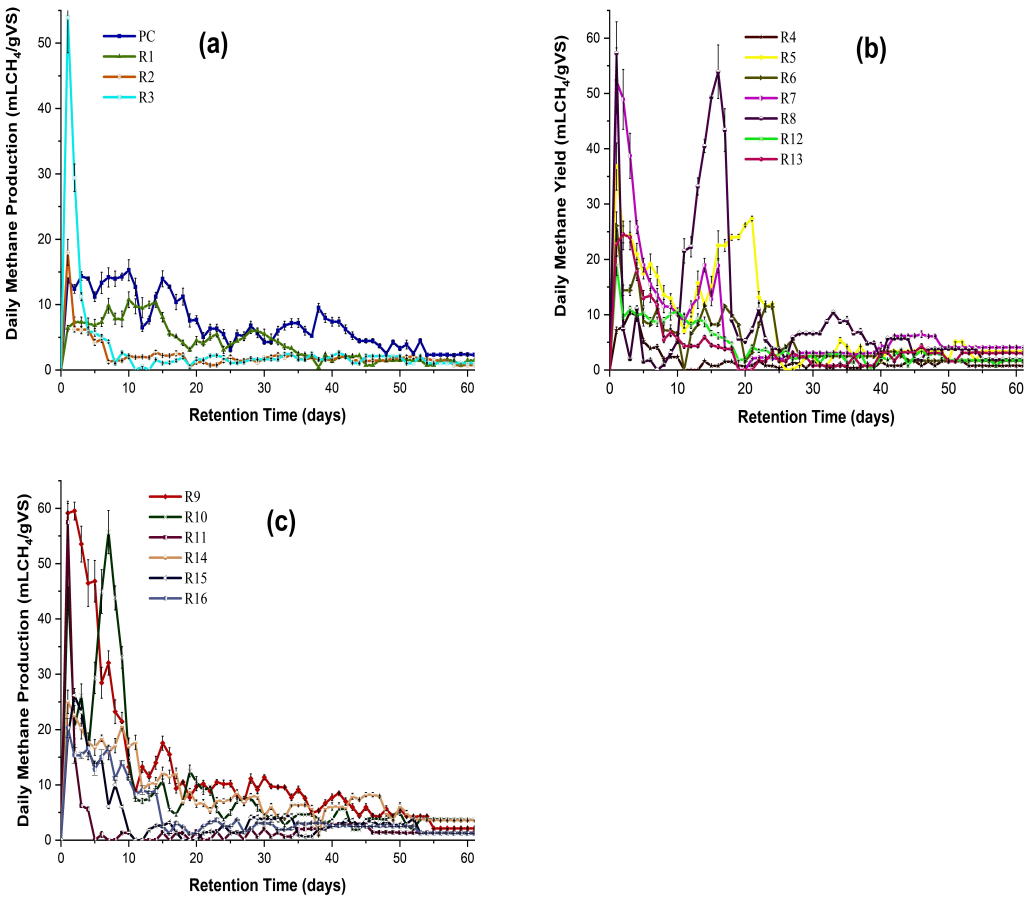

Figure 5.3: Effects of different mixing ratios on daily methane yields: (a) mono-digestion, (b) co-digestion, and (c) tri-digestion (mean±S.D; n=3) 90 % of measurements have RSD of less than 5 %

Filer et al. (2019) recommend that alkalinity be kept at 3000 mg $CaCO_3$ L^{-1} to maximize methane yield. As in the case of the daily yields, the substrate mixtures with HE percentages of 50% or higher (R5=544.96 mLCH_4/gVS, R7=494.84, R8=573.18 mLCH_4/gVS, R9=764.79 mLCH_4/gVS, R10=595.78 mLCH_4/gVS) had higher cumulative methane production. In the tri-digestion test, R9 produced the most methane (764.79 mLCH_4/gVS), followed by R10 (595.78 mLCH_4/gVS), which were all having a greater amount of HE (>50%).

The cumulative methane output of R9 was 66.80% higher than that obtained for the mono-digestion of HE (R1). This was presumably due to the fact that there were varieties of substrates available, which provided the different useful microbial population

with enough native nutrients to promote the breakdown of substrates and increase biogas generation (Arthur and Scherer, 2020). The high methane content in the co and tri-digestions might be due to the strong methanogenic activity and sufficient buffer that could majorly convert VFAs into methane.

Conversely, the rapid buildup of intermediates like VFAs with consequently low buffer capacity, may have caused the low methane levels of the mono-digestion test (Huang et al., 2016). Despite variations in the rate of methane production and yield between all BMP operations, methane was produced continuously without any lag phase. This could be explained by the high percentage of inoculation (40%) used in the BMP testing, which might have offered a significant amount of active bacteria and a supply of nutrients for microbial development.

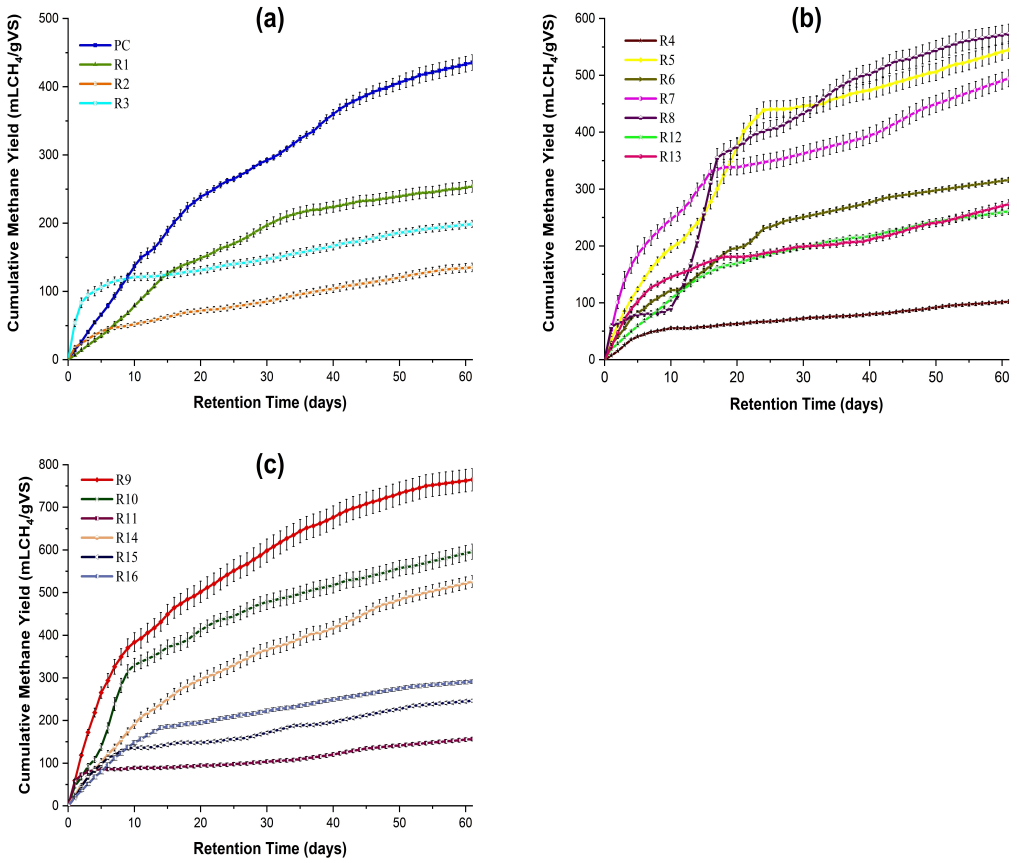

Figure 5.4: Effects of different mixing ratios on cumulative methane yields: (a) mono-digestion, (b) co-digestion, and (c) tri-digestion (mean±S.D; n=3) 90 % of measurements have RSD of less than 5 %

Additionally, it might be stated that the biodegradable organic content of the substrate mixtures had a significant role in determining the effectiveness of co-digestion. For each of the tests (R1-R16), the mean values of methane content was reported (Table 5.3 and Figure 5.4). A one-way ANOVA with a p-value of $p<0.001$ revealed a statistically significant difference between the compositions. After that, the average compositions were compared using the Tukey pairwise comparison. Average methane yields that did not have common letters were significantly different (Appendix A1). As seen in A1, the tri-digestion ratio R9 which had no similar letters with other treatments differed significantly from the other co-ratios. Therefore, different mixing ratios have different methane yields.

5.4.4 Effects of VS reduction, CN Ratio, pH, Alkalinity and VFA on Biogas and Methane Yields

The initial and final VS contents for the mono-, co-, and tri-digested substrates revealed an overall decreasing tendency for all mix ratios. Table 5.3 displays the VS reduction values for all treatments from R1 to R16. The VS reduction trend was connected with the generation of biogas and methane. In this study, HE had a very low C/N ratio compared to FLO and KR. Similarly, Singh et al. (2021b) reports of lower C/N ratio for HE. Combining HE with carbon-rich organic wastes like FLO and KR improves nutrient balance and the C/N ratio (Singh et al., 2021b). Tri-digestion of R9 exhibited the highest biogas and methane yields, followed by R10 (Table 5.3). This can be traced to the C/N ratios of R9 (23.9) and R10 (22.5).

Generally, a C/N ratio of 20-30 gives a more stable anaerobic digestion process (Dar et al., 2021; Rahman et al., 2017; Chiu and Lo, 2016). It was found that co- and tri-digestion could maintain C/N ratios at ideal values due to the mixture of various substrates, which enhanced biogas production (Table 5.1). Combining HE with FLO and KR helped achieve the optimal C/N ratio, thereby improving digestion. A considerable amount of biogas and methane was also produced in the co-digestion treatments R5, containing high amounts of HE, even at the low C/N ratio of 15.45. This could be because HE is nutrient-rich and contains adequate amounts of native trace elements like Fe, Ni, Zn and Co essential for the growth of anaerobic

Table 5.3: Biogas and Methane Yields,VFA, pH, Alkalinity and VS Reduction for Different Mix Ratios of HE, FLO and KR

Parameter	R1	R2	R3	R4	R5	R6	R7	R8	R9	R10	R11	R12	R13	R14	R15	R16	PC
Specific Biogas Yield (mL/gVS)	453.37	375.76	473.47	254.61	802.59	527.82	782.97	887.27	1167.62	881.33	322.75	611.12	482.27	990.54	417.56	632.94	762.45
Methane Content(%)	56.00	36.00	42.00	40.00	67.90	59.90	63.20	64.60	65.50	67.60	48.50	42.70	56.70	53.10	59.00	46.00	57.10
Specific Methane Yield (mLCH_4/gVS)	253.89	135.27	198.86	101.84	544.96	316.16	494.83	573.18	764.79	595.78	157.50	260.95	273.45	525.98	246.36	291.15	435.36
Specific Methane Yield Correction with 8%	274.20	146.09	214.77	109.99	588.56	341.45	534.42	619.03	825.97	643.44	170.10	281.83	295.33	568.06	266.07	314.44	470.19
Theoretical Methane Potential (mL/gVS)	461.12	833.60	745.18	727.27	657.10	586.04	602.69	644.13	852.27	689.99	609.60	646.77	565.84	659.05	773.17	774.99	551.35
Biodegradability (%) Corrected	55.06	16.23	26.69	14.00	82.93	53.95	82.10	88.99	89.74	86.35	25.84	40.35	48.33	79.81	31.86	37.57	78.96
Biodegradability (%)	59.46	17.53	28.82	15.12	89.57	58.26	88.67	96.10	96.91	93.25	27.90	43.57	52.19	86.19	34.41	40.57	85.28
VS Reduction (%)	47.81	41.79	46.94	36.71	60.72	50.69	59.68	62.67	67.62	63.49	38.43	51.76	47.19	66.79	43.75	53.08	57.99
Initial pH	7.1	6.3	6.1	6.0	7.1	7.3	7.4	7.5	7.9	7.4	6.7	6.7	6.6	6.8	6.7	7.0	7.3
Final pH	6.3	5.0	5.3	4.9	6.1	6.2	6.6	6.2	6.1	6.3	5.4	6.3	6.0	6.3	5.2	5.6	6.7
Initial Alkalinity (mg/L)	7432.50	2662.50	2525.00	1712.50	4537.50	5537.50	5887.50	5975.00	6587.50	6412.50	1512.50	1925.00	3437.50	3850.00	3537.50	1687.50	3512.50
Final Alkalinity (mg/L)	3950.00	1775.00	1900.00	1287.50	1362.50	2087.50	2825.00	2987.50	2700.00	1725.00	1275.00	1637.50	1437.50	1112.50	1625.00	1562.50	3100.00
Initial VFA (mg/L)	3652.12	4141.89	3543.28	3549.33	2956.77	1711.18	3507.00	3555.38	2890.25	2309.79	3537.24	3017.23	2920.49	3597.70	4147.94	4153.99	1747.46
Final VFA (mg/L)	2866.07	3567.47	2962.81	3005.14	1668.85	1064.19	1680.94	1674.90	1481.41	1082.33	2309.79	2932.58	1711.18	1106.52	3500.96	2902.35	1124.66

bacteria (Miah et al., 2016).

On the other hand, low pH and buffer capacities were observed for FLO and KW. Li et al. (2013) has reported a similar trend. Hence, mono-digestion of FLO and KR is not always desirable. Co-digestion of these substrates at certain optimum proportions may improve methane production performance. The initial and final pH and alkalinity values for all treatments are summarized in Table 5.3. Mixing feedstocks raised the pH of the mixtures containing FLO and KR relative to their individual pH values. This could be observed from Table 5.3 where combinations of FLO and KR with higher proportions of HE had high pH values at the start of digestion and vice versa. The initial pH values of R5, R7, R8, R9 and R10 were within the range of 7.1-7.9, while the pH values after digestion were within the range of 6.1-6.6 (Table 5.3). The observed pHs of the digesters (R5, R7, R8, R9 and R10) were within the acceptable range for anaerobic digestion (Abubakar and Ismail, 2012).

In addition, the intial and final alkalinity of R5, R7, R8, R9 and R10 lies within the ranges 4537.5-6587.5 mg/L and 1362.5-2987.5 mg/L respectively. Due to the optimal pH values and the strong alkalinity providing a very good buffer for the rectors, biogas and methane production were stable (Scherer et al., 2021; Scherer, 2007), obtaining a biodegradability range of 82.1-89.7 % (Table 5.3). On the other hand, treatments R2, R3, R4, R11 and R16 with very low initial alkalinity in the range of 1512.5-2662.5 mg/L and final pH in the range of 4.9-5.6, had very low biogas and methane yields and hence very low biodegradability values as expected (Table 5.3). This observation is consistent with the information in Table 5.3 and could be explained by the buildup of VFAs from the conversion of readily biodegradable components in the digestive media.

Conversely, treatments with 50 % or more HE added like R9 and R10 were observed to ensure a stable AD system stability due to the least initial and final VFA values ranging between 2309.8- 3555.4 mg/L and 1082.3-1680.9 mg/L respectively and this finding might provide an explanation for the best biogas yield, methane yield and biodegradability data recorded (Table 5.3). The VFA/Alkalinity ratios of 0.43 and

0.35 for R9 and R10 respectively is a confirmation of how stable the anaerobic digestion process was. According to Feng et al. (2013), a VFA/Alkalinity ratio of 0.4 indicates stability of anaerobic digestion process.

5.4.5 Effect of Native Trace Elements in Substrate Mixtures on Methane Yield

Trace elements that are often present in human-generated waste, such as iron (Fe), nickel (Ni), zinc (Zn) and molybdenum (Mo) (Appiagyei Osei-Owusu et al., 2023), were studied to investigate their effect on methane yields of the different mixtures (R1-R16). All treatments contained Fe, Ni, Zn and Mo concentrations in the range 1.7150-8.5298, 0.0017-0.0530, 0.1552-0.5541 and 0.0067-0.0700 mg/L respectively (Table 5.4).

Table 5.4: Concentration of Trace Elements in Substrate Mix

Treatment	Mo(mg/L)	Zn (mg/L)	Fe(mg/L)	Ni (mg/L)
R1	0.0171	0.2108	2.8353	0.0029
R2	0.0144	0.1995	1.9148	0.0017
R3	0.0117	0.2074	1.7150	0.0025
R4	0.0127	0.2637	2.9204	0.0051
R5	0.0675	0.3080	4.3026	0.0427
R6	0.0085	0.2121	2.9789	0.0138
R7	0.0700	0.2547	3.3521	0.0326
R8	0.0124	0.3011	3.7329	0.0374
R9	0.0072	0.5541	3.8201	0.0530
R10	0.0083	0.4141	2.9879	0.0431
R11	0.0100	0.2155	7.6721	0.0050
R12	0.0077	0.2552	4.0839	0.0092
R13	0.0070	0.2309	2.5650	0.0032
R14	0.0067	0.2348	2.5491	0.0358
R15	0.0085	0.3010	3.0142	0.0018
R16	0.0103	0.2285	8.5298	0.0034

Fe had all treatments outside the stimulatory concentration of <0.3 (Worm et al., 2009), with the highest and lowest concentrations for R16 (8.53 mg/L) and R3 (1.72 mg/L), respectively. Also, with stimulatory concentrations of 0.03<Zn<2 and 0.03<Ni<27 for

Zn and Ni respectively, all treatments were within the stimulatory range (Gikas, 2007; Li and Fang, 2007).

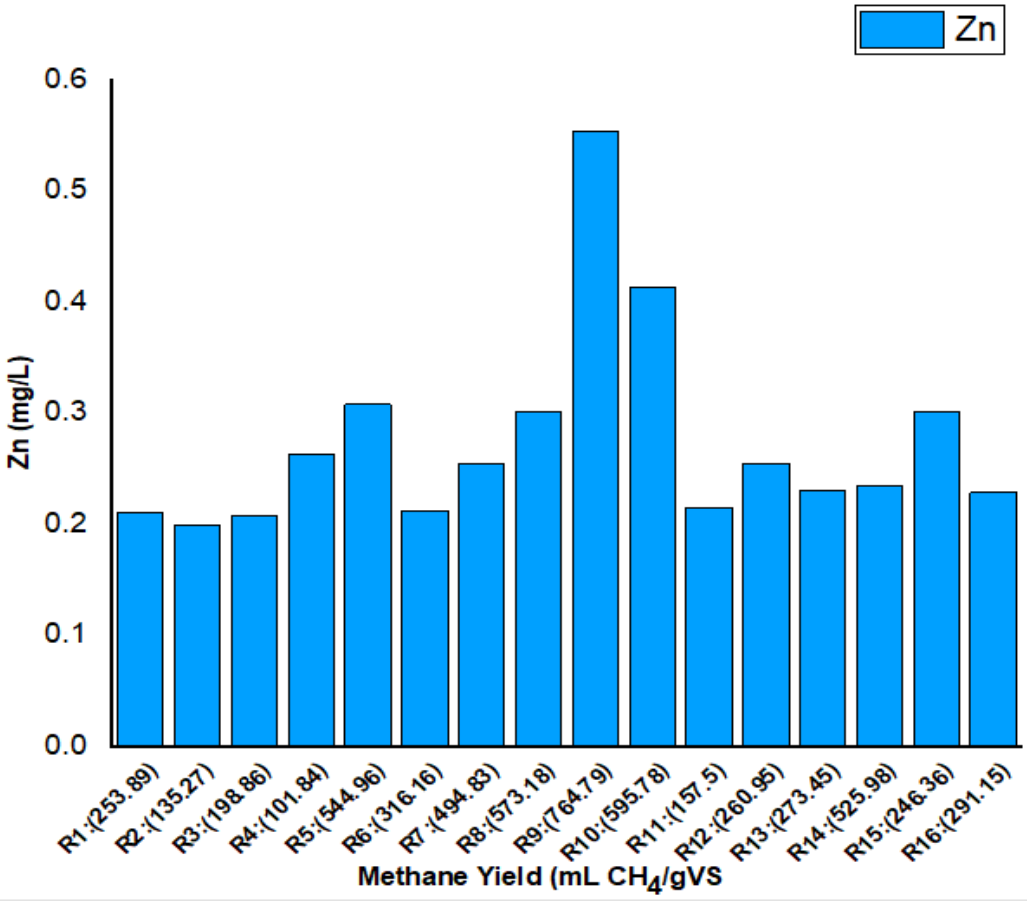

Figure 5.5: Effects of zinc concentrations on methane yields

The treatments with the highest Zn concentrations were R9 (0.554 mg/L) and R10 (0.414 mg/L), while the least concentrations were found in R1 (0.211 mg/L), R2 (0.200 mg/L) and R3 (0.210 mg/L) respectively (Figure 5.5). Considering the important roles of the trace element (Zn) for activating and maintaining enzyme activities of anaerobic microorganisms (Agler et al., 2008; Zitomer et al., 2008), they were possibly insufficient for stable and efficient anaerobic digestion in the mono-digestion tests R1,R2 and R3. It is therefore expected that the concentrations of essential trace elements could be properly adjusted by mixing HE, FLO and KR (Zhang et al., 2011).

Contrarily, R9 and R10 had the highest methane yields and were found to contain the highest concentrations of Zn. This results confirms the positive influence of

Zn on enzymes such as coenzyme *M. methyltransferase*, involved in methanogenesis (Romero-Güiza et al., 2016). Similarly, optimum concentrations of Ni in R5 (0.043 mg/L), R7 (0.033 mg/L), R8 (0.027 mg/L), R9 (0.053 mg/L) and R10 (0.022 mg/L) significantly imcreased their methane yields (Figure 5.6). Arthur et al. (2022) reported an increase in the number of methanogens present in reactors containing nickel. The author also documented that nickel concentration of less than 0.1 mg/L improved the stability of the anaerobic digestion process because intermediary products were readily digested by methanogens (Arthur et al., 2022). Further, Schmidt et al. (2014) reports a rapid accumulation of VFAs when Ni is depleted.

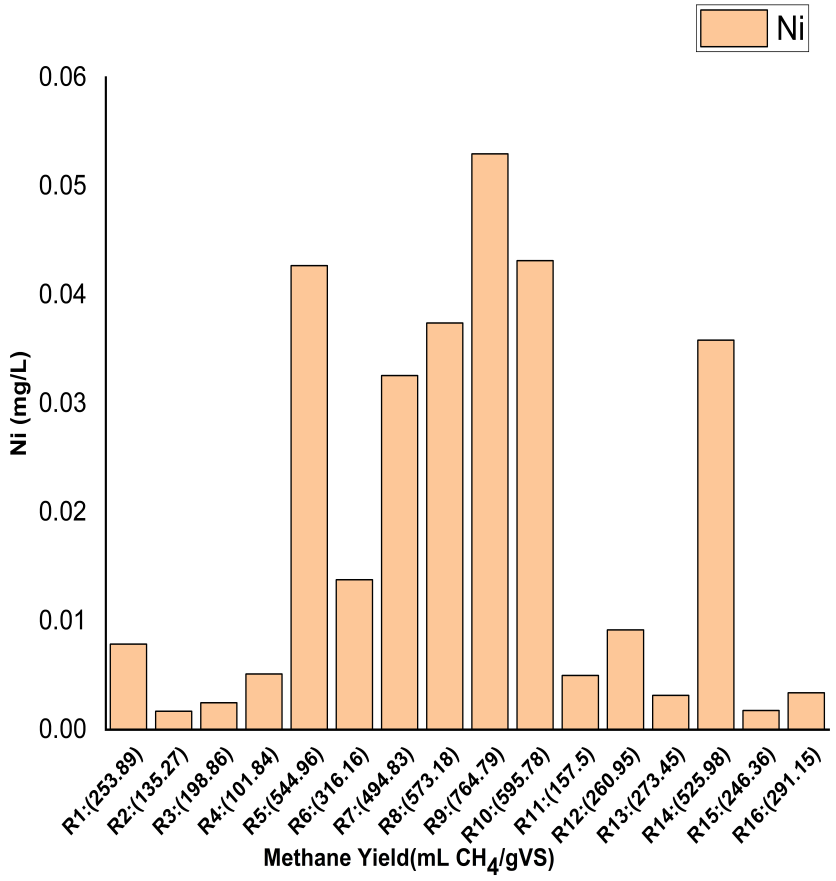

Figure 5.6: Effects of nickel concentrations on methane yields

The trace elements bottles (R7, R8 R9 and R10) with high methane yields are in the order Fe>Zn>Ni>Mo. Fermoso et al. (2009) illustrated the fundamental role of these micro nutrients by demonstrating their interactions with microbe cells. Overall, the elements in methanogens cells were in the following order Fe>Zn>Ni>Cu=Co=Mo>Mn.

Also, Schönheit et al. (1979) discovered that *Methanobacterium thermoautotrophicum* grew in response to trace elements of Fe>Ni>Co=Mo. As mentioned above, the trace elements supplied from the mixtures seemed to increase the process stability of anaerobic co- and tri-digestions. However, due to factors like C/N ratio, pH and alkalinity values of the individual co- and tri-digestion tests, some process upsets were observed in some treatments like R6 and R15 as indicated by VFA accumulation even though they had sufficient amounts of Zn and Ni.

5.4.6 Synergistic Effects of Co- and Tri-digestion

Figure. 5.7 compares the synergy index (SI) for multiple substrate digestion of HE, FLO and KR among the BMP runs. The SI values for the co- and tri-digestion runs (R4–R16) ranging from 0.61 to 3.26 are used to access how the individual mixtures affect the amount of methane generated.

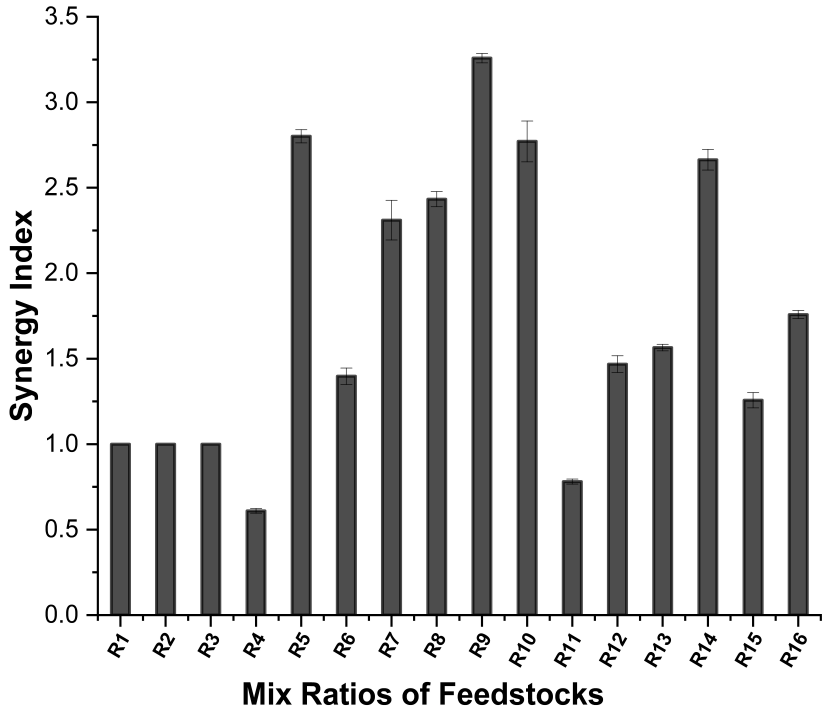

Figure 5.7: Synergy index of substrate mix at different HE/FLO/KR ratios. SI > 1 indicates synergistic effect, and SI < 1 indicates antagonistic effect (mean±S.D; n=3)

R5, R6, R7, R8, R9, R10, R12, R13, R14, R15,16 with SI values in the range 1.26-3.26 depicted stronger positive synergic effects. Additionally, R9 showed the highest SI value (3.26). The co- and tri-digestion runs containing an appropriate mix of FLO, and KR tended to produce more methane with higher HE percentages. The properties and ratios of the AD mixtures may have a bearing on the synergistic impact. These factors might have balanced the nutrients, promote microbial proliferation, boost buffer capacity, and dilute toxic substances during digestion. Wang et al. (2018c) have shown that the synergistic impact is caused by the addition of beneficial nutrients, which can improve biodegradability and enhance the metabolism of microorganisms.

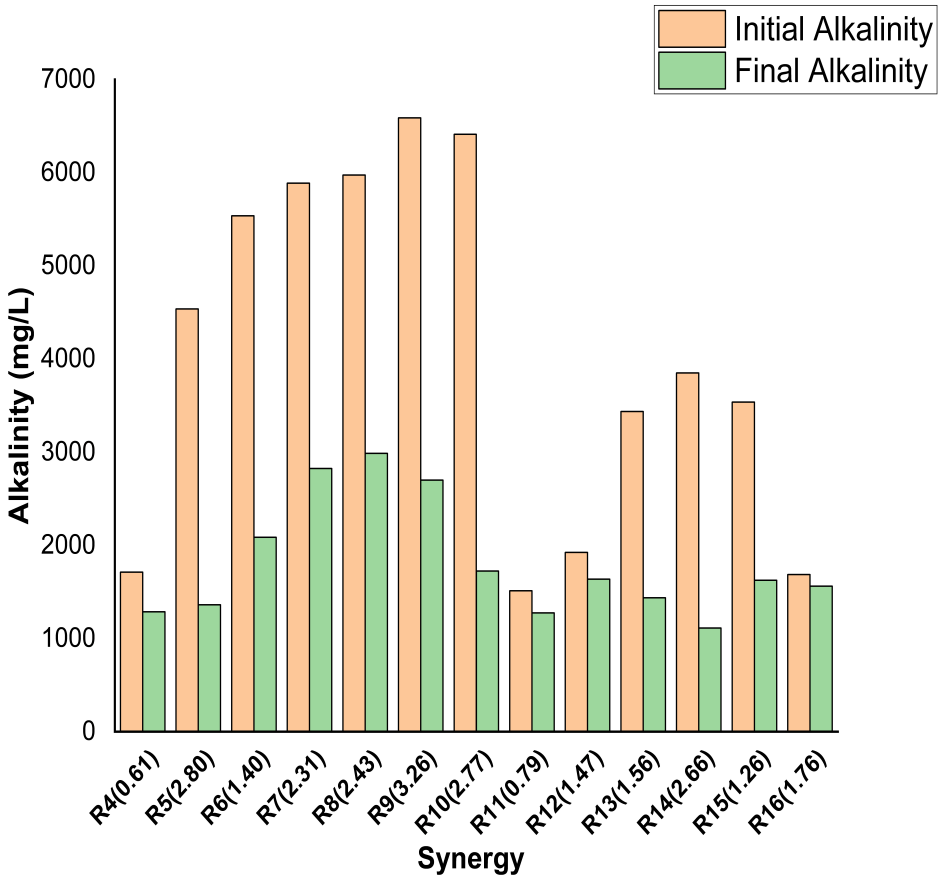

Figure 5.8: Effect of alkalinity on synergy index of substrate mixtures

It can also be observed from Figure 5.8 that bottles (R5,R6,R7,R8,R9 and R10) with initial alkalinity values of over 4500 mg/L and final alkalinity of close to 2000 mg/L and above showed a positive synergistic effect. Conversely, R4 and R11 with initial alkalinity values around 2000 mg/L and final alkalinity around 1000 mg/L exhibited

an antagonistic effect with SI values of 0.61 and 0.78, respectively (Figure 5.8). This is because R4 and R11 contained no or less amounts of HE. Also, the high amounts of KR (mainly composed of lignin-containing feed stock like plantain peels, cassava peels, cocoyam peels and yam peels) in R4 and R11 might have led to the negative synergistic effects. Kim et al. (2019b), in their study of food waste, human faeces and toilet tissue, reported no obvious positive or negative synergic effects with reported SI values of 0.939 to 1.05. However, Ebner et al. (2016) reported an SI value of 0.68 for the co-digestion of food waste and dairy manure, indicating a clear antagonistic effect. Conversely, Hou et al. (2020) reported significantly positive synergic effects for food waste, rice straw and bran.

5.4.7 Modelling of Responses

Analysis of the experimental data revealed that quartic models (Dan-Asabe et al., 2019) shown in Equations 5.7-5.9 were suitable for expressing biogas yield, methane yield and synergy as a function of the mixture components (Human Excreta-A, Food Leftovers-B and Kitchen Residue-C). The validity of the models were checked by plots of the model predicted values against the experimental (actual) values as shown in Figure 5.9. The plot of biogas yield (Figure 5.9a) showed that the slope line passes exactly through all points while the plots of methane yield (Figure 5.9b) and synergy (Figure 5.9c) passes approximately through the data points. The relative similarity between the experimental observations and the model predictions indicates the validity, precision and good predictive capacity of the RSM model.

$$BiogasYield = 452.73A + 375.54B + 474.13C + 1587.49AB + 264.52AC - 680.02BC + 7387.14ABC + 1842.66AB(A-B) - 1139.33AC(A-C) + 10187.44A^2BC - 44978.31ABC^2 - 5628.27AB(A-B)^2 + 18180.83AC(A-C)^2 + 12644.33BC(B-C)^2 \quad (5.7)$$

$$MethaneYield = 250.47A + 138.25B + 196.17C + 1363.05AB + 318.22AC - 320.97BC$$
$$+1178.90AB(A-B) + 13479.78A^2BC - 22626.90ABC^2 - 4195.21AB(A-B)^2$$
$$+11530.09AC(A-C)^2 + 7085.93BC(B-C)^2$$

(5.8)

$$Synergy = 0.97A + 1.02B + 0.99C + 7.03AB + 1.29AC - 1.94BC + 4.90AB(A-B)$$
$$+66.34A^2BC - 106.95ABC^2 - 23.27AB(A-B)^2 + 51.58AC(A-C)^2 + 40.93BC(B-C)^2$$

(5.9)

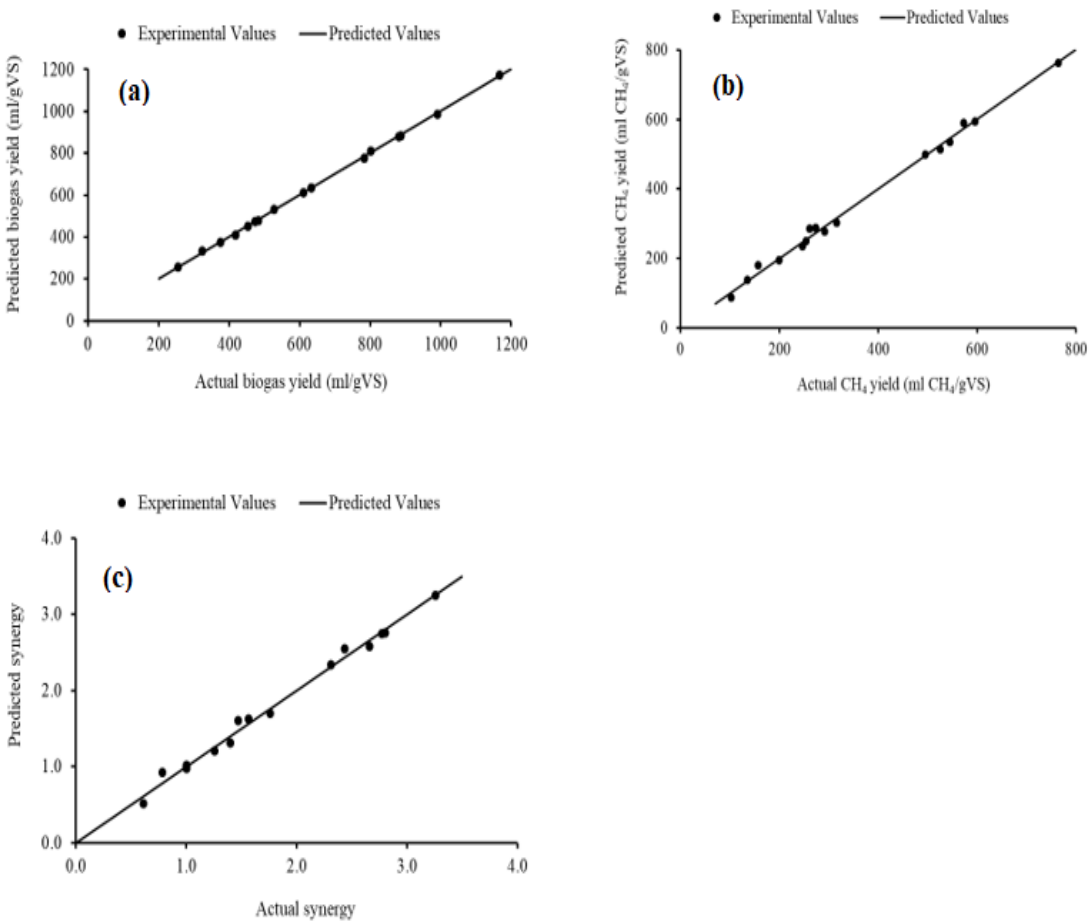

Figure 5.9: Parity plots of experimental and predicted (a)biogas yield, (b) methane yield and (c) synergy as a function of the mixture components

The statistical significance of the RSM model was assessed by carrying out ANOVA, with results shown in Table 5.5. Model terms with *p-values* less than 5 % (0.05) are significant, while the reverse is also the case (Dan-Asabe et al., 2019). In this context, the biogas yield, methane yield and synergy models with *p-values* of 0.0023, 0.0004 and 0.0013, respectively, were significant (good in predicting the output responses) as they were characterized by p-values significantly less than 0.05. Also, the model *F-values* of 431.81, 81.14 and 42.34 for biogas yield, methane yield and synergy, respectively, showed that the model is significant implying that there is only a 0.23, 0.04 and 0.13 % chance that *F-values* this large could occur due to noise (Table 5.5). Hence the model is very good at predicting the responses.

Further, the Adequate Precision (AP) values of 72.31,30.75 and 21.16 for biogas yield, methane yield and synergy, respectively, indicate an adequate signal and the ability of the model to be used to navigate the design space (Table 5.5). This is because the measure of the signal-to-noise ratio is desirable when greater than 4 (Amenaghawon et al., 2022; Betiku and Adesina, 2013). In addition, the linear terms representing the amount of HE (A), FLO (B) and KR (C) were all significant, indicating that varying the amount of feedstocks mixture components will have a significant influence on biogas yield (0.00169), methane yield (0.00016) and synergy (0.00156). There is therefore the need to test different amounts of household-generated waste in order to find the best ratios for a stable household biogas generation process.

However, the terms representing the interaction between HE and KR (AC and AC(A-C)) as well as HE, FLO and KR (ABC and A^2BC) in the biogas yield and synergy models were not significant. These terms were nonetheless retained in the model to maintain model hierarchy (Table 5.5). The biogas yield, methane yield and synergy predicted by the RSM model were respectively characterized by small magnitudes of standard deviation (13.58, 25.38, and 0.15) compared to the mean value of 629.00, 358.38 and 1.75, indicating minimal dispersion of the data sets (Table 5.5). This was confirmed by the coefficient of variation, CV, values of 2.16, 7.08 and 8.50 %, respectively, for biogas yield, methane yield, and synergy. These CV values were low enough to indicate the precision and reliability of the data (Table 5.5).

Table 5.5: ANOVA Results for the RSM Models of Biogas Yield, Methane Yield and Synergy

Parameter	Biogas Yield					Methane Yield					Synergy				
Source	Sum of Squares	DF	Mean	F-Value	P-Value	Sum of Squares	DF	Mean	F-Value	P-Value	Sum of Squares	DF	Mean	F-Value	P-Value
Model	1.03E6	13	79583.31	431.81	0.00231	5.75E5	11	52259.87	81.14	0.00035	10.36	11	0.94	42.34	0.00126
Linear Mixture	218,353.15	2	109176.58	592.38	0.00169	203884.21	2	101942.11	158.27	0.00016	2.16	2	1.08	48.67	0.00156
AB	122,998.06	1	122998.06	667.38	0.00150	96561.44	1	96561.44	149.92	0.00026	2.57	1	2.57	115.53	0.00042
AC	3020.38	1	3020.38	16.39	0.05595	5180.83	1	5180.83	8.04	0.04705	0.08	1	0.08	3.81	0.12257
BC	20,604.35	1	20604.35	111.80	0.00883	4860.01	1	4860.01	7.55	0.05154	0.18	1	0.18	8.01	0.04735
ABC	1935.39	1	1935.39	10.50	0.08348			NA					NA		
AB(A-B)	34,244.95	1	34244.95	185.81	0.00534	15820.60	1	15820.60	24.56	0.00773	0.27	1	0.27	12.29	0.02478
AC(A-C)	2193.77	1	2193.77	11.90	0.07472			NA					NA		
A^2BC	1879.83	1	1879.83	10.20	0.08564	17402.08	1	17402.08	27.02	0.00653	0.42	1	0.42	18.95	0.01213
ABC^2	17178.31	1	17178.31	93.21	0.01056	47077.28	1	47077.28	73.09	0.00103	1.05	1	1.05	47.29	0.00234
$AB(A-B)^2$	23297.21	1	23297.21	126.41	0.00782	17484.53	1	17484.53	27.15	0.00647	0.54	1	0.54	24.19	0.00794
$AC(A-C)^2$	121,489.29	1	121489.29	659.19	0.00151	133044.11	1	133044.11	206.56	0.00014	2.66	1	2.66	119.72	0.00040
$BC(B-C)^2$	76420.15	1	76420.15	414.65	0.00240	37525.29	1	37525.29	58.26	0.00158	1.25	1	1.25	56.31	0.00169
Residual	368.60	2	184.30			2576.37	4	644.09			0.09	4	0.02		
Cor Total	1.04E6	15				5.77E5	15				10.45	15			
CV (%)	2.16					7.0817					8.4991				
Mean	629.00					358.3755					1.7546				
SD	13.58					25.3790					0.1491				
AP	72.31					30.7516					21.1644				

RSM performance assessment for the biogas yield, methane yield, and synergy models was carried out using standard statistical metrics, as shown in Table 5.6. According to Fatoni (2012), a good model is one that gives an R^2, adjusted R^2 and or predicted R^2 values approaching unity. In addition, Le Man et al. (2010) documented that a model is only adequate when R^2 values are not less than 0.75. Nonetheless, Koocheki et al. (2009) stated that a high R^2 value does not necessarily imply a good regression model until there are similarly high values of adjusted R^2. Therefore, high R^2 and adjusted R^2 values can both be used to explain how adequate a model is to predict within the range of experimental values. That notwithstanding, the difference between R^2 and adjusted R^2 should not be more than 10 % (Osunkanmibi et al., 2015).

The reported R^2 values in this study indicate that the quartic model was very accurate in predicting the biogas yield (0.999), methane yield (0.996), and synergy (0.992) as shown in Table 5.6. Although all models showed good predictive performance, as seen in their high R^2 values, the biogas yield model was relatively better in its prediction because it had the highest R^2 (0.999) value and a low error value (RMSE of 4.798). This was corroborated by the results in the parity plots presented in Figure 5.6 where the predictions were closer to the experimental data. Furthermore, the difference between the R^2 values and the adjusted R^2 values for biogas yield, methane yield and synergy were not more than 10 % (Osunkanmibi et al., 2015). Also, the low RMSE and the MSE values for biogas yield and synergy show that the model is able to forecast values accurately (Table 5.6) and this can be attributed to the closeness of the error values to zero which further shows how close the experimental values are to the predicted values.

Table 5.6: RSM Performance Assessment for Biogas Yield, Methane Yield, and Synergy

Parameter	Biogas Yield	Methane Yield	Synergy
R^2	0.999	0.996	0.992
Adjusted R^2	0.997	0.983	0.968
RMSE	4.798	12.690	0.075
MSE	23.020	161.046	0.006
MAE	3.677	10.559	0.061
MAPE (%)	0.661	4.411	4.774

5.4.8 Response Surface Plots

Figures 5.7 -5.9 show the 3D response surface plots that illustrate the influence of the mixture components on biogas yield, methane yield, and synergy respectively. The 3D plots were characterized by different levels of curvature, which corroborates the relationship between substrate mix and biogas yield, methane yield, and synergy and mixture components. The shape of the plot shows that there were notable and shared interactions between HE (A), FLO (B), and KR(C). Both HE and KR had a similar positive synergistic effect on biogas yield, methane yield, and synergy, which was not comparable with that of FLO.

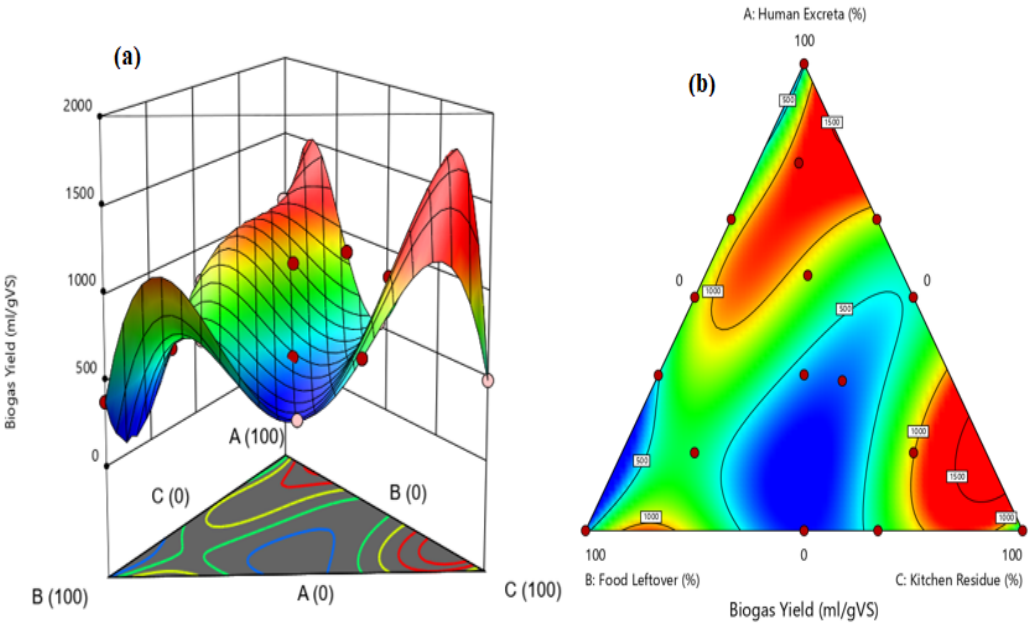

Figure 5.10: (a)Three-dimensional and (b)Two-dimensional response surface plots depicting the effect of the substrate mixing ratio on biogas yield. Contour colors represent the levels of model response: blue for low and red for high responses.

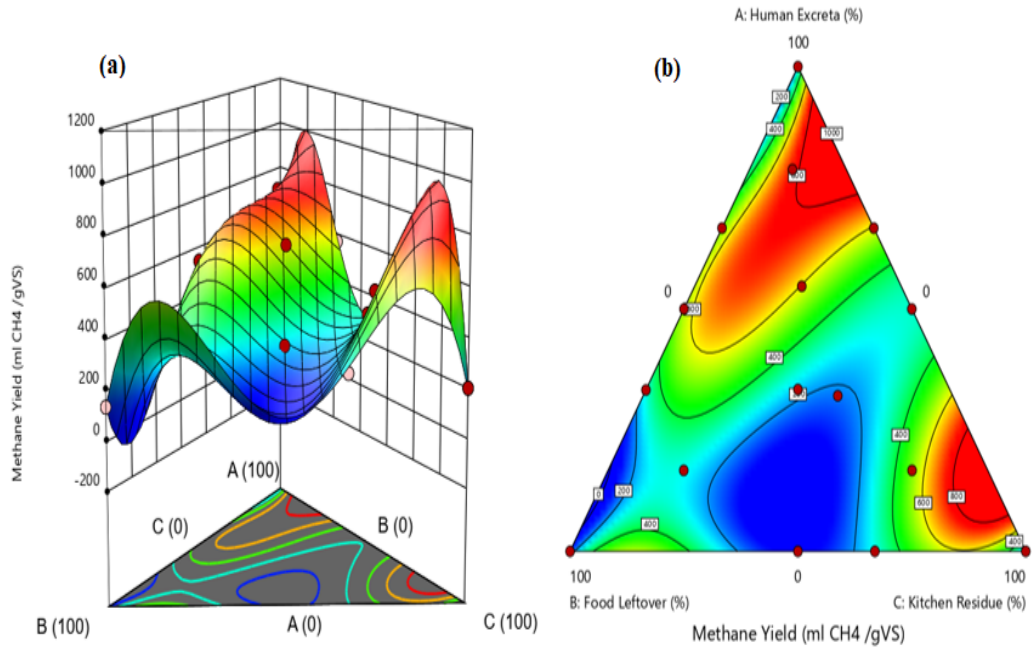

Figure 5.11: (a)Three-dimensional and (b)Two-dimensional response surface plots depicting the effect of the substrate mixing ratio on methane yield. Contour colors represent the levels of model response: blue for low and red for high responses.

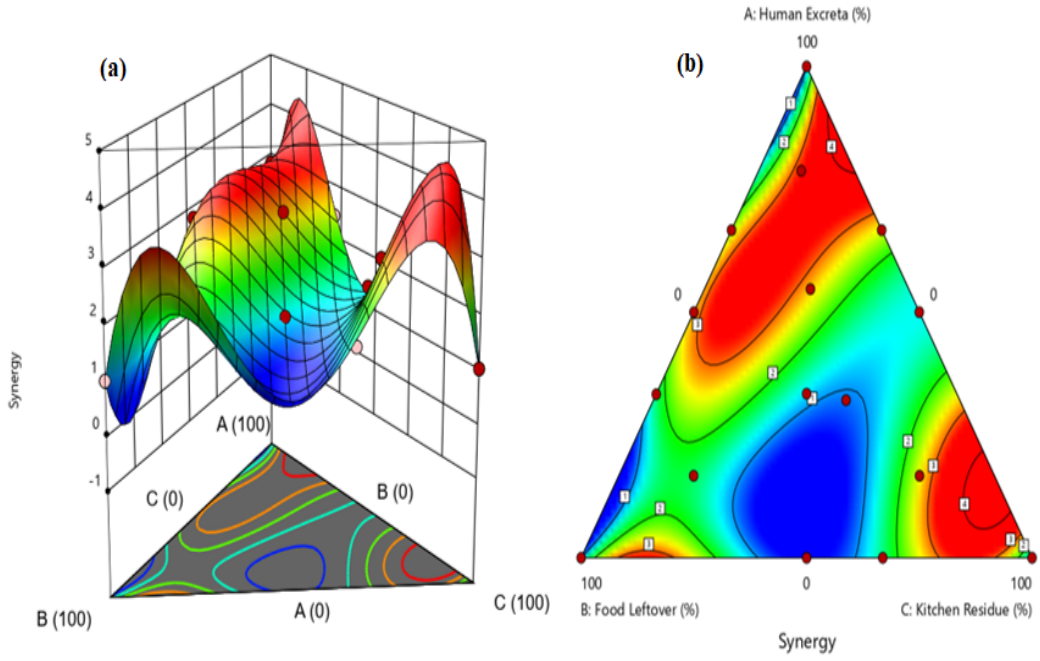

Figure 5.12: (a)Three-dimensional and (b)Two-dimensional response surface plots depicting the effect of the substrate mixing ratio on synergy index. Contour colors represent the levels of model response: blue for low and red for high responses.

This can also be seen from the coefficients of A and C in the regression model (Equations 5.8 and 5.9), i.e., 452.73 and 474.13, as well as 250.47 and 196.17 respectively, for biogas yield and methane yield compared to 375.54 and 138.25 for B.

Contextually, increasing the levels of HE and KR in the substrate mix would increase biogas yield, methane yield, and synergy. This observation could be attributed to the fact that HE and KR are rich in nutrients needed for microbial growth, complement each other in buffering the system, and have an optimum C/N ratio. The impact of FLO was not significantly seen. Although FLO could have provided a good carbon source, its insufficient buffer due to low alkalinity levels and its ability to easily degrade and lead to VFA accumulation, pH reduction, and process instability might have led to its less influence.

In general, the response surface plots show that the predicted response increases with an increasing HE and KR fractions and decreases with an increasing FLO fraction in the substrate mixtures (Figures 5.7 -5.9). This is because the maximum and minimum model outputs were found at the HE-KR and FLO vertices, respectively. This result shows that biogas yield, methane yield, and synergy were more significantly affected by the interaction between HE and KR than between FLO and HE and between FLO and KR. Similar observations were reported by Baek et al. (2020), who used a substrate mix of food waste, cattle manure, and pig manure to produce biomethane. The study reported increased methane yield and synergy when food waste and cattle manure were increased but low when pig manure was increased.

5.5 Conclusion

Ternary substrate mixtures of HE, FLO, and KR formulated for the batch experiment showed that substrate mix R9(78.8:11.8:9.4) produced the highest amount of biogas and methane. R9(78.8:11.8:9.4) also showed the strongest synergistic effect. The experimental results for the substrate mixtures were used to model the responses of biogas yield, methane yield, and synergistic effects using RSM. Results of the statistical modeling showed that different mixing ratios of HE, FLO and KR can be suitably

modeled to provide ease and robustness of determining results of different and best-performing formulations of the feedstocks.

The overall results showed that biogas yield, methane yield, and synergy are significantly influenced by the composition and interactions of feedstock mixtures. Co-digesting substrate mixtures with high amounts of HE and/or KR increased biogas yield, methane yield, and synergy. This finding suggests that it is possible to effectively treat household HE and KR onsite to produce methane for cooking. The 61-day response surface model for synergistic effects predicted an antagonistic effect (SI < 1) only for the co-digestion setting where the FLO fraction is higher than roughly 25 % or the combination of FLO and KR is greater than HE. In order to prevent the potential antagonistic effect, it is advisable to keep the FLO and KR fraction in the substrate combination below 50 %.

It is therefore recommended that in setting up an anaerobic digestion system at the household level, the amount of HE is kept relatively higher (>50 %) than KR and FLO. This is because the higher the amount of HE, the more likely the digestion process would be stable due to the ability of HE to provide a buffering support with its relatively high alkalinity compared to FLO and KR. Also, the high biodegradability of R9(78.8:11.8:9.4) depicts the ability of the microbial culture to convert the feedstocks in that particular mixing ratio to biogas. Additionally, there is no need to add trace elements to the household biogas system because the household-generated wastes have proven to contain sufficient amounts of trace element such as Zn and Ni that are very beneficial to methanogens.

CHAPTER 6

Kinetics Study of Methane Yield from Anaerobic Co-Digestion of Human Excreta, Food Leftovers and Kitchen Residue

6.1 Abstract

Following the rapid growth in household energy demand and the rising generation of household human generated waste, options for sustainable waste management and energy supply have received a lot of attention. The anaerobic digestion of human excreta (HE), food leftover (FLO) and kitchen residue (KR) with the proportions 78.8 % HE; 11.8 % FLO; 9.4 % KR proved to be an optimum co-digestion ratio with a methane yield of 764.79 mLCH_4/gVS, a biodegradability of 89.74 % and a synergy index of 3.26. Having established that, the experimental cumulative methane yield from the same ratio was fitted to five kinetic models namely Fitzhugh, Modified Gompertz, Logistic, Cone and Monod in this study to find the model with the best fit. The kinetic study showed that the cone model out of the five models had the best fit compared to the experimental data, recording an R^2 value of 0.9909.

6.2 Introduction

The large amounts of human-generated household waste, including human excreta (HE), food leftovers (FLO), and kitchen residue (KR), can be treated using the highly recommended anaerobic co-digestion (AD) technology, which also generates methane as a renewable energy source for cooking and other household purposes. Due to the potential of anaerobic digestion to improve the sustainability of sanitation systems and produce renewable energy, it has gained attention in recent years. The anaerobic biochemical methane potential (bmp) batch test is employed as the industry standard method for determining methane yield of potential feedstocks (Adl et al., 2012).

Data from batch tests have proven particularly valuable in forecasting the behaviour of methane yield of full-scale biogas systems due to advancements in computer models and the intricacy of mathematical expressions used to describe the anaerobic digestion processes (Filer et al., 2019). The rate and extent of biogas production and feedstock degradation are some of the important aspects of anaerobic digestion that determines the kinetics. However, the kinetics of the anaerobic digestion process are complex, and the optimal conditions for this process are still unclear. Therefore, studying the kinetics of the anaerobic co-digestion of human excreta and food waste to improve its efficiency is necessary.

Two crucial factors for anaerobic bio-degradation are the quantity of organic matter that can readily be broken down by microorganism and the hydrolysis rates of substrates (Angelidaki et al., 2009). These factors influence the design of biogas facilities to some extent. Numerous researches (Latinwo and Agarry, 2015a; Syaichurrozi et al., 2013) describe the generation of biogas using growth kinetics because anaerobic microorganisms are responsible for producing biogas. The growth curves frequently show a phase where the particular growth rate starts at zero at a given time frame (resulting in a lag time) and then rises to a maximum value. Moreover, the simulation of biomethane generation from anaerobic treatment uses structured kinetic models.

Additionally, the kinetics of anaerobic digestion is influenced by various factors, such as temperature, pH and hydraulic retention time in addition to the types and concentrations of microorganisms present. Hence, a thorough understanding of the kinetics of the anaerobic digestion process leads to a more accurate forecast of digester performance in general (López et al., 2021). According to Nielfa et al. (2015), some models can forecast eventual methane productions from the beginning of testing in addition to replicating the behaviour of the methane curve. Also, kinetic models can aid in understanding the processes that control biodegradation (Cecchi et al., 1990). Consequently, developing a full-scale anaerobic digestion system begins with kinetic modeling of the anaerobic digestion process (Chan et al., 2017; Andara and Esteban, 1999).

Several mathematical models have been developed to describe the kinetics of the anaerobic digestion process, including the first-order model, modified Gompertz model, the logistic model, the monod model, the fitzhugh model, hill model and cone model. The Fitzhugh model is an expansion of the first-order model that incorporates the constant n (Ihoeghian et al., 2022), whilst the modified Gompertz model (Etuwe et al., 2016; Kafle and Kim, 2012; Donoso-Bravo et al., 2010) offers more details on the lag phase and the maximum biogas or methane production rate (Bedoić et al., 2020; Pramanik et al., 2019; Zahan et al., 2018). In addition, the Logistic Function model is appropriate for simulating the initial exponential increase that stabilizes at the highest levels of biogas production and the accumulated biogas or methane yield (Latinwo and Agarry, 2015a; Donoso-Bravo et al., 2010).

The Logistic and modified Gompertz models (Latinwo and Agarry, 2015a; Schofield et al., 1994) can perfectly simulate the final phase of a growth curve, in which the growth rate declines until it eventually reaches zero, resulting in the asymptote (Zwietering et al., 1990). Also, the Monod kinetic model is a mechanistic model that links the concentrations of biomass and substrate to the growth rate. It suggests that microbial species growing under specific conditions have characteristics like a maximum cell growth rate and a saturation constant (Velázquez-Martí et al., 2018). Furthermore, the cone model predicts that methane production in a batch test will increase in direct proportion to the growth rate of methanogenic bacteria (Prajapati et al., 2018).

These models are based on different assumptions and principles and can be used to predict biogas and methane production rates as well as substrate degradation rates under different conditions. Additionally, not all models are suitable for a robust simulation of various substrates and process conditions due to structural and computational complexity (Weinrich and Nelles, 2015). Hence, the most appropriate kinetic model should be chosen to accurately examine the metabolic pathways and mechanisms involved in the AD process and predict the efficacy of specific reactors (Nguyen et al., 2019).

To fit the experimental methane production as well as evaluate kinetic parameters, this study will implement the modified Gompertz model (Yusuf et al., 2011; Budiyono and Sumardiono, 2014), logistics function model (Burnham, 2017), cone model (El-Mashad, 2013; Pitt et al., 1999), Fitzhugh (Li et al., 2018d) and Monod (Lawrence and McCarty, 1969) models. This research seeks to determine the best-fitting kinetic model for the anaerobic co-digestion of HE, FLO, and KR using a mixture of 78.8 % HE : 11.8 % FLO : 9.4 % KR.

6.3 Materials and Method

6.3.1 Feedstock and Inoculum Collection and Preparation

Fresh HE was collected from a KVIP at Ayeduase, a suburb of Kumasi, Ghana. Fresh CD was collected from the animal farm of the Department of Agriculture, KNUST. Anaerobically mono-digested cow dung with a pH of 7.8 and alkalinity of 8150 mg/L, was used as inoculum in the BMP Tests. Prior to use, the inoculum was degassed for two weeks under mesophilic condition $30\,^{\circ}$C until no gas production was recorded. The total solids (TS) and volatile solids (VS of TS) of the inoculum were 3.80 ±0.14 % and 78.29 ±0.12 %, respectively. FLO and KR were also collected from households of staff and the canteen at a Senior High School in Kumasi. FLO was mainly composed of rice, cassava, fufu, kenkey, yam, egg, fish, gari, beans, bread, banku, kontomire (cocoyam leaves) and some vegetable sauce.

KR, on the other hand, comprised of cassava peels, yam peels, cocoyam peels, plantain peels, lettuce residue, cucumber residue, tomato residue, carrot residue, garden eggs residue, avocado peels, banana peels, mango peels, orange peels, pineapple peels, onion peels, pawpaw peels and watermelon peels. FLO and KR were manually sorted to remove non-biodegradable fractions before the organic fractions were shredded into smaller pieces, blended and homogenized into a slurry to maintain a particle size below 3mm using a household food grinder and 3mm sieve. Samples were frozen at a temperature of $-20\,^{\circ}$C before use. The frozen samples were allowed to thaw at a temperature of $4\,^{\circ}$C and used within a day to prevent biological decomposition.

6.3.2 Feedstock Characterization

The physical and chemical compositions of the feedstocks (HE, FLO, and KR) were evaluated before and after digestion using standard procedure (APHA, 1998). The feedstocks were analyzed for pH, total solid (TS), volatile solid (VS), organic carbon content, total nitrogen content, hydrogen content, oxygen content, sulphur content, C/N ratio, chemical oxygen demand (COD), alkalinity and volatile fatty acids (VFA). pH was analyzed using a digital hanner H1 98136 pH meter. The total solid and volatile solid were analyzed employing APHA methods 2540 B and APHA method 2540 E respectively (APHA, 1998).

Total nitrogen was calculated using the Kjeldahl method (Bremner, 1965), and the total amount of sulfur was determined using the spectrophotometer method (Singh et al., 1999). Hydrogen was determined using titrimetric method (McLean, 1965) and organic carbon by Walkley – Black Wet Oxidation Method (Heanes, 1984; Nelson, 1982). The oxygen content was calculated as the positive difference between 100 and the sum of C, H, N, S, and ash content (AC) (Fajobi et al., 2022). The C:N ratios of the samples was calculated by dividing the measured value of C and N (Dahunsi et al., 2019; Anderson and Ingram, 1993).

6.3.3 Biochemical Methane Potential Test

A no-block, randomised ternary mixture experimental design with three variables serving as mixture components was adopted in this study to formulate the substrate mix from HE, FLO and KR. In 500 mL bottles with a working capacity of 300 mL, BMP tests of the different mixtures were carried out. 233 g of the inoculum and 7 g VS of a substrate combination were put into each bottle. A 1:1 inoculum to substrate ratio (ISR) (VS basis) was adhered to. In total, 18 BMP runs (16 runs with the substrate mixtures, one with the inoculum-only control and one run with a positive control of pure cellulose) were carried out in triplicates making 54 trials. The BMP bottles were tightly sealed, incubated at $30\,^{\circ}\mathrm{C}$ and manually shaked intermittently for 60 days, and biogas production and composition were periodically monitored. The generated biogas was collected in gas bags and measured through downward water displacement

technique using an inverted glass chamber of 1000 mL capacity (Filer et al., 2019). The measured biogas was corrected to standard conditions of $0\,^{\circ}$C and 1 atm. Biogas composition was also determined with a portable Biogas 5000, Geotech UK) analyzer.

6.3.4 Kinetics of Methane Production

Five kinetic models i.e., the modified gompertz model, the logistic function models, cone model, fitzhugh model and monod model were selected to fit the methane production obtained from the experimental data. The experimental cumulative methane yield data were used to predict kinetic parameters by employing the least squares fitting method (non-linear regression approach) with the aid of the solver function in MS Excel ToolPak (Dinh et al., 2018). The equations for the various kinetic models used in this study are presented in the subsections below.

6.3.4.1 Modified Gompertz Model

The modified Gompertz equation can be presented as shown in Equation 6.1 (Budiyono and Sumardiono, 2014; Yusuf et al., 2011).

$$Y = Aexp(-exp[\frac{R_m e}{A}(\lambda - t) + 1]) \tag{6.1}$$

where *Y* is the cumulative methane yield at any time, t ($mlCH_4/gVS$), *A* is the simulated maximum methane yield ($mlCH_4/gVS$), R_m is the maximum methane production rate ($mlCH_4/gVS/day$), *e* is Euler's function with a value of 2.718282, λ is the lag phase for methane production (day) and *t* is the time in (day).

6.3.4.2 Logistic Function Model

The logistic kinetic model equation is shown in Equation 6.2.

$$Y = (\frac{A}{1 + exp[4R_m\frac{\lambda - t}{A} + 2]}) \tag{6.2}$$

where *Y* is the cumulative methane yield at any time, t ($mlCH_4/gVS$), *A* is the simulated maximum methane yield ($mlCH_4/gVS$), R_m is the maximum methane production rate ($mlCH_4/gVS/day$) and λ is the lag phase for methane production (day).

6.3.4.3 Cone Model

The cone model described by Bedoić et al. (2020) and Ma et al. (2019b) is shown in Equation 6.3.

$$Y = (\frac{A}{1 + (k \times t)^{-n}}) \tag{6.3}$$

where *Y* is the cumulative methane yield at any time, t ($mlCH_4/gVS$), *A* is the simulated maximum methane yield ($mlCH_4/gVS$), *k* is the rate constant and *n* is the dimensionless shape factor.

6.3.4.4 Fitzhugh Model

Pitt et al. (1999) applied the Fitzhugh kinetic model using Equation 6.4.

$$Y = A(1 - exp(-kt)^n) \tag{6.4}$$

where *Y* is the cumulative methane yield at any time, t ($mlCH_4/gVS$), *A* is the simulated maximum methane yield ($mlCH_4/gVS$), *k* is the rate constant and *n* is the dimensionless shape factor.

6.3.4.5 Monod Model

Lawrence and McCarty (1969) applied the monod model using Equation 6.5.

$$Y = A \times (\frac{k \times t}{1 + (k \times t)}) \tag{6.5}$$

where *Y* is the cumulative methane yield at any time, t ($mlCH_4/gVS$), *A* is the simulated maximum methane yield ($mlCH_4/gVS$) and *k* is the rate constant.

6.3.5 Model Evaluation

Experimental validation was done for each kinetic model to make sure the expected methane yields matched the results of the experiments. Equations 6.6–6.12 provide statistical measures of the goodness of fit for the models, including the coefficient

of determination (R^2), adjusted (R^2), Akaike's information criterion *(AIC)* and error terms such as the mean square error *(MSE)*, root mean square error *(RMSE)*, standard error of prediction *(SEP)* and mean absolute error *(MAE)* as shown in Equations 6.6-6.12 (Venkateshkumar et al., 2020; El-Mashad, 2013).

$$R^2 = 1 - (\frac{\sum_{i=1}^{n}(P_i - (P_i)^{est})^2}{\sum_{i=1}^{n}(P_i)^{est} - P_{avg})^2}) \tag{6.6}$$

$$AdjustedR^2 = 1 - [(1 - R^2) \times (\frac{n-1}{n-N-1})] \tag{6.7}$$

$$MSE = 1/n \sum_{i=1}^{n}(P_i)^{est} - (P_i)^2 \tag{6.8}$$

$$RMSE = \sqrt{1/n \sum_{i=1}^{n}((P_i)^{est} - (P_i))^2} \tag{6.9}$$

$$SEP = (\frac{RMSE}{P_{avg}}) \times 100 \tag{6.10}$$

$$MAE = 1/n \sum_{i=1}^{n} |(P_i)^{est} - (P_i)| \tag{6.11}$$

$$AIC = nln(\frac{RSS}{n}) + 2(N+1) + \frac{2(N+1)(N+2)}{(n-N-2)} \tag{6.12}$$

where *n* is the number of data points, Pi^{est} is the estimated value, *Pi* is the experimental value, P_{avg} is the average experimental value, *N* is the number of model parameters and *RSS* is the residual sum of squares.

6.4 Results and Discussion

6.4.1 Feedstock Characteristics

Table 6.1 provides information about the properties of the feedstocks (HE, FLO, and KR) employed in this study. The TS concentrations for HE, FLO, and KR were 11.34 ± 0.14, 25.80 ± 0.32 and 9.44 ± 0.00 %, respectively, while their VS (of TS) contents were 82.81 ± 0.84, 83.99 ± 0.61 and 88.10 ± 0.37 %. According to Capson-Tojo et al. (2017) and Li et al. (2013), feedstocks with high VS and VS/TS values (Table 6.1) may contain organic materials that are highly biodegradable.

Table 6.1: Physicochemical Characteristics of Substrates (mean (standard deviation))

Parameter	HE	FLO	KR
TS (%)	11.34 (0.14)	25.80 (0.32)	9.44 (0.00)
VS (% TS)	82.81 (0.84)	83.99 (0.61)	88.10 (0.37)
VS/TS	0.83 (0.001)	0.84 (0.001)	0.88 (0.001)
pH	7.1 (0.1)	5.0 (0.1)	5.3(0.1)
C (%)	61.22 (0.02)	41.16 (0.01)	38.10 (0.01)
N (%)	7.32 (0.02)	1.26 (0.01)	1.30 (0.02)
H (%)	9.02 (0.02)	9.52 (0.01)	8.52 (0.01)
O (%)	12.25 (0.01)	45.66 (0.01)	43.72 (0.01)
S (%)	0.200 (0.00)	0.135 (0.00)	0.031 (0.00)
C/N	8.36 (0.01)	32.59 (0.13)	29.34 (0.44)

6.4.2 Kinetic Modeling

The optimal co-digestion ratio was found to be 78.8 % HE: 11.8 % FLO: 9.4 % KR, and the methane yield data for that ratio was fitted to five kinetic models to ascertian which model best fit the data based on the parameters and criteria given. The fitzhugh, modified gompertz, logistic, cone, and monod models were employed. Table 6.2 shows the kinetic parameters and their associated values for these models. Also, Table 6.3 displays the goodness of fit statistics of the models. The subsequent sections discuss the fit of the kinetic models based on the coefficient of determination (R^2), root mean square error (RMSE), Akaike information criterion (AIC), sum squared error (SSE)

and the difference between the measured and predicted methane values. This is because it is suitable to have a model with small error terms as well as R^2 and adjusted R^2 values approaching unity (Amenaghawon et al., 2021).

Table 6.2: Parameters for Kinetic Models

MODEL	PARAMETER	VALUE
Modified Gompertz	A $(mLCH_4/gVS)$	659.15
	Rm $(mlCH_4/gVS/d)$	38.31
	λ (d)	0.00
Fitzhugh	A $(mLCH_4/gVS)$	798.49
	k (1/d)	0.0916
	n	0.8214
Cone	A $(mLCH_4/gVS)$	979.09
	k (1/d)	0.0587
	n	0.9254
Logistic	A $(mLCH_4/gVS)$	648.02
	Rm $(mlCH_4/gVS/d)$	35.16
	λ (d)	0.1241
Monod	A $(mLCH_4/gVS)$	798.49
	k (1/d)	0.0916

Table 6.3: ANOVA Results for RSM Experiment

Parameter	Model				
	Modified Gompertz	Fitzhugh	Cone	Logistic	Monod
R_2	0.8725	0.9885	0.9909	0.8551	0.9748
Adj R_2	0.8704	0.9883	0.9908	0.8527	0.9743
MSE	4040.35	357.55	284.61	4788.54	2304.36
RMSE	63.56	18.91	16.87	69.20	48.00
SEP	11.45	3.36	2.99	12.64	8.98
MAE	56.49	16.58	14.96	61.40	36.64
AIC	515.26	367.35	353.43	525.63	478.72
Difference (%)	13.83	2.74	2.05	15.27	11.45
SSE	1.01	0.15	0.09	1.40	0.30

6.4.2.1 Fitzhugh Model

The Fitzhugh model is a modified version of the first order with the inclusion of the constant *"n"*. In this study, the Fitzhugh model estimated a rate constant, *k*, of 0.092 1/d and a biomethane yield of 798.49 $mlCH_4/gVS$ (Table 6.2), that is comparable to the value of 764.79 $mlCH_4/gVS$ from the experiment. *k* and *n* values were validated in an earlier study for *k* less than 0.30 and *"n"* less than 4.81 (El-Mashad, 2013). The Fitzhugh model predicted an *"n"* value of 0.8214 which lies within the range reported in literature. The model had reasonably small error values and an R^2 value of 0.989.

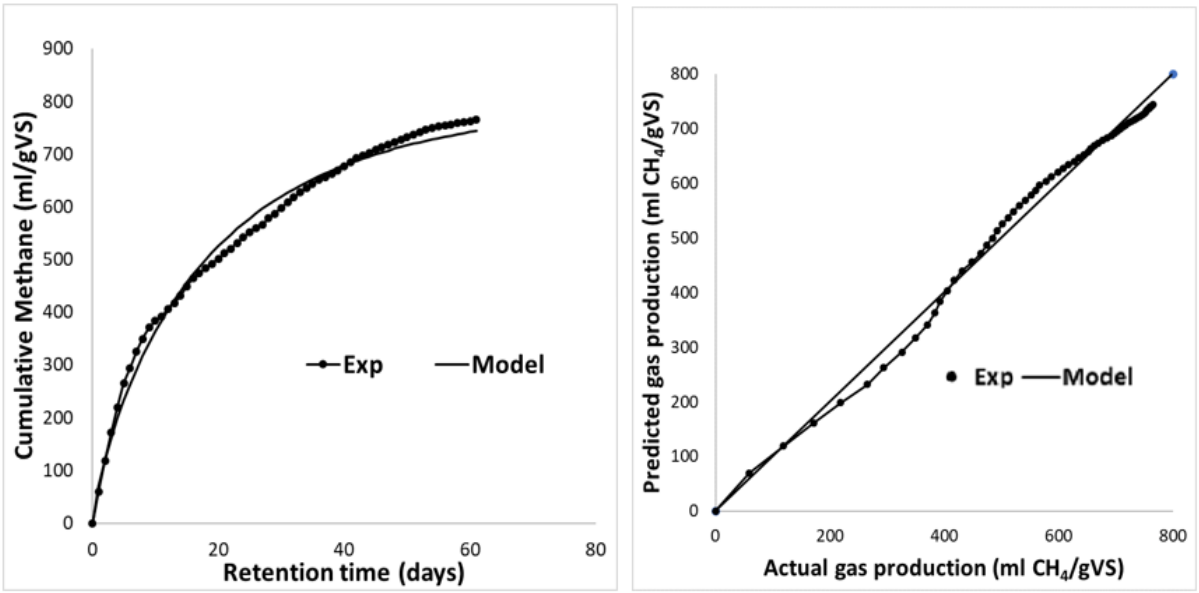

Figure 6.1: Comparison of measured and projected biomethane yield (a) time trajectory for fitzhugh model (b) parity plot for the fitzhugh model

R^2 values for the fitzhugh kinetic model ranged from 0.738 to 0.992, according to an earlier study by Cai et al. (2019). Figure 6.1 displays the results of the non-linear fitting of experimental methane yield values to the Fitzhugh model. Figure 6.1a displays the methane yield from the actual experiment and the predicted methane yields of the fitzhugh kinetic model. The extremely remarkable closeness of the experimental and predicted methane production data indicated a strong correlation between the two data sets.

Similar findings were recorded regarding the parity plot in Figure 6.1 b, where the majority of the data points are located along the slope line. All the data points in Fig. 6.1 b should cluster around the $45\,^{\circ}$C-line, demonstrating a perfect agreement between the experimental and model predictions, in the ideal scenario of a perfect fit. This further confirms that the Fitzhugh model recorded a high R^2 value (0.989) relative to the other models (Table 6.3). The Fitzhugh data performed well as evidenced by the fit and correlation for both the time trajectory (Fig. 6.1a) and the parity plot (Fig. 6.1b). Additionally, the Fitzhugh model fits well based on the relatively small difference (2.74 $\%$) between predicted and measured methane values.

6.4.2.2 Logistic Model

More advanced kinetic models are employed to investigate the duration of the lag phase during the anaerobic digestion process. The logistic model is one such model used to describe a time-dependent process (Lim et al., 2022). The logistic model predicted λ of 0.12 d^{-1}, *A* of 648.02 $mlCH_4/gVS$ and ***Rm*** of 35.16 $mlCH_4/gVS/d$. The logistic model performed poorly relative to the fitzhugh model with a low R^2 (0.855) and high error values (Table 6.3). The findings of the logistic model non-linear fitting of the experimental methane yield values for the substrates under study are shown in Figure 6.2. Figure 6.2a displays the experimental and expected methane yields derived for the logistic models. The highly substantial variance in the data showed that experimental and forecasted methane production data did not correlate well. The parity plot of Fig. 6.2 b was noted with the same observation. Furthermore, the 15.27 $\%$ disparity between actual and anticipated methane values shows that the logistic model does not fit the data well.

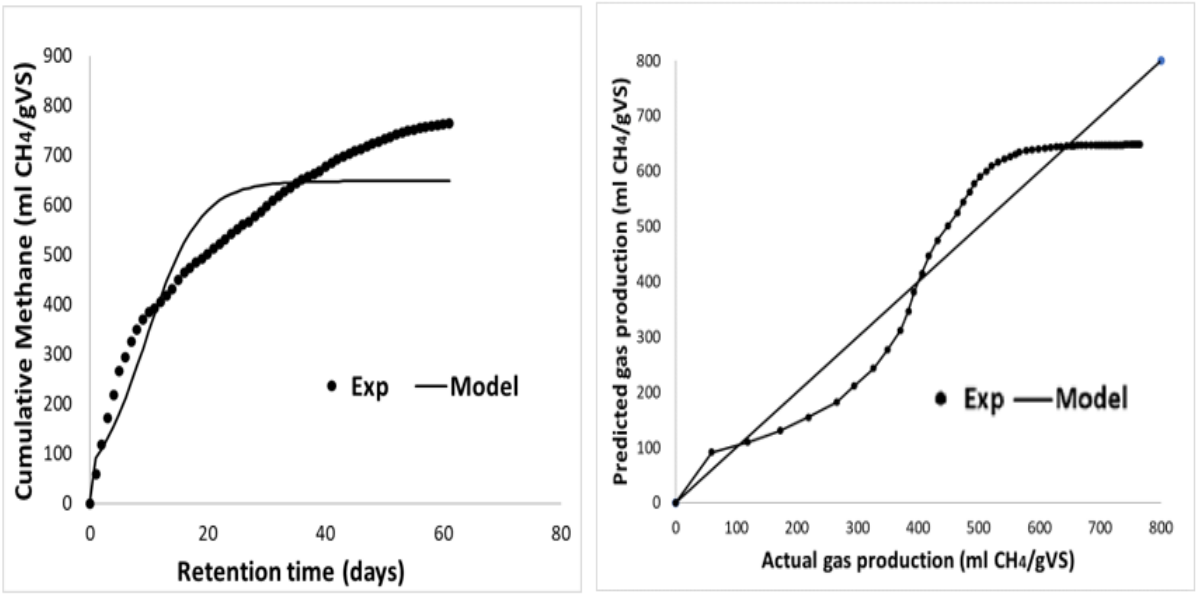

Figure 6.2: Comparison of measured and projected biomethane yield (a) time trajectory for logistic model (b) parity plot for the logistic model

6.4.2.3 Modified Gompertz model

In comparison to the methane yield from the experiment (764.79 $mlCH_4/gVS$,), the modified gompertz model estimated a lower methane yield ($659.15mlCH_4/gVS$). The results of the non-linear fitting of experimental methane yield values for substrates using the modified Gompertz model are shown in Figure 6.3. Figure 6.3a displays the observed experimental methane yield and the projected methane yields for the modified Gompertz model. The very considerable variance in the data revealed little correlation between observed and anticipated methane yield statistics. The same discovery was made about the parity plot in Figure 6.3 b. The modified Gompertz model also showed a poor fit for the experimental data, with a difference of 13.83 % between projected and measured methane concentrations. The lag phase is represented by the constant λ. In this study, the lag phase was 0.00 days based on the outcomes of the modified Gompertz model.

Usually, AD processes with less λ values show that the micro-organisms in the digester required minimal time for adaptation. When Deepanraj et al. (2015) used the modified Gompertz model to analyze the anaerobic digestion of food waste from a

hostel under mesophilic conditions, they discovered values in the range 0.1-1.0. Also, Cai et al. (2019) documented lag periods between 1.1 to 4.3 days when digesting vegetable wastes, whereas a lag phase of 2.7 to 4.2 days were reported by Gu et al. (2020) for the co-digestion of food waste and sewage sludge. The study's relatively short lag time indicates that the bacteria in the feedstocks could adapt quickly, allowing the AD process to start producing biogas. This confirms the finding that biogas generation started practically right away after the AD setup was done, possibly due to the use of cow dung as inoculum (fermentation already starts in the rumen of ruminants).

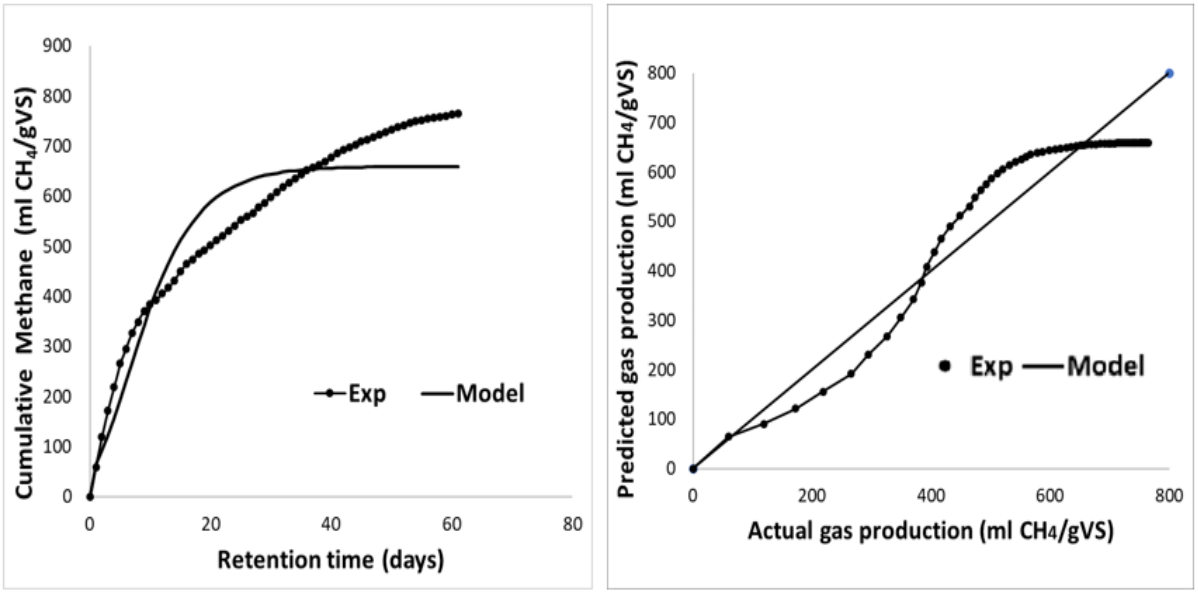

Figure 6.3: Comparison of measured and projected biomethane yield (a) time trajectory for modified Gompertz model (b) parity plot for the modified Gompertz model

Comparatively, the Rm (38.31 $mlCH_4/gVS/d$) value reported in this study for modified Gompertz was within the range that Orangun et al. (2021) reported for food waste and goat manure. Also, Andriamanohiarisoamanana et al. (2018) reported Rm values between 20 and 60 $mlCH_4/gVS/d$ for the co-digestion of dairy manure, crude glycerol, meat and bone meal. The Gompertz model in this study showed quite high error values and an R^2 of 0.873. (Table 6.3). Venkateshkumar et al. (2020) provided R^2 scores between 0.9022 and 0.9837. Because there was no lag period in the experimental data, the results from this study are ultimately lower and less impressive.

6.4.2.4 Monod Model

In comparison to the experimental value of 764.79 $mlCH_4/gVS$, the Monod model predicted a simulated biomethane yield of 798.49 $mlCH_4/gVS$ and a rate constant of 0.092 1/d. R^2 was 0.975 for the model, and error values were comparatively low (Table 6.3). Figure 6.4 shows the methane yields obtained experimentally and by prediction using the monod models. The almost exact alignment between the trends of the measured methane yields and model projections showed that the measured and projected methane production data were well correlated with a difference of 4.43 % between projected and measured methane concentrations (Figure 6.4a). The parity plot in Figure 6.4b also showed the same observation.

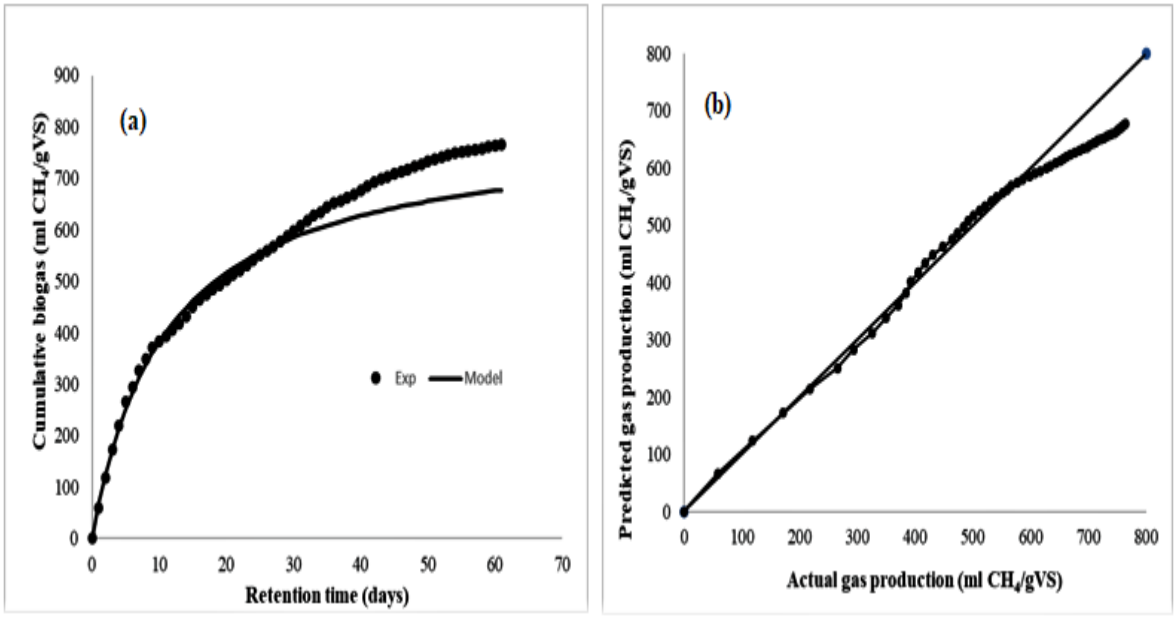

Figure 6.4: Comparison of measured and projected biomethane yield (a) time trajectory for the monod model (b) parity plot for the monod model

6.4.2.5 Cone Model

The biomethane yield (A = 979.09 $mlCH_4/gVS$) predicted by the cone model in this study was higher than what was seen in the experimental data (Table 6.2). Additionally, the model forecasted a "k" value of 0.059 1/d. In principle, a big k value indicates a quick rate of degradation. With the greatest R^2 value of 0.991, the cone model in this

investigation performed better than the other models. Venkateshkumar et al. (2020) reported R^2 values between 0.9622 and 0.9960, while between 0.9592 and 0.9929 were reported by Prajapati et al. (2018). For all the error terms used to analyze the models' accuracy, the cone model had the lowest value. The results of the non-linear fitting of experimental methane yield values for substrates using the cone model are shown in Figure 6.5.

Figure 6.5a displays the measured and projected methane yields for the cone model. The patterns of the measured methane yields and model projections almost perfectly fit each other, demonstrating that the cone model performed best (Figure 6.5a).

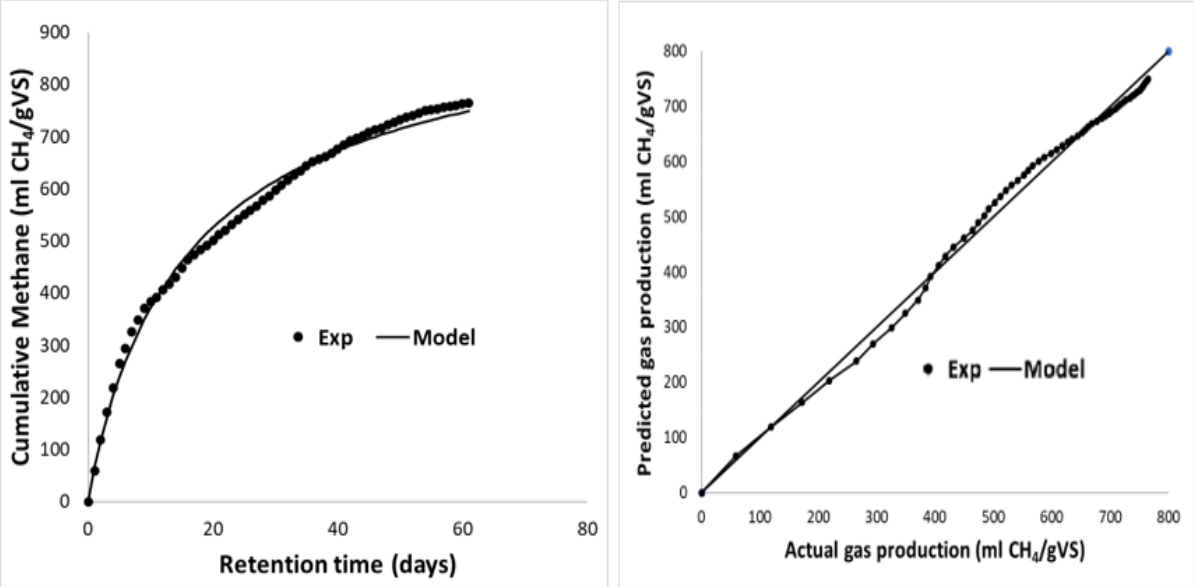

Figure 6.5: Comparison of measured and projected biomethane yield (a) time trajectory for the cone model (b) parity plot for the cone model

Additionally,the measured and projected methane yield results were all nearly aligned along the $45\,^{\circ}$C-line in the parity plot, demonstrating high agreement between the two data sets (Figure. 6.5 b). The fact that the highest R^2 value was obtained using the cone model lends further credence to this situation (Table 6.3). Consequently, the cone model provides a good fit with a difference of 2.05 % between predicted and measured methane values. Therefore, a tri-digestion of HE, FLO, and KR at a ratio of 78.8 % HE: 11.8 % FLO: 9.4 % KR was accurately predicted by the cone model. Both El-Mashad

(2013) and Karki et al. (2022) reported that the cone model had great predictive power.

6.5 Conclusion

All of the models had R^2 values that were generally high. However, the three models with the greatest fit for the methane yield data can be rated as Cone > Fitzhugh > Monod based on how low the AIC, RMSE, and SSE are. Consequently, the logistic and modified gompertz models were the least performing. Hence, the cone model can describe the anaerobic tri-digestion process of 78.8 % HE: 11.8 % FLO: 9.4 % KR with outstanding statistical indicators. Tri-digested HE, FLO and KR could therefore serve as suitable anaerobic digestion process for sustainable biogas production in households for the purposes of cooking.

CHAPTER 7

Optimization of Batch Anaerobic Co-Digestion of Human Excreta, Food Left-overs and Kitchen Residue using Biochar Additives.

7.1 Abstract

The treatment of biowaste using anaerobic digestion (AD) is prevalent, however it has drawbacks such as intermediate inhibition, system instability and low methane output. In this study, the effects of two different types of biochar (coconut shell, CCN and palm kernel shell, PKN) and three biochar dosages on the anaerobic co-digestion of human excreta (HE), foodleftovers (FLO) and kitchen residues (KR) were investigated using batch mesophilic experiments. The results showed differences in the peak occurrence times and methane yields with the biochar-amended treatments peaking earlier than the treatment without biochar. Also, the anaerobic co-digestion of HE, FLO and KR with CCN shell biochar had the highest cumulative methane yield (456.25 $mLCH_4/gVS$), followed by PKN shell biochar (410.11 $mLCH_4/gVS$). Further, the cumulative methane production increased when 3 g of CCN biochar was used depicting a 23.31 % increase compared to the control. However, too high biochar dosages of 6 g and 10 g CCN restricted methane production due to a potential stress on the anaerobic digestion process brought on by the accumulation of potential H_2 competitors. On the other hand, the cumulative methane yield was equivalent to that of the control when 3 g of PKN shell biochar was added to the substrate mixture. However, the use of 6 g of PKN shell biochar resulted in a 10.83 % rise in cumulative methane yield whereas PKN10g saw a decline in cumulative methane output compared to the control. The observed results suggest that a greater digestive efficiency may not necessarily follow from adding more biochar.

7.2 Introduction

Anaerobic co-digestion is a technology that can be used to process organic waste streams and produce renewable energy sources like biogas (Song et al., 2018). The process entails the breaking down of organic material in the absence of oxygen, generating methane-rich biogas. The low digestibility and low stability of some feedstocks, as well as the inhibition brought on by the buildup of volatile fatty acids (VFAs) and ammonia, do, however, frequently limit the process (Shen et al., 2020; Chen et al., 2008). Biochar, a carbon-rich and charcoal-like material (Tan et al., 2017), has been documented to improve anaerobic digestion by fostering microbial colonization, adsorbing inhibitory substances such heavy metals, organic compounds, and ammonia, and increasing the physical qualities of digestate (Li et al., 2019a; Zhang et al., 2018b; Fagbohungbe et al., 2017).

The adoption of biochar additives in AD systems has drawn much attention due to its potential of increasing the stability and effectiveness of the AD process (Pan et al., 2019; Cha et al., 2016). The properties and efficiency of biochar depend on the kind of biomass used, the pyrolysis conditions, and any post-processing procedures applied, like chemical or nutrient impregnation (Ruan et al., 2019; Tripathi et al., 2016). The high pore volume and surface area of biochar allow for the development of a diversified microbial population that can contribute to the breaking down of complex organic compounds (Li et al., 2020b; Arif et al., 2018). Furthermore, biochar addition has been shown to reduce the risk of acidification, by increasing the pH and buffer capacity of the anaerobic digestion process (Wang et al., 2017b).

Several researchers have explored the effects of biochar addition on the efficiency of anaerobic co-digestion systems (Shen et al., 2020; Pan et al., 2019). However, the ideal conditions for biochar addition in anaerobic co-digestion systems, such as the type and quantity of biochar, the characteristics of the feedstock, and the operational parameters, are still poorly understood and need further research. (Luz et al., 2018; Fagbohungbe et al., 2017). While some studies have reported positive effects of biochar on biogas production, methane content, and process stability, others have found no significant improvement or even negative effects.

Shen et al. (2020) found that adding peanut shell biochar to the co-digestion of food waste increased the methane yield and decreased ammonia inhibition, whereas Wang et al. (2022) discovered that adding bamboo, rice husk, and pecan shell biochar to the dry co-digestion of food waste and pig manure had no significant impact on the peak methane production rate. Hence, additional research is required to clarify the mechanisms underlying the interactions between biochar and anaerobic microorganisms and the optimal conditions for biochar addition in co-digestion systems.

Using coconut shells (CCN) and palm kernel shells (PKN), a typical agricultural wastes generated in several parts of Ghana, this study aims to produce and evaluate the effectiveness of low-cost coconut and palm kernel shell biochar additives and their optimal dosage on the anaerobic digestion of 78.8 % human excreta (HE), 11.8 % food leftovers (FLO) and 9.4 % kitchen residue (KR) to enhance biogas production. Although various carbon additives have been utilised in anaerobic digestion, this study is the first to introduce biochar additives to the mixture of feedstocks comprising almost all the organic waste generated in households.

7.3 Materials and Methods

7.3.1 Origin and Properties of Feedstock and Inoculum

The substrates used in this study are Human excreta (HE), Food leftovers (FLO) and Kitchen residue (KR) at a ratio of 78.8 % HE:11.8 % FLO:9.4 % KR. Fresh HE was collected from a KVIP at Ayeduase, a suburb of Kumasi, Ghana. FLO and KR were also collected from households of staff and the canteen of a Senior High School in Kumasi. FLO was mainly composed of rice, cassava, fufu, kenkey, yam, egg, fish, gari, beans, bread, banku, kontomire (cocoyam leaves) and some vegetable sauce which are very common foods eaten in most houses in Ghana. KR, on the other hand, comprised of cassava peels, yam peels, cocoyam peels, plantain peels, lettuce residue, cucumber residue, tomato residue, carrot residue, garden eggs residue, avocado peels, banana peels, mango peels, orange peels, pineapple peels, onion peels, pawpaw peels and watermelon peels.

FLO and KR were manually sorted to remove non-biodegradable fractions like polyethene bags before organic fractions were shredded into smaller pieces, blended and homogenized into a slurry to maintain a particle size below 3 mm using a household food grinder and 3 mm sieve. Samples were frozen at a temperature of $-20\,^{\circ}$C before use. The frozen samples were allowed to thaw at a temperature of $4\,^{\circ}$C and used within a day to prevent biological decomposition. Fresh CD was collected from the animal farm of the Department of Agriculture, KNUST. Anaerobically mono-digested cow dung with a chemical oxygen demand (COD) of 183.01±0.01 g/L, pH of 7.72±0.01 and alkalinity of 8075 mg/L was used as inoculum. The inoculum was degassed for two weeks under mesophilic condition ($30\,^{\circ}$C) until no gas production prior to use,. The total solids (TS) and volatile solids (VS) of the inoculum were 3.25±0.09 % and 71.28±0.84 %, respectively.

7.3.2 Feedstock and Inoculum Characterization

The physical and chemical compositions of the feedstocks were evaluated before and after digestion using standard procedure (APHA, 1998). The feedstock were analyzed for pH, total solid (TS), volatile solid (VS), organic carbon content, total nitrogen content, hydrogen content, oxygen content, sulphur content, C/N ratio, alkalinity and volatile fatty acids (VFA). The pH was analyzed using a digital hanner H1 98136 pH meter. The TS and VS were analyzed using APHA methods 2540 B and APHA method 2540 E, respectively (APHA, 1998).

Total nitrogen was calculated following the Kjeldahl method (Bremner, 1965), and the total amount of sulfur was determined using the spectrophotometer method (Singh et al., 1999). Hydrogen was determined using titrimetric method (McLean, 1965) and organic carbon by Walkley – Black Wet Oxidation Method (Heanes, 1984; Nelson, 1982). The oxygen content was calculated as the positive difference between 100 and the sum of C, H, N, S, and ash content (AC) (Fajobi et al., 2022). The C/N ratios of the samples was calculated by dividing the measured value of C and N (Dahunsi et al., 2019; Anderson and Ingram, 1993). Also, the alkalinity was determined according to the APHA method 2320B using Potentiometric titration (APHA, 1998). VFA was determined titrimetrically (Singh et al., 2021a, 2019a,b).

7.3.3 Biochar Preparation

The coconut shells (Figure 7.1a) and oil palm kennels (Figure 7.1b) were collected from the markets within the Kumasi Central Business District.

Figure 7.1: (a) Washed and crushed coconut shell (b) Washed and crushed oil palm kennel shell

Figure 7.2: (a) Coconut shell biochar (b) Oil palm kennel shell biochar

The crushed and washed biomass samples were incubated at 105 °C for 24 h to dry. The samples were put in crucibles, covered and put in the furnace and slowly pyrolysed to 600 °C for two hours at a heating rate of 5 °C/min. This was done in the absence of air. Subsequently, the biochar samples (Figures 7.2a and 7.2b) were milled, sieved

to separate out sizes of less than 600 μg diameter and then transferred to an air-tight sealed jar until needed. The biochar samples of size less than 600 μg at dosing amounts of 3, 6 and 10 g were utilized for the experiment.

7.3.4 Biochar Characterization

X-ray Diffraction (XRD) techniques described by Khan et al. (2020) and Chauhan and Chauhan (2014) were used to elucidate the crystalline nature of the biochar samples. XRD patterns of biochar were obtained on a powder X-ray diffractometer Model, Philips, with $CuK\alpha$ radiation having a scanning speed of $0.04\,°$/s. The scattering of X-rays from atoms produced a diffraction pattern that contained information about the atomic arrangement in crystal. Fourier Transform Infrared (FTIR) spectroscopy reported by Liu et al. (2015) was employed to investigate the structural features and molecular composition of biochar samples. All infrared spectra were collected with an FTIR Bruker Alpha spectrometer equipped with platinum attenuated total reflectance (ATR-FTIR, Bruker, Karlsruhe, Germany). The ATR-FTIR diamond crystal and all accessories were thoroughly cleaned with isopropanol between samples and background scans. The spectra was measured from 4000 cm^{-1} to 400 cm^{-1} with a scanning time of 32 s at a spectral resolution of 4 cm^{-1}. The spectra were obtained with the OPUS software (Bruker, Karlsruhe, Germany).

X-ray fluorescence (XRF) spectroscopy documented by Abdel-Fattah et al. (2015) was performed using a Rigaku NEX CG XRF to determine the elemental and oxide composition of the samples. Brunauer, Emmett and Teller (BET) surface analysis described by Abdel-Fattah et al. (2015) was carried out using a Nova 4200e surface area and pore analyzer (Quantachrome Instruments, USA). The pore volume and pore diameter were determined using the method of Barrett–Joyner–Halenda (BJH). The samples were degassed at $250\,°$C for 3 h prior to analysis. Nitrogen was used as the adsorptive gas at 77 K. Also, the pH of the biochar samples were measured by mixing 10 g of each sample to 100 ml of ionized water stirred at 170 rpm for 2 days at room temperature. The pH of the extractable water fraction of the biochar samples were 10.43 for CCN and 9.91 for PKN.

7.3.5 Theoretical BioMethane Potential (BMP_{TH})

The empirical relationship between the components of the feedstocks were determined using a modified Buswell equation by Boyle (1976), as shown in Equation 7.1.

$$C_aH_bO_cN_dS_e + (a - \frac{b}{4} - \frac{c}{2} + \frac{3d}{4} + \frac{e}{2}) \times H_2O \rightarrow (\frac{a}{2} - \frac{b}{8} + \frac{c}{4} + \frac{3d}{8} + \frac{e}{4}) \times CO_2 + (\frac{a}{2} + \frac{b}{8} - \frac{c}{4} - \frac{3d}{8} - \frac{e}{4}) \times CH_4 + d \times NH_3 + e \times H_2S \tag{7.1}$$

The theoretical methane yield was estimated using Equation 7.2 (Scherer et al., 2021; Steffen et al., 2016; Fagbohungbe et al., 2015; Raposo et al., 2013).

$$BMP_{TH} = (\frac{(\frac{a}{2} + \frac{b}{8} - \frac{c}{4} - \frac{3d}{8} - \frac{e}{4}) \times 22400}{12a + b + 16c + 14d + 32e}) \tag{7.2}$$

7.3.6 Anaerobic Digestion Set-up and Biogas Sampling

The AD experiments were performed adhering to the well-known biochemical methane potential test using a completely randomized block design. Human excreta (HE), food leftovers (FLO) and kitchen residue (KR) at a ratio of 78.8 % HE: 11.8 % FLO: 9.4 % KR (wet weight), identified from our previous studies (Chapter 5) was used as the feedstock mixture for this study. The inoculum to substrate ratio (ISR) on VS basis was 1. The experiments were conducted using 500 ml bottles (320 ml (60 %) of working volume and 180 ml of headspace) and eight different treatments with three replications. Each bottle was filled with 248 g of inoculum and 7 gVS of the feedstock mixture. For biochar-amended co-digestion systems, 3,6 or 10 g of each biochar type was added to the different treatment bottles. Dosage was decided based on the optimization experiments performed on similar systems by Flores (2020) and Jang et al. (2018).

The experimental sets are labelled as PC, SM, CCN3g, CCN6g, CCN10g, PKN3g, PKN6g and PKN10g where PC is the positive control (pure cellulose) and SM is the control; the substrate mix with no biochar addition (Table 7.1). CCN and PKN represents the biochar type and the number after CCN and PKN represents the amount (g) of biochar used. A blank of only inoculum was also run. The BMP bottles were tightly sealed, incubated at $30\,^{\circ}$C and manually shaken daily for 62 days. Biogas production and composition were monitored daily. The generated biogas was collected in gas bags and measured through downward water displacement technique using an inverted glass chamber of 1000 mL capacity (Filer et al., 2019). The measured biogas was corrected to standard conditions of $0\,^{\circ}$C and 1 atm. Biogas composition was also determined with a portable Biogas 5000, Geotech UK) analyzer.

Table 7.1: Batch experimental conditions with different biochar types.

	Mix Ratios(78.8% HE:11.8%FLO:9.4%KR)				Biochar Types	
Treatment	Inoculum (g)	HE (g)	FLO (g)	KR (g)	CCN (g)	PKN (g)
SM(no biochar)	248	60	4	8	0	0
CCN3	248	60	4	8	3	0
CCN6	248	60	4	8	6	0
CCN10	248	60	4	8	10	0
PKN3	248	60	4	8	0	3
PKN6	248	60	4	8	0	6
PKN10	248	60	4	8	0	10

7.3.7 Methane-Production Determination

Daily CH_4 production was calculated using the daily total biogas volume (T_{biogas}) collected and the percentage composition of CH_4 determined ($\%\ CH_4$). The daily CH_4 production of each treatment was further calibrated by subtracting the daily CH_4 production from the digesters with inoculant only ($T_{inoculant}$); this excluded any residual CH_4 production from the inoculant. Methane production was recorded as cumulative CH_4 production, in ml/gVS, over 62 days. Equation 7.3 shows the daily CH_4 measurements

$$Daily\ CH_4 = (T_{biogas} \times \%CH_4) - (T_{inoculant} \times \%CH_4) \quad (7.3)$$

7.3.8 Biodegradability (BD)

The extent of anaerobic biodegradability, BD, was calculated by dividing experimental methane yield (BMP_{exp}) by the theoretical methane potential (BMP_o) according to the Equation 7.4 (Wang et al., 2014a).

$$BD(\%) = (\frac{BMP_{exp}}{BMP_o}) \times 100 \quad (7.4)$$

7.3.9 Statistical Analysis

Samples were analysed in triplicates and reported as the mean value ± standard deviation (SD) in results and discussion. One-way analysis of variance (ANOVA) was then used to test the biochar types and dosages on mean methane composition. Also, Tukey's honestly significant difference (HSD) test was used for the pairwise comparison of the mean biomethane composition obtained during co-digestion using Minitab v.19 software. $p < 0.05$ was used as threshold for statistical significance.

7.4 Results and Discussion

7.4.1 Feedstock Characteristics

The properties of the feedstocks (HE, FLO, and KR) employed in this study are shown in Table 7.2. The TS concentrations for HE, FLO, and KR were 9.81 ± 0.10, 26.10 ± 0.22 and 9.48 ± 0.10 %, respectively, while the VS contents were 88.46 ± 1.04, 94.57 ± 0.09 and 90.51 ± 1.91 %. The TS value reported in this study for FLO is within the range of 18.1–37.8 % documented in literature (Dhamodharan et al., 2015; Zhang et al., 2014; Uncu and Cekmecelioglu, 2011; Wang and Zhao, 2009; Ohkouchi and Inoue, 2006). Also, the TS content of KR in this study (9.48 %) was as low as the value of 12.23 % reported by Li et al. (2020a) due to the high moisture content of kitchen residues like fruit and vegetable waste. Literature reports TS values of HE ranging from 14 % to 37 %, which is higher than the value (9.81 %) obtained in this

study (Singh et al., 2021b; Miller et al., 2015; Rose et al., 2015; Wignarajah et al., 2006)

Moreover, VS values in this study are close to the literature reported values of 81.0 % for HE (Singh et al., 2021b), 90.7-91.9 % for FLO (Pax et al., 2020; Paritosh et al., 2017; El-Mashad and Zhang, 2010) and 85.94 % for KR (Li et al., 2020a). While the pH values of FLO (5.26 ± 0.01) and KR (5.53 ± 0.01) were in the acidic range, that of HE (7.23 ± 0.01) was alkaline. The C/N ratios for FLO (32.43±0.06) and KR (32.65±0.24) were within the range of 9 to 50 documented by Guarino et al. (2016) whereas the C/N ratio for HE (8.47±0.01) was close to the lower threshold of the range. The properties of HE, FLO and KR as well as their suitability for household biogas production has been discussed in detail in previous studies (Appiagyei Osei-Owusu et al., 2023).

Table 7.2: Physicochemical Characteristics of Feedstocks (mean (standard deviation); n=3)

Parameter	HE	FLO	KR
TS (%)	9.81 (0.10)	26.10 (0.22)	9.48 (0.10)
VS (% TS)	88.46 (1.04)	94.57 (0.09)	90.51 (1.91)
VS/TS	0.88 (0.001)	0.95 (0.001)	0.91 (0.001)
COD (g/L)	79.26 (0.01)	114.55 (0.03)	118.26(0.01)
pH	7.23 (0.01)	5.26 (0.01)	5.53(0.01)
C (%)	63.01 (0.02)	48.21 (0.01)	4377.10 (0.01)
N (%)	7.44 (0.01)	1.49 (0.01)	1.34 (0.01)
H (%)	9.34 (0.03)	8.92 (0.01)	9.33 (0.01)
O (%)	10.14 (0.01)	34.90 (0.06)	41.36 (0.01)
S (%)	0.21 (0.00)	0.02 (0.00)	0.05 (0.00)
C/N	8.47 (0.01)	32.43 (0.06)	32.65 (0.24)

7.4.2 Biochar Characteristics

7.4.2.1 X-ray fluorescence (XRF)

XRF identified the presence and proportions of elements and oxides in the CCN and PKN biochar samples as shown in Table 7.3 (Details in Appendix A2) before usage

in the batch anaerobic co-digestion test. The main elemental constituents of the PKN biochar were silicon (Si), aluminium (Al), calcium (Ca) and potassium (K) while the main elemental constituents of CCN biochar were sodium (Na) and potassium (K) (Table 7.3). For CCN biochar, Na was the highest component while the highest for PKN was Si. Notably, both additives contained trace elements such as iron (Fe), nickel (Ni), zinc (Zn), chromium (Cr) and copper (Cu) in concentrations less than 1 %.

Previous studies have reported the presence of similar elements (Si, Al, Ca, Mg, Fe, Mn, P and S) when PKN and CCN were pyrolyzed (IkhtiarBakti and Gareso, 2018; Wang et al., 2014b; Werther et al., 2000). The characteristics exhibited by the macro and micro nutrients in CCN and PKN biochar samples with regards to their influence on microorganisms are very essential for the stability of the anaerobic co-digestion process. Ca is critical for the formation of microbial aggregates and a key component for the growth of some methanogens (Murray and Zinder, 1985). Fe, Zn and Ni are also required for hydrogenase activity (Choong et al., 2016; Romero-Güiza et al., 2016; Kida et al., 2001).

Table 7.3: Percentage Chemical Composition of CCN and PKN from XRF Analyses

Elemental			Oxides		
ID	Composition of CCN (%)	Composition of PKN (%)	ID	Composition of CCN (%)	Composition of PKN (%)
Fe	0.06	0.10	Fe_2O_3	1.25	4.32
Zn	0.001	0.002	ZnO	0.04	0.09
Ni	0.001	0.001	NiO	0.02	0.02
Co	0.0000	0.0001	Co_2O_3	0.01	0.01
Cr	0.01	0.01	Cr_2O_3	1.16	0.23
Cu	0.01	0.01	CuO	0.20	0.22
Mn	0.01	0.01	MnO	0.15	0.35
Si	0.16	3.74	SiO_2	19.00	65.20
Ca	0.08	0.27	CaO	7.87	8.35
Na	2.59	0.00	SrO	0.03	0.10
K	1.15	0.44	K_2O	36.75	9.36
P	0.01	0.03	P_2O_5	6.47	0.00
Cl	0.11	0.01	TiO_2	0.15	0.26
S	0.05	0.06	SO_3	9.26	2.08
Al	0.06	0.57	Al_2O_3	5.64	5.49
Mg	0.14	0.29	MgO	7.72	0.00

In addition, Fe is a key component for methane monooxygenase and nitrogenase (Schindelin et al., 1997). Also, cobalt (Co) is an essential cofactor in numerous enzymatic reactions involved in the biochemistry of methane formation (Garuti et al., 2018; Romero-Güiza et al., 2016; Choong et al., 2016). Even though these macro and micro nutrients have been shown to improve biogas production, their presence in excess could inhibit the AD process (Atasoy et al., 2020).

Table 7.3 further presents silicon dioxide (silica, SiO_2), potassium oxide (K_2O), calcium oxide (CaO), aluminium oxide (alumina, Al_2O_3) and Iron(III) oxide (Fe_2O_3) as the main oxides found in PKN biochar. Similarly, Kareem et al. (2018) documented predominant proportion of SiO_2 (81.75 %) followed by CaO (2.67 %), K_2O (2.01 %), Al_2O_3 (1.63 %), MgO (0.25 %) and Fe_2O_3 (0.17 %) for PKN biochar. The high silica and alumina contents may imply potential pozzolamic property which reveals why ash generated from PKN has been studied as potential replacement for cement

(Uchegbulam et al., 2022). According to Ezema and Aigbodion (2020), the high Si and Al in PKN biochar has also proven to improve its corrosion resistance. Similar to what is reported in Ahmad et al. (2022) and Ajien et al. (2023), the CCN biochar in this study had potassium oxide ((K_2O), silicon dioxide (SiO_2), calcium oxide (CaO), sulphur trioxide (SO_3) and Phosphorus pentoxide (P_2O_5) as the main oxides constituents.

7.4.2.2 Brunauer, Emmett and Teller (BET)

The CCN and PKN biochar samples were characterized by surface areas, pore volumes and pore diameters of 238.73 m^2/g and 382.79 m^2/g, 0.12 cm^3/g and 0.19 cm^3/g and 2.45 nm and 2.01 nm respectively. Notably, PKN had the highest surface area and pore volume among the two biochar types. Windeatt et al. (2014) reported a surface area and pore volume of 222.50 m^2/g and 0.15 cm^3/g respectively for CCN biochar pyrolised at a temperature of $600\,^{\circ}C$. The surface area of CCN biochar reported in this study is therefore higher. On the other hand, Kong et al. (2019) documented a surface area and pore volume range of 106-329 m^2/g and 0.01-0.31 cm^3/g respectively with the PKN biochar results from this study falling within range. According to Xie et al. (2022), the specific surface area, total pore volume and pore diameter of biochar are largely dependent on properties of the raw biomass and production conditions. For instance, biochar produced at a high temperatures has a larger surface and more micro and mesopores, making it more suitable for organic pollutants removal and adsorption.

The pore distribution and nitrogen isothermal adsorption graphs for CCN and PKN biochar samples are shown in Appendix (A3) . The graph of nitrogen isothermal adsorption can be compared to that of type (II) according to the IUPAC classification (Sing, 1985). Biochar with such classification has mesopores, an indication that abundant pores were formed in the biochar. A high biochar surface area and pore size distribution are essential for biofilm formation on the surface of the biochar; which further enhances microbial proliferation (Luz et al., 2018). Also, Type (II) isotherms represent unrestricted monolayer-multilayer adsorption (Rouquerol et al., 1994). When used in AD, biochar with a large surface area makes it easier to sequester undesired solutes such CO_2 and H_2S as well as ammonia and VFAs, aiding in situ biogas upgrading (Masebinu et al., 2019).

7.4.2.3 Fourier Transform Infrared (FTIR) Analysis

The FTIR spectra detailed peaks of the prevalent functional groups present in CCN and PKN biochar samples (Details in Appendix A4). The characteristic absorption bands in FTIR spectra detected the behaviour and performance of materials to a significant extent by profiling the chemical bonds as molecular fingerprints of the functional groups present. The FTIR spectra of CCN biochar were found at few major peaks of 2324.28, 2183.74, 1555.05 and 447.26 cm^{-1} (Figure 7.3). Also, PKN biochar showed few major peaks at 2079.14, 1555.39, 1024.13 and 436.98 cm^{-1} (Figure 7.3).

Uchegbulam et al. (2022) reported a similar trend of few peaks and functional groups for PKN biochar whereas raw PKN showed abundant peaks and functional groups. The author attributed the disappearance and shifts of most peaks in the biochar spectra to their chemical and thermal decomposition as well as intermolecular bond breakages during the activation or pyrolysis process. Therefore, the absence of most functional groups in the CCN and PKN biochar samples in this study indicate that the raw CCN and PKN biomasses are likely to be thermally unstable as their functional groups evaporate in the form of volatile molecules at elevated temperatures (Uchegbulam et al., 2022).

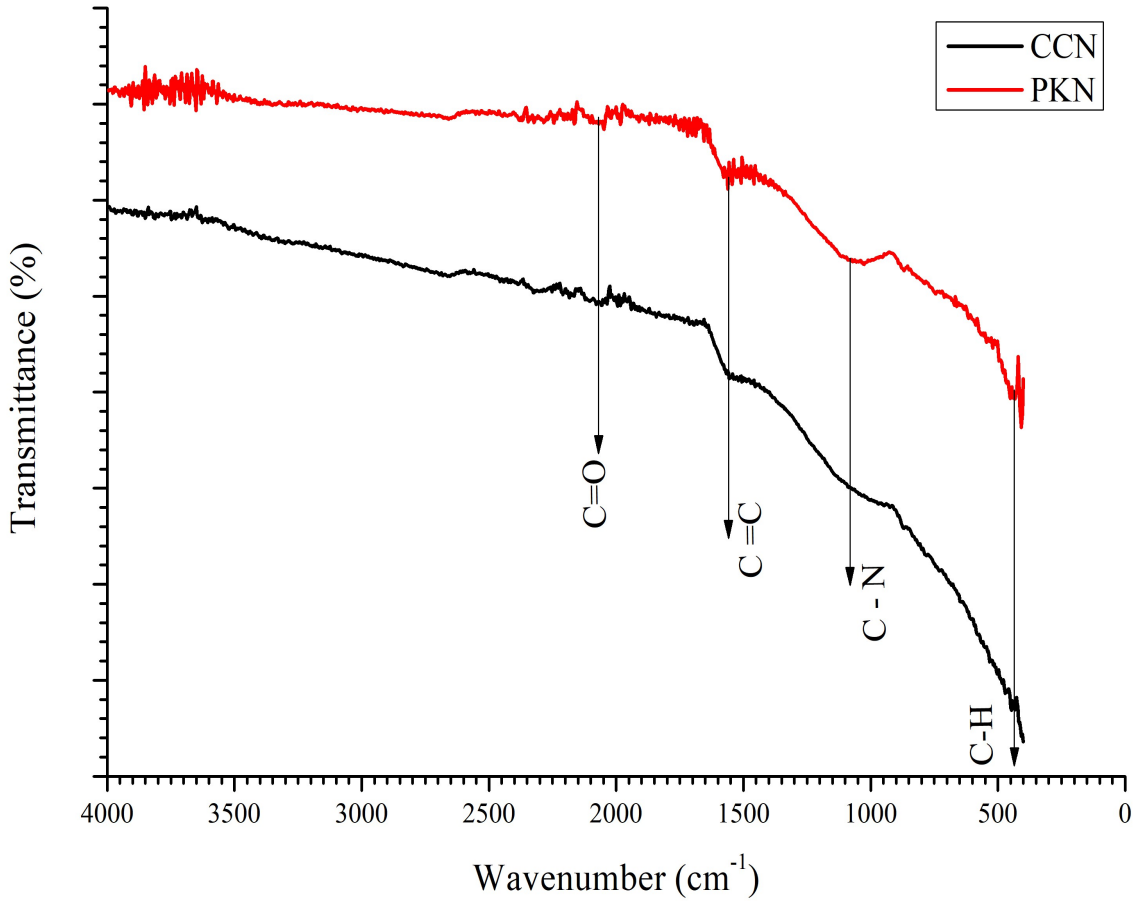

Figure 7.3: FTIR Spectra of CCN and PKN Biochar Samples

The appearance of peaks at 2079.14 and 2324.26 cm^{-1} are attributed to aromatic bands (Ihoeghian et al., 2023) while peaks at 1555.05 and 1555.39 cm^{-1} correspond to aromatic stretching vibrations of C=O and C=C (Byamba-Ochir et al., 2019; Freitas et al., 2019; Pallarés et al., 2018). The peak at 1024.13 cm^{-1} is attributed to C-O or C-N stretching (Li et al., 2019c) while the peaks at 436.98 and 447.26 cm^{-1} are attributed to a possible C-H bending. Qambrani et al. (2017) stated that CO= and CC= are main functional groups formed on the biochar surface under various conditions. Moreover, the functional groups, C=O, and C-O stretching vibration have the essential role of serving as absorbent of pollutants (Shu et al., 2017).

Further, biochar produced at a higher temperature has lower or no O/H mole ratio, indicating that the biochar surface is more aromatic and hydrophobic with high adsorb-

ing affinity to organic pollutants (Xie et al., 2022). Also, Manyà (2012) documented that the amount of carboxyl and acidic groups in biochar reduce as it is produced at severe pyrolysis conditions (increased process temperature). The reduction of the acid functional groups on the other hand leads to the increase of biochar pH.

7.4.2.4 X-ray Diffraction (XRD)

The compositional analysis of CCN and PKN biochar provides a background understanding of its chemical configuration (Details in Appendix A5). Figure 7.4 presents the phase data diagram obtained from the XRD analysis of CCN and PKN biochar samples. XRD patterns of PKN biochar showed the existence of carbon at peaks of 2θ = 23.4°, 27.5°, 38.7° and 61.1°, representing the amorphous nature of the biochar. This results was consistent with that of other studies (Jabarullah et al., 2021; Imoisili et al., 2020; Yeboah et al., 2020).

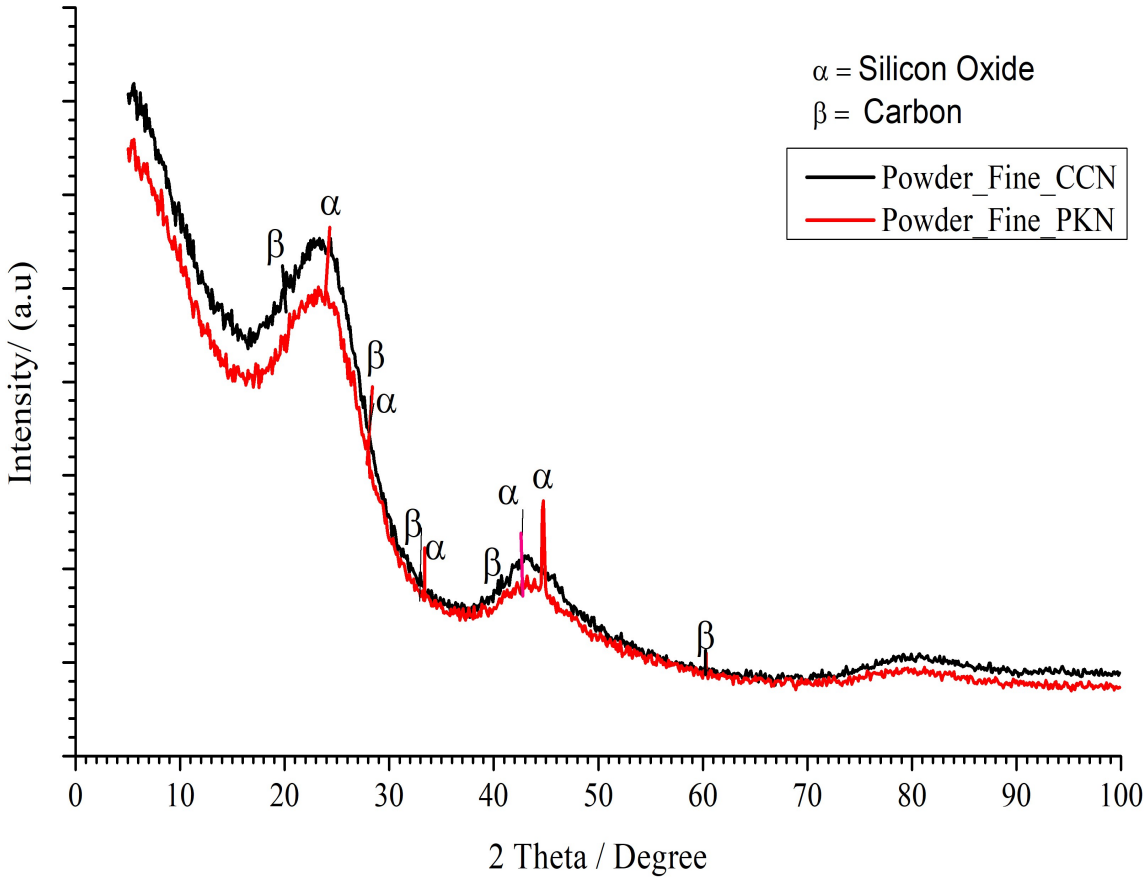

Figure 7.4: XRD Spectra of CCN and PKN Biochar Samples

Also, the PKN biochar showed some crystalline phases depicting the presence of silicon dioxide (SiO_2) at sharp peaks of 2θ equals 25.3°, 42.5° and 44.7° with 100 % intensity (Figure 7.4). According to Kareem et al. (2018), the strongest crystalline peak identified from PKN biochar XRD phase studies is SiO_2. Hence, the PKN biochar showed both amorphous and crystalline nature. The presence of broad peaks suggests an amorphous state, while crystalline materials are indicated by small sharp peaks (Ikubanni et al., 2020). According to Edmund et al. (2014), PKN is largely amorphous as its crystallinity is only 14.38 %, which is indicative of its high lignin and hemicellulose contents. While the amorphous nature of biochar enhances its adsorptive properties, its crystallinity contributes to its high surface area and buffering capability (Ihoeghian et al., 2023).

On the other hand, CCN biochar showed amorphous broad peaks at 2θ equals 26.5°, 42.2°, 44.5° and 62.1° indicating the presence of a carbonaceous material (Figure 7.4). According to IkhtiarBakti and Gareso (2018), CCN biochar results mostly succeed in becoming carbon with broad peaks showing amorphous trends. Also,other studies about CCN, have reported the presence of high carbon content material due to its high hardness, volatility and low ash content (Jain et al., 2015; Gratuito et al., 2008). Similarly, Shamsuddin et al. (2016) documented that synthesised carbons from coconut shells are mostly in the form of high amorphous state with low crystallinity.

In summary, the CCN and PKN biochar samples have unique characteristics such as large surface area, pore volume and diameter, high chemical composition as shown in the amount of trace elements present and high alkalinity. Comparatively, CCN biochar has high trace element content along with a higher alkalinity, whereas PKN biochar has a higher surface area with high trace element content.

7.4.3 Performances of Anaerobic Co-Digestion with Biochar Samples

7.4.3.1 Effects of Biochar Types on Methane Yield

The effectiveness of two different types of biochar (CCN and PKN) samples on anaerobic co-digestion of HE, FLO and KR was assessed over the course of a 62-day incubation period (Figure 7.5). All treatments showed two to three peaks at different occurrence times and persistent periods in the daily methane production time trajectory (Figure 7.5a). The daily methane yield (Figure 7.5a) recorded a rapid start-up of the anaerobic co-digestion process on the first day, ranging from 8.83 to 30.21 $mLCH_4/gVS$. On the other hand, Figure 7.5b shows that anaerobic co-digestion of HE, FLO and KR with CCN shell biochar had the highest cumulative methane yield (456.25 $mLCH_4/gVS$), followed by PKN shell biochar (410.11 $mLCH_4/gVS$).

Considering the difference of 10.11 % between cumulative methane yield of best performing CCN and PKN biochar samples and the favaourable characteristics of both biochar types, it could be said that both CCN and PKN biochar types have a high potential of being used in anaerobic digestion systems. Furthermore, the cumulative methane yield (370.03 $mLCH_4/gVS$) of the control (SM) was lower than the best performing CCN and PKN treatments. This could be attributed to the influence of biochar on alkalinity, micro-organism activity and trace element availability during the anaerobic digestion process. Similarly, other studies have reported that adding biochar to treatments increases the methane yield during anaerobic digestion in comparison to treatments without biochar (Shen et al., 2020; Jiang et al., 2018; Wang et al., 2018c; Shen et al., 2016).

Additionally, the experimental groups with biochar experienced higher daily methane yields that peaked earlier than that of the control group. PKN biochar reached its peak on the 1^{st} day of fermentation with a daily methane yield of 30.21 $mLCH_4/gVS$. This was followed by CCN biochar, which also reached its peak on the first day of fermentation but with a lower daily methane yield of 22.58 $mLCH_4/gVS$.

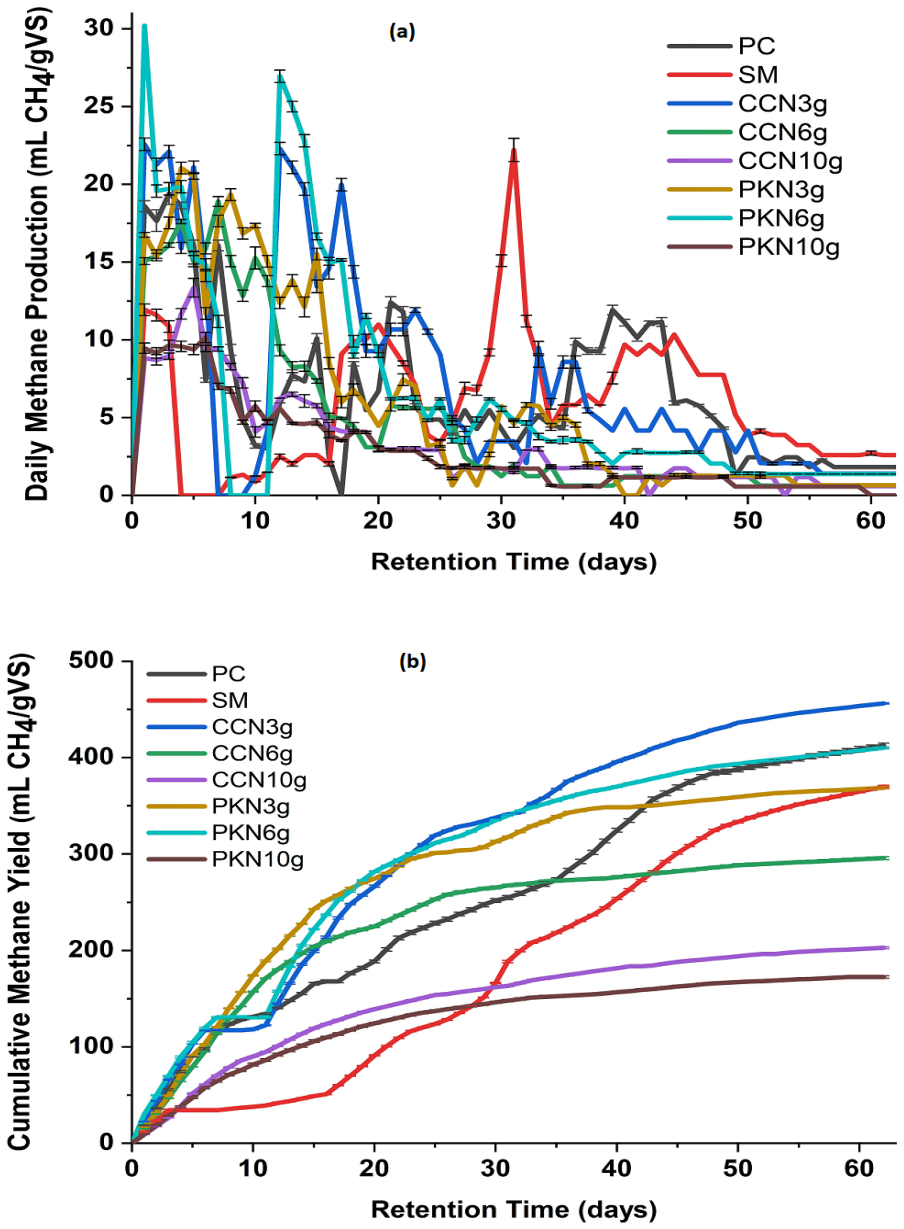

Figure 7.5: Methane yield of CCN and PKN biochar samples at different dosages; (a) Daily methane production and (b) Cumulative methane production (values are presented as mean ± SD with n=3)

Although PKN biochar had the highest methane yield peak, there was an abrupt lag phase from days 8 to 11 where no gas production was observed. As a result, the cumulative methane yields of CCN biochar (456.25 mLCH_4/gVS) eventually outperformed that of PKN biochar (410.11 mLCH_4/ gVS). Comparatively, On the 31^{st} day of fermentation, the control test, SM, reached its highest methane yield peak, with a maximum daily methane yield of 22.21 mLCH_4/gVS.

Further, the first peak window for daily methane yield was recorded between the 1^{st} and 7^{th} days of digestion. The quick hydrolysis and degradation of organics in HE, FLO, and KR might be the reason for this observation (Hou et al., 2020). However, following the 7^{th} day, the methane generation plateaued for most of the treatments until day 11, during which there was less or no methane measured. The decline of the methane production was most likely caused by a drop in system pH brought on by the rapid hydrolytic acidification conversion of feedstock to volatile fatty acids (VFAs), whose buildup might have prevented biogas synthesis (Lin et al., 2011).

The second peak window of the biochar-amended treatments observed an occurrence time between days 12 to 26. However, the control (SM) had a delayed first peak window from day 16 to 24. Due to a strong buffering support from the alkaline biochar, inhibitions caused by the early accumulation of VFAs might have been alleviated. Also, a high biochar surface area could have improved the growth and activity of methanogens resulting in the appearance of the second peak window (Wang et al., 2017b). Additionally, the stress from the inhibition after the first window could have been mitigated by the ability of the biochar additives to enhance microbial acid utilization efficiency, hence the second peak (Luo et al., 2015).

That notwithstanding, the treatments with biochar plateaued again on the 27^{th} to 33^{rd} days. Even though a decline in methane production was observed after the second peak, the treatments recorded a recovery in between the 34^{th} to 48^{th} day, depicting a third peak. The observation of the third peak could be as a result of the possible degradation of recalcitrant material like lignin in the KR feedstock which was not digested at the early stage of the fermentation process. Besides, the addition of biochar might have improved the degradation of complex substances by enhancing the recovery rate of the anaerobic bacteria as documented by Fagbohungbe et al. (2016). Eventually, methane production declined until end of experiment. Pan et al. (2019) documented a similar trend of methane production in the anaerobic digestion of chicken manure and biochar additives.

7.4.3.2 Effects of Biochar Dosage on Methane Yield

In addition to biochar types, biochar dose also affects how much AD is enhanced (Lonappan et al., 2018). Figure 7.6 illustrates impact of CCN biochar dosage on the effectiveness of anaerobic digestion.

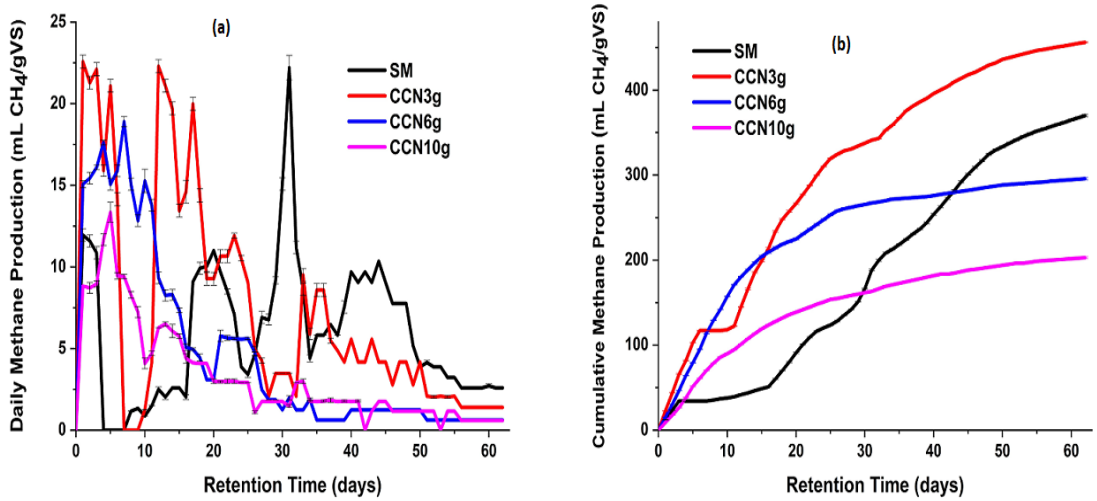

Figure 7.6: Methane yield of CCN samples at different dosages; (a) Daily methane production and (b) Cumulative methane production (values are presented as mean ± SD with n=3)

According to the findings, cumulative methane production first increased and subsequently dropped as CCN biochar dosage was raised. When 3 g of CCN biochar was added, the cumulative methane yield was 456.25 mL/gVS (Figure 7.6b). Comparatively, a 23.31 % increase in cumulative methane was observed for CCN3g as opposed to the control of cumulative methane yield of 370.03 mLCH_4/gVS ($p<0.001$). However, when the dosage of CCN biochar was raised to 6 g, the methane yield was unstable, depicting a sharp reduction of cumulative methane yield to 295.18 mLCH_4/gVS. In comparison to the control, CCN6g experienced a 20.21 % reduction ($p<0.001$) due to a potential stress on the anaerobic digestion process brought on by excess biochar addition.

Moreover, the anaerobic digestion process experienced a further reduction (45.20 %) in cumulative methane yields with an addition of 10 g of CCN biochar as compared with the control ($p=0.0002$). Hence, stabilizing the methane output and speeding up

the fermentation cycle were not made possible by adding too much CCN biochar. Even though treatment with CCN3g observed an intial increase in methane yield, too high biochar dosage restricted methane production. From the anaerobic digestion of food waste and fruit-wood biochar, a comparable outcome was attained (Cai et al., 2016; Shen et al., 2016; Luo et al., 2015).

Also, a similar trend was reported by Shen et al. (2020) when 2 % and 4 % straw biochar were used in the anaerobic digestion of straw and cow manure with 2 % performing well and 4 % inhibiting methane yields. According to Shao et al. (2019), potential H_2 competitors (e.g. *Hydrogenophaga*) of methanogens could clone onto excess biochar and weaken its DIET benefit for methanogenesis. This was observed throughout sequencing in previous studies when suspended microbes which cannot conduct DIET with biochar, were far more extensive than those attached to additives (Shao et al., 2019).

The amount of added PKN shell biochar displayed a distinct pattern than that of CCN shell biochar. The cumulative methane yield was 368.69 mLCH_4/gVS, similar to that of the control (SM=370.03 mLCH_4/gVS) with just a 0.36 % reduction ($p<0.001$) when 3 g of PKN shell biochar was added to the mixture of feedstocks. Figure 7.7 illustrates this result. Nonetheless, the cumulative methane yield increased to 410.11 mLCH_4/gVS when the dose of PKN shell biochar was increased to 6 g (Figure 7.7b), and the greatest daily methane yield of 30.21 (Figure 7.7a) was attained on the first day of fermentation. Compared with the control (SM=370.03 mLCH_4/gVS), maximum cumulative methane yields increased by 10.83 %. Since PKN6g recorded a high and early peak in daily methane yields as compared to the control (SM), 6 g PKN biochar dosage could be said to have significantly ($p<0.001$) increased methane yield and shortened the fermentation period of HE, FLO and KR.

However, with a recorded cumulative methane yield of 202.76 mL/gVS, PKN10g depicted an extreme downward trend with a 46.57 % reduction in cumulative yield as compared to the control ($p<0.001$). The observed results indicated that microbial activity and kinetics could possibly be inhibited by the high dosage of biochar amendment

(Shen et al., 2016).

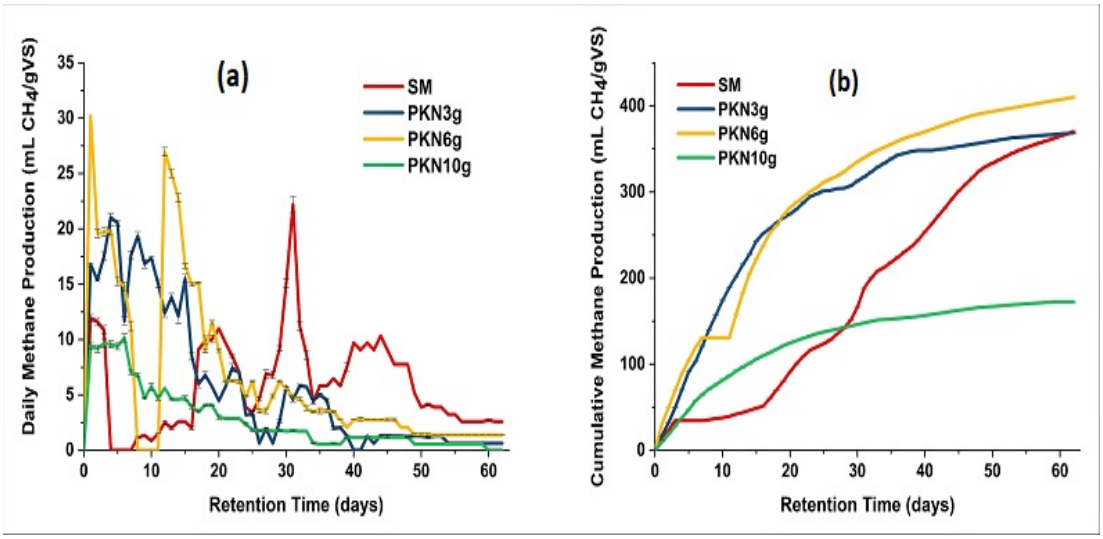

Figure 7.7: Methane yield of PKN samples at different dosages; (a) Daily methane production and (b) Cumulative methane production (values are presented as mean ± SD with n=3)

Shen et al. (2016) reported a similar observation where the less doses of pine (P250) and white oak (WO250) biochar ended up with similar cumulative volume of biogas production as the control while the higher doses of pine (P500) and white oak (WO500) biochar produced lower volumes of biogas than the control. According to Shao et al. (2019), biochar has been observed to only assist stressed situations brought on by external voltage or microbial inactivity, and has little to no effect on situations that function normally. This could be attributed to the finding that biochar enriched DIET-capable *Methanosarcina* and *Methanosaeta* which are sensitive to stress (Shao et al., 2019). Also, it could be that very low dosages of biochar addition had less or no effect on the digestion environment while very high dosages introduced stress in the form of inhibitions relative to the biochar type.

Moreover, Cai et al. (2016) documented that higher amounts of added biochar did not correspond to higher digestion efficiency in their study. Finally, the p-values of each paired test between SM/CCN3g, SM/CCN6g, SM/CCN10g, SM/PKN3g, SM/PKN6g and SM/PKN10g in this study was less than 0.001 ($p<0.001$). Therefore, the difference

between the methane production of control group and biochar-added group is significant. Clearly, different amounts of CCN and PKN shell biochar samples have significantly different impacts on methane yield and this is because the functional qualities and impacts on the anaerobic digestion process using biochars vary according to their physical and chemical parameters.

7.4.4 Effect of CN Ratio, pH, Alkalinity and VFAs on Methane Yield

The C/N ratios of all treatments were from 20.24±0.04 to 28.51±0.26 and within the 20–30 range recommended for anaerobic digestion treatments (Haider et al., 2015). It was expected that all treatments in the anaerobic digestion process will perform very well considering the range of C/N ratios but that was not the case because of the influence from other process parameters. The percentage methane content of the biogas generated for all biochar-amended treatments ranged from 51.9 to 61.8 % while the methane content for the control (SM) was 58.4 %. The biochar-amended treatments (CCN3g and PKN6g) that performed better than the control had higher methane content (62.8 and 61.8 % respectively) than the control. The in-situ CO_2 capture by the porous biochar could be the reason for the improved biogas purity (Shen et al., 2016).

However, biochar dosages that did not improve biogas generation had lower methane contents than the control as shown on Table 7.4. Similarly, with a biodegradability of 76.79 % to 89.51 %, the best performing biochar-amended treatments (CCN3g and PKN6g) had higher biodegradability values (89.51 and 88.26 % respectively) than the control (SM=87.38 %) (Table 7.4). The increase in biodegradability can be attributed to the presence of immobilized micro-organisms enhancing the digestibility of HE, FLO

Table 7.4: Biogas and Methane Yields,VFA, pH, Alkalinity and VS Reduction for Biochar Amended Treatments and Control(mean (standard deviation); n=3)

Parameter	SM	CCN3g	CCN6g	CCN10g	PKN3g	PKN6g	PKN10g
C/N	22.09(0.05)	24.63(0.07)	25.50(0.04)	20.24(0.04)	28.51(0.26)	24.83(0.20)	22.41(0.44)
Biogas Yield (mL/gVS)	643.60	726.52	529.24	384.75	640.28	656.67	332.03
Methane Yield (mL/gVS)	370.03	456.25	295.84	202.76	368.80	410.11	172.32
% Methane	58.40	62.80	55.90	52.70	57.60	61.80	51.90
VS Reduction (%)	86.48	90.87	84.59	76.89	88.24	90.12	71.37
Biodegradability (%)	87.38	89.51	84.09	79.61	84.28	88.26	76.79
Initial pH	7.53 (0.01)	7.86 (0.01)	7.93(0.01)	8.30(0.01)	7.73(0.01)	7.79(0.01)	8.01(0.01)
Final pH	6.27 (0.01)	7.21 (0.01)	7.38(0.01)	7.72(0.01)	7.04(0.01)	7.29(0.01)	7.55(0.01)

and KR. Subsequently, the low biodegradability of high dosed biochar-amended treatments compared to the control can be due to a potential inhibition of methanogenesis caused by the adsorption of VFAs by biochar. Moreover, potential H_2 competitors (e.g. *Hydrogenophaga*) of methanogens could also clone onto biochar and weaken its direct interspicies electron transfer (DIET) benefit for methanogenesis (Shao et al., 2019). The intial and final VFA concentrations are shown in Figure 7.8.

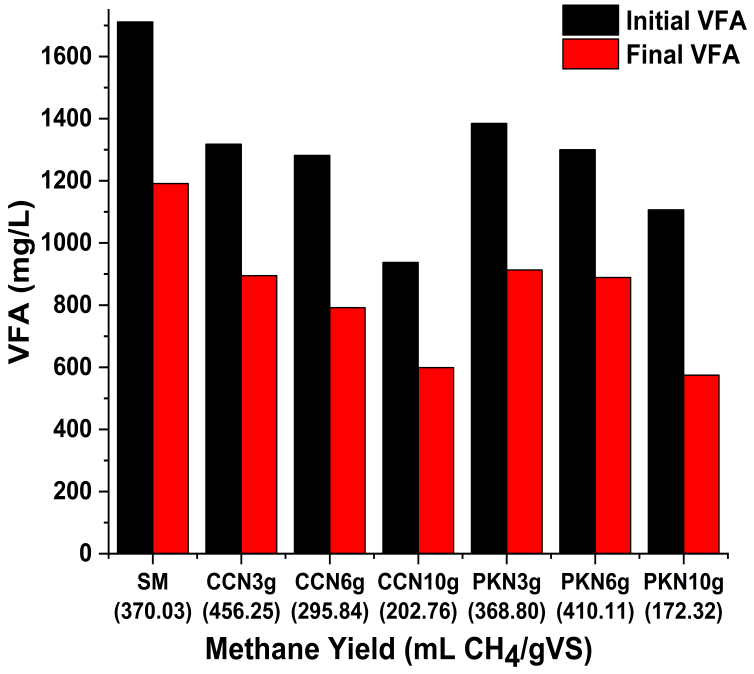

Figure 7.8: Initial and Final VFA Levels in Anaerobic Co-digestion Treatments

For all treatments, VFA concentrations were higher at the start of experiment than after digestion. Although all treatments observed low VFA concentration after digestion,

the VFA values (598.61 and 574.42 mg/L) of the least performing biochar amended treatments (CCN10g and PKN10g respectively) were very low confirming the possible VFAs adsorption by biochar. Since VFAs are crucial building blocks for the synthesis of methane, their adsorption on biochar decreases their bioavailability for conversion into methane, resulting in a restrained methanogenesis activity (Chen et al., 2021).

Also, the biochar-amended treatments recorded an initial and final pH of 7.73 to 8.30 and 7.21 to 7.72 respectively. It was expected that the digester pH increased with the biochar addition (Table 7.4) because of the alkaline nature of biochar and the buffer from the substrate mix of HE, FLO, KR and inoculum used. Also, all the biochar-amended treatments maintained pH values in the alkaline range even after digestion. According to Awosusi et al. (2021), the alkaline nature of biochar could elevate the pH in an anaerobic digestion system, thus possibly restricting methanogens which operate at a slightly acidic pH range and are very pH-sensitive. The inhibition of such metanogens has a concomitant impact on methane generation. Further, the pH of the control (SM) unsurprisingly dropped to 6.27(slightly acidic) as shown in Table 7.4 due to the production of VFAs.

Furthermore, the initial and final total alkalinity concentrations (Figure 7.9) of all biochar-amended treatments were above the optimum value of 3000 mg/l reported by Filer et al. (2019). The alkali and alkaline earth metals such as K, Ca, and Mg released as cations from the biochar could be mostly responsible for this. Suprisingly, the final alkalinity for CCN10g and PKN10g increased from 9362.5 to 9487.5 mg$CaCO_3/L$ and 9575 to 9950 mg$CaCO_3/L$ respectively. This was comparable to the rise in alkalinity observed by Shen et al. (2016) after digestion. This finding might be related to the adsorption of VFAs onto biochar samples. Although the alkalinity range was expected to boost the anaerobic digestion process, treatments like CCN10g and PKN10g experienced inhibitions possibly due to alterations in the dynamics and structure of the microbial community resulting from the use of high dosages of biochar which might have created competition for methanogens by favoring the growth of specific microbial groupings. (Ihoeghian et al., 2023).

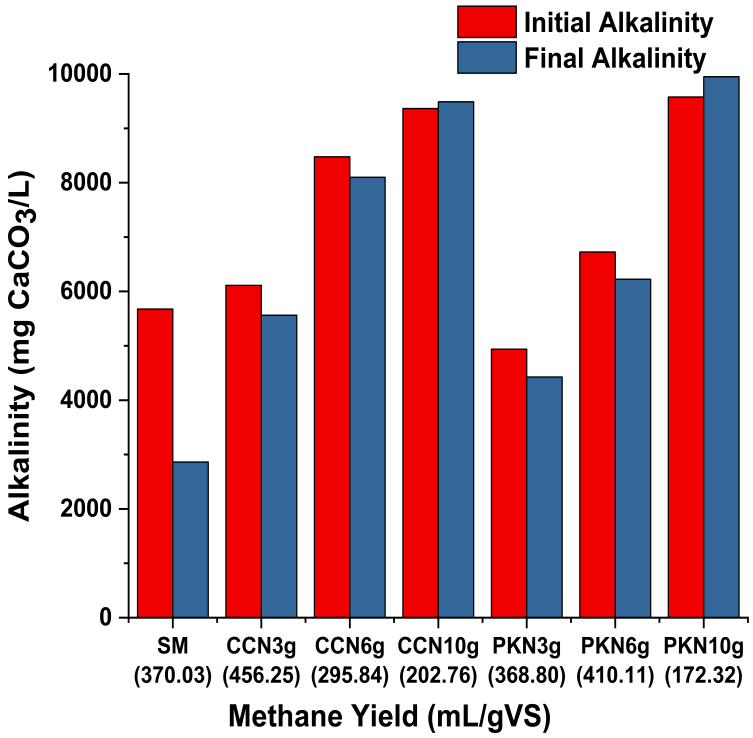

Figure 7.9: Initial and Final Alkalinity Levels in Anaerobic Co-digestion Treatments

Chen et al. (2015) documented the dominant presence of acetoclastic methanogens like *Methanosaeta* (found in biochar surface) and *Methanosarcina* (found in biochar pores) in digesters with biochar. Also, Shen et al. (2020) reported a dominance shift from *Methanosaeta* to *Methanosarcina* (74.75 %) when straw biochar dose was increased from 2 % t0 4 %. Shen et al. (2020) further documented that methane yields correlated with the characteristics of the archaeal community, and when biochar doses were extremely high, cumulative methane yields fell in response to modifications in the archaeal community.

Finally, anaerobic digestion (AD) systems with biochar encouraged the proliferation of acetoclastic methanogens other than hydrogenotrophic methanogens, as evidenced by the fact that *Methanobacterium* and *Methanospirillum* were numerous in AD without biochar addition than in the biochar-amended AD system (Shen et al., 2020). On the otherhand, the control ,SM, had alkalinity values reducing from 5675 to 2862.5 mg$CaCO_3/L$ but still maintaining the stability of the process. Hence, the excessive alkalinity generated by biochar addition may fail to provide stimulatory effects for the

AD process.

7.5 Conclusion

The effect of two biochar types and three dosages in the anaerobic co-digestion of HE, FLO and KR of ratio 78.8 % : 11.8 % : 9.4 % was examined in this study. The results showed different types and dosages of biochar resulted in varying degrees of impact on the AD process. In an ideal case, the addition of biochar is expected to improved process stability and increase methane yield, however, in some rare cases, biochar addition rather introduced stress to the AD system. While an excessive biochar dosage impeded the anaerobic digestion process, an optimal biochar dosage improved cumulative methane output. This observation further indicates that the strength of biochar in anaerobic digestion depends on the type and amount of biochar added. Despite the reported positive impacts of biochar on the anaerobic digestion process, its influence on methanogenesis has been observed to be complex. Therefore, further research is necessary to elucidate comprehensively the mechanisms behind the behaviour of biochar in anaerobic digestion systems, focusing on microbial studies.

CHAPTER 8

Conclusions and Recommendations

8.1 Conclusions

Anaerobic co-digestion was used in this research study as a sustainable method for converting human excreta (HE), food leftovers (FLO) and kitchen residue (KR) into biogas rich in methane. The research included several experimental phases designed to bridge the gaps found in literature such as; determining the individual characteristics of HE, FLO and KR that makes them suitable for household biogas production and finding the optimum mixing ratio of HE, FLO and KR that promotes an enhanced anaerobic co-digestion performance and maximum methane yield. The model that best fits the anaerobic digestion of HE, FLO and KR in this work and the impact of two different biochar additives (coconut shell and palm kernel shell) and three dosages on the co-digestion of feedstocks were also determined. The research revealed a number of intriguing discoveries and results, which are outlined below.

The main goal of Chapter 4 with the title "Physico-Chemical Characterization of Selected Feedstocks as Co-Substrates in Household Biogas Generation" was to investigate various household generated waste with the potential of being used for biogas production. This was done through the characterization of HE, FLO, KR and CD. Using the findings from the physico-chemical characterisation, an initial computation of the theoretical biogas and methane yields of the selected feedstocks was done. From the results obtained, the suitability of HE, FLO, KR and CD for household biogas production was established since all feedstocks contained readily available biodegradable components that could easily be converted to biogas.

However, HE, proposed as the main substrate for household biogas generation in this study, had a very low C/N ratio, which could possibly lead to a low anaerobic digestion performance. Therefore, the use of small portions of FLO and KR as co-substrates was proposed to balance the C/N ratio during co-digestion. In addition, it was concluded that feedstocks like FLO and KR with low pH and alkalinity levels could be complimented by HE which had optimum pH and alkalinity levels. Also,

CD as inoculum, was found to be a good source of microbial community and buffer for the co-digestion of HE, FLO and KR. This information was established through the results obtained for the various characterization analysis done in this study, which mostly met the requirements for suitable anaerobic digestion feedstocks available in literature. Having established that HE, FLO and KR have suitable characteristics for household anaerobic digestion, co-digestion studies using the selected feedstocks were performed.

Chapter 5 with the title "Anaerobic Co-Digestion of Human Excreta, Food Leftovers and Kitchen Residue: Ternary Mixture Design, Synergistic Effects and RSM Approach." aimed to determine the co-digestion performance of HE, FLO and KR at sixteen different mix ratios (based on volatile solids) using a ternary mixture design, biochemical methane potential (BMP) assay and a response surface method. Ternary substrate mixtures of HE, FLO, and KR formulated for the mesophilic batch experiment showed that substrate mix R9 with feedstock ratio 78.8 % HE: 11.8 % FLO: 9.4 % KR produced the highest amount of biogas and methane.

R9(78.8 % HE: 11.8 % FLO: 9.4 % KR) also showed the strongest positive synergistic effect. It could be inferred from the results that co-digestion with the right substrate proportions, such as R9, can significantly improve biogas production and methane yield. Also, the high biodegradability of R9(78.8 % HE: 11.8 % FLO: 9.4 % KR) depicts the ability of the microbial culture to convert the feedstocks in that mixing ratio to biogas. This study thus suggests that the mesophilic co-digestion of 78.8 % HE:11.8 % FLO:9.4 % KR is a promising ratio which could be adapted in household biogas systems. Furthermore, the analysis of variance test amongst the methane yields indicated that different co-digestion mixtures have significantly different effects on the ultimate biogas and methane yields.

Additionally, the experimental results for the substrate mixtures were used to model the responses of biogas yield, methane yield, and synergistic effects using the response surface model (RSM). The RSM model proved that different mixing ratios of HE, FLO and KR can be suitably modeled to provide ease and robustness of determining results

of different and best-performing formulations of the feedstocks. Most importantly, the RSM results showed that biogas yield, methane yield, and synergy were considerably impacted by the composition of the substrate combination and the interactions between the substrates in many ways. Co-digesting feedstocks mixtures with high amounts of HE and/or KR increased biogas yield, methane yield, and synergy.

Moreover, the 61-day response surface model for synergistic effects predicted an antagonistic effect (SI < 1) only for the co-digestion conditions where the FLO fraction was higher than approximately 25 % or the combination of FLO and KR was greater than HE. Therefore, in an effort to prevent a potential antagonistic impact, it was discovered that keeping the FLO and KR fraction in the substrate combination below 50 % was important. Additionally, there is no need to add trace elements to the household biogas system because the household-generated wastes have proven to contain sufficient amounts of trace element such as Zn, Fe, Co, Mo and Ni that are very beneficial to methanogens. With the promising performance of the 78.8 % HE:11.8 % FLO:9.4 % KR co-digestion ratio, kinetic modelling of the methane performance was thus conducted in Chapter 6.

Chapter 6 entitled "Kinetics Study of Methane Production from Anaerobic Co-Digestion of Human Excreta, Food Leftovers and Kitchen Residue" focused on fitting the cumulative methane yield data for the substrate mix of 78.8 % HE: 11.8 % FLO: 9.4 % KR to different kinetic models (Fitzhugh, Modified Gompertz, Logistic, Monod and Cone) to determine the best fit. The study showed that all the models had R^2 values that were generally high. However, the three models with the best fit for the methane yield data were in the order; Cone > Fitzhugh > Monod based on the closeness of R^2 to unity and how low the error terms (AIC, RMSE, and SSE) were. Consequently, the logistic and modified gompertz models were the least performing. Further investigations and optimization of the mesophilic co-digestion of substrate mix 78.8 % HE: 11.8 % FLO: 9.4 % KR with coconut shell and palm kernel shell biochar additives were conducted in chapter 7.

Chapter 7 entitled "Optimization of Batch Anaerobic Co-Digestion of Human Excreta, Food Leftovers and Kitchen Residue using Biochar additives" focused on studying the effectiveness of two different types of biochar (coconut shell, CCN and palm kernel shell, PKN) samples and three different dosages (3 g, 6 g and 10 g) on anaerobic co-digestion of HE, FLO and KR over the course of a 62-day incubation period. All biochar-amended treatments showed two to three peaks at different occurrence times and persistent periods in the daily methane production time trajectory.

The anaerobic co-digestion of HE, FLO and KR with CCN shell biochar had the highest cumulative methane yield (456.25 $mLCH_4$/gVS), followed by PKN shell biochar (410.11 $mLCH_4$/gVS). Considering the difference of 10.11 % between cumulative methane yield of best performing CCN and PKN biochar samples and the favourable characteristics of both biochar types, it could be said that both CCN and PKN biochar types have a high potential of being used in household anaerobic digestion systems. In addition, the cumulative methane yield (370.03 $mLCH_4$/gVS) of the control (SM) was lower than the best performing CCN and PKN treatments. This could be attributed to the influence of biochar on alkalinity, micro-organism activity and trace element availability during the anaerobic digestion process.

Subsequently, biochar dosage was used to determine the level of anaerobic co-digestion enhancement. According to the findings of this study, cumulative methane production increased when 3 g of CCN biochar was used depicting a 23.31 % increase in cumulative methane for CCN3g compared to the control (SM). Even though treatment with CCN3g observed an initial increase in methane yield, too high biochar dosages of 6 g and 10 g CCN restricted methane production due to a potential stress on the anaerobic digestion process brought on by excess biochar addition. The non-performance of the high dosed treatment could also be attributed to the accumulation of potential H_2 competitors (e.g. *Hydrogenophaga*) of methanogens that could clone onto excess biochar and weaken its DIET benefit for methanogenesis.

The addition of PKN shell biochar displayed a distinct pattern compared to that of CCN shell biochar. The cumulative methane yield was 368.69 $mLCH_4$/gVS, sim-

ilar to that of the control (SM=370.03 mLCH_4/gVS) with just a 0.36 % reduction ($p<0.001$) when 3 g of PKN shell biochar was added to the mixture of feedstocks. This observation was not surprising because the composition of feedstocks used in this study was the best performing ratio and biochar has been shown to only assist stressed situations brought on by external voltage or microbial inactivity, and had little to no effect on situations that were functioning normally. This also confirms the finding that biochar enriches DIET-capable *Methanosarcina* and *Methanosaeta* which are sensitive to stress. Nonetheless, the cumulative methane yield increased by 10.83 % when the dose of PKN shell biochar was increased to 6 g, depicting improved process and environmental conditions of the digester.

Conversely, PKN10g observed a decrease in cumulative methane yield as compared to the control. The observed results indicated that microbial activity and kinetics could possibly be restricted by excessive dosage of biochar. Also, higher amounts of added biochar may not necessarily correspond to higher digestion efficiency. Finally, the p-values of each paired test between biochar- amended treatments and control (SM/CCN3g, SM/CCN6g, SM/CCN10g, SM/PKN3g, SM/PKN6g and SM/PKN10g) in this study was less than 0.001 ($p<0.001$). This indicates that the difference between the methane production of control group and biochar-added group is significant. Clearly, different amounts of CCN and PKN shell biochar samples have significantly different impacts on methane yield and this is because the functional qualities and impacts on the anaerobic digestion process using biochars vary according to their physical and chemical parameters.

It was expected that all treatments in the anaerobic digestion process will perform very well considering the range of C/N ratios (20.24 – 28.51) but that was not the case because of the influence from other process parameters. The biochar-amended treatments (CCN3g and PKN6g) that performed better than the control had higher methane contents (62.8 and 61.8 % respectively) than the control. The in-situ CO_2 capture by the porous biochar could be the reason for the improved biogas purity. Similarly, the best performing biochar-amended treatments (CCN3g and PKN6g) had higher biodegradability values (89.51 and 88.26 % respectively) than the control (SM=87.38

%). The increase in biodegradability can be attributed to the presence of immobilized micro-organisms enhancing the digestibility of HE, FLO and KR.

Subsequently, the low biodegradability of the high dosed biochar amended treatments compared to the control can be due to a potential inhibition of methanogenesis caused by the adsorption of VFAs by biochar. For all treatments, VFA concentrations were higher at the start of experiment and low after digestion. Although all treatments observed low VFA concentration after digestion, the results (598.61 and 574.42 mg/L) of the least performing biochar amended treatments (CCN10g and PKN10g respectively) were very low confirming the possible VFAs adsorption onto biochar. Since VFAs are crucial building blocks for the synthesis of methane, their adsorption on biochar decreases their bio-availability for conversion into methane, resulting in a restrained methanogenesis activity.

Also, it was expected that the digester pH increased with the biochar addition because of the alkaline nature of biochar and the buffer from the substrate mix of HE, FLO, KR and inoculum used. Consequently, all the biochar-amended treatments maintained pH values in the alkaline range even after digestion. The buffering action of the alkaline biochar in CCN10g and PKN10g elevated the pH in the anaerobic digestion system thereby potentially inhibiting the activity of methanogens which operate at a slightly acidic pH range and are very pH-sensitive. The inhibition of such metanogens had a concomitant effect on methane production. Further, the pH of the control (SM) unsurprisingly dropped to 6.27 after digestion due to the production of VFAs.

Furthermore, the initial and final total alkalinity concentrations of all biochar-amended treatments were above the optimum value of 3000 mg/l. This could mostly be attributed to the cation release of the alkali and alkaline earth metals (K, Ca and Mg) from the biochar. Suprisingly, the final alkalinity of CCN10g and PKN10g increased from 9362.5 to 9487.5 mg$CaCO_3/L$ and 9575 to 9950 mg$CaCO_3/L$ respectively. Although the alkalinity range was expected to boost the anaerobic digestion process, treatments like CCN10g and PKN10g experienced inhibitions possibly due to changes in the microbial community structure and dynamics resulting from the use of high

dosages of biochar which might have selectively favored the growth of certain microbial groups, thus creating competition for methanogens. Hence, the excessive alkalinity generated by biochar addition may fail to provide stimulatory effects for the AD process.

8.1.1 Overall Conclusions

(i) HE, FLO and KR are proposed to be very well developed as feedstock sources for household biogas generation due to their availability in households, readily available biodegradable components and complimenting individual physico-chemical characteristics.

(ii) Mixing feedstocks raised the pH of the mixtures containing FLO and KR relative to their pH values. This could be seen at the start of digestion, where co-substrates having higher proportions of HE also had higher pH values and vice versa.

(iii) The strong alkalinity values of treatments, R5, R7, R8, R9 and R10 provided a very good buffer leading to a biodegradability range of 82.1-89.7 % and stable biogas and methane production processes. On the other hand, treatments R2, R3, R4, R11, R12 and R16 with very low initial alkalinity had very low biogas and methane yields and hence very low biodegradability values.

(iv) Mesophilic anaerobic co-digestion of HE, FLO and KR proved to significantly improve methane production during the BMP assays. It was discovered that the mono-digestion tests for FLO and KR produced less methane than the mixed groups. This might be explained by the high levels of VFA buildup in FLO and KR (R2:4141.89 mg/L and R3: 3543.28 mg/L, respectively) as well as the lower levels of alkalinity in FLO (R2:1775.0 mg/L) and KR (R3:1900.0 mg/L). Also, the low C/N ratio of HE might have led to the low methane production in its mono-digestion.

(v) The co-digestion substrate- mix with HE percentages of 50 % or higher (R5, R6, R7, R8, R9, R10) had higher cumulative methane production with R9 producing the most methane (764.79.5 mLCH4/g VS), followed by R10, which were all having a greater amount of HE (>50 %).

(vi) Conversely, treatments with 50 % or more HE were seen to be able to maintain system stability as it had the lowest final VFA accumulation ranging from 1082.3 mg/L to 1680.9 mg/L.

(vii) Compared to the mono-digestion of HE (R1), the cumulative methane output of R9 was 66.80 % higher. This was presumably due to the fact that there were varieties of substrates available, which provided the microbial population with enough nutrients to promote the breakdown of substrates and increase biogas generation.

(viii) The response surface plots show that the predicted response increases with an increasing HE and KR fractions and decreased with an increasing FLO fraction in the substrate mixtures.

(ix) The three models with the greatest fit for the methane yield data were in the order Cone > Fitzhugh > Monod.

(x) The anaerobic co-digestion of HE, FLO and KR with CCN shell biochar had the highest cumulative methane yield (456.25 mL CH_4/gVS), followed by PKN shell biochar (410.11 mLCH_4/gVS). Considering the difference between the cumulative methane yields and the favourable characteristics of both biochar types, it could be said that both CCN and PKN biochar types have high potentials in being used in anaerobic digestion systems.

(xi) Different dosages of biochar resulted in varying degrees of influence on the anaerobic co-digestion process. In an ideal case, the addition of biochar was expected to improve process stability and increase methane yield, however, in some rare cases, the addition of biochar rather introduced stress to the anaerobic co-digestion system. An appropriate biochar dosage increased cumulative methane yield, whereas excess or high biochar dosages inhibited the anaerobic co-digestion process. Hence, the effectiveness of biochar in anaerobic co-digestion depends on the type and amount of biochar added.

8.2 Contribution to Knowledge

(i) This study has highlighted the efficiency and benefits of co-digestion of household-generated wastes(HE, FLO and KR) and demonstrated its superiority over mono-digestion in terms of biogas and methane production. This is very important because some households still operate digesters that use only foodwaste as feed-stock resulting in less or no gas production.

(ii) Previous co-digestion studies of food waste and human excreta has often been characterised by limitations in the sense that, they arbitrarily combine the feed-stocks with no guide to the choice of mixing ratios. Because the mixing ratios are chosen at random, just a few experimental setups are carried out with less accurracy in predicting the best performing ratio. Therefore this study adapts an experimental strategy like the mixture design and the response surface model for a wider coverage of mixing ratios and an accurate model prediction.

(iii) This study is the first to use mixture design and response surface model to predict the best performing mixing ratio of household-generated waste (HE, FLO and KR).

(iv) By comparing the biogas and methane yields of the different mixing ratios of HE, FLO and KR, using the RSM model, this study has provided insights into how the different mixture compositions affect biogas and methane yields. The study has also documented reasons and understanding of the characteristics of feedstocks, important AD process parameters and environmental conditions that lead to enhanced or inhibited biogas production in the various mixing ratios.

(v) This study has in addition determined the most effective and efficient mixing ratio R9(78.8 % HE:11.8 % FLO:9.4 % KR) for higher biogas and methane yields, better process stability and reduced digester volumes.

(vi) This study has reported the need to keep HE above 50 %, FLO, approximately 25 % and below or the combination of FLO and KR, lesser than HE in the anaerobic co-digestion of HE, FLO and KR for enhanced biogas and methane yields.

(vii) This research has contributed to identifying optimal biochar types and dosages that can lead to enhanced biogas and methane yields. Also,the research provided

understanding on some of the mechanisms by which biochar improves or inhibits the anaerobic co-digestion process.

8.3 Implication for Further Studies

(i) Further studies could focus on exploring the micro-organism activity in the best performing anaerobic co-digestion ratio R9(78.8 % HE:11.8 % FLO:9.4 % KR).

(ii) Further studies could also explore how seasonal variations in food leftovers and kitchen residues will affect the stability and efficiency of the co-digestion mix ratio R9(78.8 % HE:11.8 % FLO:9.4 % KR).

(iii) Further research could focus on the modelling of the anaerobic co-digestion process using artificial intelligence techniques (Artificial Neural Network).

(iv) In addition, further research could focus on the scalability of the anaerobic co-digestion of the best performing ratio R9(78.8 % HE:11.8 % FLO:9.4 % KR). This is because a pilot or case study could provide information on technical, economical and operational challenges.

(v) Subsequent research could examine the potential challenges and opportunities in digestate management. This may include assessing the suitability of digestate for soil amendment.

(vi) Comparing the effects of biochar produced using different pyrolysis temperatures or activation methods can help identify the most effective and sustainable biochar production techniques for anaerobic co-digestion systems.

(vii) Further in-situ studies could investigate the interactions between biochar and microbial consortia involved in anaerobic co-digestion. Understanding how biochar influences microbial communities, their activities and methabolic pathways could provide insights into the mechanisms behind enhanced or inhibited AD processes.

(viii) Finally, subsequent research could focus on integrating the biochar in the form of a compressed film in the design of household bio-digesters for large scale implementation.

8.4 Recommendations

(i) It is recommended that in setting up a full-scale anaerobic co-digestion system at the household level, the amount of HE is kept relatively higher (>50 %) than KR and FLO. A high amount of HE would lead to a more stable digestion process brought on by the buffering support provided by HE with its relatively high alkalinity compared to FLO and KR. Moreover, the use of less FLO and KR is beneficial for households that use them as feed for animals.

(ii) Also, it is suggested that households would adhere to the best-performing ratio, R9(78.8 % HE:11.8 % FLO:9.4 % KR) for enhanced biogas production.

(iii) Lastly, digester designers and builders could adhere to the information from the cone model to aid in designing an upscale household biogas system that co-digests 78.8 % HE: 11.8 % FLO: 9.4 % KR with excellent statistical metrics.

(iv) CCN and PKN biochar samples are recommended as potential additives for household anaerobic co-digestion process due to their unique characteristics that favour enhanced AD processes.

(v) Lastly, it is also recommended that excess use of biochar is avoided in order to mitigate process inhibitions.

Bibliography

Abalo, E. M., Peprah, P., Nyonyo, J., Ampomah-Sarpong, R., and Agyemang-Duah, W. (2018). A review of the triple gains of waste and the way forward for ghana. *Journal of Renewable Energy*, 2018.

Abbas, I., Liu, J., Noor, R. S., Faheem, M., Farhan, M., Ameen, M., and Shaikh, S. A. (2020). Development and performance evaluation of small size household portable biogas plant for domestic use. *Biomass Conversion and Biorefinery*, pages 1–13.

Abbas, T., Ali, G., Adil, S. A., Bashir, M. K., and Kamran, M. A. (2017). Economic analysis of biogas adoption technology by rural farmers: The case of faisalabad district in pakistan. *Renewable energy*, 107:431–439.

Abdel-Fattah, T. M., Mahmoud, M. E., Ahmed, S. B., Huff, M. D., Lee, J. W., and Kumar, S. (2015). Biochar from woody biomass for removing metal contaminants and carbon sequestration. *Journal of Industrial and Engineering Chemistry*, 22:103–109.

Abiti, B., Hartard, S., Bradl, H. B., Pishva, D., and Ahiakpa, J. K. (2017). Resource prospects of municipal solid wastes generatedin the ga east municipal assembly of ghana. *Journal of Health and Pollution*, 7(14):37–47.

Abubakar, B. and Ismail, N. (2012). Anaerobic digestion of cow dung for biogas production. *ARPN journal of engineering and applied sciences*, 7(2):169–172.

Aceves-Lara, C.-A., Latrille, E., Conte, T., and Steyer, J.-P. (2012). Online estimation of vfa, alkalinity and bicarbonate concentrations by electrical conductivity measurement during anaerobic fermentation. *Water Science and Technology*, 65(7):1281–1289.

Achinas, S., Achinas, V., and Euverink, G. J. W. (2017). A technological overview of biogas production from biowaste. *Engineering*, 3(3):299–307.

Adeoti, O., Ilori, M., Oyebisi, T., and Adekoya, L. (2000). Engineering design and

economic evaluation of a family-sized biogas project in nigeria. *Technovation*, 20(2):103–108.

Adl, M., Sheng, K., and Gharibi, A. (2012). Technical assessment of bioenergy recovery from cotton stalks through anaerobic digestion process and the effects of inexpensive pre-treatments. *Applied energy*, 93:251–260.

Afifah, U. and Priadi, C. R. (2017). Biogas potential from anaerobic co-digestion of faecal sludge with food waste and garden waste. In *AIP Conference Proceedings*, volume 18, page 020032. AIP Publishing LLC.

Agler, M. T., Garcia, M. L., Lee, E. S., Schlicher, M., and Angenent, L. T. (2008). Thermophilic anaerobic digestion to increase the net energy balance of corn grain ethanol. *Environmental science & technology*, 42(17):6723–6729.

Agyei, P. A., Awuah, E., and Oduro-Kwarteng, S. (2011). Faecal sludge management in madina, ghana. *Journal of Applied Technology and Environmental Sanitation*, 1(3):239–249.

Agyeman, F. O. and Tao, W. (2014). Anaerobic co-digestion of food waste and dairy manure: Effects of food waste particle size and organic loading rate. *Journal of environmental management*, 133:268–274.

Ahiataku-Togobo, W. (2008). Biogas experience in africa: the case of ghana. In *Workshop on research and development programme for Biogas for Better Life–an African initiative. The Energy Centre, KNUST, Kumasi, Ghana.*

Ahiataku-Togobo, W. (2016). Renewable energy resources and potentials in ghana. *Ministry of Power-RAED*.

Ahmad, M., Rajapaksha, A. U., Lim, J. E., Zhang, M., Bolan, N., Mohan, D., Vithanage, M., Lee, S. S., and Ok, Y. S. (2014). Biochar as a sorbent for contaminant management in soil and water: a review. *Chemosphere*, 99:19–33.

Ahmad, R. K., Sulaiman, S. A., Yusup, S., Dol, S. S., Inayat, M., and Umar, H. A. (2022). Exploring the potential of coconut shell biomass for charcoal production. *Ain Shams Engineering Journal*, 13(1):101499.

Ahmed, I., Ofori-Amanfo, D., Awuah, E., and Cobbold, F. (2018a). Performance assessment of the rehabilitated mudor sewage treatment plant at james town accra-ghana. *Journal of Water Resource and Protection*, 10(8):725–739.

Ahmed, I., Ofori-Amanfo, D., Awuah, E., and Cobbold, F. (2019). A comprehensive study on the physicochemical characteristics of faecal sludge in greater accra region and analysis of its potential use as feedstock for green energy. *Journal of Renewable Energy*, 2019.

Ahmed, I., Quarshie, A. M., Ofori-Amanfo, D., Cobbold, F., Amofa-Sarkodie, E. S., and Awuah, E. (2018b). Assessment of foreign material load in the management of faecal sludge in the greater accra region of ghana. *International Journal of Energy and Environmental Science*, 3(1):27–36.

Ahou, Y. S., Bautista Angeli, J.-R., Awad, S., Baba-Moussa, L., and Andres, Y. (2021). Assessment of inoculum to substrate ratio to recover energy from cassava wastes through anaerobic digestion. *Waste and Biomass Valorization*, 12(4):1891–1900.

Ahring, B. K., Sandberg, M., and Angelidaki, I. (1995). Volatile fatty acids as indicators of process imbalance in anaerobic digestors. *Applied microbiology and biotechnology*, 43(3):559–565.

Ahring, B. K. and Westermann, P. (1985). Sensitivity of thermophilic methanogenic bacteria to heavy metals. *Current Microbiology*, 12(5):273–276.

Aisien, F. A., Aisien, E. T., et al. (2020). Biogas from cassava peels waste. *Detritus*, 10:100.

Ajieh, M. U., Isagba, E. S., Ihoeghian, N., Edosa, V. I., Amenaghawon, A., Oshoma, C. E., Erhunmwunse, N., Obuekwe, I. S., Tongo, I., Emokaro, C., et al. (2021). Assessment of sociocultural acceptability of biogas from faecal waste as an alternative energy source in selected areas of benin city, edo state, nigeria. *Environment, Development and Sustainability*, 23(9):13182–13199.

Ajien, A., Idris, J., Md Sofwan, N., Husen, R., and Seli, H. (2023). Coconut shell and husk biochar: A review of production and activation technology, economic, financial aspect and application. *Waste Management & Research*, 41(1):37–51.

Alakangas, E. (2015). Quality guidelines for wood fuels in finland.

Alatriste-Mondragón, F., Samar, P., Cox, H. H., Ahring, B. K., and Iranpour, R. (2006). Anaerobic codigestion of municipal, farm, and industrial organic wastes: a survey of recent literature. *Water Environment Research*, 78(6):607–636.

Altaş, L. (2009). Inhibitory effect of heavy metals on methane-producing anaerobic granular sludge. *Journal of hazardous materials*, 162(2-3):1551–1556.

Amenaghawon, A. N., Evbarunegbe, N. I., and Obahiagbon, K. (2021). Optimum biodiesel production from waste vegetable oil using functionalized cow horn catalyst: a comparative evaluation of some expert systems. *Cleaner Engineering and Technology*, 4:100184.

Amenaghawon, A. N., Orukpe, P. I., Nwanbi-Victor, J., Okedi, M. O., and Aburime, E. I. (2022). Enhanced lipase production from a ternary substrate mix of agricultural residues: a case of optimization of microbial inducers and global sensitivity analysis. *Bioresource Technology Reports*, 17:101000.

Amigun, B., Parawira, W., Musango, J., Aboyade, A., and Badmos, A. (2012). Anaerobic biogas generation for rural area energy provision in africa. *Biogas*, pages 36–62.

Ampofo, K. (1996). National biogas resource assessment. *Ministry of Energy, Accra, Ghana*.

An, V. T. H., Thanh, V. T. M., and Anh, N. V. (2017). Bio-methane potential test for anaerobic co-digestion of faecal sludge and sewage sludge. *Vietnam Journal of Science and Technology*, 55(4C):27–32.

Andara, A. R. and Esteban, J. L. (1999). Kinetic study of the anaerobic digestion of the solid fraction of piggery slurries. *Biomass and bioenergy*, 17(5):435–443.

Anderson, J. and Ingram, J. (1993). A handbook of methods. *CAB International, Wallingford, Oxfordshire*, 221:62–65.

Andriamanohiarisoamanana, F. J., Saikawa, A., Kan, T., Qi, G., Pan, Z., Yamashiro, T., Iwasaki, M., Ihara, I., Nishida, T., and Umetsu, K. (2018). Semi-continuous anaerobic co-digestion of dairy manure, meat and bone meal and crude glycerol: Process performance and digestate valorization. *Renewable Energy*, 128:1–8.

Andriamanohiarisoamanana, F. J., Saikawa, A., Tarukawa, K., Qi, G., Pan, Z., Yamashiro, T., Iwasaki, M., Ihara, I., Nishida, T., and Umetsu, K. (2017). Anaerobic co-digestion of dairy manure, meat and bone meal, and crude glycerol under mesophilic conditions: Synergistic effect and kinetic studies. *Energy for Sustainable Development*, 40:11–18.

Angelidaki, I. and Ahring, B. (1992). Effects of free long-chain fatty acids on thermophilic anaerobic digestion. *Applied microbiology and biotechnology*, 37:808–812.

Angelidaki, I., Alves, M., Bolzonella, D., Borzacconi, L., Campos, J., Guwy, A., Kalyuzhnyi, S., Jenicek, P., and Van Lier, J. (2009). Defining the biomethane potential (bmp) of solid organic wastes and energy crops: a proposed protocol for batch assays. *Water science and technology*, 59(5):927–934.

Angelidaki, I. and Sanders, W. (2004). Assessment of the anaerobic biodegradability of macropollutants. *Re/Views in Environmental Science & Bio/Technology*, 3(2):117–129.

Anggarini, S., Hidayat, N., Sunyoto, N. M. S., and Wulandari, P. S. (2015). Optimization of hydraulic retention time (hrt) and inoculums addition in wastewater treatment using anaerobic digestion system. *Agriculture and Agricultural Science Procedia*, 3:95–101.

Antwi, E., Bensah, E. C., Quansah, D. A., Arthur, R., and Ahiekpor, J. (2010). Ghana's biofuels policy: challenges and the way forward. *International Journal of Energy and Environment*, 1(5):805–814.

Anuar, M. F., Fen, Y. W., Zaid, M. H. M., Matori, K. A., and Khaidir, R. E. M. (2018). Synthesis and structural properties of coconut husk as potential silica source. *Results in Physics*, 11:1–4.

Anwar, N., Wang, W., Zhang, J., Li, Y., Chen, C., Liu, G., and Zhang, R. (2016). Effect of sodium salt on anaerobic digestion of kitchen waste. *Water Science and Technology*, 73(8):1865–1871.

AOAC (1990). Official methods of analysis.

AOAC (1995). Protein (crude) in animal feed and pet food 984.13. *Official methods of analysis of official analytical chemists international*, 1:30–31.

AOAC (2006). Aoac official method 2003.05: Crude fat in feeds, cereal grains, and forages.

APHA (1992). Standard methods for water and wastewater examination.

APHA, W. (1998). Standard methods for the examination of water and wastewater 20th edition. *American Public Health Association, American Water Work Association, Water Environment Federation, Washington, DC*.

Appiagyei Osei-Owusu, B., Baidoo, M. F., Arthur, R., and Oduro-Kwarteng, S. (2023). Physico-chemical characterization of selected feedstocks as co-substrates for household biogas generation in ghana. *International Journal of Sustainable Engineering*, 16(1):117–128.

Appiah-Effah, E., NYARKO, K. B., and AWUAH, E. (2014). Characterization of public toilet sludge from peri-urban and rural areas of ashanti region of ghana. *Journal of Applied Sciences in Environmental Sanitation*, 9(3).

Arif, S., Liaquat, R., and Adil, M. (2018). Applications of materials as additives in anaerobic digestion technology. *Renewable and Sustainable Energy Reviews*, 97:354–366.

Arifan, F., Abdullah, A., and Sumardiono, S. (2021). Kinetic study of biogas production from animal manure and organic waste in semarang city by using anaerobic digestion method. *Indonesian Journal of Chemistry*, 21(5):1221–1230.

Ariunbaatar, J., Di Perta, E. S., Panico, A., Frunzo, L., Esposito, G., Lens, P. N., and Pirozzi, F. (2015). Effect of ammoniacal nitrogen on one-stage and two-stage anaerobic digestion of food waste. *Waste management*, 38:388–398.

Ariunbaatar, J., Esposito, G., Yeh, D. H., and Lens, P. N. (2016). Enhanced anaerobic digestion of food waste by supplementing trace elements: role of selenium (vi) and iron (ii). *Frontiers in Environmental Science*, 4:8.

Arthur, R., Antonczyk, S., Off, S., and Scherer, P. A. (2022). Mesophilic and thermophilic anaerobic digestion of wheat straw in a cstr system with 'synthetic manure': impact of nickel and tungsten on methane yields, cell count, and microbiome. *Bioengineering*, 9(1):13.

Arthur, R., Baidoo, M. F., and Antwi, E. (2011). Biogas as a potential renewable energy source: A ghanaian case study. *Renewable energy*, 36(5):1510–1516.

Arthur, R., Baidoo, M. F., Osei, G., Boamah, L., and Kwofie, S. (2020). Evaluation of potential feedstocks for sustainable biogas production in ghana: Quantification, energy generation, and co2 abatement. *Cogent Environmental Science*, 6(1):1868162.

Arthur, R. and Scherer, P. A. (2020). Monitoring dissolved active trace elements in biogas plants using total reflection x-ray fluorescence spectrometry. *X-Ray Spectrometry*, 49(5):560–571.

Astals, S., Batstone, D., Mata-Alvarez, J., and Jensen, P. (2014). Identification of synergistic impacts during anaerobic co-digestion of organic wastes. *Bioresource technology*, 169:421–427.

Astals, S., Musenze, R., Bai, X., Tannock, S., Tait, S., Pratt, S., and Jensen, P. (2015). Anaerobic co-digestion of pig manure and algae: Impact of intracellular algal products recovery on co-digestion performance. *Bioresource technology*, 181:97–104.

Atasoy, M., Eyice, Ö., and Cetecioglu, Z. (2020). Volatile fatty acid production from semi-synthetic milk processing wastewater under alkali ph: the pearls and pitfalls of microbial culture. *Bioresource Technology*, 297:122415.

Awosusi, A., Sethunya, V., and Matambo, T. (2021). Synergistic effect of anaerobic co-digestion of south african food waste with cow manure: Role of low density-polyethylene in process modulation. *Materials Today: Proceedings*, 38:793–803.

Baek, G., Kim, D., Kim, J., Kim, H., and Lee, C. (2020). Treatment of cattle manure by anaerobic co-digestion with food waste and pig manure: Methane yield and synergistic effect. *International Journal of Environmental Research and Public Health*, 17(13):4737.

Baek, G., Kim, J., Kim, J., and Lee, C. (2018). Role and potential of direct interspecies electron transfer in anaerobic digestion. *Energies*, 11(1):107.

Bah, H., Zhang, W., Wu, S., Qi, D., Kizito, S., and Dong, R. (2014). Evaluation of batch anaerobic co-digestion of palm pressed fiber and cattle manure under mesophilic conditions. *Waste Management*, 34(11):1984–1991.

Banks, C. J., Zhang, Y., Jiang, Y., and Heaven, S. (2012). Trace element requirements for stable food waste digestion at elevated ammonia concentrations. *Bioresource technology*, 104:127–135.

Barnes, R. B., Richardson, D., Berry, J. W., and Hood, R. L. (1945). Flame photometry a rapid analytical procedure. *Industrial & Engineering Chemistry Analytical Edition*, 17(10):605–611.

Batstone, D. J. (2006). Mathematical modelling of anaerobic reactors treating domestic wastewater: Rational criteria for model use. *Reviews in Environmental Science and Bio/Technology*, 5(1):57–71.

Bedi, A. S., Sparrow, R., and Tasciotti, L. (2017). The impact of a household biogas programme on energy use and expenditure in east java. *Energy Economics*, 68:66–76.

Bedoić, R., Špehar, A., Puljko, J., Čuček, L., Ćosić, B., Pukšec, T., and Duić, N. (2020). Opportunities and challenges: Experimental and kinetic analysis of anaerobic co-digestion of food waste and rendering industry streams for biogas production. *Renewable and Sustainable Energy Reviews*, 130:109951.

Bensah, E. C. and Brew-Hammond, A. (2010). Biogas technology dissemination in ghana: history, current status, future prospects, and policy significance. *International Journal of Energy and Environment*, 1(2):277–294.

Bensah, E. C., Senya, O., Ahiekpor, J., Antwi, E., and Ribeiro, J. (2015). A study of the effluent quality of excrement-based biogas plants in ghana. *Int J Sci Eng Appl Sci (IJSEAS)*, 1(6).

Bernardo, G., Marroccoli, M., Nobili, M., Telesca, A., and Valenti, G. (2007). The use of oil well-derived drilling waste and electric arc furnace slag as alternative raw

materials in clinker production. *Resources, Conservation and Recycling*, 52(1):95–102.

Betiku, E. and Adesina, O. A. (2013). Statistical approach to the optimization of citric acid production using filamentous fungus aspergillus niger grown on sweet potato starch hydrolyzate. *Biomass and Bioenergy*, 55:350–354.

Bin, C. (1989). The current status of agricultural geothermal utilization in china. *Biomass*, 20(1-2):69–76.

Björnsson, L., Murto, M., and Mattiasson, B. (2000). Evaluation of parameters for monitoring an anaerobic co-digestion process. *Applied microbiology and biotechnology*, 54(6):844–849.

Bo, Z. and Pin-Jing, H. (2014). Performance assessment of two-stage anaerobic digestion of kitchen wastes. *Environmental technology*, 35(10):1277–1285.

Boadi, K. O. and Kuitunen, M. (2003). Municipal solid waste management in the accra metropolitan area, ghana. *Environmentalist*, 23(3):211–218.

Boakye, F. A. (2008). *Sustainability of Alternative Energy Resources for Ghanaian Women: A Case Stody of the Appolonia Biogas Project*. PhD thesis, Cornell University.

Boateng, S. (2015). Factors influencing solid waste management in ghana [mphil thesis]. *Lambert Academic Publication*, 1.

Bodík, I. and Miroslavakubaská, M. (2014). Possibilities of anaerobic fermentation of food waste on municipal wastewater treatment plants. *Int. J. Eng. Sci. Innov. Technol*, 3:523–532.

Bolzonella, D., Fatone, F., Pavan, P., and Cecchi, F. (2005). Anaerobic fermentation of organic municipal solid wastes for the production of soluble organic compounds. *Industrial & Engineering Chemistry Research*, 44(10):3412–3418.

Bouallagui, H., Touhami, Y., Cheikh, R. B., and Hamdi, M. (2005). Bioreactor performance in anaerobic digestion of fruit and vegetable wastes. *Process biochemistry*, 40(3-4):989–995.

Boyacı, İ. H. (2005). A new approach for determination of enzyme kinetic constants using response surface methodology. *Biochemical Engineering Journal*, 25(1):55–62.

Boyle, W. (1976). Energy recovery from sanitary landfills-a review. *Microbial energy conversion*, pages 119–138.

Braun, R. (1982). Biogas—methane treatment of organic waste. *Monograph. Wien New York*.

Braun, R. (2007). Anaerobic digestion: a multi-faceted process for energy, environmental management and rural development. In *Improvement of crop plants for industrial end uses*, pages 335–416. Springer.

Bremner, J. (1965). Total nitrogen. *Methods of soil analysis: part 2 chemical and microbiological properties*, 9:1149–1178.

Browne, J. D. and Murphy, J. D. (2013). Assessment of the resource associated with biomethane from food waste. *Applied Energy*, 104:170–177.

Brulé, M., Bolduan, R., Seidelt, S., Schlagermann, P., and Bott, A. (2013). Modified batch anaerobic digestion assay for testing efficiencies of trace metal additives to enhance methane production of energy crops. *Environmental technology*, 34(13-14):2047–2058.

Bryant, M. (1979). Microbial methane production—theoretical aspects. *Journal of animal science*, 48(1):193–201.

Budiyono, I. S. and Sumardiono, S. (2014). Kinetic model of biogas yield production from vinasse at various initial ph: comparison between modified gompertz model and first order kinetic model. *Research Journal of Applied Sciences, Engineering and Technology*, 7(13):2798–2805.

Bukari, F. I. M., Annan-Prah, E. C., and Abdul, R. (2019). Urban household solid waste management: Livelihood implications of reuse in the wa municipality. In *The China-Africa Urban Development Forum (CAUDF) University of Cape Coast, Cape Coast,Ghana 3rd–4th October, 2019*, page 32.

Bułkowska, K., Białobrzewski, I., Gusiatin, Z. M., Klimiuk, E., and Pokój, T. (2015). Adm1-based modeling of anaerobic codigestion of maize silage and cattle manure: calibration of parameters and model verification. part 2. *Archives of Environmental Protection*, 41(3).

Burnham, A. K. (2017). Use and misuse of logistic equations for modeling chemical kinetics. *Journal of Thermal Analysis and Calorimetry*, 127(1):1107–1116.

Buswell, A. and Boruff, C. (1932). The relation between the chemical composition of organic matter and the quality and quantity of gas produced during sludge digestion. *Sewage Works Journal*, pages 454–460.

Buswell, A. and Mueller, H. (1952). Mechanism of methane fermentation. *Industrial & Engineering Chemistry*, 44(3):550–552.

Butnan, S., Deenik, J. L., Toomsan, B., Antal, M. J., and Vityakon, P. (2015). Biochar characteristics and application rates affecting corn growth and properties of soils contrasting in texture and mineralogy. *Geoderma*, 237:105–116.

Byamba-Ochir, N., Buyankhishig, B., Byambasuren, N., and Surenjav, E. (2019). Characterization of silver loaded activated carbon prepared under supercritical water condition. *Solid State Phenomena*, 288:59–64.

Cabbai, V., Ballico, M., Aneggi, E., and Goi, D. (2013). Bmp tests of source selected ofmsw to evaluate anaerobic codigestion with sewage sludge. *Waste management*, 33(7):1626–1632.

Cai, F., Yan, H., Zhang, R., Liu, G., and Chen, C. (2019). Prediction of methane production performances based on determination of organic components for different vegetable wastes. *International Journal of Agricultural and Biological Engineering*, 12(3):154–159.

Cai, J., He, P., Wang, Y., Shao, L., and Lü, F. (2016). Effects and optimization of the use of biochar in anaerobic digestion of food wastes. *Waste Management & Research*, 34(5):409–416.

Cantrell, K. B., Hunt, P. G., Uchimiya, M., Novak, J. M., and Ro, K. S. (2012). Impact

of pyrolysis temperature and manure source on physicochemical characteristics of biochar. *Bioresource technology*, 107:419–428.

Capson-Tojo, G., Moscoviz, R., Ruiz, D., Santa-Catalina, G., Trably, E., Rouez, M., Crest, M., Steyer, J.-P., Bernet, N., Delgenès, J.-P., et al. (2018). Addition of granular activated carbon and trace elements to favor volatile fatty acid consumption during anaerobic digestion of food waste. *Bioresource technology*, 260:157–168.

Capson-Tojo, G., Rouez, M., Crest, M., Steyer, J.-P., Delgenès, J.-P., and Escudié, R. (2016). Food waste valorization via anaerobic processes: a review. *Reviews in Environmental Science and Bio/Technology*, 15(3):499–547.

Capson-Tojo, G., Rouez, M., Crest, M., Trably, E., Steyer, J.-P., Bernet, N., Delgenès, J.-P., and Escudié, R. (2017). Kinetic study of dry anaerobic co-digestion of food waste and cardboard for methane production. *Waste Management*, 69:470–479.

Carucci, G., Carrasco, F., Trifoni, K., Majone, M., and Beccari, M. (2005). Anaerobic digestion of food industry wastes: effect of codigestion on methane yield. *Journal of Environmental Engineering*, 131(7):1037–1045.

Casallas-Ojeda, M. R., Marmolejo-Rebellón, L. F., and Torres-Lozada, P. (2020). Evaluation of simultaneous incidence of head space and temperature on biochemical methane potential in food waste. *Cogent Engineering*, 7(1):1729514.

Cavaleiro, A., Pereira, M., and Alves, M. (2008). Enhancement of methane production from long chain fatty acid based effluents. *Bioresource technology*, 99(10):4086–4095.

Cavinato, C., Fatone, F., Bolzonella, D., and Pavan, P. (2010). Thermophilic anaerobic co-digestion of cattle manure with agro-wastes and energy crops: comparison of pilot and full scale experiences. *Bioresource technology*, 101(2):545–550.

Cecchi, F., Alvarez, J. M., Traverso, P. G., Medici, F., and Fazzini, G. (1990). A new approach to the kinetic study of anaerobic degradation of the organic fraction of municipal solid waste. *Biomass*, 23(2):79–102.

Cha, J. S., Park, S. H., Jung, S.-C., Ryu, C., Jeon, J.-K., Shin, M.-C., and Park, Y.-K.

(2016). Production and utilization of biochar: A review. *Journal of Industrial and Engineering Chemistry*, 40:1–15.

Chan, Y. J., Chong, M. F., and Law, C. L. (2017). Performance and kinetic evaluation of an integrated anaerobic–aerobic bioreactor in the treatment of palm oil mill effluent. *Environmental technology*, 38(8):1005–1021.

Chauhan, A. and Chauhan, P. (2014). Powder xrd technique and its applications in science and technology. *J Anal Bioanal Tech*, 5(5):1–5.

Chen, M., Liu, S., Yuan, X., Li, Q. X., Wang, F., Xin, F., and Wen, B. (2021). Methane production and characteristics of the microbial community in the co-digestion of potato pulp waste and dairy manure amended with biochar. *Renewable Energy*, 163:357–367.

Chen, S., Zhang, J., and Wang, X. (2015). Effects of alkalinity sources on the stability of anaerobic digestion from food waste. *Waste Management & Research*, 33(11):1033–1040.

Chen, X., Romano, R. T., and Zhang, R. (2010a). Anaerobic digestion of food wastes for biogas production. *International Journal of Agricultural and Biological Engineering*, 3(4):61–72.

Chen, Y. and Cheng, J. J. (2007). Effect of potassium inhibition on the thermophilic anaerobic digestion of swine waste. *Water environment research*, 79(6):667–674.

Chen, Y., Cheng, J. J., and Creamer, K. S. (2008). Inhibition of anaerobic digestion process: a review. *Bioresource technology*, 99(10):4044–4064.

Chen, Y., Hu, W., Chen, P., and Ruan, R. (2017). Household biogas cdm project development in rural china. *Renewable and Sustainable Energy Reviews*, 67:184–191.

Chen, Y., Hu, W., and Sweeney, S. (2013). Resource availability for household biogas production in rural china. *Renewable and Sustainable Energy Reviews*, 25:655–659.

Chen, Y., Yang, G., Sweeney, S., and Feng, Y. (2010b). Household biogas use in rural china: A study of opportunities and constraints. *Renewable and sustainable energy reviews*, 14(1):545–549.

Chiu, S. L. and Lo, I. (2016). Reviewing the anaerobic digestion and co-digestion process of food waste from the perspectives on biogas production performance and environmental impacts. *Environmental Science and Pollution Research*, 23(24):24435–24450.

Choong, Y. Y., Norli, I., Abdullah, A. Z., and Yhaya, M. F. (2016). Impacts of trace element supplementation on the performance of anaerobic digestion process: A critical review. *Bioresource technology*, 209:369–379.

Chow, W. L., Chan, Y. J., and Chong, M. F. (2015). A new energy source from the anaerobic co-digestion (acd) treatment of oleo chemical effluent with glycerin pitch. *Asia-Pacific Journal of Chemical Engineering*, 10(4):556–564.

Christiaensen, L. and Heltberg, R. (2014). Greening china's rural energy: new insights on the potential of smallholder biogas. *Environment and Development Economics*, 19(1):8–29.

Chu, C.-F., Li, Y.-Y., Xu, K.-Q., Ebie, Y., Inamori, Y., and Kong, H.-N. (2008). A ph- and temperature-phased two-stage process for hydrogen and methane production from food waste. *International Journal of Hydrogen Energy*, 33(18):4739–4746.

Chua, K. H., Cheah, W., Tan, C., and Leong, Y. (2013). Harvesting biogas from wastewater sludge and food waste. In *IOP Conference Series: Earth and Environmental Science*, volume 16 (1), page 012118. IOP Publishing.

Chynoweth, D., Turick, C., Owens, J., Jerger, D. E., and Peck, M. (1993). Biochemical methane potential of biomass and waste feedstocks. *Biomass and bioenergy*, 5(1):95–111.

Coimbra-Araújo, C. H., Mariane, L., Júnior, C. B., Frigo, E. P., Frigo, M. S., Araújo, I. R. C., and Alves, H. J. (2014). Brazilian case study for biogas energy: Production of electric power, heat and automotive energy in condominiums of agroenergy. *Renewable and Sustainable Energy Reviews*, 40:826–839.

Cooney, M. J., Lewis, K., Harris, K., Zhang, Q., and Yan, T. (2016). Start up performance of biochar packed bed anaerobic digesters. *Journal of water process engineering*, 9:e7–e13.

Cozzolino, C., Bassetti, A., and Rondelli, P. (1992). Industrial application of semi-dry anaerobic digestion process of organic solid waste. In *Proc. Int. Symp. on Anaerobic Digestion of Solid Waste*, pages 551–555.

Cruz, I. A., Andrade, L. R. S., Bharagava, R. N., Nadda, A. K., Bilal, M., Figueiredo, R. T., and Ferreira, L. F. R. (2021). Valorization of cassava residues for biogas production in brazil based on the circular economy: An updated and comprehensive review. *Cleaner Engineering and Technology*, 4:100196.

Cruz Viggi, C., Rossetti, S., Fazi, S., Paiano, P., Majone, M., and Aulenta, F. (2014). Magnetite particles triggering a faster and more robust syntrophic pathway of methanogenic propionate degradation. *Environmental science & technology*, 48(13):7536–7543.

Curry, N. and Pillay, P. (2012). Biogas prediction and design of a food waste to energy system for the urban environment. *Renewable Energy*, 41:200–209.

Da Silva, C., Astals, S., Peces, M., Campos, J., and Guerrero, L. (2018). Biochemical methane potential (bmp) tests: Reducing test time by early parameter estimation. *Waste Management*, 71:19–24.

Dadaser-Celik, F., Azgin, S. T., and Yildiz, Y. S. (2016). Optimization of solid content, carbon/nitrogen ratio and food/inoculum ratio for biogas production from food waste. *Waste Management & Research*, 34(12):1241–1248.

Dahunsi, S., Osueke, C., Olayanju, T., and Lawal, A. (2019). Co-digestion of theobroma cacao (cocoa) pod husk and poultry manure for energy generation: Effects of pretreatment methods. *Bioresource technology*, 283:229–241.

Dai, X., Hu, C., Zhang, D., and Chen, Y. (2017). A new method for the simultaneous enhancement of methane yield and reduction of hydrogen sulfide production in the anaerobic digestion of waste activated sludge. *Bioresource Technology*, 243:914–921.

Daifullah, A. and Girgis, B. (1998). Removal of some substituted phenols by activated carbon obtained from agricultural waste. *Water research*, 32(4):1169–1177.

Dan-Asabe, B., Yaro, S., Yawas, D., and Aku, S. (2019). Statistical modeling and optimization of the flexural strength, water absorption and density of a doum palm-kankara clay filler hybrid composite. *Journal of King Saud University-Engineering Sciences*, 31(4):385–394.

Dar, R., Parmar, M., Dar, E., Sani, R., and Phutela, U. (2021). Biomethanation of agricultural residues: Potential, limitations and possible solutions. *Renewable and Sustainable Energy Reviews*, 135:110217.

Dareioti, M. A. and Kornaros, M. (2015). Anaerobic mesophilic co-digestion of ensiled sorghum, cheese whey and liquid cow manure in a two-stage cstr system: Effect of hydraulic retention time. *Bioresource technology*, 175:553–562.

Dasa, K. T., Westman, S. Y., Millati, R., Cahyanto, M. N., Taherzadeh, M. J., and Niklasson, C. (2016). Inhibitory effect of long-chain fatty acids on biogas production and the protective effect of membrane bioreactor. *BioMed Research International*, 2016.

Datong, Z. (1989). An analysis of domestic biogas storage installations in china. *Biomass*, 20(1-2):61–67.

Dechrugsa, S., Kantachote, D., and Chaiprapat, S. (2013). Effects of inoculum to substrate ratio, substrate mix ratio and inoculum source on batch co-digestion of grass and pig manure. *Bioresource Technology*, 146:101–108.

Deepanraj, B., Sivasubramanian, V., and Jayaraj, S. (2015). Experimental and kinetic study on anaerobic digestion of food waste: The effect of total solids and ph. *Journal of Renewable and Sustainable Energy*, 7(6):063104.

Deepanraj, B., Sivasubramanian, V., and Jayaraj, S. (2017). Effect of substrate pretreatment on biogas production through anaerobic digestion of food waste. *International Journal of Hydrogen Energy*, 42(42):26522–26528.

Deublein, D. and Steinhauser, A. (2011). *Biogas from waste and renewable resources: an introduction*. John Wiley & Sons.

Dhamodharan, K., Kumar, V., and Kalamdhad, A. S. (2015). Effect of different livestock dungs as inoculum on food waste anaerobic digestion and its kinetics. *Bioresource technology*, 180:237–241.

Ding, Z., Hu, X., Wan, Y., Wang, S., and Gao, B. (2016). Removal of lead, copper, cadmium, zinc, and nickel from aqueous solutions by alkali-modified biochar: Batch and column tests. *Journal of Industrial and Engineering Chemistry*, 33:239–245.

Dinh, P., Fujiwara, T., Phu, S. P., and Hoang, M. (2018). Kinetic of biogas production in co-digestion of vegetable waste, horse dung, and sludge by batch reactors. In *IOP Conference Series: Earth and Environmental Science*, volume 159, page 012041. IOP Publishing.

Dioha, I., Ikeme, C., Nafi'u, T., Soba, N., and Yusuf, M. (2013). Effect of carbon to nitrogen ratio on biogas production. *International Research Journal of Natural Sciences*, 1(3):1–10.

Divya, D., Gopinath, L., and Christy, P. M. (2015). A review on current aspects and diverse prospects for enhancing biogas production in sustainable means. *Renewable and sustainable energy reviews*, 42:690–699.

Dixon, M., Gallop, J. R., Lambert, S. C., Lardon, L., Healy, J. V., and Steyer, J.-P. (2007). Data mining to support anaerobic wwtp monitoring. *Control engineering practice*, 15(8):987–999.

Donoso-Bravo, A., Mailier, J., Martin, C., Rodríguez, J., Aceves-Lara, C. A., and Wouwer, A. V. (2011). Model selection, identification and validation in anaerobic digestion: a review. *Water research*, 45(17):5347–5364.

Donoso-Bravo, A., Pérez-Elvira, S., and Fdz-Polanco, F. (2010). Application of simplified models for anaerobic biodegradability tests. evaluation of pre-treatment processes. *Chemical Engineering Journal*, 160(2):607–614.

Drosg, B., Braun, R., Bochmann, G., and Al Saedi, T. (2013). Analysis and characterisation of biogas feedstocks. In *The biogas handbook*, pages 52–84. Elsevier.

Duan, X., Chen, Y., Yan, Y., Feng, L., Chen, Y., and Zhou, Q. (2019). New method

for algae comprehensive utilization: Algae-derived biochar enhances algae anaerobic fermentation for short-chain fatty acids production. *Bioresource technology*, 289:121637.

Duetz, W., Bouwmeester, H., Van Beilen, J., and Witholt, B. (2003). Biotransformation of limonene by bacteria, fungi, yeasts, and plants. *Applied microbiology and biotechnology*, 61:269–277.

Duku, M. H., Gu, S., and Hagan, E. B. (2011a). Biochar production potential in ghana—a review. *Renewable and Sustainable Energy Reviews*, 15(8):3539–3551.

Duku, M. H., Gu, S., and Hagan, E. B. (2011b). A comprehensive review of biomass resources and biofuels potential in ghana. *Renewable and sustainable energy reviews*, 15(1):404–415.

Ebner, J. H., Labatut, R. A., Lodge, J. S., Williamson, A. A., and Trabold, T. A. (2016). Anaerobic co-digestion of commercial food waste and dairy manure: Characterizing biochemical parameters and synergistic effects. *Waste management*, 52:286–294.

Edjekumhene, I., Atakora, S., Atta-Konadu, R., and Brew-Hammond, A. (2001). Implementation of renewable energy technologies-opportunities and barriers. ghana country study. *Office of Scientific and Technical Information (OSTI)*.

Edmund, C. O., Christopher, M. S., and Pascal, D. K. (2014). Characterization of palm kernel shell for materials reinforcement and water treatment. *Journal of Chemical Engineering and Materials Science*, 5(1):1–6.

Egwu, U., Uchenna-Egwu, B., and Ezeokpube, G. C. (2021). Ash-extracts from plant residues can provide sufficient buffering alkalinity and trace elements required to prevent operation instability to guarantee optimum methane yield during anaerobic digestion of agricultural residues. *Journal of Cleaner Production*, 318:128369.

El-Mashad, H., McGarvey, J., and Zhang, R. (2008). Performance and microbial analysis of anaerobic digesters treating food waste and dairy manure. *Biological Engineering Transactions*, 1(3):233–242.

El-Mashad, H. M. (2013). Kinetics of methane production from the codigestion of switchgrass and spirulina platensis algae. *Bioresource technology*, 132:305–312.

El-Mashad, H. M. and Zhang, R. (2010). Biogas production from co-digestion of dairy manure and food waste. *Bioresource technology*, 101(11):4021–4028.

Elbeshbishy, E., Nakhla, G., and Hafez, H. (2012). Biochemical methane potential (bmp) of food waste and primary sludge: influence of inoculum pre-incubation and inoculum source. *Bioresource technology*, 110:18–25.

Elmitwalli, T., Van Leeuwen, M., Kujawa-Roeleveld, K., Sanders, W., and Zeeman, G. (2006). Anaerobic biodegradability and digestion in accumulation systems for concentrated black water and kitchen organic-wastes. *Water science and technology*, 53(8):167–175.

Eskicioglu, C. and Ghorbani, M. (2011). Effect of inoculum/substrate ratio on mesophilic anaerobic digestion of bioethanol plant whole stillage in batch mode. *Process Biochemistry*, 46(8):1682–1687.

Esposito, G., Frunzo, L., Liotta, F., Panico, A., and Pirozzi, F. (2012). Bio-methane potential tests to measure the biogas production from the digestion and co-digestion of complex organic substrates. *The Open Environmental Engineering Journal*, 5(1).

Etuwe, C. N., Momoh, Y. O. L., and Iyagba, E. T. (2016). Development of mathematical models and application of the modified gompertz model for designing batch biogas reactors. *Waste and biomass valorization*, 7:543–550.

Ezema, I. and Aigbodion, V. (2020). Explicit microstructural evolution and electrochemical performance of value added palm kernel shell ash nanoparticle/a356 alloy composite. *Materialwissenschaft und Werkstofftechnik*, 51(3):324–329.

Ezemonye, L. I. N., Ogbomida, E. T., and Ajieh, M. U. (2018). *Contemporary Issues in Africa's Development: Whither the African Renaissance?* Cambridge Scholars Publishing.

Fabbri, D. and Torri, C. (2016). Linking pyrolysis and anaerobic digestion (py-ad) for the conversion of lignocellulosic biomass. *Current opinion in biotechnology*, 38:167–173.

Fagbohungbe, M. O., Herbert, B. M., Hurst, L., Ibeto, C. N., Li, H., Usmani, S. Q., and

Semple, K. T. (2017). The challenges of anaerobic digestion and the role of biochar in optimizing anaerobic digestion. *Waste management*, 61:236–249.

Fagbohungbe, M. O., Herbert, B. M., Hurst, L., Li, H., Usmani, S. Q., and Semple, K. T. (2016). Impact of biochar on the anaerobic digestion of citrus peel waste. *Bioresource technology*, 216:142–149.

Fagbohungbe, M. O., Herbert, B. M., Li, H., Ricketts, L., and Semple, K. T. (2015). The effect of substrate to inoculum ratios on the anaerobic digestion of human faecal material. *Environmental Technology & Innovation*, 3:121–129.

Fajobi, M., Lasode, O., Adeleke, A., Ikubanni, P., and Balogun, A. (2022). Investigation of physicochemical characteristics of selected lignocellulose biomass. *Scientific Reports*, 12(1):1–14.

Fanyin-Martin, A., Tamakloe, W., Antwi, E., Ami, J., Awarikabey, E., Apatti, J., Mensah, M., and Chandran, K. (2017). Chemical characterization of faecal sludge in the kumasi metropolis, ghana. *Gates Open Research*, 1(12):12.

Farooq, Z., REHMAN, S.-U., and Abid, M. (2013). Application of response surface methodology to optimize composite flour for the production and enhanced storability of leavened flat bread (naan). *Journal of food processing and preservation*, 37(5):939–945.

Fatoni, R. (2012). Product design of wheat straw polypropylene composite.

Fei-Baffoe, B., Nyankson, E. A., and Gorkeh-Miah, J. (2014). Municipal solid waste management in sekondi-takoradi metropolis, ghana. *Journal of Waste Management*, 2014.

Fei-Baffoe, B., Osei, K., Agyapong, E. A., and Nyankson, E. A. (2016). Co-composting of organic solid waste and sewage sludge–a waste management option for university campus. *International Journal of Environment*, 5(1):14–31.

Feng, L., Li, Y., Chen, C., Liu, X., Xiao, X., Ma, X., Zhang, R., He, Y., and Liu, G. (2013). Biochemical methane potential (bmp) of vinegar residue and the influence of feed to inoculum ratios on biogas production. *Bioresources*, 8(2):2487–2498.

Feng, L., Luo, J., and Chen, Y. (2015). Dilemma of sewage sludge treatment and disposal in china.

Feng, Y., Guo, Y., Yang, G., Qin, X., and Song, Z. (2012). Household biogas development in rural china: On policy support and other macro sustainable conditions. *Renewable and Sustainable Energy Reviews*, 16(8):5617–5624.

Fermoso, F. G., Bartacek, J., Jansen, S., and Lens, P. N. (2009). Metal supplementation to uasb bioreactors: from cell-metal interactions to full-scale application. *Science of the total environment*, 407(12):3652–3667.

Fermoso, F. G., Collins, G., Bartacek, J., and Lens, P. N. (2008). Zinc deprivation of methanol fed anaerobic granular sludge bioreactors. *Journal of Industrial Microbiology and Biotechnology*, 35(6):543–557.

Ferrer, I., Ponsá, S., Vázquez, F., and Font, X. (2008). Increasing biogas production by thermal (70 c) sludge pre-treatment prior to thermophilic anaerobic digestion. *Biochemical Engineering Journal*, 42(2):186–192.

Ferrer-Martí, L., Ferrer, I., Sánchez, E., and Garfí, M. (2018). A multi-criteria decision support tool for the assessment of household biogas digester programmes in rural areas. a case study in peru. *Renewable and Sustainable Energy Reviews*, 95:74–83.

Filer, J., Ding, H. H., and Chang, S. (2019). Biochemical methane potential (bmp) assay method for anaerobic digestion research. *Water*, 11(5):921.

Fisgativa, H., Tremier, A., and Dabert, P. (2016). Characterizing the variability of food waste quality: A need for efficient valorisation through anaerobic digestion. *Waste Management*, 50:264–274.

Flores, C. B. F. (2020). *Application of biochar as an additive to enhance biomethane potential in anaerobic digestion*. Rochester Institute of Technology.

Font-Palma, C. (2019). Methods for the treatment of cattle manure—a review. *C*, 5(2):27.

Forster-Carneiro, T., Pérez, M., and Romero, L. (2008). Influence of total solid and inoculum contents on performance of anaerobic reactors treating food waste. *Bioresource technology*, 99(15):6994–7002.

Franke-Whittle, I. H., Walter, A., Ebner, C., and Insam, H. (2014). Investigation into the effect of high concentrations of volatile fatty acids in anaerobic digestion on methanogenic communities. *Waste management*, 34(11):2080–2089.

Freitas, J. V., Nogueira, F. G., and Farinas, C. S. (2019). Coconut shell activated carbon as an alternative adsorbent of inhibitors from lignocellulosic biomass pretreatment. *Industrial Crops and Products*, 137:16–23.

Gaballah, E. S., Abdelkader, T. K., Luo, S., Yuan, Q., and Abomohra, A. E.-F. (2020). Enhancement of biogas production by integrated solar heating system: A pilot study using tubular digester. *Energy*, 193:116758.

Gao, M., Zhang, L., Florentino, A. P., and Liu, Y. (2019). Performance of anaerobic treatment of blackwater collected from different toilet flushing systems: Can we achieve both energy recovery and water conservation? *Journal of hazardous materials*, 365:44–52.

Garfí, M., Ferrer-Martí, L., Velo, E., and Ferrer, I. (2012). Evaluating benefits of low-cost household digesters for rural andean communities. *Renewable and Sustainable Energy Reviews*, 16(1):575–581.

Garoma, T. and Pappaterra, D. (2018). An investigation of ultrasound effect on digestate solubilization and methane yield. *Waste Management*, 71:728–733.

Garuti, M., Langone, M., Fabbri, C., and Piccinini, S. (2018). Methodological approach for trace elements supplementation in anaerobic digestion: Experience from full-scale agricultural biogas plants. *Journal of environmental management*, 223:348–357.

Gashaw, A. (2014). Anaerobic co-digestion of biodegradable municipal solid waste with human excreta for biogas production: A review. *American Journal of Applied Chemistry*, 2(4):55–62.

Gashaw, A. (2016). Co-digestion of municipal organic wastes with night soil and cow dung for biogas production: A review. *African Journal of Biotechnology*, 15(2):32–44.

Gashaw, A., Teshita, A., and Ethiopia, B. H. (2014). Co-digestion of ethiopian food waste with cow dung for biogas production. *BH Ethiopia*.

Gaskin, J. W., Speir, A., Morris, L., Ogden, L., Harris, K., Lee, D., and Das, K. (2007). Potential for pyrolysis char to affect soil moisture and nutrient status of a loamy sand soil. Georgia Institute of Technology.

Gavala, H. N., Yenal, U., Skiadas, I. V., Westermann, P., and Ahring, B. K. (2003). Mesophilic and thermophilic anaerobic digestion of primary and secondary sludge. effect of pre-treatment at elevated temperature. *Water research*, 37(19):4561–4572.

Georgacakis, D., Sievers, D., and Iannotti, E. (1982). Buffer stability in manure digesters. *Agricultural Wastes*, 4(6):427–441.

Ghani, W. and Idris, A. (2009). Preliminary study on biogas production of biogas from municipal solid waste (msw) leachate. *Journal of Engineering Science and Technology*, 4(4):374–380.

Ghimire, P. C. (2013). Snv supported domestic biogas programmes in asia and africa. *Renewable energy*, 49:90–94.

Gikas, P. (2007). Kinetic responses of activated sludge to individual and joint nickel (ni (ii)) and cobalt (co (ii)): an isobolographic approach. *Journal of hazardous materials*, 143(1-2):246–256.

Giwa, A. S., Xu, H., Chang, F., Wu, J., Li, Y., Ali, N., Ding, S., and Wang, K. (2019). Effect of biochar on reactor performance and methane generation during the anaerobic digestion of food waste treatment at long-run operations. *Journal of Environmental Chemical Engineering*, 7(4):103067.

Gl, H., Li, J., and Zhang, Y. (1993). Agricultural climate resources in china.

Gomec, C. Y., Kim, M., Ahn, Y., and Speece, R. E. (2002). The role of ph in mesophilic anaerobic sludge solubilization. *Journal of Environmental Science and Health, Part A*, 37(10):1871–1878.

Gómez-Quiroga, X., Aboudi, K., Fernández-Güelfo, L. A., Álvarez-Gallego, C. J., and Romero-García, L. I. (2020). Thermophilic anaerobic co-digestion of exhausted

sugar beet pulp with cow manure to boost the performance of the process: the effect of manure proportion. *Water*, 13(1):67.

González, J., Román, S., Encinar, J. M., and Martínez, G. (2009). Pyrolysis of various biomass residues and char utilization for the production of activated carbons. *Journal of Analytical and Applied Pyrolysis*, 85(1-2):134–141.

Gosens, J., Lu, Y., He, G., Bluemling, B., and Beckers, T. A. (2013). Sustainability effects of household-scale biogas in rural china. *Energy Policy*, 54:273–287.

Grando, R. L., de Souza Antune, A. M., Da Fonseca, F. V., Sánchez, A., Barrena, R., and Font, X. (2017). Technology overview of biogas production in anaerobic digestion plants: A european evaluation of research and development. *Renewable and Sustainable Energy Reviews*, 80:44–53.

Gratuito, M. K. B., Panyathanmaporn, T., Chumnanklang, R.-A., Sirinuntawittaya, N., and Dutta, A. (2008). Production of activated carbon from coconut shell: Optimization using response surface methodology. *Bioresource technology*, 99(11):4887–4895.

Grimberg, S., Hilderbrandt, D., Kinnunen, M., and Rogers, S. (2015). Anaerobic digestion of food waste through the operation of a mesophilic two-phase pilot scale digester–assessment of variable loadings on system performance. *Bioresource technology*, 178:226–229.

GSS, G. (2010). Population and housing census: Summary report of final results. *Accra: Ghana Statistical Service*.

Gu, J., Liu, R., Cheng, Y., Stanisavljevic, N., Li, L., Djatkov, D., Peng, X., and Wang, X. (2020). Anaerobic co-digestion of food waste and sewage sludge under mesophilic and thermophilic conditions: Focusing on synergistic effects on methane production. *Bioresource technology*, 301:122765.

Guarino, G., Carotenuto, C., Di Cristofaro, F., Papa, S., Morrone, B., and Minale, M. (2016). Does the c/n ratio really affect the bio-methane yield? a three years investigation of buffalo manure digestion. *Chemical Engineering Transactions*, 49:463–468.

Gunes, B., Stokes, J., Davis, P., Connolly, C., and Lawler, J. (2021). Optimisation of anaerobic digestion of pot ale after thermochemical pre-treatment through response surface methodology. *Biomass and Bioenergy*, 144:105902.

Gustavsson, J., Yekta, S. S., Sundberg, C., Karlsson, A., Ejlertsson, J., Skyllberg, U., and Svensson, B. H. (2013). Bioavailability of cobalt and nickel during anaerobic digestion of sulfur-rich stillage for biogas formation. *Applied energy*, 112:473–477.

Gwavuya, S., Abele, S., Barfuss, I., Zeller, M., and Müller, J. (2012). Household energy economics in rural ethiopia: A cost-benefit analysis of biogas energy. *Renewable Energy*, 48:202–209.

Gyamfi, S., Modjinou, M., and Djordjevic, S. (2015). Improving electricity supply security in ghana—the potential of renewable energy. *Renewable and sustainable energy reviews*, 43:1035–1045.

H Pishgar-Komleh, S., Keyhani, A., Mostofi-Sarkari, M., and Jafari, A. (2012). Application of response surface methodology for optimization of picker-husker harvesting losses in corn seed. *Iranian (Iranica) Journal of Energy & Environment*, 3(2).

Hadi, P., To, M.-H., Hui, C.-W., Lin, C. S. K., and McKay, G. (2015). Aqueous mercury adsorption by activated carbons. *Water Research*, 73:37–55.

Hafner, S. D., Koch, K., Carrere, H., Astals, S., Weinrich, S., and Rennuit, C. (2018). Software for biogas research: Tools for measurement and prediction of methane production. *SoftwareX*, 7:205–210.

Hagos, K., Zong, J., Li, D., Liu, C., and Lu, X. (2017). Anaerobic co-digestion process for biogas production: Progress, challenges and perspectives. *Renewable and sustainable energy reviews*, 76:1485–1496.

Haider, M. R., Yousaf, S., Malik, R. N., Visvanathan, C., et al. (2015). Effect of mixing ratio of food waste and rice husk co-digestion and substrate to inoculum ratio on biogas production. *Bioresource technology*, 190:451–457.

Hashimoto, A. G. (1989). Effect of inoculum/substrate ratio on methane yield and production rate from straw. *Biological wastes*, 28(4):247–255.

Hassanein, A., Lansing, S., and Tikekar, R. (2019). Impact of metal nanoparticles on biogas production from poultry litter. *Bioresource technology*, 275:200–206.

Heanes, D. (1984). Determination of total organic-c in soils by an improved chromic acid digestion and spectrophotometric procedure. *Communications in soil science and plant analysis*, 15(10):1191–1213.

Heubeck, S., Craggs, R., and Shilton, A. (2007). Influence of co2 scrubbing from biogas on the treatment performance of a high rate algal pond. *Water Science and Technology*, 55(11):193–200.

Hidalgo, D. and Martín-Marroquín, J. M. (2015). Biochemical methane potential of livestock and agri-food waste streams in the castilla y león region (spain). *Food Research International*, 73:226–233.

Ho, S.-H., Yang, Z.-k., Nagarajan, D., Chang, J.-S., Ren, N.-q., et al. (2017). High-efficiency removal of lead from wastewater by biochar derived from anaerobic digestion sludge. *Bioresource technology*, 246:142–149.

Holliger, C., Alves, M., Andrade, D., Angelidaki, I., Astals, S., Baier, U., Bougrier, C., Buffière, P., Carballa, M., De Wilde, V., et al. (2016). Towards a standardization of biomethane potential tests. *Water Science and Technology*, 74(11):2515–2522.

Hood-Nowotny, R. C. (2016). Biochar: A regional supply chain approach in view of climate change mitigation. In *Biochar: A Regional Supply Chain Approach in View of Climate Change Mitigation*, pages 351–367. Cambridge University Press.

Horváth, I. S., Tabatabaei, M., Karimi, K., and Kumar, R. (2016). Recent updates on biogas production-a review. *Biofuel research journal*, 3(2):394.

Hou, T., Chen, N., Tong, S., Li, B., He, Q., and Feng, C. (2019). Enhancement of rice bran as carbon and microbial sources on the nitrate removal from groundwater. *Biochemical Engineering Journal*, 148:185–194.

Hou, T., Zhao, J., Lei, Z., Shimizu, K., and Zhang, Z. (2020). Synergistic effects of rice straw and rice bran on enhanced methane production and process stability of anaerobic digestion of food waste. *Bioresource Technology*, 314:123775.

Huang, J. and Pinder, K. (1995). Effects of calcium on development of anaerobic acidogenic biofilms. *Biotechnology and bioengineering*, 45(3):212–218.

Huang, X., Yun, S., Zhu, J., Du, T., Zhang, C., and Li, X. (2016). Mesophilic anaerobic co-digestion of aloe peel waste with dairy manure in the batch digester: Focusing on mixing ratios and digestate stability. *Bioresource technology*, 218:62–68.

Hubenov, V., Mihaylova, S., and Simeonov, I. (2015). Anaerobic co-digestion of waste fruits and vegetables and swine manure in a pilot-scale bioreactor. *Bulgarian Chemical Communications*, 47(3):788–792.

Hussien, F. M., Hamad, A. J., and Faraj, J. J. (2020). Impact of adding cow dung with different ratios on anaerobic co-digestion of waste food for biogas production. *J. Mech. Eng. Res. Dev*, 43(7):213–221.

Hutton, G., Rehfuess, E., Tediosi, F., Weiss, S., Organization, W. H., et al. (2006). *Evaluation of the costs and benefits of household energy and health interventions at global and regional levels*. World Health Organization.

Ibikunle, R., Titiladunayo, I., Akinnuli, B., Dahunsi, S., and Olayanju, T. (2019). Estimation of power generation from municipal solid wastes: A case study of ilorin metropolis, nigeria. *Energy Reports*, 5:126–135.

Igoni, A. H., Ayotamuno, M., Eze, C., Ogaji, S., and Probert, S. (2008). Designs of anaerobic digesters for producing biogas from municipal solid-waste. *Applied energy*, 85(6):430–438.

Ihoeghian, N. A., Amenaghawon, A. N., Ajieh, M. U., Oshoma, C. E., Ogofure, A., Erhunmwunse, N. O., Edosa, V. I., Tongo, I., Obuekwe, I. S., Isagba, E. S., et al. (2022). Anaerobic co-digestion of cattle rumen content and food waste for biogas production: Establishment of co-digestion ratios and kinetic studies. *Bioresource Technology Reports*, 18:101033.

Ihoeghian, N. A., Amenaghawon, A. N., Ogofure, A., Oshoma, C. E., Ajieh, M. U., Erhunmwunse, N. O., Obuekwe, I. S., Edosa, V. I., Tongo, I., Emokaro, C., et al. (2023). Biochar-facilitated batch co-digestion of food waste and cattle rumen content: An assessment of process stability, kinetic studies, and pathogen fate. *Green Technologies and Sustainability*, page 100035.

IkhtiarBakti, A. and Gareso, P. L. (2018). Characterization of active carbon prepared from coconuts shells using ftir, xrd and sem techniques. *J. Ilm. Pendidik. Fis. Al-Biruni*, 7:33–39.

Ikpe, A., Imonitie, D., and Ndon, A. (2019). Investigation of biogas energy derivation from anaerobic digestion of different local food wastes in nigeria. *Academic Platform Journal of Engineering and Science*, 7(2):332–340.

Ikubanni, P., Oki, M., Adeleke, A., Adediran, A., and Adesina, O. (2020). Influence of temperature on the chemical compositions and microstructural changes of ash formed from palm kernel shell. *Results in Engineering*, 8:100173.

Imoisili, P. E., Ukoba, K. O., and Jen, T.-C. (2020). Synthesis and characterization of amorphous mesoporous silica from palm kernel shell ash. *boletín de la sociedad española de cerámica y vidrio*, 59(4):159–164.

Iqbal, S. A., Rahaman, S., Rahman, M., and Yousuf, A. (2014). Anaerobic digestion of kitchen waste to produce biogas. *Procedia Engineering*, 90:657–662.

Izumi, K., Okishio, Y.-k., Nagao, N., Niwa, C., Yamamoto, S., and Toda, T. (2010). Effects of particle size on anaerobic digestion of food waste. *International biodeterioration & biodegradation*, 64(7):601–608.

Jabarullah, N. H., Kamal, A. S., and Othman, R. (2021). A modification of palm waste lignocellulosic materials into biographite using iron and nickel catalyst. *Processes*, 9(6):1079.

Jackson-Moss, C., Duncan, J., and Cooper, D. (1989). The effect of calcium on anaerobic digestion. *Biotechnology Letters*, 11(3):219–224.

Jain, A., Balasubramanian, R., and Srinivasan, M. (2015). Production of high surface area mesoporous activated carbons from waste biomass using hydrogen peroxide-mediated hydrothermal treatment for adsorption applications. *Chemical Engineering Journal*, 273:622–629.

Jang, H. M., Choi, Y.-K., and Kan, E. (2018). Effects of dairy manure-derived biochar on psychrophilic, mesophilic and thermophilic anaerobic digestions of dairy manure. *Bioresource technology*, 250:927–931.

Jeuland, M., Kone, D., and Strauss, M. (2004). Private sector management of fecal sludge: A model for the future. *Focus of an Innovative Planning Experience in Bamako, Mali. Swiss Federal Institute of Aquatic Science and Technology (EAWAG), Duebendorf, Switzerland*.

Jiang, Y., Dennehy, C., Lawlor, P. G., Hu, Z., McCabe, M., Cormican, P., Zhan, X., and Gardiner, G. E. (2018). Inhibition of volatile fatty acids on methane production kinetics during dry co-digestion of food waste and pig manure. *Waste Management*, 79:302–311.

Kabir, H., Yegbemey, R. N., and Bauer, S. (2013). Factors determinant of biogas adoption in bangladesh. *Renewable and Sustainable Energy Reviews*, 28:881–889.

Kadam, R. and Panwar, N. (2017). Recent advancement in biogas enrichment and its applications. *Renewable and Sustainable Energy Reviews*, 73:892–903.

Kafle, G. K. and Chen, L. (2016). Comparison on batch anaerobic digestion of five different livestock manures and prediction of biochemical methane potential (bmp) using different statistical models. *Waste management*, 48:492–502.

Kafle, G. K. and Kim, S.-H. (2012). Kinetic study of the anaerobic digestion of swine manure at mesophilic temperature: a lab scale batch operation. *Journal of Biosystems Engineering*, 37(4):233–244.

Kafle, G. K. and Kim, S. H. (2013). Anaerobic treatment of apple waste with swine manure for biogas production: batch and continuous operation. *Applied Energy*, 103:61–72.

Kafle, G. K., Kim, S. H., and Sung, K. I. (2012). Batch anaerobic co-digestion of kimchi factory waste silage and swine manure under mesophilic conditions. *Bioresource technology*, 124:489–494.

Kallistova, A. Y., Goel, G., and Nozhevnikova, A. (2014). Microbial diversity of methanogenic communities in the systems for anaerobic treatment of organic waste. *Microbiology*, 83(5):462–483.

Kareem, B., Oladosu, K. O., Alade, A. O., and Durowoju, M. O. (2018). Optimization of combustion characteristics of palm kernel-based biofuel for grate furnace. *International Journal of Energy and Environmental Engineering*, 9:457–472.

Karekezi, S. (2002). Renewables in africa—meeting the energy needs of the poor. *Energy policy*, 30(11-12):1059–1069.

Karki, R., Chuenchart, W., Surendra, K., Shrestha, S., Raskin, L., Sung, S., Hashimoto, A., and Khanal, S. K. (2021). Anaerobic co-digestion: Current status and perspectives. *Bioresource Technology*, 330:125001.

Karki, R., Chuenchart, W., Surendra, K., Sung, S., Raskin, L., and Khanal, S. K. (2022). Anaerobic co-digestion of various organic wastes: Kinetic modeling and synergistic impact evaluation. *Bioresource Technology*, 343:126063.

Katz, S. and Jenniss, S. (1983). Regulatory compliance monitoring by atomic absorption spectroscopy.

Kaushal, R., Sandhu, S., and Soni, M. K. (2022). Anaerobic co-digestion of food waste, algae, and cow dung for biogas yield enhancement as a prospective approach for environmental sustainability. *Sustainable Energy Technologies and Assessments*, 52:102236.

Kelebe, H. E., Ayimut, K. M., Berhe, G. H., and Hintsa, K. (2017). Determinants for adoption decision of small scale biogas technology by rural households in tigray, ethiopia. *Energy Economics*, 66:272–278.

Kemausuor, F., Adaramola, M. S., and Morken, J. (2018). A review of commercial biogas systems and lessons for africa. *Energies*, 11(11):2984.

Ketibuah, E., Asase, M., Yusif, S., Mensah, M., and Fischer, K. (2004). Comparative analysis of household waste in the cities of stuttgart and kumasi–options for waste recycling and treatment in kumasi. In *Proceedings of the 19th international CODATA Conference*, pages 1–8.

Khalid, A., Arshad, M., Anjum, M., Mahmood, T., and Dawson, L. (2011). The anaerobic digestion of solid organic waste. *Waste management*, 31(8):1737–1744.

Khan, E. U., Mainali, B., Martin, A., and Silveira, S. (2014). Techno-economic analysis of small scale biogas based polygeneration systems: Bangladesh case study. *Sustainable Energy Technologies and Assessments*, 7:68–78.

Khan, H., Yerramilli, A. S., D'Oliveira, A., Alford, T. L., Boffito, D. C., and Patience, G. S. (2020). Experimental methods in chemical engineering: X-ray diffraction spectroscopy—xrd. *The Canadian Journal of Chemical Engineering*, 98(6):1255–1266.

Khoufi, S., Louhichi, A., and Sayadi, S. (2015). Optimization of anaerobic co-digestion of olive mill wastewater and liquid poultry manure in batch condition and semi-continuous jet-loop reactor. *Bioresource Technology*, 182:67–74.

Kida, K., Shigematsu, T., Kijima, J., Numaguchi, M., Mochinaga, Y., Abe, N., and Morimura, S. (2001). Influence of ni2+ and co2+ on methanogenic activity and the amounts of coenzymes involved in methanogenesis. *Journal of Bioscience and Bioengineering*, 91(6):590–595.

Kigozi, R., Aboyade, A., and Muzenda, E. (2013). Biogas production using the organic fraction of municipal solid waste as feedstock. *World*, 5:6.

Kim, J., Baek, G., Kim, J., and Lee, C. (2019a). Energy production from different organic wastes by anaerobic co-digestion: Maximizing methane yield versus maximizing synergistic effect. *Renewable energy*, 136:683–690.

Kim, J., Kim, J., and Lee, C. (2019b). Anaerobic co-digestion of food waste, human feces, and toilet paper: methane potential and synergistic effect. *Fuel*, 248:189–195.

Kim, J., Park, C., Kim, T.-H., Lee, M., Kim, S., Kim, S.-W., and Lee, J. (2003). Effects of various pretreatments for enhanced anaerobic digestion with waste activated sludge. *Journal of bioscience and bioengineering*, 95(3):271–275.

Kim, T. Y., Lee, J., and Kim, J. Y. (2014). Evaluating methane potential and kinetics of anaerobic co-digestion with feces and food waste. The 2014 World Congress on Advances in Civil Environmental and Material Research (ACEM14).

Kiran, E. U., Trzcinski, A. P., Ng, W. J., and Liu, Y. (2014). Bioconversion of food waste to energy: A review. *Fuel*, 134:389–399.

KITE (2008). Feasibility study report on domestic biogas in ghana. *Kumasi Institute of Technology Energy and Environment, Ghana: Submitted to Shell Foundation*.

Kizito, S., Luo, H., Wu, S., Ajmal, Z., Lv, T., and Dong, R. (2017). Phosphate recovery from liquid fraction of anaerobic digestate using four slow pyrolyzed biochars: Dynamics of adsorption, desorption and regeneration. *Journal of Environmental Management*, 201:260–267.

Kizito, S., Wu, S., Kirui, W. K., Lei, M., Lu, Q., Bah, H., and Dong, R. (2015). Evaluation of slow pyrolyzed wood and rice husks biochar for adsorption of ammonium nitrogen from piggery manure anaerobic digestate slurry. *Science of the Total Environment*, 505:102–112.

Kjeldsen, P., Barlaz, M. A., Rooker, A. P., Baun, A., Ledin, A., and Christensen, T. H. (2002). Present and long-term composition of msw landfill leachate: a review. *Critical reviews in environmental science and technology*, 32(4):297–336.

Kjeldsen, P. and Christophersen, M. (2001). Composition of leachate from old landfills in denmark. *Waste Management & Research*, 19(3):249–256.

Koch, K., Hafner, S. D., Weinrich, S., and Astals, S. (2019). Identification of critical problems in biochemical methane potential (bmp) tests from methane production curves. *Frontiers in Environmental Science*, page 178.

Koch, K., Plabst, M., Schmidt, A., Helmreich, B., and Drewes, J. E. (2016). Co-digestion of food waste in a municipal wastewater treatment plant: comparison of batch tests and full-scale experiences. *Waste Management*, 47:28–33.

Kohmuean, P., Boonrod, N., and Wongkoblap, A. (2020). Biogas production from cassava waste: effect of concentration. In *IOP conference series: materials science and engineering*, volume 778 (1), page 012115. IOP Publishing.

Komnitsas, K., Zaharaki, D., Pyliotis, I., Vamvuka, D., and Bartzas, G. (2015). Assessment of pistachio shell biochar quality and its potential for adsorption of heavy metals. *Waste and Biomass Valorization*, 6:805–816.

Kondusamy, D. and Kalamdhad, A. S. (2014). Pre-treatment and anaerobic digestion

of food waste for high rate methane production–a review. *Journal of Environmental Chemical Engineering*, 2(3):1821–1830.

Koné, D. and Strauss, M. (2004). Low-cost options for treating faecal sludges (fs) in developing countries–challenges and performance. In *9th International IWA Specialist Group Conference on Wetlands Systems for Water Pollution Control and to the 6th International IWA Specialist Group Conference on Waste Stabilisation Ponds, Avignon, France*, volume 27.

Kong, S.-H., Loh, S. K., Bachmann, R. T., Zainal, H., Cheong, K., et al. (2019). Palm kernel shell biochar production, characteristics and carbon sequestration potential. *J. Oil Palm Res*, 31(3):508–520.

Koocheki, A., Taherian, A. R., Razavi, S. M., and Bostan, A. (2009). Response surface methodology for optimization of extraction yield, viscosity, hue and emulsion stability of mucilage extracted from lepidium perfoliatum seeds. *Food Hydrocolloids*, 23(8):2369–2379.

Kossmann, W. and Pönitz, U. (1999). Biogas-country reports. *Biogas Digest-Information and Advisory Service on Appropriate Technology*, pages 48–49.

Kouzuma, A., Kato, S., and Watanabe, K. (2015). Microbial interspecies interactions: recent findings in syntrophic consortia. *Frontiers in microbiology*, 6:477.

Krakat, N., Demirel, B., Anjum, R., and Dietz, D. (2017). Methods of ammonia removal in anaerobic digestion: a review. *Water Science and Technology*, 76(8):1925–1938.

Krishania, M., Vijay, V., and Chandra, R. (2013). Methane fermentation and kinetics of wheat straw pretreated substrates co-digested with cattle manure in batch assay. *Energy*, 57:359–367.

Kuffour, A., Awuah, E., Anyemedu, F., Strauss, M., Koné, D., and Cofie, O. (2009). Effect of using different particle sizes of sand as filter media for dewatering faecal sludge. *Desalination*, 248(1-3):308–314.

Kugelman, I. J. and McCarty, P. L. (1965). Cation toxicity and stimulation in anaerobic waste treatment. *Journal (Water Pollution Control Federation)*, pages 97–116.

Kujawa-Roeleveld, K., Elmitwalli, T., and Zeeman, G. (2006). Enhanced primary treatment of concentrated black water and kitchen residues within desar concept using two types of anaerobic digesters. *Water Science and Technology*, 53(9):159–168.

Kumar, M., Dutta, S., You, S., Luo, G., Zhang, S., Show, P. L., Sawarkar, A. D., Singh, L., and Tsang, D. C. (2021). A critical review on biochar for enhancing biogas production from anaerobic digestion of food waste and sludge. *Journal of Cleaner Production*, 305:127143.

Kyere, R., Addaney, M., and Akudugu, J. A. (2019). Decentralization and solid waste management in urbanizing ghana: moving beyond the status quo. In *Municipal Solid Waste Management*. IntechOpen.

Labatut, R. and Gooch, C. (2012). Monitoring of anaerobic digestion process to optimize performanceand prevent system failure. In *In Proceedings of the Got Manure? Enhancing Environmental and Economic Sustainability*. Citeseer.

Labatut, R. A. and Scott, N. R. (2008). Experimental and predicted methane yields from the anaerobic co-digestion of animal manure with complex organic substrates. *ASABE Paper*, 08(085087).

Ladygina, N. and Rineau, F. (2013). *Biochar and soil biota*. CRC Press.

Lam, J., ter Heegde, F., and Teune, B. (2011). Domestic biogas compact course, technology and mass-dissemination experiences from asia. *Hand-out for students. Germany: University of Oldenburg*.

Langenhoff, A. A., Brouwers-Ceiler, D. L., Engelberting, J. H., Quist, J. J., Wolkenfelt, J. G., Zehnder, A. J., and Schraa, G. (1997). Microbial reduction of manganese coupled to toluene oxidation. *FEMS Microbiology Ecology*, 22(2):119–127.

Latha, K., Velraj, R., Shanmugam, P., and Sivanesan, S. (2019). Mixing strategies of high solids anaerobic co-digestion using food waste with sewage sludge for enhanced biogas production. *Journal of cleaner production*, 210:388–400.

Latinwo, G. and Agarry, S. (2015a). Modelling the kinetics of biogas generation from

mesophilic anaerobic co-digestion of sewage sludge with municipal organic waste. *simulation*, 31.

Latinwo, G. K. and Agarry, S. E. (2015b). Modelling the kinetics of biogas production from mesophilic anaerobic co-digestion of cow dung with plantain peels. *International Journal of Renewable Energy Development*, 4(1).

Lavagnolo, M. C., Girotto, F., Hirata, O., and Cossu, R. (2017). Lab-scale co-digestion of kitchen waste and brown water for a preliminary performance evaluation of a decentralized waste and wastewater management. *Waste Management*, 66:155–160.

Lawal, A., Dzivama, A., and Wasinda, M. (2016). Effect of inoculum to substrate ratio on biogas production of sheep paunch manure. *Research in Agricultural Engineering*, 62(1):8–14.

Lawrence, A. W. and McCarty, P. L. (1969). Kinetics of methane fermentation in anaerobic treatment. *Journal (Water Pollution Control Federation)*, pages R1–R17.

Le Man, H., Behera, S., and Park, H. (2010). Optimization of operational parameters for ethanol production from korean food waste leachate. *International Journal of Environmental Science & Technology*, 7:157–164.

Lee, Y., Park, J., Ryu, C., Gang, K. S., Yang, W., Park, Y.-K., Jung, J., and Hyun, S. (2013). Comparison of biochar properties from biomass residues produced by slow pyrolysis at 500 c. *Bioresource technology*, 148:196–201.

Lemmer, A., Merkle, W., Baer, K., and Graf, F. (2017). Effects of high-pressure anaerobic digestion up to 30 bar on ph-value, production kinetics and specific methane yield. *Energy*, 138:659–667.

Lesteur, M., Bellon-Maurel, V., Gonzalez, C., Latrille, E., Roger, J., Junqua, G., and Steyer, J.-P. (2010). Alternative methods for determining anaerobic biodegradability: a review. *Process biochemistry*, 45(4):431–440.

Li, C. and Fang, H. H. (2007). Inhibition of heavy metals on fermentative hydrogen production by granular sludge. *Chemosphere*, 67(4):668–673.

Li, C., Nges, I. A., Lu, W., and Wang, H. (2017). Assessment of the degradation efficiency of full-scale biogas plants: A comparative study of degradation indicators. *Bioresource technology*, 244:304–312.

Li, D., Liu, S., Mi, L., Li, Z., Yuan, Y., Yan, Z., and Liu, X. (2015a). Effects of feedstock ratio and organic loading rate on the anaerobic mesophilic co-digestion of rice straw and cow manure. *Bioresource Technology*, 189:319–326.

Li, K., Liu, R., and Sun, C. (2015b). Comparison of anaerobic digestion characteristics and kinetics of four livestock manures with different substrate concentrations. *Bioresource technology*, 198:133–140.

Li, L., Qiu, Y., Huang, J., Li, F., and Sheng, G. D. (2014). Mechanisms and factors influencing adsorption of microcystin-lr on biochars. *Water, Air, & Soil Pollution*, 225(12):1–10.

Li, L., Zou, D., Xiao, Z., Zeng, X., Zhang, L., Jiang, L., Wang, A., Ge, D., Zhang, G., and Liu, F. (2019a). Biochar as a sorbent for emerging contaminants enables improvements in waste management and sustainable resource use. *Journal of Cleaner Production*, 210:1324–1342.

Li, P., Li, W., Sun, M., Xu, X., Zhang, B., and Sun, Y. (2018a). Evaluation of biochemical methane potential and kinetics on the anaerobic digestion of vegetable crop residues. *Energies*, 12(1):26.

Li, P., Liu, Z., Zhao, M., Dai, X., and Ruan, W. (2020a). Evaluation of biogas performance and process stability from food, kitchen, and fruit/vegetable waste by mono-, co-, and tridigestion. *Energy & Fuels*, 34(10):12734–12742.

Li, Q., Xu, M., Wang, G., Chen, R., Qiao, W., and Wang, X. (2018b). Biochar assisted thermophilic co-digestion of food waste and waste activated sludge under high feedstock to seed sludge ratio in batch experiment. *Bioresource technology*, 249:1009–1016.

Li, R., Chen, S., and Li, X. (2010). Biogas production from anaerobic co-digestion of food waste with dairy manure in a two-phase digestion system. *Applied biochemistry and biotechnology*, 160(2):643–654.

Li, W., Loh, K.-C., Zhang, J., Tong, Y. W., and Dai, Y. (2018c). Two-stage anaerobic digestion of food waste and horticultural waste in high-solid system. *Applied Energy*, 209:400–408.

Li, X., Huang, J., Liu, Y., Huang, T., Maurer, C., and Kranert, M. (2019b). Effects of salt on anaerobic digestion of food waste with different component characteristics and fermentation concentrations. *Energies*, 12(18):3571.

Li, X., Wang, Y., Zhang, G., Sun, W., Bai, Y., Zheng, L., Han, X., and Wu, L. (2019c). Influence of mg-promoted ni-based catalyst supported on coconut shell carbon for co2 methanation. *ChemistrySelect*, 4(3):838–845.

Li, Y., Jin, Y., Li, H., Borrion, A., Yu, Z., and Li, J. (2018d). Kinetic studies on organic degradation and its impacts on improving methane production during anaerobic digestion of food waste. *Applied energy*, 213:136–147.

Li, Y., Xing, B., Ding, Y., Han, X., and Wang, S. (2020b). A critical review of the production and advanced utilization of biochar via selective pyrolysis of lignocellulosic biomass. *Bioresource Technology*, 312:123614.

Li, Y., Zhang, R., Liu, X., Chen, C., Xiao, X., Feng, L., He, Y., and Liu, G. (2013). Evaluating methane production from anaerobic mono-and co-digestion of kitchen waste, corn stover, and chicken manure. *Energy & Fuels*, 27(4):2085–2091.

Li, Y., Zhao, J., Krooneman, J., and Euverink, G. J. W. (2021). Strategies to boost anaerobic digestion performance of cow manure: Laboratory achievements and their full-scale application potential. *Science of the Total Environment*, 755:142940.

Lim, J., Chen, C.-L., Ho, I., and Wang, J.-Y. (2013). Study of microbial community and biodegradation efficiency for single-and two-phase anaerobic co-digestion of brown water and food waste. *Bioresource technology*, 147:193–201.

Lim, J. W. (2011). Anaerobic co-digestion of brown water and food waste for energy recovery. In *11th edition of the World Wide Workshop for Young Environmental Scientists (WWW-YES-2011)-Urban Waters: resource or risks?*, volume 1 (14).

Lim, Y. F., Chan, Y. J., Abakr, Y. A., Sethu, V., Selvarajoo, A., Singh, A., Lee, J., and Gareth, M. (2022). Evaluation of potential feedstock for biogas production via

anaerobic digestion in malaysia: kinetic studies and economics analysis. *Environmental technology*, 43(16):2492–2509.

Lin, C.-Y. (1992). Effect of heavy metals on volatile fatty acid degradation in anaerobic digestion. *Water Research*, 26(2):177–183.

Lin, C.-Y. and Shei, S.-H. (2008). Heavy metal effects on fermentative hydrogen production using natural mixed microflora. *International Journal of Hydrogen Energy*, 33(2):587–593.

Lin, D., Kakizono, T., Nishio, N., and Nagai, S. (1990). Enhanced cytochrome formation and stimulate methanogenesis rate by the increased ferrous concentrations in methanosarcina barkeri culture. *FEMS microbiology letters*, 68(1-2):89–92.

Lin, J., Zuo, J., Gan, L., Li, P., Liu, F., Wang, K., Chen, L., and Gan, H. (2011). Effects of mixture ratio on anaerobic co-digestion with fruit and vegetable waste and food waste of china. *Journal of Environmental Sciences*, 23(8):1403–1408.

Lindmark, J., Thorin, E., Fdhila, R. B., and Dahlquist, E. (2014). Effects of mixing on the result of anaerobic digestion. *Renewable and Sustainable Energy Reviews*, 40:1030–1047.

Linville, J. L., Shen, Y., Ignacio-de Leon, P. A., Schoene, R. P., and Urgun-Demirtas, M. (2017). In-situ biogas upgrading during anaerobic digestion of food waste amended with walnut shell biochar at bench scale. *Waste Management & Research*, 35(6):669–679.

Lippert, T., Bandelin, J., Musch, A., Drewes, J. E., and Koch, K. (2018). Energy-positive sewage sludge pre-treatment with a novel ultrasonic flatbed reactor at low energy input. *Bioresource technology*, 264:298–305.

Liu, B., Guo, W., Wang, H., Si, Q., Zhao, Q., Luo, H., and Ren, N. (2020). B-doped graphitic porous biochar with enhanced surface affinity and electron transfer for efficient peroxydisulfate activation. *Chemical Engineering Journal*, 396:125119.

Liu, F., Rotaru, A.-E., Shrestha, P. M., Malvankar, N. S., Nevin, K. P., and Lovley, D. R. (2012). Promoting direct interspecies electron transfer with activated carbon. *Energy & Environmental Science*, 5(10):8982–8989.

Liu, L. and Fan, S. (2018). Removal of cadmium in aqueous solution using wheat straw biochar: effect of minerals and mechanism. *Environmental science and pollution research*, 25(9):8688–8700.

Liu, M., Wei, Y., and Leng, X. (2021). Improving biogas production using additives in anaerobic digestion: A review. *Journal of Cleaner Production*, 297:126666.

Liu, Y. (1996). Bioenergetic interpretation on the s0x0 ratio in substrate-sufficient batch culture. *Water Research*, 30(11):2766–2770.

Liu, Y., He, Z., and Uchimiya, M. (2015). Comparison of biochar formation from various agricultural by-products using ftir spectroscopy. *Modern Applied Science*, 9(4):246.

Liu, Z. and Lv, J. (2016). The effect of total solids concentration and temperature on biogas production by anaerobic digestion. *Energy sources, Part A: Recovery, utilization, and environmental effects*, 38(23):3534–3541.

Lo, H., Chiang, C., Tsao, H., Pai, T., Liu, M., Kurniawan, T., Chao, K., Liou, C., Lin, K., Chang, C., et al. (2012). Effects of spiked metals on the msw anaerobic digestion. *Waste management & research*, 30(1):32–48.

Lohani, S. P. and Havukainen, J. (2018). Anaerobic digestion: factors affecting anaerobic digestion process. In *Waste Bioremediation*, pages 343–359. Springer.

Lonappan, L., Rouissi, T., Brar, S. K., Verma, M., and Surampalli, R. Y. (2018). Adsorption of diclofenac onto different biochar microparticles: Dataset–characterization and dosage of biochar. *Data in brief*, 16:460–465.

Longjan, G. G. and Dehouche, Z. (2020). Biogas production potential of co-digested food waste and water hyacinth common to the niger delta. *Biofuels*, 11(3):277–287.

López, I., Benzo, M., Passeggi, M., and Borzacconi, L. (2021). A simple kinetic model applied to anaerobic digestion of cow manure. *Environmental Technology*, 42(22):3451–3462.

Lovley, D. R. (2017). Syntrophy goes electric: direct interspecies electron transfer. *Annual review of microbiology*, 71:643–664.

Lü, F., Hao, L., Zhu, M., Shao, L., and He, P. (2012). Initiating methanogenesis of vegetable waste at low inoculum-to-substrate ratio: importance of spatial separation. *Bioresource technology*, 105:169–173.

Lü, F., Liu, Y., Shao, L., and He, P. (2019). Powdered biochar doubled microbial growth in anaerobic digestion of oil. *Applied Energy*, 247:605–614.

Lü, F., Luo, C., Shao, L., and He, P. (2016). Biochar alleviates combined stress of ammonium and acids by firstly enriching methanosaeta and then methanosarcina. *Water research*, 90:34–43.

Luo, C., Lü, F., Shao, L., and He, P. (2015). Application of eco-compatible biochar in anaerobic digestion to relieve acid stress and promote the selective colonization of functional microbes. *Water research*, 68:710–718.

Luo, G. and Angelidaki, I. (2012). Integrated biogas upgrading and hydrogen utilization in an anaerobic reactor containing enriched hydrogenotrophic methanogenic culture. *Biotechnology and bioengineering*, 109(11):2729–2736.

Luo, T., Khoshnevisan, B., Huang, R., Chen, Q., Mei, Z., Pan, J., and Liu, H. (2020). Analysis of revolution in decentralized biogas facilities caused by transition in chinese rural areas. *Renewable and Sustainable Energy Reviews*, 133:110133.

Luostarinen, S., Normak, A., Edström, M., et al. (2011). Overview of biogas technology. *Overview of Biogas Technology. Baltic manure WP6 Energy potentials*, 47.

Luste, S., Luostarinen, S., and Sillanpää, M. (2009). Effect of pre-treatments on hydrolysis and methane production potentials of by-products from meat-processing industry. *Journal of hazardous materials*, 164(1):247–255.

Luz, F. C., Cordiner, S., Manni, A., Mulone, V., and Rocco, V. (2018). Biochar characteristics and early applications in anaerobic digestion-a review. *Journal of Environmental Chemical Engineering*, 6(2):2892–2909.

Lwiza, F., Mugisha, J., Walekhwa, P. N., Smith, J., and Balana, B. (2017). Disadoption of household biogas technologies in central uganda. *Energy for Sustainable Development*, 37:124–132.

Lybæk, R., Ackom, E. K., and Bensah, E. C. (2017). A review of biogas application across continents-case study of thailand, ghana and denmark. In *12th GMSARN International Conference*, page 6.

Ma, H. (2003). Main technical points for household methane pool gas production. *Renew Energ*, 108:29–30.

Ma, J., Mungoni, L. J., Verstraete, W., and Carballa, M. (2009). Maximum removal rate of propionic acid as a sole carbon source in uasb reactors and the importance of the macro-and micro-nutrients stimulation. *Bioresource Technology*, 100(14):3477–3482.

Ma, J., Pan, J., Qiu, L., Wang, Q., and Zhang, Z. (2019a). Biochar triggering multipath methanogenesis and subdued propionic acid accumulation during semi-continuous anaerobic digestion. *Bioresource technology*, 293:122026.

Ma, J., Zhao, Q.-B., Laurens, L. L., Jarvis, E. E., Nagle, N. J., Chen, S., and Frear, C. S. (2015). Mechanism, kinetics and microbiology of inhibition caused by long-chain fatty acids in anaerobic digestion of algal biomass. *Biotechnology for biofuels*, 8(1):1–12.

Ma, X., Yu, M., Yang, M., Gao, M., Wu, C., and Wang, Q. (2019b). Synergistic effect from anaerobic co-digestion of food waste and sophora flavescens residues at different co-substrate ratios. *Environmental Science and Pollution Research*, 26(36):37114–37124.

Manyà, J. J. (2012). Pyrolysis for biochar purposes: a review to establish current knowledge gaps and research needs. *Environmental science & technology*, 46(15):7939–7954.

Manyà, J. J., Ortigosa, M. A., Laguarta, S., and Manso, J. A. (2014). Experimental study on the effect of pyrolysis pressure, peak temperature, and particle size on the potential stability of vine shoots-derived biochar. *Fuel*, 133:163–172.

Mao, C., Feng, Y., Wang, X., and Ren, G. (2015). Review on research achievements of biogas from anaerobic digestion. *Renewable and sustainable energy reviews*, 45:540–555.

Martens, E. C., Koropatkin, N. M., Smith, T. J., and Gordon, J. I. (2009). Complex glycan catabolism by the human gut microbiota: the bacteroidetes sus-like paradigm. *Journal of Biological Chemistry*, 284(37):24673–24677.

Martínez, E. J., Rosas, J. G., Sotres, A., Moran, A., Cara, J., Sánchez, M. E., and Gómez, X. (2018). Codigestion of sludge and citrus peel wastes: Evaluating the effect of biochar addition on microbial communities. *Biochemical Engineering Journal*, 137:314–325.

Masebinu, S., Akinlabi, E., Muzenda, E., and Aboyade, A. (2019). A review of biochar properties and their roles in mitigating challenges with anaerobic digestion. *Renewable and Sustainable Energy Reviews*, 103:291–307.

Massanet-Nicolau, J., Dinsdale, R., Guwy, A., and Shipley, G. (2013). Use of real time gas production data for more accurate comparison of continuous single-stage and two-stage fermentation. *Bioresource Technology*, 129:561–567.

Mata-Alvarez, J. (2002). *Biomethanization of the organic fraction of municipal solid wastes*. IWA publishing.

Mata-Alvarez, J., Dosta, J., Romero-Güiza, M., Fonoll, X., Peces, M., and Astals, S. (2014). A critical review on anaerobic co-digestion achievements between 2010 and 2013. *Renewable and sustainable energy reviews*, 36:412–427.

Mata-Alvarez, J., Macé, S., and Llabres, P. (2000). Anaerobic digestion of organic solid wastes. an overview of research achievements and perspectives. *Bioresource technology*, 74(1):3–16.

Matheri, A., Ndiweni, S., Belaid, M., Muzenda, E., and Hubert, R. (2017). Optimising biogas production from anaerobic co-digestion of chicken manure and organic fraction of municipal solid waste. *Renewable and Sustainable Energy Reviews*, 80:756–764.

McLean, E. (1965). Aluminum. *Methods of Soil Analysis: Part 2 Chemical and Microbiological Properties*, 9:978–998.

Mel, M., Ihsan, S. I., Setyobudi, R. H., et al. (2015). Process improvement of biogas production from anaerobic co-digestion of cow dung and corn husk. *Procedia Chemistry*, 14:91–100.

Mengel, D. B. (1993). Fundamentals of soil cation exchange capacity (cec). *Purdue University Cooperative Extension Service West Lafayette, Indiana, USA*.

Mengistu, M. G., Simane, B., Eshete, G., and Workneh, T. S. (2016). Factors affecting households' decisions in biogas technology adoption, the case of ofla and mecha districts, northern ethiopia. *Renewable Energy*, 93:215–227.

Mensah, A. and Larbi, E. (2005). Solid waste disposal in ghana. *WELLFACT Sheet—Regional Annex in Developing Countries, WELL—Resource Centre Network*.

Mensah, J. T., Marbuah, G., and Amoah, A. (2016). Energy demand in ghana: A disaggregated analysis. *Renewable and Sustainable Energy Reviews*, 53:924–935.

Metcalf, E. E. and Eddy, H. (2003). Wastewater engineer treatment disposal, reuse. *New York: McGRaw*, 191.

Meyer-Kohlstock, D., Haupt, T., Heldt, E., Heldt, N., and Kraft, E. (2016). Biochar as additive in biogas-production from bio-waste. *Energies*, 9(4):247.

Meyers, D. J. and Lorimor, J. (2003). Field experiences with two iowa dairy farm plug flow digesters. In *2003 ASAE Annual Meeting*, page 1. American Society of Agricultural and Biological Engineers.

Miah, M. R., Rahman, A. K. M. L., Akanda, M. R., Pulak, A., and Rouf, M. A. (2016). Production of biogas from poultry litter mixed with the co-substrate cow dung. *Journal of Taibah university for science*, 10(4):497–504.

Miezah, K., Obiri-Danso, K., Kádár, Z., Fei-Baffoe, B., and Mensah, M. Y. (2015). Municipal solid waste characterization and quantification as a measure towards effective waste management in ghana. *Waste management*, 46:15–27.

Miezah, K., Obiri-Danso, K., Kádár, Z., Heiske, S., Fei-Baffoe, B., Mensah, M., and

Meyer, A. S. (2017). Municipal solid waste management in a low income economy through biogas and bioethanol production. *Waste and biomass valorization*, 8(1):115–127.

Miller, A., Espanani, R., Junker, A., Hendry, D., Wilkinson, N., Bollinger, D., Abelleira-Pereira, J., Deshusses, M., Inniss, E., and Jacoby, W. (2015). Supercritical water oxidation of a model fecal sludge without the use of a co-fuel. *Chemosphere*, 141:189–196.

Minale, M. and Worku, T. (2014). Anaerobic co-digestion of sanitary wastewater and kitchen solid waste for biogas and fertilizer production under ambient temperature: waste generated from condominium house. *International Journal of Environmental Science and Technology*, 11(2):509–516.

Mirmohamadsadeghi, S., Karimi, K., Tabatabaei, M., and Aghbashlo, M. (2019). Biogas production from food wastes: A review on recent developments and future perspectives. *Bioresource Technology Reports*, 7:100202.

Miron, Y., Zeeman, G., Van Lier, J. B., and Lettinga, G. (2000). The role of sludge retention time in the hydrolysis and acidification of lipids, carbohydrates and proteins during digestion of primary sludge in cstr systems. *Water research*, 34(5):1705–1713.

Mital, K. M. (1997). *Biogas systems: policies, progress and prospects*. Taylor & Francis.

Mohammed, M., Egyir, I., Donkor, A., Amoah, P., Nyarko, S., Boateng, K., and Ziwu, C. (2017). Feasibility study for biogas integration into waste treatment plants in ghana. *Egyptian Journal of Petroleum*, 26(3):695–703.

Mohan, D., Sarswat, A., Ok, Y. S., and Pittman Jr, C. U. (2014). Organic and inorganic contaminants removal from water with biochar, a renewable, low cost and sustainable adsorbent–a critical review. *Bioresource technology*, 160:191–202.

Möller, K. and Müller, T. (2012). Effects of anaerobic digestion on digestate nutrient availability and crop growth: A review. *Engineering in life sciences*, 12(3):242–257.

Monney, I., Tiimub, B. M., and Bagah, H. C. (2013). Characteristics and management of household solid waste in urban areas in ghana: the case of wa. *Civil and Environmental Research*, 3(9):10–21.

Moreno-Castilla, C. (2004). Adsorption of organic molecules from aqueous solutions on carbon materials. *Carbon*, 42(1):83–94.

Morita, M. and Sasaki, K. (2012). Factors influencing the degradation of garbage in methanogenic bioreactors and impacts on biogas formation. *Applied Microbiology and Biotechnology*, 94(3):575–582.

Moset, V., Al-zohairi, N., and Møller, H. B. (2015). The impact of inoculum source, inoculum to substrate ratio and sample preservation on methane potential from different substrates. *Biomass and Bioenergy*, 83:474–482.

Moset, V., Fontaine, D., and Møller, H. B. (2017). Co-digestion of cattle manure and grass harvested with different technologies. effect on methane yield, digestate composition and energy balance. *Energy*, 141:451–460.

Mshandete, A., Björnsson, L., Kivaisi, A. K., Rubindamayugi, M. S., and Mattiasson, B. (2006). Effect of particle size on biogas yield from sisal fibre waste. *Renewable energy*, 31(14):2385–2392.

Mshandete, A., Kivaisi, A., Rubindamayugi, M., and Mattiasson, B. (2004). Anaerobic batch co-digestion of sisal pulp and fish wastes. *Bioresource technology*, 95(1):19–24.

Mshandete, A. M. and Parawira, W. (2009). Biogas technology research in selected sub-saharan african countries–a review. *African Journal of Biotechnology*, 8(2).

Msibi, S. S. and Kornelius, G. (2017). Potential for domestic biogas as household energy supply in south africa. *Journal of Energy in Southern Africa*, 28(2):1–13.

Mu, L., Zhang, L., Zhu, K., Ma, J., Ifran, M., and Li, A. (2020). Anaerobic co-digestion of sewage sludge, food waste and yard waste: Synergistic enhancement on process stability and biogas production. *Science of the Total Environment*, 704:135429.

Muha, I., Zielonka, S., Lemmer, A., Schönberg, M., Linke, B., Grillo, A., and Wittum, G. (2013). Do two-phase biogas plants separate anaerobic digestion phases?–a mathematical model for the distribution of anaerobic digestion phases among reactor stages. *Bioresource technology*, 132:414–418.

Muhammad Nasir, I., Mohd Ghazi, T. I., and Omar, R. (2012). Production of biogas from solid organic wastes through anaerobic digestion: a review. *Applied microbiology and biotechnology*, 95(2):321–329.

Mukherjee, A., Zimmerman, A., and Harris, W. (2011). Surface chemistry variations among a series of laboratory-produced biochars. *Geoderma*, 163(3-4):247–255.

Muratçobanoğlu, H., Gökçek, Ö. B., Mert, R. A., Zan, R., and Demirel, S. (2020). Simultaneous synergistic effects of graphite addition and co-digestion of food waste and cow manure: Biogas production and microbial community. *Bioresource technology*, 309:123365.

Murovec, B., Kolbl, S., and Stres, B. (2015). Methane yield database: online infrastructure and bioresource for methane yield data and related metadata. *Bioresource Technology*, 189:217–223.

Murray, P. A. and Zinder, S. H. (1985). Nutritional requirements of methanosarcina sp. strain tm-1. *Applied and environmental microbiology*, 50(1):49–55.

Mwirigi, J., Balana, B. B., Mugisha, J., Walekhwa, P., Melamu, R., Nakami, S., and Makenzi, P. (2014). Socio-economic hurdles to widespread adoption of small-scale biogas digesters in sub-saharan africa: A review. *Biomass and Bioenergy*, 70:17–25.

Nabegu, A. B. (2010). An analysis of municipal solid waste in kano metropolis, nigeria. *Journal of Human Ecology*, 31(2):111–119.

Nagabooshnam, J. K. (2011). Solid waste generation and composition in gaborone, botswana, potential for resource recovery. *J. Eng. Technol. Environ. Eng*, 6:4878–4884.

Nagao, N., Tajima, N., Kawai, M., Niwa, C., Kurosawa, N., Matsuyama, T., Yusoff, F. M., and Toda, T. (2012). Maximum organic loading rate for the single-stage wet anaerobic digestion of food waste. *Bioresource technology*, 118:210–218.

Nah, I. W., Kang, Y. W., Hwang, K.-Y., and Song, W.-K. (2000). Mechanical pretreatment of waste activated sludge for anaerobic digestion process. *Water research*, 34(8):2362–2368.

Nandi, R., Saha, C. K., Sarker, S., Huda, M. S., and Alam, M. M. (2020). Optimization of reactor temperature for continuous anaerobic digestion of cow manure: Bangladesh perspective. *Sustainability*, 12(21):8772.

Nartey, O. D. and Zhao, B. (2014). Biochar preparation, characterization, and adsorptive capacity and its effect on bioavailability of contaminants: an overview. *Advances in Materials Science and Engineering*, 2014.

Nasrin, T., Saha, C. K., Nandi, R., Huda, M., Alam, M., et al. (2021). Kinetic study and optimization of total solids for anaerobic digestion of kitchen waste: Bangladesh perspective. *Water Science and Technology*, 84(5):1136–1145.

Nelson, D. W. (1982). Total carbon, organic, and organic matter. *Chemical and microbiological properties*, pages 539–577.

Nene, Y. (1999). Utilizing traditional knowledge in agriculture. *Traditional knowledge system of India and Sri Lanka*, pages 32–38.

Neshat, S. A., Mohammadi, M., Najafpour, G. D., and Lahijani, P. (2017). Anaerobic co-digestion of animal manures and lignocellulosic residues as a potent approach for sustainable biogas production. *Renewable and Sustainable Energy Reviews*, 79:308–322.

Neves, L., Oliveira, R., and Alves, M. (2009). Co-digestion of cow manure, food waste and intermittent input of fat. *Bioresource technology*, 100(6):1957–1962.

Neves, L., Ribeiro, R., Oliveira, R., and Alves, M. (2006). Enhancement of methane production from barley waste. *Biomass and Bioenergy*, 30(6):599–603.

Nguyen, D. D., Jeon, B.-H., Jeung, J. H., Rene, E. R., Banu, J. R., Ravindran, B., Vu, C. M., Ngo, H. H., Guo, W., and Chang, S. W. (2019). Thermophilic anaerobic digestion of model organic wastes: Evaluation of biomethane production and multiple kinetic models analysis. *Bioresource technology*, 280:269–276.

Nguyen, N. N., Nguyen, A. V., and Dang, L. X. (2017). The inhibition of methane hydrate formation by water alignment underneath surface adsorption of surfactants. *Fuel*, 197:488–496.

Ni, J.-Q. and Nyns, E.-J. (1996). New concept for the evaluation of rural biogas management in developing countries. *Energy Conversion and Management*, 37(10):1525–1534.

Nielfa, A., Cano, R., and Fdz-Polanco, M. (2015). Theoretical methane production generated by the co-digestion of organic fraction municipal solid waste and biological sludge. *Biotechnology Reports*, 5:14–21.

Nsamba, H. K., Hale, S. E., Cornelissen, G., Bachmann, R. T., et al. (2015). Sustainable technologies for small-scale biochar production—a review. *Journal of Sustainable Bioenergy Systems*, 5(01):10.

Nweke, C. N. and Nwabanne, J. T. (2021). Anaerobic digestion of yam peel for biogas production: A kinetic study. *Journal of Engineering and Applied Sciences*, 18(1):275–286.

Obileke, K., Onyeaka, H., and Nwokolo, N. (2021). Materials for the design and construction of household biogas digesters for biogas production: A review. *International Journal of Energy Research*, 45(3):3761–3779.

Ofori-Amanfo, D., Rockson, G. N. K., Arthur, A., and Ahmed, I. (2018). Processing dewatered faecal sludge into un pelletized fertilizer for crop production in greater accra-ghana. *International Journal of Environmental Monitoring and Analysis*, 6(1):18–25.

Ofori-Boateng, C., Lee, K. T., and Mensah, M. (2013). The prospects of electricity generation from municipal solid waste (msw) in ghana: A better waste management option. *Fuel Processing Technology*, 110:94–102.

Ohkouchi, Y. and Inoue, Y. (2006). Direct production of l (+)-lactic acid from starch and food wastes using lactobacillus manihotivorans lmg18011. *Bioresource Technology*, 97(13):1554–1562.

Okello, C., Pindozzi, S., Faugno, S., and Boccia, L. (2013). Development of bioenergy technologies in uganda: A review of progress. *Renewable and Sustainable Energy Reviews*, 18:55–63.

Okot-Okumu, J. (2012). Solid waste management in african cities–east africa. *Waste Management–An Integrated Vision*.

Oladejo, O. S., Dahunsi, S. O., Adesulu-Dahunsi, A. T., Ojo, S. O., Lawal, A. I., Idowu, E. O., Olanipekun, A. A., Ibikunle, R. A., Osueke, C. O., Ajayi, O. E., et al. (2020). Energy generation from anaerobic co-digestion of food waste, cow dung and piggery dung. *Bioresource technology*, 313:123694.

Orangun, A., Kaur, H., and Kommalapati, R. R. (2021). Batch anaerobic co-digestion and biochemical methane potential analysis of goat manure and food waste. *Energies*, 14(7):1952.

Ortiz, W., Terrapon-Pfaff, J., and Dienst, C. (2017). Understanding the diffusion of domestic biogas technologies. systematic conceptualisation of existing evidence from developing and emerging countries. *Renewable and Sustainable Energy Reviews*, 74:1287–1299.

Osei-Marfo, M., Awuah, E., and de Vries, N. (2018). Biogas technology diffusion and shortfalls in the central and greater accra regions of ghana. *Water Practice & Technology*, 13(4):932–946.

O'Shaughnessy, S., Deasy, M., Doyle, J., and Robinson, A. (2014). Field trial testing of an electricity-producing portable biomass cooking stove in rural malawi. *Energy for Sustainable development*, 20:1–10.

Osunkanmibi, O. B., Owolabi, T. O., and Betiku, E. (2015). Comparison of artificial neural network and response surface methodology performance on fermentation parameters optimization of bioconversion of cashew apple juice to gluconic acid. *International Journal of Food Engineering*, 11(3):393–403.

Owen, W., Stuckey, D., Healy Jr, J., Young, L., and McCarty, P. (1979). Bioassay for monitoring biochemical methane potential and anaerobic toxicity. *Water research*, 13(6):485–492.

Pallarés, J., González-Cencerrado, A., and Arauzo, I. (2018). Production and characterization of activated carbon from barley straw by physical activation with carbon dioxide and steam. *Biomass and bioenergy*, 115:64–73.

Pan, J., Ma, J., Zhai, L., Luo, T., Mei, Z., and Liu, H. (2019). Achievements of biochar application for enhanced anaerobic digestion: a review. *Bioresource Technology*, 292:122058.

Parameswaran, P. and Rittmann, B. E. (2012). Feasibility of anaerobic co-digestion of pig waste and paper sludge. *Bioresource technology*, 124:163–168.

Parawira, W. (2009). Biogas technology in sub-saharan africa: status, prospects and constraints. *Reviews in Environmental Science and Bio/Technology*, 8(2):187–200.

Paritosh, K., Kushwaha, S. K., Yadav, M., Pareek, N., Chawade, A., and Vivekanand, V. (2017). Food waste to energy: an overview of sustainable approaches for food waste management and nutrient recycling. *BioMed research international*, 2017.

Parra-Orobio, B. A., Donoso-Bravo, A., Ruiz-Sánchez, J. C., Valencia-Molina, K. J., and Torres-Lozada, P. (2018). Effect of inoculum on the anaerobic digestion of food waste accounting for the concentration of trace elements. *Waste management*, 71:342–349.

Patel, H. and Madamwar, D. (2000). Biomethanation of low ph petrochemical wastewater using up-flow fixed-film anaerobic bioreactors. *World Journal of Microbiology and Biotechnology*, 16:69–75.

Patinvoh, R. J., Feuk-Lagerstedt, E., Lundin, M., Sárvári Horváth, I., and Taherzadeh, M. J. (2016). Biological pretreatment of chicken feather and biogas production from total broth. *Applied biochemistry and biotechnology*, 180(7):1401–1415.

Paudel, S., Kang, Y., Yoo, Y.-S., and Seo, G. T. (2017). Effect of volumetric organic loading rate (olr) on h2 and ch4 production by two-stage anaerobic co-digestion of food waste and brown water. *Waste Management*, 61:484–493.

Pax, M. E., Muzenda, E., and Lekgoba, T. (2020). Effect of co-digestion of food waste and cow dung on biogas yield. In *E3S Web of Conferences*, volume 181, page 01005. EDP Sciences.

Pecchi, M. and Baratieri, M. (2019). Coupling anaerobic digestion with gasification, pyrolysis or hydrothermal carbonization: A review. *Renewable and Sustainable Energy Reviews*, 105:462–475.

Pellegrini, L. A., De Guido, G., and Langé, S. (2018). Biogas to liquefied biomethane via cryogenic upgrading technologies. *Renewable Energy*, 124:75–83.

Pignatello, J. J. (2011). Interactions of anthropogenic organic chemicals with natural organic matter and black carbon in environmental particles. *Biophysico-Chemical Processes of Anthropogenic Organic Compounds in Environmental Systems*, pages 1–50.

Pind, P. F., Angelidaki, I., Ahring, B. K., Stamatelatou, K., and Lyberatos, G. (2003). Monitoring and control of anaerobic reactors. *Biomethanation II*, pages 135–182.

Pitt, R., Cross, T., Pell, A., Schofield, P., and Doane, P. (1999). Use of in vitro gas production models in ruminal kinetics. *Mathematical biosciences*, 159(2):145–163.

Pohland, F. and Ghosh, S. (1971). Developments in anaerobic stabilization of organic wastes-the two-phase concept. *Environmental letters*, 1(4):255–266.

Pöschl, M., Ward, S., and Owende, P. (2010). Evaluation of energy efficiency of various biogas production and utilization pathways. *Applied energy*, 87(11):3305–3321.

Prabhu, M., Waigaonkar, S., Dube, R., Walther, D., and Mutnuri, S. (2015). Anaerobic co-digestion of food waste and septage—a waste to energy project in nashik city. *Carbon Sci Technol*, 7(2):87–98.

Prajapati, K. K., Pareek, N., and Vivekanand, V. (2018). Pretreatment and multi-feed anaerobic co-digestion of agro-industrial residual biomass for improved biomethanation and kinetic analysis. *Frontiers in Energy Research*, 6:111.

Pramanik, S. K., Suja, F. B., Porhemmat, M., and Pramanik, B. K. (2019). Performance and kinetic model of a single-stage anaerobic digestion system operated at different successive operating stages for the treatment of food waste. *Processes*, 7(9):600.

Procházka, J., Dolejš, P., Máca, J., and Dohányos, M. (2012). Stability and inhibition of anaerobic processes caused by insufficiency or excess of ammonia nitrogen. *Applied microbiology and biotechnology*, 93(1):439–447.

Pujar, A., Yadawe, M., and Pujeri, U. (2030). Shivan and mathapati, hiremath d (2014) determination of bod, cod, do and other physico-chemical properties of sugar and cement industries. *Res. J. Pharm. Biol. Chem. Sci*, 5(6):1075–1078.

Puyol, D., Flores-Alsina, X., Segura, Y., Molina, R., Padrino, B., Fierro, J., Gernaey, K., Melero, J., and Martinez, F. (2018). Exploring the effects of zvi addition on resource recovery in the anaerobic digestion process. *Chemical Engineering Journal*, 335:703–711.

Qambrani, N. A., Rahman, M. M., Won, S., Shim, S., and Ra, C. (2017). Biochar properties and eco-friendly applications for climate change mitigation, waste management, and wastewater treatment: A review. *Renewable and Sustainable Energy Reviews*, 79:255–273.

Quan, C., Gao, N., and Song, Q. (2016). Pyrolysis of biomass components in a tga and a fixed-bed reactor: Thermochemical behaviors, kinetics, and product characterization. *Journal of Analytical and Applied Pyrolysis*, 121:84–92.

Rahman, M. A., Møller, H. B., Saha, C. K., Alam, M. M., Wahid, R., and Feng, L. (2017). Optimal ratio for anaerobic co-digestion of poultry droppings and lignocellulosic-rich substrates for enhanced biogas production. *Energy for Sustainable Development*, 39:59–66.

Rajagopal, R., Lim, J. W., Mao, Y., Chen, C.-L., and Wang, J.-Y. (2013). Anaerobic co-digestion of source segregated brown water (feces-without-urine) and food waste: for singapore context. *Science of the Total Environment*, 443:877–886.

Rajendran, K., Aslanzadeh, S., and Taherzadeh, M. J. (2012). Household biogas digesters—a review. *Energies*, 5(8):2911–2942.

Rakić, N., Šušteršič, V., Gordić, D., Jovičić, N., Bošković, G., and Bogdanović, I. (2022). Characterizing production parameters and synergistic effect of primary sludge and food waste co-digestion. *Research Square*, 1.

Randhawa, G. K. and Kullar, J. S. (2011). Bioremediation of pharmaceuticals, pesticides, and petrochemicals with gomeya/cow dung. *International Scholarly Research Notices*, 2011.

Raposo, F., Banks, C., Siegert, I., Heaven, S., and Borja, R. (2006). Influence of inoculum to substrate ratio on the biochemical methane potential of maize in batch tests. *Process Biochemistry*, 41(6):1444–1450.

Raposo, F., Borja, R., Cacho, J., Mumme, J., Orupõld, K., Esteves, S., Noguerol-Arias, J., Picard, S., Nielfa, A., Scherer, P., et al. (2013). First international comparative study of volatile fatty acids in aqueous samples by chromatographic techniques: Evaluating sources of error. *TrAC Trends in Analytical Chemistry*, 51:127–143.

Raposo, F., Borja, R., Rincon, B., and Jimenez, A. (2008). Assessment of process control parameters in the biochemical methane potential of sunflower oil cake. *Biomass and Bioenergy*, 32(12):1235–1244.

Raposo, F., De la Rubia, M., Fernández-Cegrí, V., and Borja, R. (2012). Anaerobic digestion of solid organic substrates in batch mode: an overview relating to methane yields and experimental procedures. *Renewable and sustainable energy reviews*, 16(1):861–877.

Raposo, F., Fernández-Cegrí, V., De la Rubia, M., Borja, R., Béline, F., Cavinato, C., Demirer, G., Fernández, B., Fernández-Polanco, M., Frigon, J., et al. (2011). Biochemical methane potential (bmp) of solid organic substrates: evaluation of anaerobic biodegradability using data from an international interlaboratory study. *Journal of Chemical Technology & Biotechnology*, 86(8):1088–1098.

Rasit, N., Idris, A., Harun, R., and Ghani, W. A. W. A. K. (2015). Effects of lipid inhibition on biogas production of anaerobic digestion from oily effluents and sludges: An overview. *Renewable and Sustainable Energy Reviews*, 45:351–358.

Resasco, J., Chen, L. D., Clark, E., Tsai, C., Hahn, C., Jaramillo, T. F., Chan, K., and Bell, A. T. (2017). Promoter effects of alkali metal cations on the electrochemical reduction of carbon dioxide. *Journal of the American Chemical Society*, 139(32):11277–11287.

Rice, E. W., Baird, R. B., Eaton, A. D., Clesceri, L. S., et al. (2012). *Standard methods for the examination of water and wastewater*, volume 10. American public health association Washington, DC.

Rico, C., Muñoz, N., Fernández, J., and Rico, J. L. (2015). High-load anaerobic co-digestion of cheese whey and liquid fraction of dairy manure in a one-stage uasb process: Limits in co-substrates ratio and organic loading rate. *Chemical Engineering Journal*, 262:794–802.

Rodriguez-Chiang, L. M. and Dahl, O. P. (2015). Effect of inoculum to substrate ratio on the methane potential of microcrystalline cellulose production wastewater. *BioResources*, 10(1):898–911.

Romero-Güiza, M., Vila, J., Mata-Alvarez, J., Chimenos, J., and Astals, S. (2016). The role of additives on anaerobic digestion: a review. *Renewable and Sustainable Energy Reviews*, 58:1486–1499.

Ronsse, F., Van Hecke, S., Dickinson, D., and Prins, W. (2013). Production and characterization of slow pyrolysis biochar: influence of feedstock type and pyrolysis conditions. *Gcb Bioenergy*, 5(2):104–115.

Roopnarain, A. and Adeleke, R. (2017). Current status, hurdles and future prospects of biogas digestion technology in africa. *Renewable and Sustainable Energy Reviews*, 67:1162–1179.

Rosales, E., Meijide, J., Pazos, M., and Sanromán, M. A. (2017). Challenges and recent advances in biochar as low-cost biosorbent: From batch assays to continuous-flow systems. *Bioresource technology*, 246:176–192.

Rose, C., Parker, A., Jefferson, B., and Cartmell, E. (2015). The characterization of feces and urine: a review of the literature to inform advanced treatment technology. *Critical reviews in environmental science and technology*, 45(17):1827–1879.

Rouf, M., Bajpai, P., and Jotshi, C. (2010). Optimization of biogas generation from press mud in batch reactor. *Bangladesh Journal of Scientific and Industrial Research*, 45(4):371–376.

Rouquerol, J., Avnir, D., Fairbridge, C. W., Everett, D. H., Haynes, J., Pernicone, N., Ramsay, J. D., Sing, K. S. W., and Unger, K. K. (1994). Recommendations for the characterization of porous solids (technical report). *Pure and applied chemistry*, 66(8):1739–1758.

Ruan, X., Sun, Y., Du, W., Tang, Y., Liu, Q., Zhang, Z., Doherty, W., Frost, R. L., Qian, G., and Tsang, D. C. (2019). Formation, characteristics, and applications of environmentally persistent free radicals in biochars: a review. *Bioresource technology*, 281:457–468.

Safari, M., Abdi, R., Adl, M., and Kafashan, J. (2018). Optimization of biogas productivity in lab-scale by response surface methodology. *Renewable Energy*, 118:368–375.

Saitawee, L., Hussaro, K., Teekasap, S., Cheamsawat, N., et al. (2014). Biogas proction from anaerobic co-digestion of cow dung and organic wastes (napier pak chong i and food waste) in thailand: temperature effect on biogas product. *American Journal of Environmental Sciences*, 10(2):129–139.

Sakah, M., Diawuo, F. A., Katzenbach, R., and Gyamfi, S. (2017). Towards a sustainable electrification in ghana: A review of renewable energy deployment policies. *Renewable and Sustainable Energy Reviews*, 79:544–557.

Salminen, E., Einola, J., and Rintala, J. (2003). The methane production of poultry slaughtering residues and effects of pre-treatments on the methane production of poultry feather. *Environmental Technology*, 24(9):1079–1086.

Salvador, F., Martin-Sanchez, N., Sanchez-Hernandez, R., Sanchez-Montero, M. J., and Izquierdo, C. (2015). Regeneration of carbonaceous adsorbents. part i: thermal regeneration. *Microporous and Mesoporous Materials*, 202:259–276.

Samuel, J., Gujjala, L., Rintu, B., et al. (2017). Kinetic modeling of mixed culture process of anaerobic co-digestion of vegetable wastes with pistia stratiotes: a scientific attempt on biomethanationy. *Journal of Microbial and Biochemical Technology*, 9(1):554–566.

Sanchez-Monedero, M., Cayuela, M., Roig, A., Jindo, K., Mondini, C., and Bolan, N. (2018). Role of biochar as an additive in organic waste composting. *Bioresource Technology*, 247:1155–1164.

Sandhu, S. and Kaushal, R. (2022a). Anaerobic co-digestion of food wastes, algae, pond sludge and cow dung for biogas yield enhancement as a potent approach to reduce carbon footprints. *Australian Journal of Mechanical Engineering*, pages 1–20.

Sandhu, S. and Kaushal, R. (2022b). Optimisation of anaerobic digestion of layer manure, breeding manure and cow dung using grey relational analysis. *Biomass Conversion and Biorefinery*, pages 1–13.

Sauer, K. and Thauer, R. K. (2000). Methyl-coenzyme m formation in methanogenic archaea: Involvement of zinc in coenzyme m activation. *European Journal of Biochemistry*, 267(9):2498–2504.

Sawant, A. A., Hegde, N. V., Straley, B. A., Donaldson, S. C., Love, B. C., Knabel, S. J., and Jayarao, B. M. (2007). Antimicrobial-resistant enteric bacteria from dairy cattle. *Applied and environmental microbiology*, 73(1):156–163.

Sawasdee, V., Hasin, S., and Pisutpaisal, N. (2021). Fly ash utilization for methane production improvement from co-digestion between cow dung and pennisetum purpureum. *Energy Reports*, 7:591–598.

Sawayama, S., Tada, C., Tsukahara, K., and Yagishita, T. (2004). Effect of ammonium addition on methanogenic community in a fluidized bed anaerobic digestion. *Journal of bioscience and bioengineering*, 97(1):65–70.

Schattauer, A., Abdoun, E., Weiland, P., Plöchl, M., and Heiermann, M. (2011). Abundance of trace elements in demonstration biogas plants. *Biosystems engineering*, 108(1):57–65.

Scherer, P. (2007). Operating analytics of biogas plants to improve efficiency and to ensure process stability. *Progress in Biogas Stuttgart-Hohenheim*, pages 77–84.

Scherer, P. A., Arthur, R., and Antonczyk, S. (2021). Accelerated biomethane potential

assay for straw with artificially flocculated sludge and defined 'synthetic manure'. *Bioresource Technology Reports*, 15:100787.

Schindelin, H., Kisker, C., Schlessman, J. L., Howard, J. B., and Rees, D. C. (1997). Structure of adp· aif4—stabilized nitrogenase complex and its implications for signal transduction. *Nature*, 387(6631):370–376.

Schink, B. (1997). Energetics of syntrophic cooperation in methanogenic degradation. *Microbiology and molecular biology reviews*, 61(2):262–280.

Schmidt, T., Nelles, M., Scholwin, F., and Pröter, J. (2014). Trace element supplementation in the biogas production from wheat stillage–optimization of metal dosing. *Bioresource technology*, 168:80–85.

Schofield, P., Pitt, R., and Pell, A. (1994). Kinetics of fiber digestion from in vitro gas production. *Journal of animal science*, 72(11):2980–2991.

Schönheit, P., Moll, J., and Thauer, R. K. (1979). Nickel, cobalt, and molybdenum requirement for growth of methanobacterium thermoautotrophicum. *Archives of Microbiology*, 123(1):105–107.

Sedighi, A., Karrabi, M., Shahnavaz, B., and Mostafavinezhad, M. (2022). Bioenergy production from the organic fraction of municipal solid waste and sewage sludge using mesophilic anaerobic co-digestion: An experimental and kinetic modeling study. *Renewable and Sustainable Energy Reviews*, 153:111797.

Shah, F. A., Mahmood, Q., Rashid, N., Pervez, A., Raja, I. A., and Shah, M. M. (2015). Co-digestion, pretreatment and digester design for enhanced methanogenesis. *Renewable and Sustainable Energy Reviews*, 42:627–642.

Shamsuddin, M., Yusoff, N., and Sulaiman, M. (2016). Synthesis and characterization of activated carbon produced from kenaf core fiber using h3po4 activation. *Procedia Chemistry*, 19:558–565.

Shamurad, B., Sallis, P., Petropoulos, E., Tabraiz, S., Ospina, C., Leary, P., Dolfing, J., and Gray, N. (2020). Stable biogas production from single-stage anaerobic digestion of food waste. *Applied energy*, 263:114609.

Shane, A., Gheewala, S. H., and Phiri, S. (2017). Rural domestic biogas supply model for zambia. *Renewable and Sustainable Energy Reviews*, 78:683–697.

Shao, L., Li, S., Cai, J., He, P., and Lü, F. (2019). Ability of biochar to facilitate anaerobic digestion is restricted to stressed surroundings. *Journal of Cleaner Production*, 238:117959.

Sharma, A., Pareek, V., and Zhang, D. (2015). Biomass pyrolysis—a review of modelling, process parameters and catalytic studies. *Renewable and sustainable energy reviews*, 50:1081–1096.

Sharma, P. and Melkania, U. (2017). Biochar-enhanced hydrogen production from organic fraction of municipal solid waste using co-culture of enterobacter aerogenes and e. coli. *International Journal of Hydrogen Energy*, 42(30):18865–18874.

Sharma, S. K., Mishra, I., Sharma, M., and Saini, J. (1988). Effect of particle size on biogas generation from biomass residues. *Biomass*, 17(4):251–263.

Shen, R., Jing, Y., Feng, J., Luo, J., Yu, J., and Zhao, L. (2020). Performance of enhanced anaerobic digestion with different pyrolysis biochars and microbial communities. *Bioresource technology*, 296:122354.

Shen, X., Huang, G., Yang, Z., and Han, L. (2015a). Compositional characteristics and energy potential of chinese animal manure by type and as a whole. *Applied Energy*, 160:108–119.

Shen, Y., Forrester, S., Koval, J., and Urgun-Demirtas, M. (2017). Yearlong semi-continuous operation of thermophilic two-stage anaerobic digesters amended with biochar for enhanced biomethane production. *Journal of cleaner production*, 167:863–874.

Shen, Y., Linville, J. L., Ignacio-de Leon, P. A. A., Schoene, R. P., and Urgun-Demirtas, M. (2016). Towards a sustainable paradigm of waste-to-energy process: Enhanced anaerobic digestion of sludge with woody biochar. *Journal of Cleaner Production*, 135:1054–1064.

Shen, Y., Linville, J. L., Urgun-Demirtas, M., Schoene, R. P., and Snyder, S. W. (2015b). Producing pipeline-quality biomethane via anaerobic digestion of sludge

amended with corn stover biochar with in-situ co2 removal. *Applied energy*, 158:300–309.

Shih, J., Fanyin-Martin, A., Taher, E., and Chandran, K. (2017). Implementation and process analysis of pilot scale multi-phase anaerobic fermentation and digestion of faecal sludge in ghana. *Gates Open Research*, 1.

Shu, J., Cheng, S., Xia, H., Zhang, L., Peng, J., Li, C., and Zhang, S. (2017). Copper loaded on activated carbon as an efficient adsorbent for removal of methylene blue. *RSC advances*, 7(24):14395–14405.

Sibisi, N. and Green, J. (2005). A floating dome biogas digester: perceptions of energising a rural school in maphephetheni, kwazulu-natal. *Journal of Energy in Southern Africa*, 16(3):45–52.

Siddique, M. N. I., Munaim, M. S. A., and Wahid, Z. B. A. (2017). The combined effect of ultrasonic and microwave pre-treatment on bio-methane generation from co-digestion of petrochemical wastewater. *Journal of Cleaner Production*, 145:303–309.

Siddique, M. N. I., Munaim, M. S. A., and Zularisam, A. (2015a). Feasibility analysis of anaerobic co-digestion of activated manure and petrochemical wastewater in kuantan (malaysia). *Journal of Cleaner Production*, 106:380–388.

Siddique, M. N. I. and Wahid, Z. A. (2018). Achievements and perspectives of anaerobic co-digestion: A review. *Journal of cleaner production*, 194:359–371.

Siddique, N. and Wahid, Z. A. (2012). Application of chemical and biological coupled treatment technology in pomie and petroleum waste water as biodegradation. *Journal of Environmental Science and Technology*, 5(3):155–167.

Siddique, N. I., Munaim, M. S. A., and Wahid, Z. A. (2015b). Role of biogas recirculation in enhancing petrochemical wastewater treatment efficiency of continuous stirred tank reactor. *Journal of Cleaner Production*, 91:229–234.

Sing, K. S. (1985). Reporting physisorption data for gas/solid systems with special reference to the determination of surface area and porosity (recommendations 1984). *Pure and applied chemistry*, 57(4):603–619.

Singh, D., Chhonkar, P., and Pandey, R. (1999). Soil plant water analysis: a methods manual. *IARI, New Delhi*, pages 80–82.

Singh, M. and Maharjan, K. L. (2003). Contribution of biogas technology in well-being of rural hill areas of nepal: a comparative study between biogas users and non-users. *Journal of international Development and Cooperation*, 9(2):43–63.

Singh, P. K., Srichandan, H., Ojha, S. K., Mishra, S., and Naik, K. (2019a). A comparative study of biogasification of wheat straw, sugarcane bagasse and pressmud. *Journal of Environmental Science and Health, Part A*, 54(4):306–314.

Singh, P. K., Srichandan, H., Ojha, S. K., Pattnaik, R., Verma, S. K., Pal, S., Singh, J., and Mishra, S. (2021a). Evaluation of biomethane potential of codigested sheep manure and kitchen refuse. *Biomass Conversion and Biorefinery*, pages 1–11.

Singh, P. K., Verma, S. K., Ojha, S. K., Panda, P. K., Srichandan, H., Jha, E., and Mishra, S. (2019b). Intrinsic molecular insights to enhancement of biogas production from kitchen refuse using alkaline-microwave pretreatment. *Scientific reports*, 9(1):1–12.

Singh, S., Hariteja, N., Sharma, S., Raju, N. J., and Prasad, T. R. (2021b). Production of biogas from human faeces mixed with the co-substrate poultry litter & cow dung. *Environmental Technology & Innovation*, 23:101551.

Sinpaisansomboon, N., Intanon, P., Rakwichian, W., and Kongsricharoern, N. (2007). Development of two-stage anaerobic digesters for biogas production from biodegradable waste of phitsanulok municipal, thailand. *Journal of Renewable Energy and Smart Grid Technology*, 2(2):73–83.

Somanathan, E. and Bluffstone, R. (2015). Biogas: Clean energy access with low-cost mitigation of climate change. *Environmental and Resource Economics*, 62(2):265–277.

Song, Y.-C., Kim, M., Shon, H., Jegatheesan, V., and Kim, S. (2018). Modeling methane production in anaerobic forward osmosis bioreactor using a modified anaerobic digestion model no. 1. *Bioresource technology*, 264:211–218.

Soyingbe, A., Olayinka, O., Bamgbose, O., and Adetunji, M. (2019). Effective management of faecal sludge through co-digestion for biogas generation. *Journal of Applied Sciences and Environmental Management*, 23(6):1159–1168.

Speece, R. E. (1983). Anaerobic biotechnology for industrial wastewater treatment. *Environmental science & technology*, 17(9):416A–427A.

Spierling, R. E. (2011). Anaerobic co-digestion of microalgae with food waste and wastewater sludge. *California Polytechnic State University*, 1.

Sreekrishnan, T., Kohli, S., Rana, V., et al. (2004). Enhancement of biogas production from solid substrates using different techniques—-a review. *Bioresource technology*, 95(1):1–10.

Sri Bala Kameswari, K., Kalyanaraman, C., Porselvam, S., and Thanasekaran, K. (2012). Optimization of inoculum to substrate ratio for bio-energy generation in co-digestion of tannery solid wastes. *Clean Technologies and Environmental Policy*, 14(2):241–250.

Stams, A. J. and Plugge, C. M. (2009). Electron transfer in syntrophic communities of anaerobic bacteria and archaea. *Nature Reviews Microbiology*, 7(8):568–577.

Steffen, F., Requejo, A., Ewald, C., Janzon, R., and Saake, B. (2016). Anaerobic digestion of fines from recovered paper processing–influence of fiber source, lignin and ash content on biogas potential. *Bioresource technology*, 200:506–513.

Steffen, R., Szolar, O., and Braun, R. (1998). Feedstocks for anaerobic digestion. *Institute of Agrobiotechnology Tulin, University of Agricultural Sciences, Vienna*.

Strauss, M., Drescher, S., Zurbrügg, C., Montangero, A., Cofie, O., and Drechsel, P. (2003). Co-composting of faecal sludge and municipal organic waste: a literature and state-of-knowledge review. *International Water Management Institute (IWMI) Accra, Ghana*.

Stroot, P. G., McMahon, K. D., Mackie, R. I., and Raskin, L. (2001). Anaerobic codigestion of municipal solid waste and biosolids under various mixing conditions—i. digester performance. *Water research*, 35(7):1804–1816.

Sulaiman, S. M. and Seswoya, R. (2019). Kinetics modelling of batch anaerobic co-digestion of domestic primary sewage sludge and food waste in a stirred reactor. In *IOP Conference Series: Materials Science and Engineering*, volume 601, page 012012. IOP Publishing.

Sumardiono, S., Syaichurrozi, I., Budiyono, B., and Budi Sasongko, S. (2013). The effect of cod/n ratios and ph control to biogas production from vinasse. *International Journal of Biochemistry Research & Review*, 3(4):278–290.

Sunyoto, N. M., Zhu, M., Zhang, Z., and Zhang, D. (2016). Effect of biochar addition on hydrogen and methane production in two-phase anaerobic digestion of aqueous carbohydrates food waste. *Bioresource technology*, 219:29–36.

Surendra, K., Takara, D., Hashimoto, A. G., and Khanal, S. K. (2014). Biogas as a sustainable energy source for developing countries: Opportunities and challenges. *Renewable and Sustainable Energy Reviews*, 31:846–859.

Syaichurrozi, I., Sumardiono, S., et al. (2013). Biogas production kinetic from vinasse waste in batch mode anaerobic digestion. *World applied sciences journal*, 26(11):1464–1472.

Syaichurrozi, I., Sumardiono, S., et al. (2014). Effect of total solid content to biogas production rate from vinasse (research note). *International Journal of Engineering*, 27(2):177–184.

Taghizadeh-Toosi, A., Clough, T. J., Sherlock, R. R., and Condron, L. M. (2012). Biochar adsorbed ammonia is bioavailable. *Plant and soil*, 350:57–69.

Tampio, E., Ervasti, S., Paavola, T., Heaven, S., Banks, C., and Rintala, J. (2014). Anaerobic digestion of autoclaved and untreated food waste. *Waste Management*, 34(2):370–377.

Tan, L., Qu, Y., Zhou, J., Ma, F., and Li, A. (2009). Dynamics of microbial community for x-3b wastewater decolorization coping with high-salt and metal ions conditions. *Bioresource Technology*, 100(12):3003–3009.

Tan, X.-f., Liu, S.-b., Liu, Y.-g., Gu, Y.-l., Zeng, G.-m., Hu, X.-j., Wang, X., Liu, S.-h., and Jiang, L.-h. (2017). Biochar as potential sustainable precursors for activated

carbon production: Multiple applications in environmental protection and energy storage. *Bioresource technology*, 227:359–372.

Tisma, M., Kojic, A. B., Zelic, B., and Planinic, M. (2017). Biological pre-treatment of lignocellulose waste for its further application in biogas production. *Journal of Biotechnology*, 256:S12.

Tripathi, M., Sahu, J. N., and Ganesan, P. (2016). Effect of process parameters on production of biochar from biomass waste through pyrolysis: A review. *Renewable and sustainable energy reviews*, 55:467–481.

Tufaner, F. and Avşar, Y. (2016). Effects of co-substrate on biogas production from cattle manure: a review. *International journal of environmental science and technology*, 13(9):2303–2312.

Uchegbulam, I., Momoh, E. O., and Agan, S. A. (2022). Potentials of palm kernel shell derivatives: A critical review on waste recovery for environmental sustainability. *Cleaner Materials*, page 100154.

Uncu, O. N. and Cekmecelioglu, D. (2011). Cost-effective approach to ethanol production and optimization by response surface methodology. *Waste management*, 31(4):636–643.

Van Haandel, A. C. and Lettinga, G. (1994). Anaerobic sewage treatment. *A practical guide for regions with a hot climate. John Whiley and sons. Gran Bretaña*.

Vats, N., Khan, A. A., and Ahmad, K. (2019). Effect of substrate ratio on biogas yield for anaerobic co-digestion of fruit vegetable waste & sugarcane bagasse. *Environmental Technology & Innovation*, 13:331–339.

VDI, V. D. I. (2006). 4630: Fermentation of organic materials-characterisation of the substrate, sampling, collection of material data, fermentation tests. *Verein Deutscher Ingenieure (VDI), editor. VDI Handbuch Energietechnik. Berlin: Beuth Verlag GmbH*, pages 44–59.

VDI.4630 (2016). *VDI 4630: Fermentation of Organic Materials: Characterisation of the Substrate, Sampling, Collection of Material Data, Fermentation Tests*. Beuth Verlag.

Velázquez-Martí, B., Meneses-Quelal, O. W., Gaibor-Chavez, J., Niño-Ruiz, Z., et al. (2018). Review of mathematical models for the anaerobic digestion process. In *Anaerobic Digestion*. IntechOpen.

Velimirovic, M., Schmid, D., Wagner, S., Micić, V., von der Kammer, F., and Hofmann, T. (2016). Agar agar-stabilized milled zerovalent iron particles for in situ groundwater remediation. *Science of The Total Environment*, 563:713–723.

Venkateshkumar, R., Shanmugam, S., and Veerappan, A. (2020). Anaerobic co-digestion of cow dung and cotton seed hull with different blend ratio: experimental and kinetic study. *Biomass Conversion and Biorefinery*, pages 1–11.

Vigueras-Carmona, S., Trujillo, M., García Rivero, M., Membrillo Venegas, I., and Zafra Jiménez, G. (2016). Effect of particle size on mesophilic anaerobic digestion of thermally pre-treated waste activated sludge. *Journal of Biotech research*, 7.

Vintiloiu, A., Boxriker, M., Lemmer, A., Oechsner, H., Jungbluth, T., Mathies, E., and Ramhold, D. (2013). Effect of ethylenediaminetetraacetic acid (edta) on the bioavailability of trace elements during anaerobic digestion. *Chemical engineering journal*, 223:436–441.

Wagner, A. O., Lins, P., Malin, C., Reitschuler, C., and Illmer, P. (2013). Impact of protein-, lipid-and cellulose-containing complex substrates on biogas production and microbial communities in batch experiments. *Science of the Total Environment*, 458:256–266.

Wahid, R., Feng, L., Cong, W.-F., Ward, A. J., Møller, H. B., and Eriksen, J. (2018). Anaerobic mono-digestion of lucerne, grass and forbs–influence of species and cutting frequency. *Biomass and bioenergy*, 109:199–208.

Walekhwa, P. N., Mugisha, J., and Drake, L. (2009). Biogas energy from family-sized digesters in uganda: Critical factors and policy implications. *Energy policy*, 37(7):2754–2762.

Walker, L. (2009). *An investigation into the bioprocesses of DiCOM®: A technology combining composting and thermophilic anaerobic digestion for the treatment of municipal solid waste*. PhD thesis, Murdoch University.

Wang, B., Björn, A., Strömberg, S., Nges, I. A., Nistor, M., and Liu, J. (2017a). Evaluating the influences of mixing strategies on the biochemical methane potential test. *Journal of environmental management*, 185:54–59.

Wang, B., Nges, I. A., Nistor, M., and Liu, J. (2014a). Determination of methane yield of cellulose using different experimental setups. *Water science and technology*, 70(4):599–604.

Wang, C., Zhang, Y., Zhang, L., and Pang, M. (2016). Alternative policies to subsidize rural household biogas digesters. *Energy Policy*, 93:187–195.

Wang, D., Ai, J., Shen, F., Yang, G., Zhang, Y., Deng, S., Zhang, J., Zeng, Y., and Song, C. (2017b). Improving anaerobic digestion of easy-acidification substrates by promoting buffering capacity using biochar derived from vermicompost. *Bioresource technology*, 227:286–296.

Wang, G., Li, Q., Dzakpasu, M., Gao, X., Yuwen, C., and Wang, X. C. (2018a). Impacts of different biochar types on hydrogen production promotion during fermentative co-digestion of food wastes and dewatered sewage sludge. *Waste management*, 80:73–80.

Wang, G., Li, Q., Gao, X., and Wang, X. C. (2018b). Synergetic promotion of syntrophic methane production from anaerobic digestion of complex organic wastes by biochar: Performance and associated mechanisms. *Bioresource technology*, 250:812–820.

Wang, J. (2014). Decentralized biogas technology of anaerobic digestion and farm ecosystem: opportunities and challenges. *Frontiers in Energy Research*, 2:10.

Wang, J. and Li, Y. (2016). Synergistic pretreatment of waste activated sludge using cao2 in combination with microwave irradiation to enhance methane production during anaerobic digestion. *Applied Energy*, 183:1123–1132.

Wang, L., Lovas, T., and Houshfar, E. (2014b). Effect of sewage sludge addition on potassium release and ash transformation during wheat straw combustion. *CHEMICAL ENGINEERING*, 37.

Wang, L., Shen, F., Yuan, H., Zou, D., Liu, Y., Zhu, B., and Li, X. (2014c). Anaerobic co-digestion of kitchen waste and fruit/vegetable waste: Lab-scale and pilot-scale studies. *Waste management*, 34(12):2627–2633.

Wang, T., Shao, L., Li, T., Lü, F., and He, P. (2014d). Digestion and dewatering characteristics of waste activated sludge treated by an anaerobic biofilm system. *Bioresource technology*, 153:131–136.

Wang, X., Yang, G., Feng, Y., Ren, G., and Han, X. (2012). Optimizing feeding composition and carbon–nitrogen ratios for improved methane yield during anaerobic co-digestion of dairy, chicken manure and wheat straw. *Bioresource technology*, 120:78–83.

Wang, X. and Zhao, Y.-c. (2009). A bench scale study of fermentative hydrogen and methane production from food waste in integrated two-stage process. *International journal of hydrogen energy*, 34(1):245–254.

Wang, Y., Li, G., Chi, M., Sun, Y., Zhang, J., Jiang, S., and Cui, Z. (2018c). Effects of co-digestion of cucumber residues to corn stover and pig manure ratio on methane production in solid state anaerobic digestion. *Bioresource technology*, 250:328–336.

Wang, Z., Jiang, Y., Wang, S., Zhang, Y., Hu, Y., Hu, Z.-h., Wu, G., and Zhan, X. (2020). Impact of total solids content on anaerobic co-digestion of pig manure and food waste: Insights into shifting of the methanogenic pathway. *Waste Management*, 114:96–106.

Wang, Z., Wang, S., Xie, S., Jiang, Y., Meng, J., Wu, G., Hu, Y., and Zhan, X. (2022). Stimulatory effects of biochar addition on dry anaerobic co-digestion of pig manure and food waste under mesophilic conditions. *Environmental Science and Pollution Research*, pages 1–12.

Ward, A. J., Hobbs, P. J., Holliman, P. J., and Jones, D. L. (2008). Optimisation of the anaerobic digestion of agricultural resources. *Bioresource technology*, 99(17):7928–7940.

Weber, K. and Quicker, P. (2018). Properties of biochar. *Fuel*, 217:240–261.

Wegener, G., Krukenberg, V., Riedel, D., Tegetmeyer, H. E., and Boetius, A. (2015). Intercellular wiring enables electron transfer between methanotrophic archaea and bacteria. *Nature*, 526(7574):587–590.

Weiland, P. (2010). Biogas production: current state and perspectives. *Applied microbiology and biotechnology*, 85(4):849–860.

Weinrich, S. and Nelles, M. (2015). Critical comparison of different model structures for the applied simulation of the anaerobic digestion of agricultural energy crops. *Bioresource Technology*, 178:306–312.

Werther, J., Saenger, M., Hartge, E.-U., Ogada, T., and Siagi, Z. (2000). Combustion of agricultural residues. *Progress in energy and combustion science*, 26(1):1–27.

Wignarajah, K., Litwiller, E., Fisher, J. W., and Hogan, J. (2006). Simulated human feces for testing human waste processing technologies in space systems. *SAE Transactions*, pages 424–430.

Williams, S. (1984). Aoac official methods of analysis. *Association of Official Analytical Chemists, 14th Edition, Arlington, VA*, pages 8–34.

Windeatt, J. H., Ross, A. B., Williams, P. T., Forster, P. M., Nahil, M. A., and Singh, S. (2014). Characteristics of biochars from crop residues: potential for carbon sequestration and soil amendment. *Journal of environmental management*, 146:189–197.

Woolf, D., Amonette, J. E., Street-Perrott, F. A., Lehmann, J., and Joseph, S. (2010). Sustainable biochar to mitigate global climate change. *Nature communications*, 1(1):56.

Worm, P., Fermoso, F. G., Lens, P. N., and Plugge, C. M. (2009). Decreased activity of a propionate degrading community in a uasb reactor fed with synthetic medium without molybdenum, tungsten and selenium. *Enzyme and Microbial Technology*, 45(2):139–145.

Xie, S., Hai, F. I., Zhan, X., Guo, W., Ngo, H. H., Price, W. E., and Nghiem, L. D. (2016). Anaerobic co-digestion: A critical review of mathematical modelling for performance optimization. *Bioresource Technology*, 222:498–512.

Xie, S., Wickham, R., and Nghiem, L. D. (2017a). Synergistic effect from anaerobic co-digestion of sewage sludge and organic wastes. *International Biodeterioration & Biodegradation*, 116:191–197.

Xie, T., Xie, S., Sivakumar, M., and Nghiem, L. D. (2017b). Relationship between the synergistic/antagonistic effect of anaerobic co-digestion and organic loading. *International Biodeterioration & Biodegradation*, 124:155–161.

Xie, Y., Wang, L., Li, H., Westholm, L. J., Carvalho, L., Thorin, E., Yu, Z., Yu, X., and Skreiberg, Ø. (2022). A critical review on production, modification and utilization of biochar. *Journal of Analytical and Applied Pyrolysis*, 161:105405.

Xu, R., Zhang, K., Liu, P., Khan, A., Xiong, J., Tian, F., and Li, X. (2018). A critical review on the interaction of substrate nutrient balance and microbial community structure and function in anaerobic co-digestion. *Bioresource technology*, 247:1119–1127.

Ya'aba, Y. and Ramalan, A. S. (2021). Isolation, identification and characterization of some bacteria associated with biogas production from cow dung. *Equity Journal of Science and Technology*, 7(2):91–91.

Yang, G. and Wang, J. (2019). Synergistic enhancement of biohydrogen production from grass fermentation using biochar combined with zero-valent iron nanoparticles. *Fuel*, 251:420–427.

Yang, H., Deng, R., Jin, J., Wu, Y., Jiang, X., and Shi, J. (2022). Hydrolytic performances of different organic compounds in different lignocellulosic biomass during anaerobic digestion. *Environmental Engineering Research*, 27(4).

Yang, Y., Zhang, Y., Li, Z., Zhao, Z., Quan, X., and Zhao, Z. (2017). Adding granular activated carbon into anaerobic sludge digestion to promote methane production and sludge decomposition. *Journal of cleaner production*, 149:1101–1108.

Yang, Z., Wang, W., He, Y., Zhang, R., and Liu, G. (2018). Effect of ammonia on methane production, methanogenesis pathway, microbial community and reactor performance under mesophilic and thermophilic conditions. *Renewable Energy*, 125:915–925.

Yargicoglu, E. N., Sadasivam, B. Y., Reddy, K. R., and Spokas, K. (2015). Physical and chemical characterization of waste wood derived biochars. *Waste management*, 36:256–268.

Yavini, T. D., Chia, A. I., and John, A. (2014). Evaluation of the effect of total solids concentration on biogas yields of agricultural wastes. *International Research Journal of Environment Sciences*, 3(2):70–75.

Ye, M., Liu, J., Ma, C., Li, Y.-Y., Zou, L., Qian, G., and Xu, Z. P. (2018). Improving the stability and efficiency of anaerobic digestion of food waste using additives: a critical review. *Journal of Cleaner Production*, 192:316–326.

Yeboah, M. L., Li, X., and Zhou, S. (2020). Facile fabrication of biochar from palm kernel shell waste and its novel application to magnesium-based materials for hydrogen storage. *Materials*, 13(3):625.

Yenigün, O. and Demirel, B. (2013). Ammonia inhibition in anaerobic digestion: a review. *Process Biochemistry*, 48(5-6):901–911.

Yi, J., Dong, B., Jin, J., and Dai, X. (2014). Effect of increasing total solids contents on anaerobic digestion of food waste under mesophilic conditions: performance and microbial characteristics analysis. *PloS one*, 9(7):e102548.

Yılmaz, Ş. and Şahan, T. (2020). Utilization of pumice for improving biogas production from poultry manure by anaerobic digestion: a modeling and process optimization study using response surface methodology. *Biomass and Bioenergy*, 138:105601.

Yirong, C., Zhang, W., Heaven, S., and Banks, C. J. (2017). Influence of ammonia in the anaerobic digestion of food waste. *Journal of environmental chemical engineering*, 5(5):5131–5142.

Yoon, Y.-M., Kim, S.-H., Shin, K.-S., and Kim, C.-H. (2014). Effects of substrate to inoculum ratio on the biochemical methane potential of piggery slaughterhouse wastes. *Asian-Australasian journal of animal sciences*, 27(4):600.

Yuan, Z., Yang, H., Zhi, X., and Shen, J. (2010). Increased performance of continuous

stirred tank reactor with calcium supplementation. *International journal of hydrogen energy*, 35(7):2622–2626.

Yue, Z.-B., Yu, H.-Q., and Wang, Z.-L. (2007). Anaerobic digestion of cattail with rumen culture in the presence of heavy metals. *Bioresource Technology*, 98(4):781–786.

Yusuf, M., Debora, A., and Ogheneruona, D. (2011). Ambient temperature kinetic assessment of biogas production from co-digestion of horse and cow dung. *Research in Agricultural Engineering*, 57(3):97–104.

Zahan, Z., Othman, M. Z., and Muster, T. H. (2018). Anaerobic digestion/co-digestion kinetic potentials of different agro-industrial wastes: A comparative batch study for c/n optimisation. *Waste Management*, 71:663–674.

Zahedi, S., Solera, R., Micolucci, F., Cavinato, C., and Bolzonella, D. (2016). Changes in microbial community during hydrogen and methane production in two-stage thermophilic anaerobic co-digestion process from biowaste. *Waste management*, 49:40–46.

Zeng, X., Sun, Q., Huo, B., Wan, H., and Jing, C. (2010). Integrated solid waste management under global warming. *The Open waste management journal*, 3(1).

Zhai, N., Zhang, T., Yin, D., Yang, G., Wang, X., Ren, G., and Feng, Y. (2015). Effect of initial ph on anaerobic co-digestion of kitchen waste and cow manure. *Waste management*, 38:126–131.

Zhang, C., Su, H., Baeyens, J., and Tan, T. (2014). Reviewing the anaerobic digestion of food waste for biogas production. *Renewable and Sustainable Energy Reviews*, 38:383–392.

Zhang, C., Yun, S., Li, X., Wang, Z., Xu, H., and Du, T. (2018a). Low-cost composited accelerants for anaerobic digestion of dairy manure: Focusing on methane yield, digestate utilization and energy evaluation. *Bioresource technology*, 263:517–524.

Zhang, J., Zhao, W., Zhang, H., Wang, Z., Fan, C., and Zang, L. (2018b). Recent achievements in enhancing anaerobic digestion with carbon-based functional materials. *Bioresource technology*, 266:555–567.

Zhang, L., Lee, Y.-W., and Jahng, D. (2011). Anaerobic co-digestion of food waste and piggery wastewater: focusing on the role of trace elements. *Bioresource technology*, 102(8):5048–5059.

Zhang, L., Loh, K.-C., and Zhang, J. (2018c). Food waste enhanced anaerobic digestion of biologically pretreated yard waste: Analysis of cellulose crystallinity and microbial communities. *Waste Management*, 79:109–119.

Zhang, L., Ouyang, W., and Lia, A. (2012). Essential role of trace elements in continuous anaerobic digestion of food waste. *Procedia Environmental Sciences*, 16:102–111.

Zhang, R., El-Mashad, H. M., Hartman, K., Wang, F., Liu, G., Choate, C., and Gamble, P. (2007). Characterization of food waste as feedstock for anaerobic digestion. *Bioresource technology*, 98(4):929–935.

Zhang, W., Wu, S., Guo, J., Zhou, J., and Dong, R. (2015a). Performance and kinetic evaluation of semi-continuously fed anaerobic digesters treating food waste: role of trace elements. *Bioresource technology*, 178:297–305.

Zhang, W., Zhang, L., and Li, A. (2015b). Anaerobic co-digestion of food waste with msw incineration plant fresh leachate: process performance and synergistic effects. *Chemical Engineering Journal*, 259:795–805.

Zhang, Y., Fan, R., Zhang, Q., Chen, Y., Sharifi, O., Leszczynska, D., Zhang, R., and Dai, Q. (2019). Synthesis of cawo4-biochar nanocomposites for organic dye removal. *Materials Research Bulletin*, 110:169–173.

Zhao, S.-X., Ta, N., and Wang, X.-D. (2017). Effect of temperature on the structural and physicochemical properties of biochar with apple tree branches as feedstock material. *Energies*, 10(9):1293.

Zhao, Z., Zhang, Y., Woodard, T., Nevin, K., and Lovley, D. (2015). Enhancing syntrophic metabolism in up-flow anaerobic sludge blanket reactors with conductive carbon materials. *Bioresource technology*, 191:140–145.

Zhen, G., Lu, X., Kato, H., Zhao, Y., and Li, Y.-Y. (2017). Overview of pretreatment

strategies for enhancing sewage sludge disintegration and subsequent anaerobic digestion: Current advances, full-scale application and future perspectives. *Renewable and Sustainable Energy Reviews*, 69:559–577.

Zhen, G., Lu, X., Kobayashi, T., Kumar, G., and Xu, K. (2016). Anaerobic co-digestion on improving methane production from mixed microalgae (scenedesmus sp., chlorella sp.) and food waste: Kinetic modeling and synergistic impact evaluation. *Chemical Engineering Journal*, 299:332–341.

Zhou, J., Zhang, Y., Khoshnevisan, B., and Duan, N. (2021). Meta-analysis of anaerobic co-digestion of livestock manure in last decade: Identification of synergistic effect and optimization synergy range. *Applied Energy*, 282:116128.

Zhou, Y., Zhang, Z., Nakamoto, T., Li, Y., Yang, Y., Utsumi, M., and Sugiura, N. (2011). Influence of substrate-to-inoculum ratio on the batch anaerobic digestion of bean curd refuse-okara under mesophilic conditions. *Biomass and bioenergy*, 35(7):3251–3256.

Ziemiński, K. and Kowalska-Wentel, M. (2015). Effect of enzymatic pretreatment on anaerobic co-digestion of sugar beet pulp silage and vinasse. *Bioresource technology*, 180:274–280.

Zitomer, D. H., Johnson, C. C., and Speece, R. E. (2008). Metal stimulation and municipal digester thermophilic/mesophilic activity. *Journal of environmental engineering*, 134(1):42–47.

Zwietering, M. H., Jongenburger, I., Rombouts, F. M., and Van't Riet, K. (1990). Modeling of the bacterial growth curve. *Applied and environmental microbiology*, 56(6):1875–1881.

Appendix

WORKSHEET 4

One-way ANOVA: PC (mL CH4/g VS), R1(mL CH4/g VS), R2(mL CH4/g VS), R3(mL CH4/g VS), R4(mL CH4/g VS), R5(mL CH4

*** NOTE * Cannot draw the interval plot for the Tukey procedure. Interval plots for comparisons are illegible with more than 45 intervals.**

Method

Null hypothesis	All means are equal
Alternative hypothesis	Not all means are equal
Significance level	α = 0.05

Equal variances were assumed for the analysis.

Factor Information

Factor	Levels	Values
Factor	17	PC (mL CH4/g VS), R1(mL CH4/g VS), R2(mL CH4/g VS), R3(mL CH4/g VS), R4(mL CH4/g VS), R5(mL CH4/g VS), R6(mL CH4/g VS), R7(mL CH4/g VS), R8(mL CH4/g VS), R9(mL CH4/g VS), R10(mL CH4/g VS), R11(mL CH4/g VS), R12 (mL CH4/g VS), R13 (mL CH4/g VS), R14 (mL CH4/g VS), R15 (mL CH4/g VS), R16 (mL CH4/g VS)

Analysis of Variance

Source	DF	Adj SS	Adj MS	F-Value	P-Value
Factor	16	18481923	1155120	111.59	0.00000
Error	1020	10558030	10351		
Total	1036	29039953			

Model Summary

S	R-sq	R-sq(adj)	R-sq(pred)
101.740	63.64%	63.07%	62.42%

Means

Factor	N	Mean	StDev	95% CI
PC (mL CH4/g VS)	61	281.5	122.3	(255.9, 307.1)
R1(mL CH4/g VS)	61	173.70	73.72	(148.14, 199.26)
R2(mL CH4/g VS)	61	87.48	31.47	(61.92, 113.04)
R3(mL CH4/g VS)	61	150.14	32.53	(124.58, 175.70)
R4(mL CH4/g VS)	61	71.09	20.87	(45.52, 96.65)
R5(mL CH4/g VS)	61	388.8	145.2	(363.2, 414.3)
R6(mL CH4/g VS)	61	224.2	81.7	(198.7, 249.8)
R7(mL CH4/g VS)	61	354.8	100.2	(329.2, 380.4)
R8(mL CH4/g VS)	61	389.1	175.2	(363.6, 414.7)
R9(mL CH4/g VS)	61	564.7	177.3	(539.1, 590.3)
R10(mL CH4/g VS)	61	438.8	139.9	(413.3, 464.4)
R11(mL CH4/g VS)	61	111.57	25.14	(86.01, 137.13)
R12 (mL CH4/g VS)	61	183.09	64.88	(157.52, 208.65)
R13 (mL CH4/g VS)	61	192.52	53.61	(166.96, 218.09)
R14 (mL CH4/g VS)	61	345.7	136.6	(320.2, 371.3)
R15 (mL CH4/g VS)	61	174.03	51.10	(148.47, 199.59)
R16 (mL CH4/g VS)	61	211.91	67.81	(186.35, 237.47)

Pooled StDev = 101.740

Tukey Pairwise Comparisons

Grouping Information Using the Tukey Method and 95% Confidence

Factor	N	Mean	Grouping						
R9(mL CH4/g VS)	61	564.7	A						
R10(mL CH4/g VS)	61	438.8		B					
R8(mL CH4/g VS)	61	389.1		B	C				
R5(mL CH4/g VS)	61	388.8		B	C				
R7(mL CH4/g VS)	61	354.8			C				
R14 (mL CH4/g VS)	61	345.7			C				
PC (mL CH4/g VS)	61	281.5				D			
R6(mL CH4/g VS)	61	224.2				D	E		
R16 (mL CH4/g VS)	61	211.91					E	F	
R13 (mL CH4/g VS)	61	192.52					E	F	
R12 (mL CH4/g VS)	61	183.09					E	F	
R15 (mL CH4/g VS)	61	174.03					E	F	G
R1(mL CH4/g VS)	61	173.70					E	F	G
R3(mL CH4/g VS)	61	150.14						F	G
R11(mL CH4/g VS)	61	111.57							G
R2(mL CH4/g VS)	61	87.48							
R4(mL CH4/g VS)	61	71.09							

	H	I
	H	I
		I

Means that do not share a letter are significantly different.

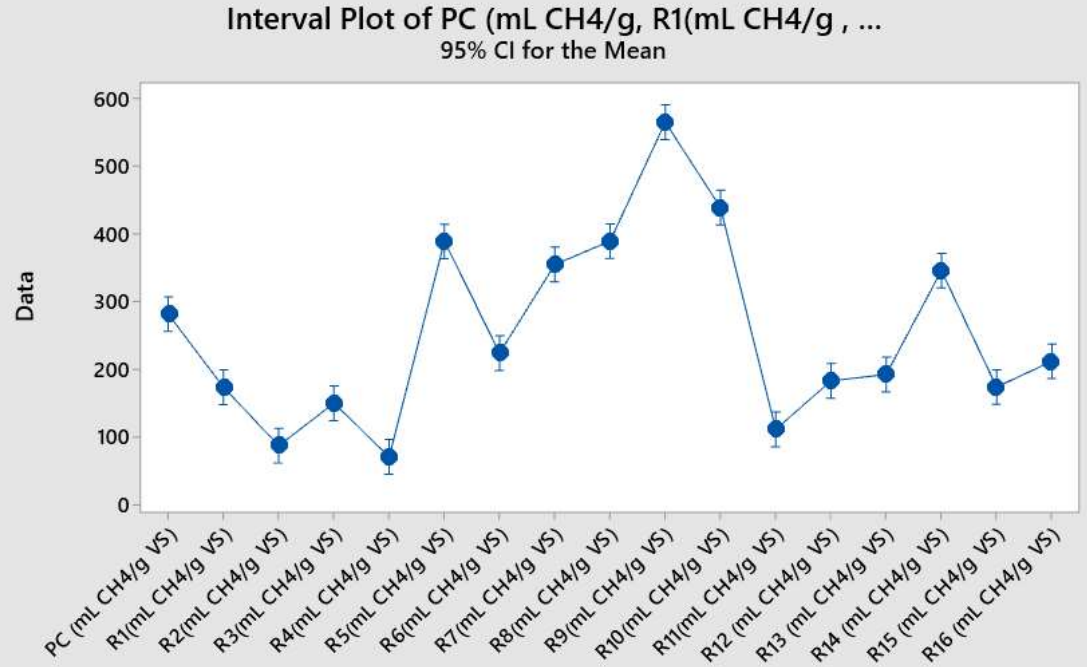

The pooled standard deviation is used to calculate the intervals.

APPENDIX A2

Type	FP analysis
Folder	<Common>
File	CCNCCN_202212071341
Counts	All
Analysis date	07-12-22 13:41
Sample name	CCN
Application	CCN

[Analyzed result]

Component	Result 1	Result 2	Unit	Number	Average
MgO	8.1	7.34	mass%	2	**7.72**
Al2O3	6.19	5.09	mass%	2	**5.64**
SiO2	20.9	17.1	mass%	2	**19**
P2O5	7.03	5.9	mass%	2	**6.465**
SO3	10.5	8.01	mass%	2	**9.255**
K2O	32.2	41.3	mass%	2	**36.75**
CaO	7.31	8.43	mass%	2	**7.87**
TiO2	0.131	0.163	mass%	2	**0.147**
V2O5	ND	ND	mass%	0	**0**
Cr2O3	1.08	1.24	mass%	2	**1.16**
MnO	0.165	0.125	mass%	2	**0.145**
Fe2O3	1.52	0.981	mass%	2	**1.2505**
Co2O3	0.007	0.0054	mass%	2	**0.0062**
NiO	0.0241	0.0151	mass%	2	**0.0196**
CuO	0.236	0.167	mass%	2	**0.2015**
ZnO	0.0453	0.0308	mass%	2	**0.03805**
Ga2O3	ND	ND	mass%	0	**0**
GeO2	ND	ND	mass%	0	**0**
As2O3	ND	ND	mass%	0	**0**
SeO2	ND	ND	mass%	0	**0**
Rb2O	0.0976	0.0709	mass%	2	**0.08425**
SrO	0.0367	0.027	mass%	2	**0.03185**
Y2O3	0.0161	0.0112	mass%	2	**0.01365**
Nb2O5	ND	ND	mass%	0	**0**
MoO3	ND	ND	mass%	0	**0**
RuO2	ND	ND	mass%	0	**0**
Rh2O3	ND	ND	mass%	0	**0**
PdO	ND	ND	mass%	0	**0**
Ag2O	ND	ND	mass%	0	**0**
CdO	ND	ND	mass%	0	**0**
In2O3	ND	ND	mass%	0	**0**
SnO2	0.0174	ND	mass%	1	**0.0174**
Sb2O3	ND	ND	mass%	0	**0**
TeO2	0.0181	ND	mass%	1	**0.0181**
Cs2O	ND	ND	mass%	0	**0**
BaO	ND	ND	mass%	0	**0**
La2O3	ND	ND	mass%	0	**0**

CeO2	ND	ND	mass%	0	**0**
Pr6O11	ND	ND	mass%	0	**0**
Nd2O3	ND	ND	mass%	0	**0**
HfO2	0.0049	ND	mass%	1	**0.0049**
Ta2O5	ND	ND	mass%	0	**0**
WO3	ND	ND	mass%	0	**0**
Ir2O3	ND	ND	mass%	0	**0**
PtO2	ND	ND	mass%	0	**0**
Au2O	0.0032	ND	mass%	1	**0.0032**
HgO	ND	ND	mass%	0	**0**
Tl2O3	ND	ND	mass%	0	**0**
PbO	ND	ND	mass%	0	**0**
Bi2O3	ND	ND	mass%	0	**0**
ThO2	ND	ND	mass%	0	**0**
U3O8	ND	ND	mass%	0	**0**
Na2O	2.59	2.9	mass%	2	**2.745**
Sc2O3	0.0276	ND	mass%	1	**0.0276**
ZrO2	1.76	1.09	mass%	2	**1.425**

Type	FP analysis
Folder	<Common>
File	PKNPKN
Counts	All
Analysis date	07-12-22 10:23
Sample name	PKN
Application	PKN

[Analyzed result]

Component	Result 1	Result 2	Unit	Number	Average
MgO	ND	ND	mass%	0	**0**
Al2O3	5.32	5.65	mass%	2	**5.49**
SiO2	64.8	65.7	mass%	2	**65.2**
P2O5	ND	ND	mass%	0	**0**
SO3	2.14	2.03	mass%	2	**2.08**
K2O	9.58	9.14	mass%	2	**9.36**
CaO	8.48	8.22	mass%	2	**8.35**
TiO2	0.271	0.24	mass%	2	**0.255**
V2O5	0.0044	0.01	mass%	2	**0.0072**
Cr2O3	0.235	0.23	mass%	2	**0.232**
MnO	0.358	0.34	mass%	2	**0.349**
Fe2O3	4.4	4.24	mass%	2	**4.32**
Co2O3	0.0084	0.0168	mass%	2	**0.0126**
NiO	0.0205	0.0137	mass%	2	**0.0171**
CuO	0.229	0.213	mass%	2	**0.221**
ZnO	0.088	0.0841	mass%	2	**0.086**

Ga2O3	ND	ND	mass%	0	**0**
GeO2	ND	ND	mass%	0	**0**
As2O3	ND	ND	mass%	0	**0**
SeO2	ND	ND	mass%	0	**0**
Rb2O	0.0647	0.0619	mass%	2	**0.0633**
SrO	0.102	0.095	mass%	2	**0.0982**
Y2O3	ND	ND	mass%	0	**0**
Nb2O5	ND	ND	mass%	0	**0**
MoO3	ND	ND	mass%	0	**0**
RuO2	ND	ND	mass%	0	**0**
Rh2O3	ND	ND	mass%	0	**0**
PdO	ND	ND	mass%	0	**0**
Ag2O	ND	ND	mass%	0	**0**
CdO	ND	ND	mass%	0	**0**
In2O3	ND	ND	mass%	0	**0**
SnO2	0.0346	0.0365	mass%	2	**0.0356**
Sb2O3	ND	ND	mass%	0	**0**
TeO2	ND	0.0264	mass%	1	**0.0264**
Cs2O	ND	ND	mass%	0	**0**
BaO	ND	ND	mass%	0	**0**
La2O3	ND	ND	mass%	0	**0**
CeO2	ND	ND	mass%	0	**0**
Pr6O11	ND	ND	mass%	0	**0**
Nd2O3	ND	ND	mass%	0	**0**
HfO2	ND	0.0057	mass%	2	**0.0029**
Ta2O5	0.0004	ND	mass%	1	**0.0004**
WO3	ND	ND	mass%	0	**0**
Ir2O3	ND	ND	mass%	0	**0**
PtO2	ND	ND	mass%	0	**0**
Au2O	ND	0.0021	mass%	1	**0.0021**
HgO	ND	ND	mass%	0	**0**
Tl2O3	ND	ND	mass%	0	**0**
PbO	ND	ND	mass%	0	**0**
Bi2O3	ND	ND	mass%	0	**0**
ThO2	ND	ND	mass%	0	**0**
U3O8	ND	ND	mass%	0	**0**
Na2O	ND	ND	mass%	0	**0**
Sc2O3	0.0151	0.0211	mass%	2	**0.0181**
ZrO2	3.88	3.65	mass%	2	**3.76**

Type	FP analysis
Folder	<Common>
File	CCN_ECCN_E
Counts	All
Analysis date	07-12-22 11:08
Sample name	CCN_E
Application	CCN_E

[Analyzed result]

Component	Result 1	Result 2	Unit	Number	Average
Mg	1410	1370	ppm	2	**1391**
Al	584	574	ppm	2	**579**
Si	1630	1620	ppm	2	**1628**
P	81.9	59.2	ppm	2	**70.6**
S	487	485	ppm	2	**486**
Cl	1070	1070	ppm	2	**1076**
K	11400	11400	ppm	2	**11485**
Ca	820	828	ppm	2	**824**
Ti	13.3	10.9	ppm	2	**12.1**
V	2.23	ND	ppm	1	**2.23**
Cr	83.4	85.4	ppm	2	**84.4**
Mn	74.1	73.4	ppm	2	**73.8**
Fe	568	564	ppm	2	**566**
Co	ND	ND	ppm	0	**0**
Ni	7.17	7.29	ppm	2	**7.23**
Cu	79.7	79.8	ppm	2	**79.8**
Zn	14	13.6	ppm	2	**13.8**
Ga	ND	ND	ppm	0	**0**
Ge	ND	ND	ppm	0	**0**
As	ND	ND	ppm	0	**0**
Se	ND	ND	ppm	0	**0**
Br	4.49	3.99	ppm	2	**4.24**
Rb	32.9	32.8	ppm	2	**32.9**
Sr	11.4	11	ppm	2	**11.2**
Y	ND	3.97	ppm	1	**3.97**
Nb	ND	ND	ppm	0	**0**
Mo	ND	ND	ppm	0	**0**
Ru	ND	ND	ppm	0	**0**
Rh	ND	ND	ppm	0	**0**
Pd	ND	ND	ppm	0	**0**
Ag	0.701	ND	ppm	1	**0.701**
Cd	ND	ND	ppm	0	**0**
In	ND	ND	ppm	0	**0**
Sn	8.69	9.33	ppm	2	**9.01**
Sb	ND	ND	ppm	0	**0**
Te	8.81	7.86	ppm	2	**8.34**
I	ND	ND	ppm	0	**0**

Cs	ND	ND	ppm	0	**0**
Ba	ND	ND	ppm	0	**0**
La	ND	ND	ppm	0	**0**
Ce	ND	ND	ppm	0	**0**
Pr	ND	ND	ppm	0	**0**
Nd	ND	ND	ppm	0	**0**
Hf	ND	ND	ppm	2	**0**
Ta	ND	ND	ppm	2	**0.535**
W	ND	ND	ppm	0	**0**
Ir	ND	ND	ppm	0	**0**
Pt	ND	ND	ppm	0	**0**
Au	ND	ND	ppm	2	**1.048**
Hg	ND	ND	ppm	0	**0**
Tl	ND	ND	ppm	0	**0**
Pb	ND	ND	ppm	0	**0**
Bi	ND	ND	ppm	0	**0**
Th	ND	ND	ppm	0	**0**
U	ND	ND	ppm	2	**0**
O	954000	955000	ppm	2	**954871**
Na	26100	25600	ppm	2	**25922**
Sc	ND	ND	ppm	0	**0**
Zr	744	775	ppm	2	**760**

Type	FP analysis
Folder	<Common>
File	PKN_EPKN_E
Counts	All
Analysis date	07-12-22 11:27
Sample name	PKN_E
Application	PKN_E

[Analyzed result]

Component	Result 1	Result 2	Unit	Number	**Average**
Mg	2900	2820	ppm	2	**2863**
Al	5710	5620	ppm	2	**5669**
Si	37300	37400	ppm	2	**37412**
P	292	283	ppm	2	**287**
S	590	582	ppm	2	**586**
Cl	121	120	ppm	2	**121**
K	4460	4420	ppm	2	**4444**
Ca	2670	2660	ppm	2	**2668**
Ti	56.1	61.2	ppm	2	**58.6**
V	2.12	ND	ppm	1	**2.12**
Cr	53.3	56.6	ppm	2	**55**
Mn	98.3	97	ppm	2	**97.7**

Fe	1020	1020	ppm	2	**1022**
Co	0.7643	ND	ppm	1	**0.7643**
Ni	4.23	4.24	ppm	2	**4.24**
Cu	51.3	52.4	ppm	2	**51.9**
Zn	18.8	19.2	ppm	2	**19**
Ga	ND	ND	ppm	0	**0**
Ge	ND	ND	ppm	0	**0**
As	ND	ND	ppm	0	**0**
Se	ND	ND	ppm	0	**0**
Br	2.22	2.51	ppm	2	**2.37**
Rb	15.3	15.4	ppm	2	**15.4**
Sr	22.2	22.5	ppm	2	**22.4**
Y	ND	ND	ppm	0	**0**
Nb	ND	ND	ppm	0	**0**
Mo	ND	ND	ppm	0	**0**
Ru	ND	ND	ppm	0	**0**
Rh	ND	ND	ppm	0	**0**
Pd	ND	ND	ppm	0	**0**
Ag	ND	ND	ppm	0	**0**
Cd	ND	ND	ppm	0	**0**
In	ND	ND	ppm	0	**0**
Sn	9.04	8.95	ppm	2	**9**
Sb	4.27	ND	ppm	1	**4.27**
Te	11.1	7.83	ppm	2	**9.47**
I	ND	ND	ppm	0	**0**
Cs	ND	ND	ppm	0	**0**
Ba	ND	ND	ppm	0	**0**
La	ND	ND	ppm	0	**0**
Ce	ND	ND	ppm	0	**0**
Pr	ND	ND	ppm	0	**0**
Nd	ND	ND	ppm	0	**0**
Hf	0.0057	ND	ppm	1	**0.0057**
Ta	0.0043	ND	ppm	1	**0.0043**
W	ND	ND	ppm	0	**0**
Ir	ND	ND	ppm	0	**0**
Pt	ND	ND	ppm	0	**0**
Au	ND	ND	ppm	0	**0**
Hg	ND	ND	ppm	0	**0**
Tl	ND	ND	ppm	0	**0**
Pb	ND	2.41	ppm	1	**2.41**
Bi	ND	ND	ppm	0	**0**
Th	ND	ND	ppm	0	**0**
U	ND	ND	ppm	0	**0**
O	943000	943000	ppm	2	**943755**
Na	ND	ND	ppm	0	**0**
Sc	ND	ND	ppm	0	**0**
Zr	815	830	ppm	2	**822**

APPENDIX A3

Quantachrome NovaWin - Data Acquisition and Reduction
for NOVA instruments
©1994-2013, Quantachrome Instruments
version 11.03

Analysis				Report			
Operator:	Abdulrahman Abdulkareem	Date:	2008/01/05	Operator:	Abdulrahman Abdulkareem	Date:	2022/11/14
Sample ID:	Sample CCN	Filename:		Sample CCN.qps			
Sample Desc:		Comment:					
Sample weight:	0.2 g	Sample Volume:		1 cc			
Outgas Time:	3.0 hrs	OutgasTemp:		250.0 C			
Analysis gas:	Nitrogen	Bath Temp:		273.0 K			
Press. Tolerance:	0.100/0.100 (ads/des)	Equil time:		60/60 sec (ads/des)	Equil timeout:		240/240 sec (ads/des)
Analysis Time:	62.4 min	End of run:		2008/01/05 4:53:14	Instrument:		Nova Station A
Cell ID:	1						

Multi-Point BET Plot

Data Reduction Parameters

Adsorbate	Nitrogen	Temperature	77.350K		
	Molec. Wt.: 28.013	Cross Section:	16.200 Å²	Liquid Density:	0.808 g/cc

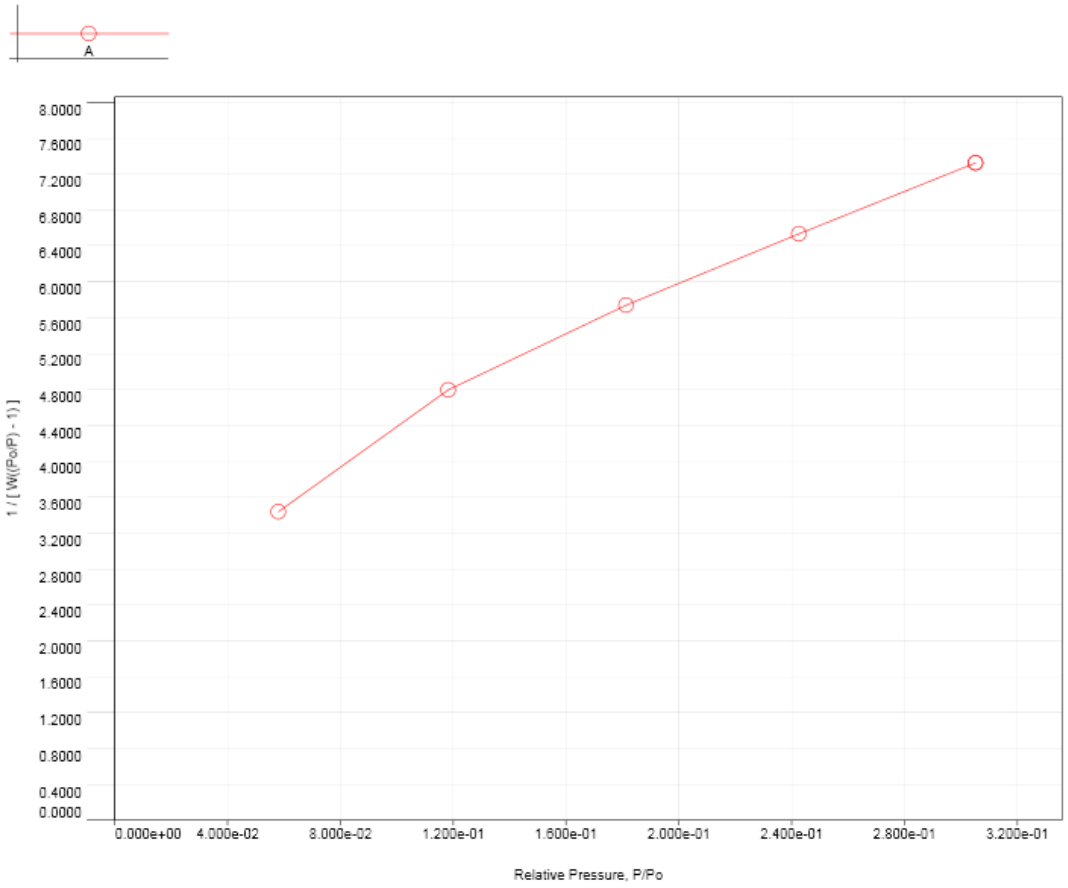

BET summary

Slope =	15.367
Intercept =	2.783e+00
Correlation coefficient, r =	0.992047
C constant=	6.522
Surface Area =	191.870 m²/g

APPENDIX A3

Quantachrome NovaWin - Data Acquisition and Reduction
for NOVA instruments
©1994-2013, Quantachrome Instruments
version 11.03

Analysis				Report			
Operator:	Abdulrahman Abdulkareem	Date:	2008/01/05	Operator:	Abdulrahman Abdulkareem	Date:	2022/11/14
Sample ID:	Sample CCN	Filename:		Sample CCN.qps			
Sample Desc:		Comment:					
Sample weight:	0.2 g	Sample Volume:		1 cc			
Outgas Time:	3.0 hrs	OutgasTemp:		250.0 C			
Analysis gas:	Nitrogen	Bath Temp:		273.0 K			
Press. Tolerance:	0.100/0.100 (ads/des)	Equil time:		60/60 sec (ads/des)	Equil timeout:		240/240 sec (ads/des)
Analysis Time:	62.4 min	End of run:		2008/01/05 4:53:14	Instrument:		Nova Station A
Cell ID:	1						

DA Plot

Data Reduction Parameters

DA Method	Incr. E:	500.000	Incr. n:	0.100	Interact. Const. (K):	2.960nm³ x kJ / mol	
Adsorbate	Nitrogen		Temperature	77.350K			
	Molec. Wt.:	28.013	Cross Section:	16.200 Å²	Liquid Density:	0.808 g/cc	

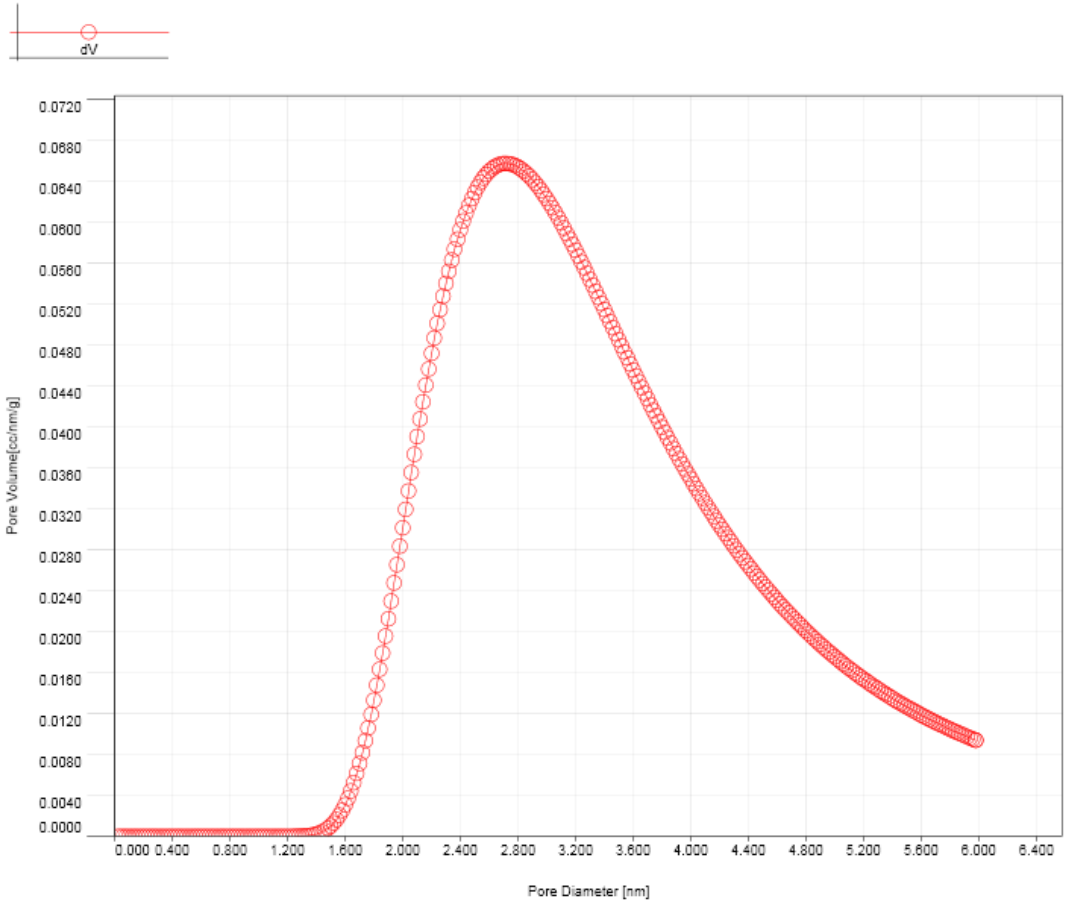

DA method summary

Best E =	0.887 kJ/mol
Best n =	1.000
DA Micropore Volume =	0.169 cc/g
Pore Diameter (mode)=	2.720e+00 nm

APPENDIX A3

Quantachrome NovaWin - Data Acquisition and Reduction
for NOVA instruments
©1994-2013, Quantachrome Instruments
version 11.03

Analysis				Report			
Operator:	Abdulrahman Abdulkareem	Date:	2008/01/05	Operator:	Abdulrahman Abdulkareem	Date:	2022/11/14
Sample ID:	Sample CCN	Filename:		Sample CCN.qps			
Sample Desc:		Comment:					
Sample weight:	0.2 g	Sample Volume:		1 cc			
Outgas Time:	3.0 hrs	OutgasTemp:		250.0 C			
Analysis gas:	Nitrogen	Bath Temp:		273.0 K			
Press. Tolerance:	0.100/0.100 (ads/des)	Equil time:		60/60 sec (ads/des)	Equil timeout:		240/240 sec (ads/des)
Analysis Time:	62.4 min	End of run:		2008/01/05 4:53:14	Instrument:		Nova Station A
Cell ID:	1						

BJH method Adsorption dV(d)

Data Reduction Parameters

t-Method	Calc. method: de Boer				
BJH/DH method	Moving pt. avg.: off				
Adsorbate	Nitrogen	Temperature	77.350K		
	Molec. Wt.: 28.013	Cross Section:	16.200 Å²	Liquid Density:	0.808 g/cc

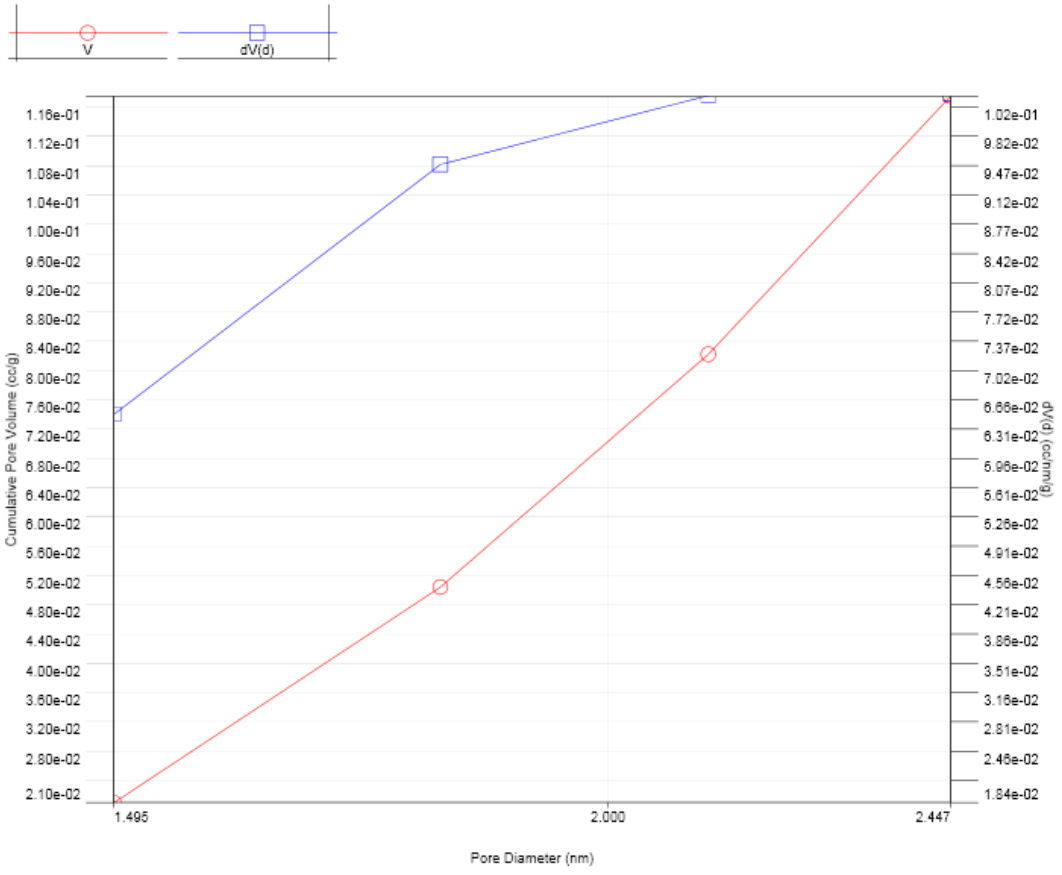

BJH adsorption summary

Surface Area =	238.732 m²/g
Pore Volume =	0.117 cc/g
Pore Diameter Dv(d) =	2.447 nm

APPENDIX A3

Quantachrome NovaWin - Data Acquisition and Reduction
for NOVA instruments
©1994-2013, Quantachrome Instruments
version 11.03

Analysis				Report			
Operator:	Abdulrahman Abdulkareem	**Date:**	2008/01/05	**Operator:**	Abdulrahman Abdulkareem	**Date:**	2022/11/14
Sample ID:	Sample CCN	**Filename:**		Sample CCN.qps			
Sample Desc:		**Comment:**					
Sample weight:	0.2 g	**Sample Volume:**		1 cc			
Outgas Time:	3.0 hrs	**OutgasTemp:**		250.0 C			
Analysis gas:	Nitrogen	**Bath Temp:**		273.0 K			
Press. Tolerance:	0.100/0.100 (ads/des)	**Equil time:**		60/60 sec (ads/des)	**Equil timeout:**		240/240 sec (ads/des)
Analysis Time:	62.4 min	**End of run:**		2008/01/05 4:53:14	**Instrument:**		Nova Station A
Cell ID:	1						

Multi-Point BET

Data Reduction Parameters Data

Adsorbate	Nitrogen		Temperature	77.350K		
	Molec. Wt.:	28.013	Cross Section:	16.200 Å²	Liquid Density:	0.808 g/cc

Multi-Point BET Data

Relative Pressure [P/Po]	Volume @ STP [cc/g]	1 / [W((Po/P) - 1)]	Relative Pressure [P/Po]	Volume @ STP [cc/g]	1 / [W((Po/P) - 1)]
5.79900e-02	14.3317	3.4368e+00	2.42569e-01	39.2114	6.5348e+00
1.18230e-01	22.3809	4.7934e+00	3.05221e-01	47.9938	7.3237e+00
1.81332e-01	30.8792	5.7392e+00			

BET summary

Slope =	15.367
Intercept =	2.783e+00
Correlation coefficient, r =	0.992047
C constant=	6.522
Surface Area =	191.870 m²/g

APPENDIX A3

Quantachrome NovaWin - Data Acquisition and Reduction
for NOVA instruments
©1994-2013, Quantachrome Instruments
version 11.03

Analysis				Report			
Operator:	Abdulrahman Abdulkareem	Date:	2008/01/05	Operator:	Abdulrahman Abdulkareem	Date:	2022/11/14
Sample ID:	Sample CCN	Filename:		Sample CCN.qps			
Sample Desc:		Comment:					
Sample weight:	0.2 g	Sample Volume:		1 cc			
Outgas Time:	3.0 hrs	OutgasTemp:		250.0 C			
Analysis gas:	Nitrogen	Bath Temp:		273.0 K			
Press. Tolerance:	0.100/0.100 (ads/des)	Equil time:		60/60 sec (ads/des)	Equil timeout:		240/240 sec (ads/des)
Analysis Time:	62.4 min	End of run:		2008/01/05 4:53:14	Instrument:		Nova Station A
Cell ID:	1						

Langmuir

Data Reduction Parameters Data

Adsorbate	Nitrogen		Temperature	77.350K		
	Molec. Wt.:	28.013	Cross Section:	16.200 Å²	Liquid Density:	0.808 g/cc

Langmuir Data

P/Po	P/Po/W [(g/g)]	P/Po	P/Po/W [(g/g)]
5.79900e-02	3.2375e+00	2.42569e-01	4.9496e+00
1.18230e-01	4.2267e+00	3.05221e-01	5.0884e+00
1.81332e-01	4.6985e+00		

Langmuir summary

Slope =	7.13755
Intercept =	3.14775
Correlation coefficient, r =	0.934
Surface Area =	487.915 m²/g

APPENDIX A3

Quantachrome NovaWin - Data Acquisition and Reduction
for NOVA instruments
©1994-2013, Quantachrome Instruments
version 11.03

Analysis				Report			
Operator:	Abdulrahman Abdulkareem	**Date:**	2008/01/05	**Operator:**	Abdulrahman Abdulkareem	**Date:**	2022/11/14
Sample ID:	Sample CCN	**Filename:**		Sample CCN.qps			
Sample Desc:		**Comment:**					
Sample weight:	0.2 g	**Sample Volume:**		1 cc			
Outgas Time:	3.0 hrs	**OutgasTemp:**		250.0 C			
Analysis gas:	Nitrogen	**Bath Temp:**		273.0 K			
Press. Tolerance:	0.100/0.100 (ads/des)	**Equil time:**		60/60 sec (ads/des)	**Equil timeout:**		240/240 sec (ads/des)
Analysis Time:	62.4 min	**End of run:**		2008/01/05 4:53:14	**Instrument:**		Nova Station A
Cell ID:	1						

Isotherm

Data Reduction Parameters Data

Adsorbate	Nitrogen		Temperature	77.350K		
	Molec. Wt.:	28.013	Cross Section:	16.200 Å²	Liquid Density:	0.808 g/cc

Isotherm Data

Relative Pressure	Volume @ STP [cc/g]	Relative Pressure	Volume @ STP [cc/g]	Relative Pressure	Volume @ STP [cc/g]
5.79900e-02	14.3317	1.81332e-01	30.8792	3.05221e-01	47.9938
1.18230e-01	22.3809	2.42569e-01	39.2114		

APPENDIX A3

Quantachrome NovaWin - Data Acquisition and Reduction
for NOVA instruments
©1994-2013, Quantachrome Instruments
version 11.03

Analysis				Report			
Operator:	Abdulrahman AbdulkareemDate:2008/01/05			**Operator:**	Abdulrahman Abdulkareem Date:2022/11/14		
Sample ID:	Sample CCN	**Filename:**		Sample CCN.qps			
Sample Desc:		**Comment:**					
Sample weight:	0.2 g	**Sample Volume:**		1 cc			
Outgas Time:	3.0 hrs	**OutgasTemp:**		250.0 C			
Analysis gas:	Nitrogen	**Bath Temp:**		273.0 K			
Press. Tolerance:	0.100/0.100 (ads/des)	**Equil time:**		60/60 sec (ads/des)	**Equil timeout:**	240/240 sec (ads/des)	
Analysis Time:	62.4 min	**End of run:**		2008/01/05 4:53:14	**Instrument:**	Nova Station A	
Cell ID:	1						

DR method

Data Reduction Parameters Data

DR method	Affinity coefficient (ß): 0.3300				
Adsorbate	Nitrogen	Temperature	77.350K		
	Molec. Wt.: 28.013	Cross Section:	16.200 Å²	Liquid Density:	0.808 g/cc
	Critical Temp.: 126.200 K	Critical Press.:	33.500 atm	SuperCritic. K.:	1.000
Adsorbent	Carbon				
	DR. Exp (n): 2.000				

DR method Data

Log2(P/Po)	Weight Adsorbed [(g)]	Log2(P/Po)	Weight Adsorbed [(g)]
1.529296e+00	3.5824e-03	3.784276e-01	9.8015e-03
8.598339e-01	5.5945e-03	2.656223e-01	1.1997e-02
5.498601e-01	7.7187e-03		

DR method summary

Slope =	-4.017e-01
Intercept =	1.380e-02
Correlation Coefficient =	0.9821
Average Pore width =	5.571nm
Adsorption energy =	4.667 kJ/mol
Micropore volume =	0.085 cc/g
Micropore surface area =	240.283 m²/g

APPENDIX A3

Analysis
Operator: Abdulrahman Abdulkareem **Date:**2008/01/05
Sample ID: Sample CCN **Filename:**

Report
Operator: Abdulrahman Abdulkareem **Date:**2022/11/14
Sample CCN.qps

DA Method Micropore Analysis Data continued

Diameter [nm]	dV(d) [cc/nm/g]	Diameter [nm]	dV(d) [cc/nm/g]
4.66000e+00	2.20891e-02	5.34000e+00	1.39954e-02
4.68000e+00	2.17871e-02	5.36000e+00	1.38147e-02
4.70000e+00	2.14897e-02	5.38000e+00	1.36366e-02
4.72000e+00	2.11966e-02	5.40000e+00	1.34612e-02
4.74000e+00	2.09079e-02	5.42000e+00	1.32885e-02
4.76000e+00	2.06235e-02	5.44000e+00	1.31183e-02
4.78000e+00	2.03434e-02	5.46000e+00	1.29506e-02
4.80000e+00	2.00674e-02	5.48000e+00	1.27854e-02
4.82000e+00	1.97955e-02	5.50000e+00	1.26227e-02
4.84000e+00	1.95277e-02	5.52000e+00	1.24624e-02
4.86000e+00	1.92640e-02	5.54000e+00	1.23045e-02
4.88000e+00	1.90041e-02	5.56000e+00	1.21489e-02
4.90000e+00	1.87482e-02	5.58000e+00	1.19956e-02
4.92000e+00	1.84961e-02	5.60000e+00	1.18445e-02
4.94000e+00	1.82478e-02	5.62000e+00	1.16957e-02
4.96000e+00	1.80032e-02	5.64000e+00	1.15491e-02
4.98000e+00	1.77623e-02	5.66000e+00	1.14046e-02
5.00000e+00	1.75250e-02	5.68000e+00	1.12623e-02
5.02000e+00	1.72913e-02	5.70000e+00	1.11220e-02
5.04000e+00	1.70611e-02	5.72000e+00	1.09838e-02
5.06000e+00	1.68344e-02	5.74000e+00	1.08477e-02
5.08000e+00	1.66111e-02	5.76000e+00	1.07135e-02
5.10000e+00	1.63911e-02	5.78000e+00	1.05812e-02
5.12000e+00	1.61744e-02	5.80000e+00	1.04509e-02
5.14000e+00	1.59610e-02	5.82000e+00	1.03225e-02
5.16000e+00	1.57508e-02	5.84000e+00	1.01960e-02
5.18000e+00	1.55438e-02	5.86000e+00	1.00712e-02
5.20000e+00	1.53398e-02	5.88000e+00	9.94832e-03
5.22000e+00	1.51390e-02	5.90000e+00	9.82718e-03
5.24000e+00	1.49411e-02	5.92000e+00	9.70779e-03
5.26000e+00	1.47462e-02	5.94000e+00	9.59012e-03
5.28000e+00	1.45542e-02	5.96000e+00	9.47414e-03
5.30000e+00	1.43652e-02	5.98000e+00	9.35982e-03
5.32000e+00	1.41789e-02		

DA method summary

Best E =	0.887 kJ/mol
Best n =	1.000
DA Micropore Volume =	0.169 cc/g
Pore Diameter (mode)=	2.720e+00 nm

APPENDIX A3

Quantachrome NovaWin - Data Acquisition and Reduction
for NOVA instruments
©1994-2013, Quantachrome Instruments
version 11.03

Analysis				Report			
Operator:	Abdulrahman Abdulkareem	Date:	2008/01/05	Operator:	Abdulrahman Abdulkareem	Date:	2022/11/14
Sample ID:	Sample CCN	Filename:		Sample CCN.qps			
Sample Desc:		Comment:					
Sample weight:	0.2 g	Sample Volume:		1 cc			
Outgas Time:	3.0 hrs	OutgasTemp:		250.0 C			
Analysis gas:	Nitrogen	Bath Temp:		273.0 K			
Press. Tolerance:	0.100/0.100 (ads/des)	Equil time:		60/60 sec (ads/des)	Equil timeout:		240/240 sec (ads/des)
Analysis Time:	62.4 min	End of run:		2008/01/05 4:53:14	Instrument:		Nova Station A
Cell ID:	1						

DFT method Pore Size Distribution

Data Reduction Parameters Data

DFT method	Calc. Model: N2 at 77 K on carbon (slit pore, NLDFT equilibrium model)				
	Rel. press. range: 0.0000 - 1.0000			Moving pt. avg: off	
Adsorbate	Nitrogen	Temperature	77.350K		
	Molec. Wt.: 28.013	Cross Section:	16.200 Å²	Liquid Density:	0.808 g/cc

DFT method Pore Size Distribution Data

Pore width [nm]	Cumulative Pore Volume [cc/g]	Cumulative Surface Area [m²/g]	dV(d) [cc/nm/g]	dS(d) [m²/nm/g]
1.7656	5.7169e-03	8.2087e+00	1.1226e-02	1.2717e+01
1.8469	9.2100e-03	1.1991e+01	4.2983e-02	4.6546e+01
1.9319	1.3407e-02	1.6336e+01	4.9366e-02	5.1106e+01
2.0208	1.6738e-02	1.9633e+01	3.7460e-02	3.7074e+01
2.1138	1.6933e-02	1.9817e+01	2.1013e-03	1.9882e+00
2.2111	2.1416e-02	2.3872e+01	4.6077e-02	4.1677e+01
2.3129	2.9909e-02	3.1216e+01	8.3449e-02	7.2159e+01
2.4194	3.7492e-02	3.7485e+01	7.1226e-02	5.8880e+01
2.5307	4.6949e-02	4.4959e+01	8.4926e-02	6.7116e+01
2.6472	5.8613e-02	5.3771e+01	1.0014e-01	7.5654e+01
2.7691	6.8214e-02	6.0706e+01	7.8799e-02	5.6914e+01

DFT method summary

Pore volume =	0.068 cc/g
Surface area =	60.706 m²/g
Lower confidence limit =	1.766 nm
Fitting error =	2.110 %
Pore width (Mode) =	2.647 nm
Moving point average :	off

APPENDIX A3

Quantachrome NovaWin - Data Acquisition and Reduction
for NOVA instruments
©1994-2013, Quantachrome Instruments
version 11.03

Analysis				Report			
Operator:	Abdulrahman Abdulkareem	**Date:**	2008/01/05	**Operator:**	Abdulrahman Abdulkareem	**Date:**	2022/11/14
Sample ID:	Sample CCN	**Filename:**		Sample CCN.qps			
Sample Desc:		**Comment:**					
Sample weight:	0.2 g	**Sample Volume:**		1 cc			
Outgas Time:	3.0 hrs	**OutgasTemp:**		250.0 C			
Analysis gas:	Nitrogen	**Bath Temp:**		273.0 K			
Press. Tolerance:	0.100/0.100 (ads/des)	**Equil time:**		60/60 sec (ads/des)	**Equil timeout:**		240/240 sec (ads/des)
Analysis Time:	62.4 min	**End of run:**		2008/01/05 4:53:14	**Instrument:**		Nova Station A
Cell ID:	1						

Area-Volume Summary

Data Reduction Parameters Data

	Thermal Transpiration: on	**Eff. mol. diameter (D):** 3.54 Å		**Eff. cell stem diam. (d):** 4.0000 mm	
t-Method	**Calc. method:** de Boer				
BJH/DH method	**Moving pt. avg.:** off				
DR method	**Affinity coefficient (ß):** 0.3300				
HK method	**Tabulated data interval:** 1				
SF method	**Tabulated data interval:** 1				
DFT method	**Calc. Model:** N2 at 77 K on carbon (slit pore, NLDFT equilibrium model)				
	Rel. press. range: 0.0000 - 1.0000			**Moving pt. avg:** off	
Adsorbate	**Nitrogen**	**Temperature**	77.350K		
	Molec. Wt.: 28.013	**Cross Section:**	16.200 Å²	**Liquid Density:**	0.808 g/cc
	Critical Temp.: 126.200 K	**Critical Press.:**	33.500 atm	**SuperCritic. K.:**	1.000
Adsorbent	Carbon				
	DR. Exp (n): 2.000				

Surface Area Data

SinglePoint BET	1.451e+02 m²/g
MultiPoint BET	1.919e+02 m²/g
Langmuir surface area	4.879e+02 m²/g
BJH method cumulative adsorption surface area	2.387e+02 m²/g
DH method cumulative adsorption surface area	2.536e+02 m²/g
t-method external surface area	1.919e+02 m²/g
DR method micropore area	2.403e+02 m²/g
DFT cumulative surface area	6.071e+01 m²/g

Pore Volume Data

BJH method cumulative adsorption pore volume	1.175e-01 cc/g
DH method cumulative adsorption pore volume	1.200e-01 cc/g
DR method micropore volume	8.539e-02 cc/g
HK method micropore volume	4.174e-02 cc/g
SF method micropore volume	1.477e-02 cc/g
DFT method cumulative pore volume	6.821e-02 cc/g

Pore Size Data

BJH method adsorption pore Diameter (Mode Dv(d))	2.447e+00 nm
DH method adsorption pore Diameter (Mode Dv(d))	2.121e+00 nm
DR method micropore Pore width	5.571e+00 nm
DA method pore Diameter (Mode)	2.720e+00 nm
HK method pore Diameter (Mode)	3.675e-01 nm
SF method pore Diameter (Mode)	4.523e-01 nm
DFT pore Diameter (Mode)	2.647e+00 nm

Analysis				Report			
Operator:	Abdulrahman Abdulkareem	Date:	2008/01/05	Operator:	Abdulrahman Abdulkareem	Date:	2022/11/14
Sample ID:	Sample PKN	Filename:		Sample PKN.qps			
Sample Desc:		Comment:					
Sample weight:	0.3 g	Sample Volume:		1 cc			
Outgas Time:	3.0 hrs	OutgasTemp:		250.0 C			
Analysis gas:	Nitrogen	Bath Temp:		273.0 K			
Press. Tolerance:	0.100/0.100 (ads/des)	Equil time:		60/60 sec (ads/des)	Equil timeout:		240/240 sec (ads/des)
Analysis Time:	103.0 min	End of run:		2008/01/05 21:16:41	Instrument:		Nova Station C
Cell ID:	3						

Multi-Point BET Plot

Data Reduction Parameters

Adsorbate	Nitrogen	Temperature	77.350K		
	Molec. Wt.: 28.013	Cross Section:	16.200 Å²	Liquid Density:	0.808 g/cc

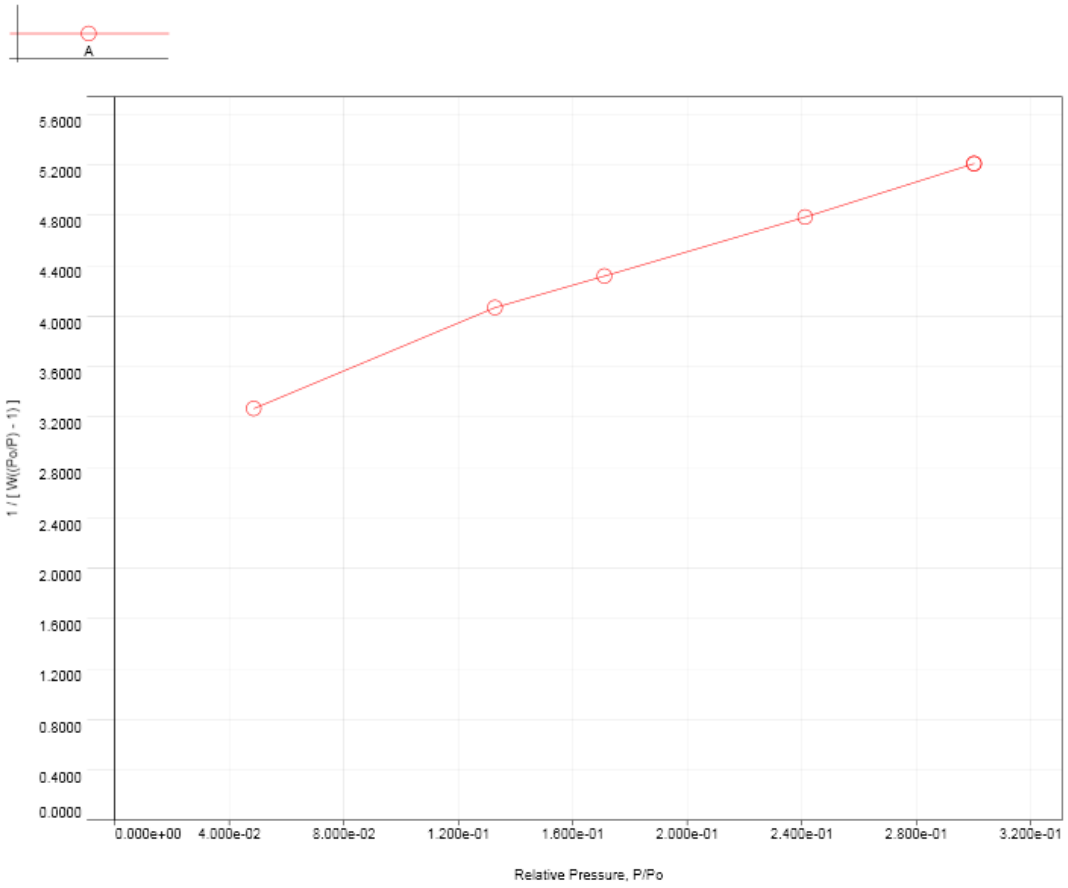

BET summary

Slope =	7.572
Intercept =	2.976e+00
Correlation coefficient, r =	0.995996
C constant=	3.545
Surface Area =	330.186 m²/g

Analysis				Report			
Operator:	Abdulrahman Abdulkareem	Date:	2008/01/05	Operator:	Abdulrahman Abdulkareem	Date:	2022/11/14
Sample ID:	Sample PKN	Filename:		Sample PKN.qps			
Sample Desc:		Comment:					
Sample weight:	0.3 g	Sample Volume:		1 cc			
Outgas Time:	3.0 hrs	OutgasTemp:		250.0 C			
Analysis gas:	Nitrogen	Bath Temp:		273.0 K			
Press. Tolerance:	0.100/0.100 (ads/des)	Equil time:		60/60 sec (ads/des)	Equil timeout:		240/240 sec (ads/des)
Analysis Time:	103.0 min	End of run:		2008/01/05 21:16:41	Instrument:		Nova Station C
Cell ID:	3						

DA Plot

Data Reduction Parameters

DA Method	Incr. E:	500.000	Incr. n:	0.100	Interact. Const. (K):	2.960nm³ x kJ / mol	
Adsorbate	Nitrogen		Temperature	77.350K			
	Molec. Wt.:	28.013	Cross Section:	16.200 Å²	Liquid Density:	0.808 g/cc	

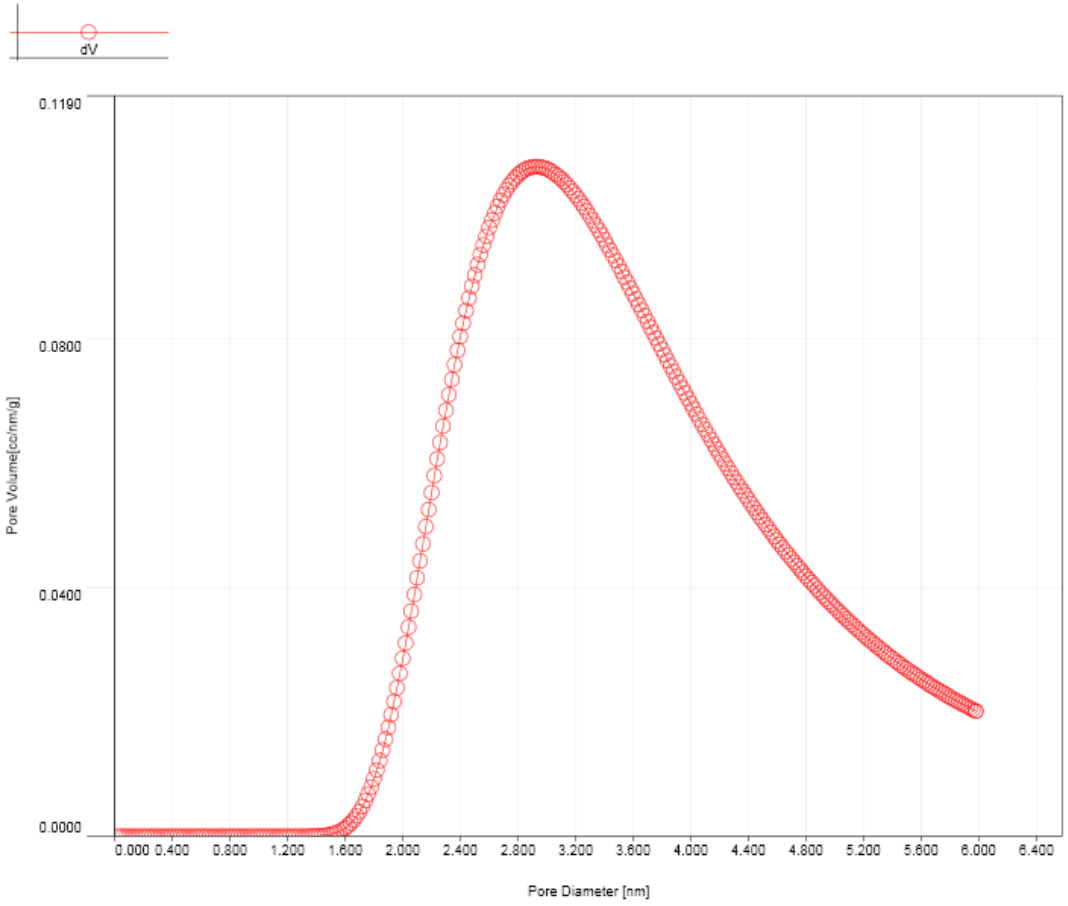

DA method summary

Best E =	0.707 kJ/mol
Best n =	1.000
DA Micropore Volume =	0.299 cc/g
Pore Diameter (mode)=	2.920e+00 nm

Analysis

Operator:	Abdulrahman AbdulkareemDate:2008/01/05		
Sample ID:	Sample PKN	**Filename:**	Sample PKN.qps
Sample Desc:		**Comment:**	
Sample weight:	0.3 g	**Sample Volume:**	1 cc
Outgas Time:	3.0 hrs	**OutgasTemp:**	250.0 C
Analysis gas:	Nitrogen	**Bath Temp:**	273.0 K
Press. Tolerance:	0.100/0.100 (ads/des)	**Equil time:**	60/60 sec (ads/des)
Analysis Time:	103.0 min	**End of run:**	2008/01/05 21:16:41
Cell ID:	3		

Report

Operator:	Abdulrahman Abdulkareem	**Date:**	2022/11/14
Equil timeout:	240/240 sec (ads/des)		
Instrument:	Nova Station C		

BJH method Adsorption dV(d)

Data Reduction Parameters

t-Method	Calc. method: de Boer				
BJH/DH method	Moving pt. avg.: off				
Adsorbate	Nitrogen	Temperature	77.350K		
	Molec. Wt.: 28.013	Cross Section:	16.200 Å²	Liquid Density:	0.808 g/cc

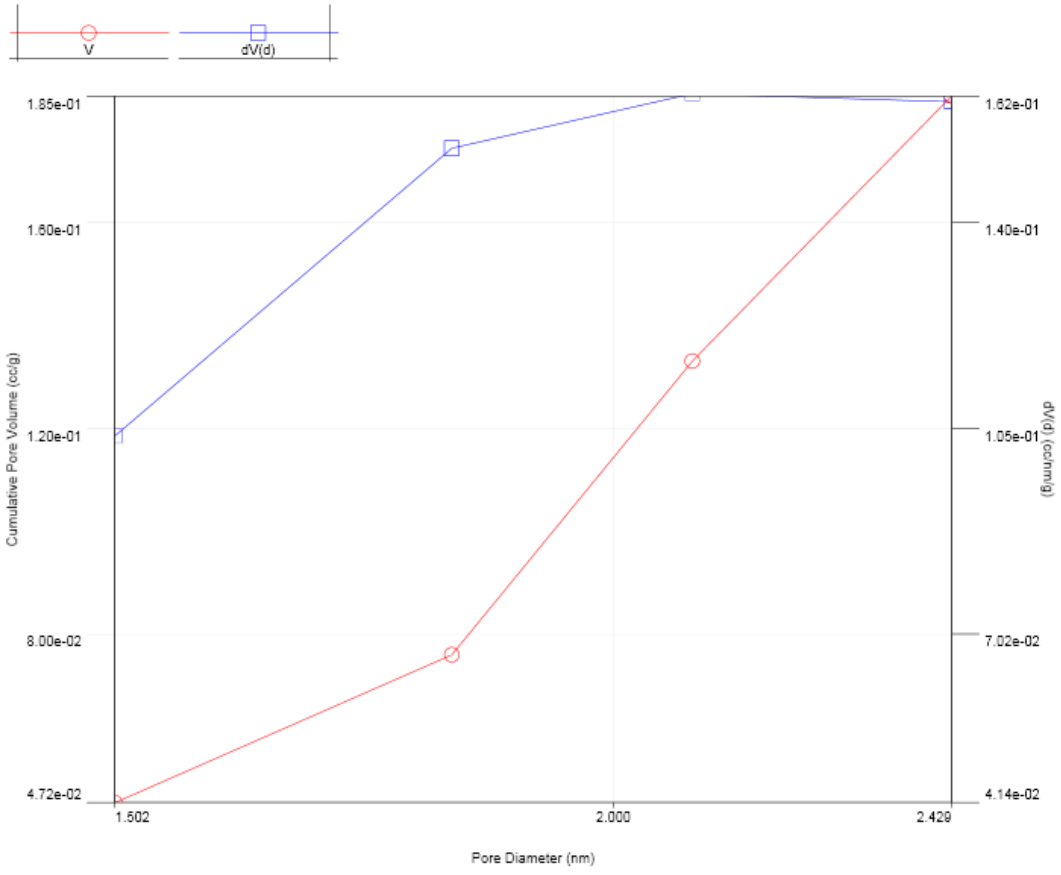

BJH adsorption summary

Surface Area =	382.787 m²/g
Pore Volume =	0.185 cc/g
Pore Diameter Dv(d) =	2.093 nm

Analysis				Report			
Operator:	Abdulrahman Abdulkareem	**Date:**	2008/01/05	**Operator:**	Abdulrahman Abdulkareem	**Date:**	2022/11/14
Sample ID:	Sample PKN	**Filename:**		Sample PKN.qps			
Sample Desc:		**Comment:**					
Sample weight:	0.3 g	**Sample Volume:**		1 cc			
Outgas Time:	3.0 hrs	**OutgasTemp:**		250.0 C			
Analysis gas:	Nitrogen	**Bath Temp:**		273.0 K			
Press. Tolerance:	0.100/0.100 (ads/des)	**Equil time:**		60/60 sec (ads/des)	**Equil timeout:**		240/240 sec (ads/des)
Analysis Time:	103.0 min	**End of run:**		2008/01/05 21:16:41	**Instrument:**		Nova Station C
Cell ID:	3						

Multi-Point BET

Data Reduction Parameters Data

Adsorbate	Nitrogen		Temperature	77.350K		
	Molec. Wt.:	28.013	Cross Section:	16.200 Å²	Liquid Density:	0.808 g/cc

Multi-Point BET Data

Relative Pressure [P/Po]	Volume @ STP [cc/g]	1 / [W((Po/P) - 1)]	Relative Pressure [P/Po]	Volume @ STP [cc/g]	1 / [W((Po/P) - 1)]
4.85470e-02	12.5014	3.2656e+00	2.41176e-01	53.1443	4.7850e+00
1.32799e-01	30.1260	4.0671e+00	3.00189e-01	65.8832	5.2094e+00
1.71069e-01	38.2396	4.3181e+00			

BET summary

Slope =	7.572
Intercept =	2.976e+00
Correlation coefficient, r =	0.995996
C constant=	3.545
Surface Area =	330.186 m²/g

Analysis				Report			
Operator:	Abdulrahman Abdulkareem	**Date:**	2008/01/05	**Operator:**	Abdulrahman Abdulkareem	**Date:**	2022/11/14
Sample ID:	Sample PKN	**Filename:**		Sample PKN.qps			
Sample Desc:		**Comment:**					
Sample weight:	0.3 g	**Sample Volume:**		1 cc			
Outgas Time:	3.0 hrs	**OutgasTemp:**		250.0 C			
Analysis gas:	Nitrogen	**Bath Temp:**		273.0 K			
Press. Tolerance:	0.100/0.100 (ads/des)	**Equil time:**		60/60 sec (ads/des)	**Equil timeout:**		240/240 sec (ads/des)
Analysis Time:	103.0 min	**End of run:**		2008/01/05 21:16:41	**Instrument:**		Nova Station C
Cell ID:	3						

Langmuir

Data Reduction Parameters Data

Adsorbate	Nitrogen		Temperature	77.350K		
	Molec. Wt.:	28.013	Cross Section:	16.200 Å²	Liquid Density:	0.808 g/cc

Langmuir Data

P/Po	P/Po/W [(g/g)]	P/Po	P/Po/W [(g/g)]
4.85470e-02	3.1071e+00	2.41176e-01	3.6310e+00
1.32799e-01	3.5270e+00	3.00189e-01	3.6456e+00
1.71069e-01	3.5794e+00		

Langmuir summary

Slope =	1.99031
Intercept =	3.14224
Correlation coefficient, r =	0.865
Surface Area =	1749.735 m²/g

Quantachrome NovaWin - Data Acquisition and Reduction
for NOVA instruments
©1994-2013, Quantachrome Instruments
version 11.03

Analysis				Report			
Operator:	Abdulrahman Abdulkareem	**Date:**	2008/01/05	**Operator:**	Abdulrahman Abdulkareem	**Date:**	2022/11/14
Sample ID:	Sample PKN	**Filename:**		Sample PKN.qps			
Sample Desc:		**Comment:**					
Sample weight:	0.3 g	**Sample Volume:**		1 cc			
Outgas Time:	3.0 hrs	**OutgasTemp:**		250.0 C			
Analysis gas:	Nitrogen	**Bath Temp:**		273.0 K			
Press. Tolerance:	0.100/0.100 (ads/des)	**Equil time:**		60/60 sec (ads/des)	**Equil timeout:**		240/240 sec (ads/des)
Analysis Time:	103.0 min	**End of run:**		2008/01/05 21:16:41	**Instrument:**		Nova Station C
Cell ID:	3						

Isotherm

Data Reduction Parameters Data

Adsorbate	Nitrogen		Temperature	77.350K		
	Molec. Wt.:	28.013	Cross Section:	16.200 Å²	Liquid Density:	0.808 g/cc

Isotherm Data

Relative Pressure	Volume @ STP [cc/g]	Relative Pressure	Volume @ STP [cc/g]	Relative Pressure	Volume @ STP [cc/g]
4.85470e-02	12.5014	1.71069e-01	38.2396	3.00189e-01	65.8832
1.32799e-01	30.1260	2.41176e-01	53.1443		

Analysis				Report			
Operator:	Abdulrahman Abdulkareem	**Date:**	2008/01/05	**Operator:**	Abdulrahman Abdulkareem	**Date:**	2022/11/14
Sample ID:	Sample PKN	**Filename:**		Sample PKN.qps			
Sample Desc:		**Comment:**					
Sample weight:	0.3 g	**Sample Volume:**		1 cc			
Outgas Time:	3.0 hrs	**OutgasTemp:**		250.0 C			
Analysis gas:	Nitrogen	**Bath Temp:**		273.0 K			
Press. Tolerance:	0.100/0.100 (ads/des)	**Equil time:**		60/60 sec (ads/des)	**Equil timeout:**		240/240 sec (ads/des)
Analysis Time:	103.0 min	**End of run:**		2008/01/05 21:16:41	**Instrument:**		Nova Station C
Cell ID:	3						

DR method

Data Reduction Parameters Data

DR method	Affinity coefficient (ß): 0.3300				
Adsorbate	Nitrogen	Temperature	77.350K		
	Molec. Wt.: 28.013	Cross Section:	16.200 Å²	Liquid Density:	0.808 g/cc
	Critical Temp.: 126.200 K	Critical Press.:	33.500 atm	SuperCritic. K.:	1.000
Adsorbent	Carbon				
	DR. Exp (n): 2.000				

DR method Data

Log2(P/Po)	Weight Adsorbed [(g)]	Log2(P/Po)	Weight Adsorbed [(g)]
1.726169e+00	4.6874e-03	3.815112e-01	1.9926e-02
7.687874e-01	1.1296e-02	2.731162e-01	2.4703e-02
5.880262e-01	1.4338e-02		

DR method summary

Slope =	-4.780e-01
Intercept =	2.964e-02
Correlation Coefficient =	0.9885
Average Pore width =	6.077nm
Adsorption energy =	4.279 kJ/mol
Micropore volume =	0.122 cc/g
Micropore surface area =	344.022 m²/g

Analysis
Operator: Abdulrahman Abdulkareem **Date:**2008/01/05
Sample ID: Sample PKN **Filename:**

Report
Operator: Abdulrahman Abdulkareem **Date:**2022/11/14
Sample PKN.qps

DA Method Micropore Analysis Data continued

Diameter [nm]	dV(d) [cc/nm/g]	Diameter [nm]	dV(d) [cc/nm/g]
4.66000e+00	4.57079e-02	5.34000e+00	2.96193e-02
4.68000e+00	4.51217e-02	5.36000e+00	2.92513e-02
4.70000e+00	4.45432e-02	5.38000e+00	2.88885e-02
4.72000e+00	4.39721e-02	5.40000e+00	2.85307e-02
4.74000e+00	4.34086e-02	5.42000e+00	2.81779e-02
4.76000e+00	4.28524e-02	5.44000e+00	2.78301e-02
4.78000e+00	4.23035e-02	5.46000e+00	2.74871e-02
4.80000e+00	4.17619e-02	5.48000e+00	2.71488e-02
4.82000e+00	4.12276e-02	5.50000e+00	2.68153e-02
4.84000e+00	4.07003e-02	5.52000e+00	2.64865e-02
4.86000e+00	4.01801e-02	5.54000e+00	2.61622e-02
4.88000e+00	3.96669e-02	5.56000e+00	2.58425e-02
4.90000e+00	3.91606e-02	5.58000e+00	2.55272e-02
4.92000e+00	3.86611e-02	5.60000e+00	2.52163e-02
4.94000e+00	3.81684e-02	5.62000e+00	2.49097e-02
4.96000e+00	3.76824e-02	5.64000e+00	2.46074e-02
4.98000e+00	3.72030e-02	5.66000e+00	2.43093e-02
5.00000e+00	3.67301e-02	5.68000e+00	2.40154e-02
5.02000e+00	3.62637e-02	5.70000e+00	2.37255e-02
5.04000e+00	3.58037e-02	5.72000e+00	2.34397e-02
5.06000e+00	3.53500e-02	5.74000e+00	2.31579e-02
5.08000e+00	3.49026e-02	5.76000e+00	2.28799e-02
5.10000e+00	3.44613e-02	5.78000e+00	2.26058e-02
5.12000e+00	3.40261e-02	5.80000e+00	2.23355e-02
5.14000e+00	3.35969e-02	5.82000e+00	2.20689e-02
5.16000e+00	3.31737e-02	5.84000e+00	2.18061e-02
5.18000e+00	3.27563e-02	5.86000e+00	2.15468e-02
5.20000e+00	3.23447e-02	5.88000e+00	2.12912e-02
5.22000e+00	3.19388e-02	5.90000e+00	2.10390e-02
5.24000e+00	3.15385e-02	5.92000e+00	2.07904e-02
5.26000e+00	3.11439e-02	5.94000e+00	2.05451e-02
5.28000e+00	3.07547e-02	5.96000e+00	2.03032e-02
5.30000e+00	3.03709e-02	5.98000e+00	2.00647e-02
5.32000e+00	2.99924e-02		

DA method summary

Best E =	0.707 kJ/mol
Best n =	1.000
DA Micropore Volume =	0.299 cc/g
Pore Diameter (mode)=	2.920e+00 nm

Analysis				Report			
Operator:	Abdulrahman Abdulkareem	**Date:**	2008/01/05	**Operator:**	Abdulrahman Abdulkareem	**Date:**	2022/11/14
Sample ID:	Sample PKN	**Filename:**		Sample PKN.qps			
Sample Desc:		**Comment:**					
Sample weight:	0.3 g	**Sample Volume:**		1 cc			
Outgas Time:	3.0 hrs	**OutgasTemp:**		250.0 C			
Analysis gas:	Nitrogen	**Bath Temp:**		273.0 K			
Press. Tolerance:	0.100/0.100 (ads/des)	**Equil time:**		60/60 sec (ads/des)	**Equil timeout:**		240/240 sec (ads/des)
Analysis Time:	103.0 min	**End of run:**		2008/01/05 21:16:41	**Instrument:**		Nova Station C
Cell ID:	3						

DFT method Pore Size Distribution

Data Reduction Parameters Data

DFT method	**Calc. Model:** N2 at 77 K on carbon (slit pore, NLDFT equilibrium model)				
	Rel. press. range: 0.0000 - 1.0000			**Moving pt. avg:** off	
Adsorbate	Nitrogen	Temperature	77.350K		
	Molec. Wt.: 28.013	**Cross Section:**	16.200 Å²	**Liquid Density:**	0.808 g/cc

DFT method Pore Size Distribution Data

Pore width [nm]	Cumulative Pore Volume [cc/g]	Cumulative Surface Area [m²/g]	dV(d) [cc/nm/g]	dS(d) [m²/nm/g]
1.6879	0.0000e+00	0.0000e+00	0.0000e+00	0.0000e+00
1.7656	0.0000e+00	0.0000e+00	0.0000e+00	0.0000e+00
1.8469	2.0906e-03	2.2640e+00	2.5725e-02	2.7858e+01
1.9319	8.3901e-03	8.7854e+00	7.4104e-02	7.6715e+01
2.0208	1.4013e-02	1.4350e+01	6.3236e-02	6.2584e+01
2.1138	1.4574e-02	1.4881e+01	6.0276e-03	5.7030e+00
2.2111	2.1957e-02	2.1559e+01	7.5888e-02	6.8641e+01
2.3129	3.5473e-02	3.3246e+01	1.3280e-01	1.1483e+02
2.4194	4.7571e-02	4.3248e+01	1.1364e-01	9.3946e+01
2.5307	6.2527e-02	5.5067e+01	1.3431e-01	1.0614e+02
2.6472	8.0694e-02	6.8793e+01	1.5596e-01	1.1783e+02
2.7691	9.4502e-02	7.8765e+01	1.1332e-01	8.1847e+01

DFT method summary

Pore volume =	0.095 cc/g
Surface area =	78.765 m²/g
Lower confidence limit =	1.688 nm
Fitting error =	2.973 %
Pore width (Mode) =	2.647 nm
Moving point average :	off

Analysis				Report			
Operator:	Abdulrahman AbdulkareemDate:2008/01/05			**Operator:**	Abdulrahman Abdulkareem Date:2022/11/14		
Sample ID:	Sample PKN	**Filename:**		Sample PKN.qps			
Sample Desc:		**Comment:**					
Sample weight:	0.3 g	**Sample Volume:**		1 cc			
Outgas Time:	3.0 hrs	**OutgasTemp:**		250.0 C			
Analysis gas:	Nitrogen	**Bath Temp:**		273.0 K			
Press. Tolerance:	0.100/0.100 (ads/des)	**Equil time:**		60/60 sec (ads/des)	**Equil timeout:**	240/240 sec (ads/des)	
Analysis Time:	103.0 min	**End of run:**		2008/01/05 21:16:41	**Instrument:**	Nova Station C	
Cell ID:	3						

Area-Volume Summary

Data Reduction Parameters Data

	Thermal Transpiration: on	**Eff. mol. diameter (D):** 3.54 Å		**Eff. cell stem diam. (d):** 4.0000 mm	
t-Method	**Calc. method:** de Boer				
BJH/DH method	**Moving pt. avg.:** off				
DR method	**Affinity coefficient (ß):** 0.3300				
HK method	**Tabulated data interval:** 1				
SF method	**Tabulated data interval:** 1				
DFT method	**Calc. Model:** N2 at 77 K on carbon (slit pore, NLDFT equilibrium model)				
	Rel. press. range: 0.0000 - 1.0000			**Moving pt. avg:** off	
Adsorbate	**Nitrogen**	**Temperature**	77.350K		
	Molec. Wt.: 28.013	**Cross Section:**	16.200 Å²	**Liquid Density:**	0.808 g/cc
	Critical Temp.: 126.200 K	**Critical Press.:**	33.500 atm	**SuperCritic. K.:**	1.000
Adsorbent	Carbon				
	DR. Exp (n): 2.000				

Surface Area Data

SinglePoint BET	2.007e+02 m²/g
MultiPoint BET	3.302e+02 m²/g
Langmuir surface area	1.750e+03 m²/g
BJH method cumulative adsorption surface area	3.828e+02 m²/g
DH method cumulative adsorption surface area	4.137e+02 m²/g
t-method external surface area	3.302e+02 m²/g
DR method micropore area	3.440e+02 m²/g
DFT cumulative surface area	7.877e+01 m²/g

Pore Volume Data

BJH method cumulative adsorption pore volume	1.846e-01 cc/g
DH method cumulative adsorption pore volume	1.910e-01 cc/g
DR method micropore volume	1.223e-01 cc/g
HK method micropore volume	5.303e-02 cc/g
SF method micropore volume	1.083e-02 cc/g
DFT method cumulative pore volume	9.450e-02 cc/g

Pore Size Data

BJH method adsorption pore Diameter (Mode Dv(d))	2.093e+00 nm
DH method adsorption pore Diameter (Mode Dv(d))	2.093e+00 nm
DR method micropore Pore width	6.077e+00 nm
DA method pore Diameter (Mode)	2.920e+00 nm
HK method pore Diameter (Mode)	1.882e+00 nm
SF method pore Diameter (Mode)	3.534e+00 nm
DFT pore Diameter (Mode)	2.647e+00 nm

APPENDIX A4

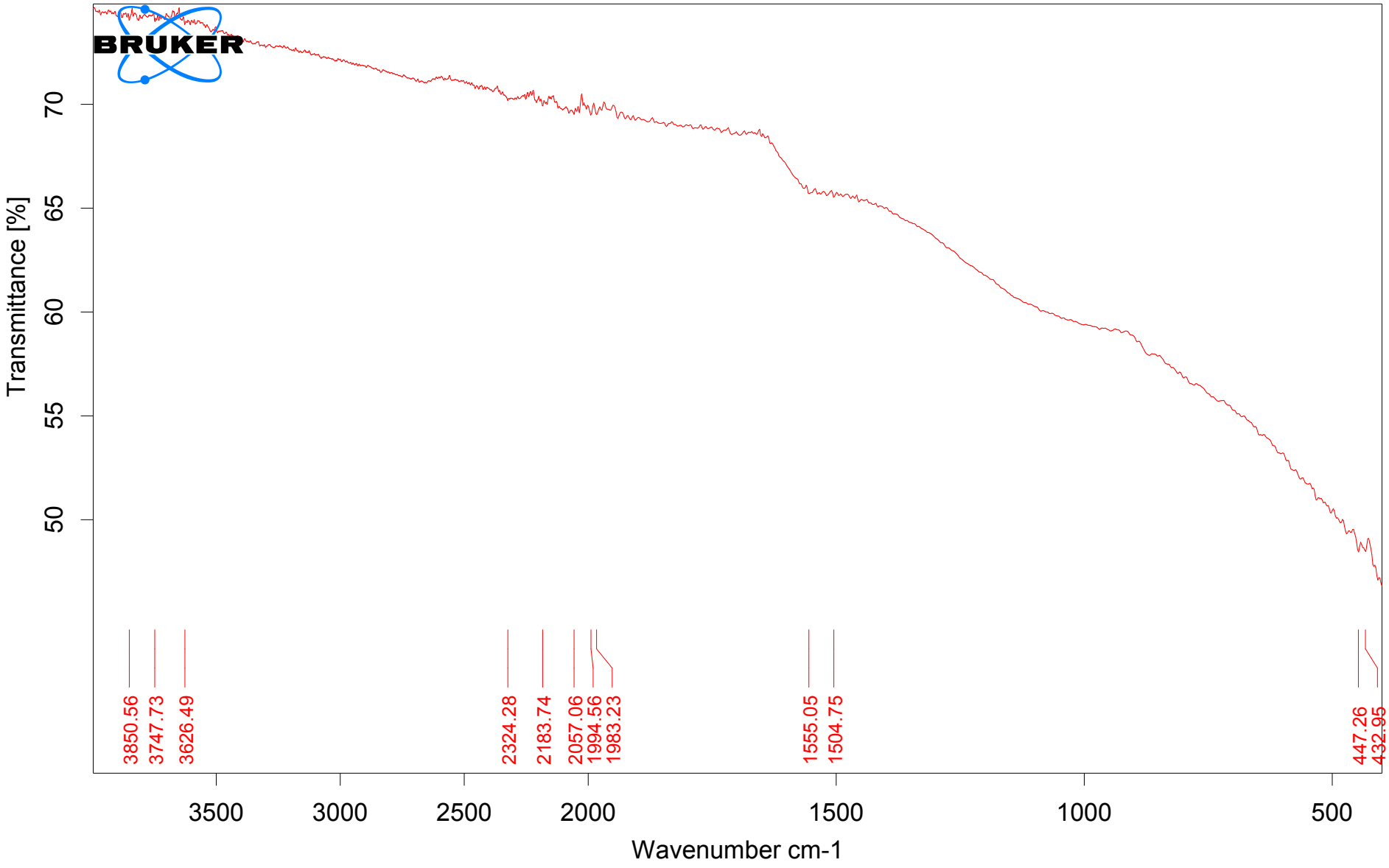

C:\OPUS_7.2.139.1294\MEAS\.5140	CCN	Instrument type and / or accessory	22/11/2022

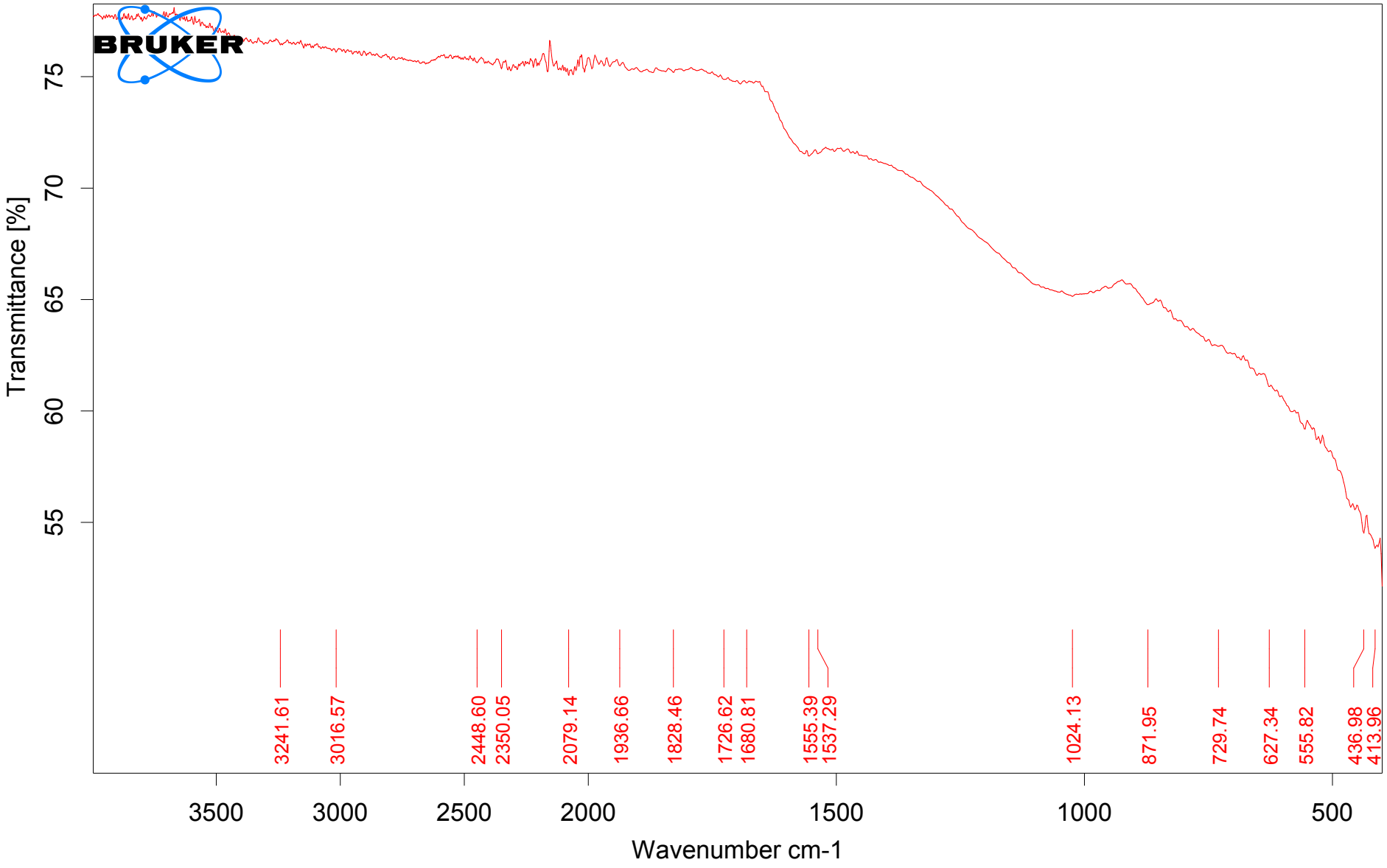

C:\OPUS_7.2.139.1294\MEAS\.5139	PKN	Instrument type and / or accessory	22/11/2022

APPENDIX A5

Measurement Conditions:

Dataset Name	Powder_Fine_CCN
File name	C:\XRD Data\Martin\Powder_Fine_CCN.xrdml
Sample Identification	Powder_Fine_CCN
Comment	Configuration=Reflection-transmission spinner, Owner=User-1, Creation date=12/11/2013 09:58:32

Goniometer=Theta/Theta; Minimum step size 2Theta:0.0001; Minimum step size Omega:0.0001
Sample stage=Reflection-transmission spinner; Minimum step size Phi:0.1
Diffractometer system=EMPYREAN
Measurement program=C:\XRD Data\Martin\Measurement Programs\Powder_Fine.xrdmp, Identifier={890F6871-C77A-4C0D-8558-ECB72383A3CA}
Fine Calibration Offset for 2Theta = 12.5809 deg
Fine Calibration Offset for Omega = -0.0009 deg

Measurement Start Date/Time	25/01/2023 15:50:47
Operator	UG leogn
Raw Data Origin	XRD measurement (*.XRDML)
Scan Axis	Gonio
Start Position [°2θ]	5.0525
End Position [°2θ]	99.8675
Step Size [°2θ]	0.1050
Scan Step Time [s]	47.6850
Scan Type	Continuous
PSD Mode	Scanning
PSD Length [°2θ]	3.35
Offset [°2θ]	0.0000
Divergence Slit Type	Fixed
Divergence Slit Size [°]	0.2177
Specimen Length [mm]	10.00
Measurement Temperature [°C]	25.00
Anode Material	Cu
K-Alpha1 [Å]	1.54060
K-Alpha2 [Å]	1.54443
K-Beta [Å]	1.39225
K-A2 / K-A1 Ratio	0.50000
Generator Settings	40 mA, 45 kV
Diffractometer Type	0000000011136412
Diffractometer Number	0
Goniometer Radius [mm]	240.00
Dist. Focus-Diverg. Slit [mm]	100.00
Incident Beam Monochromator	No
Spinning	Yes

Main Graphics, Analyze View:

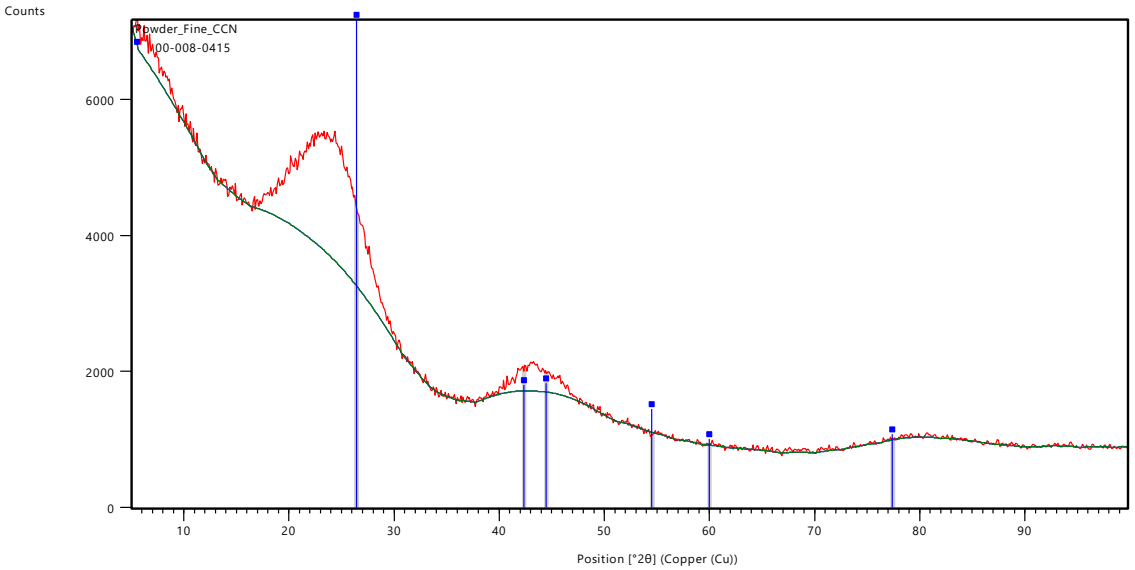

Peak List:

Pattern List:

Visible	Ref.Code	Score	Compound Name	Displ.[°2θ]	Scale Fac.	Chem. Formula
*	00-008-0415	51	Carbon	0.000	0.589	C

Measurement Conditions:

Dataset Name	Powder_Fine_PKN
File name	C:\XRD Data\Martin\Powder_Fine_PKN.xrdml
Sample Identification	Powder_Fine_PKN
Comment	Configuration=Reflection-transmission spinner, Owner=User-1, Creation date=12/11/2013 09:58:32

Goniometer=Theta/Theta; Minimum step size 2Theta:0.0001; Minimum step size Omega:0.0001
Sample stage=Reflection-transmission spinner; Minimum step size Phi:0.1
Diffractometer system=EMPYREAN
Measurement program=C:\XRD Data\Martin\Measurement Programs\Powder_Fine.xrdmp, Identifier={890F6871-C77A-4C0D-8558-ECB72383A3CA}
Fine Calibration Offset for 2Theta = 12.5809 deg
Fine Calibration Offset for Omega = -0.0009 deg

Measurement Start Date/Time	25/01/2023 16:03:53
Operator	UG leogn
Raw Data Origin	XRD measurement (*.XRDML)
Scan Axis	Gonio
Start Position [°2θ]	5.0525
End Position [°2θ]	99.8675
Step Size [°2θ]	0.1050
Scan Step Time [s]	47.6850
Scan Type	Continuous
PSD Mode	Scanning
PSD Length [°2θ]	3.35
Offset [°2θ]	0.0000
Divergence Slit Type	Fixed
Divergence Slit Size [°]	0.2177
Specimen Length [mm]	10.00
Measurement Temperature [°C]	25.00
Anode Material	Cu
K-Alpha1 [Å]	1.54060
K-Alpha2 [Å]	1.54443
K-Beta [Å]	1.39225
K-A2 / K-A1 Ratio	0.50000
Generator Settings	40 mA, 45 kV
Diffractometer Type	0000000011136412
Diffractometer Number	0
Goniometer Radius [mm]	240.00
Dist. Focus-Diverg. Slit [mm]	100.00
Incident Beam Monochromator	No
Spinning	Yes

Main Graphics, Analyze View:

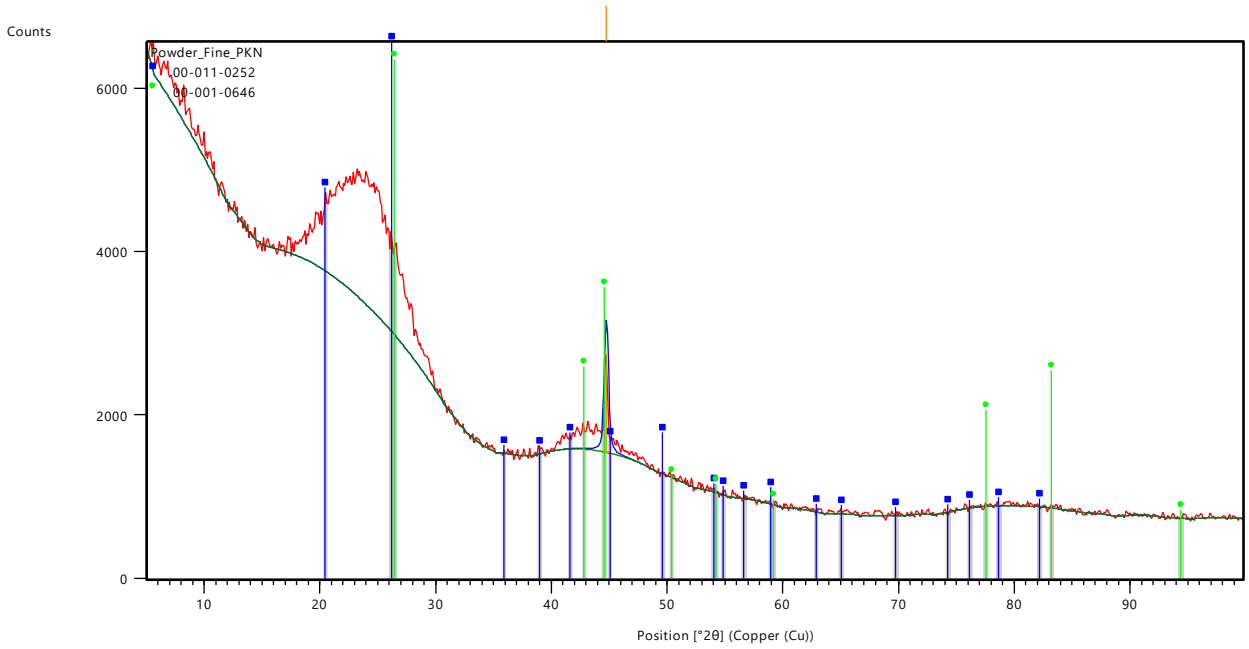

Peak List:

Pos. [°2θ]	Height [cts]	FWHM Left [°2θ]	d-spacing [Å]	Rel. Int. [%]
44.7294	1213.85	0.3780	2.02443	100.00

Pattern List:

Visible	Ref.Code	Score	Compound Name	Displ.[°2θ]	Scale Fac.	Chem. Formula
*	00-011-0252	35	Silicon Oxide	0.000	0.773	Si O2
*	00-001-0646	25	Carbon	0.000	0.511	C

APPENDIX A6

Anova: Single Factor

SUMMARY

Groups	*Count*	*Sum*	*Average*	*Variance*
SM	62	11683.62	188.4455	15465.8
CCN3g	62	19349.13	312.0827	16710.51
CCN6g	62	14482.31	233.5856	5459.841
CCN10g	62	9263.46	149.4106	2683.827
PKN3g	62	17634.87	284.4334	9330.437
PKN6g	62	18550.61	299.2033	12126.27
PKN10g	62	8140.48	131.2981	1877.186

ANOVA

Source of Variation	*SS*	*df*	*MS*	*F*	*P-value*	*F crit*
Between Groups	2011714	6	335285.7	36.87128	5.38E-36	2.119811
Within Groups	3882886	427	9093.411			
Total	5894600	433				

t-Test: Paired Two Sample for Means

	SM	*CCN3g*
Mean	188.4455	312.0827
Variance	15465.8	16710.51
Observatio	62	62
Pearson Co	0.937789	
Hypothesiz	0	
df	61	
t Stat	-21.6374	
P(T<=t) one	1.3E-30	
t Critical or	1.670219	
P(T<=t) two	2.61E-30	
t Critical tw	1.999624	

Therefore p<0.001
higher than control

t-Test: Paired Two Sample for Means

	SM	*CCN6g*
Mean	188.4455	233.5856
Variance	15465.8	5459.841
Observatio	62	62
Pearson Co	0.80937	
Hypothesiz	0	
df	61	
t Stat	-4.56934	
P(T<=t) one	1.22E-05	
t Critical or	1.670219	
P(T<=t) two	2.44E-05	
t Critical tw	1.999624	

Therefore p<0.001
lower than control

t-Test: Paired Two Sample for Means

	SM	*CCN10g*
Mean	188.4455	149.4106
Variance	15465.8	2683.827
Observatio	62	62
Pearson Co	0.8844	
Hypothesiz	0	
df	61	
t Stat	3.739996	
P(T<=t) one	0.000204	
t Critical or	1.670219	
P(T<=t) two	0.000409	
t Critical tw	1.999624	

Therefore p=0.0002
lower than control

t-Test: Paired Two Sample for Means

	SM	*PKN3g*
Mean	188.4455	284.4334
Variance	15465.8	9330.437
Observatio	62	62
Pearson Co	0.840208	
Hypothesiz	0	
df	61	
t Stat	-11.1316	
P(T<=t) one	1.26E-16	
t Critical or	1.670219	
P(T<=t) two	2.52E-16	
t Critical tw	1.999624	

Therefore p<0.001
lower than control

t-Test: Paired Two Sample for Means

	SM	*PKN6g*
Mean	188.4455	299.2033
Variance	15465.8	12126.27
Observatio	62	62
Pearson Co	0.896512	

t-Test: Paired Two Sample for Means

	SM	*PKN10g*
Mean	188.4455	131.2981
Variance	15465.8	1877.186
Observatio	62	62
Pearson Co	0.865098	

Hypothesiz	0
df	61
t Stat	-15.8244
P(T<=t) one	1.44E-23
t Critical or	1.670219
P(T<=t) two	2.88E-23
t Critical tw	1.999624

Therefore p<0.001
lower than control

Hypothesiz	0
df	61
t Stat	5.024512
P(T<=t) one	2.35E-06
t Critical or	1.670219
P(T<=t) two	4.69E-06
t Critical tw	1.999624

Therefore p<0.001
lower than control